
Universiteit
Leiden
The Netherlands

Immune modulation by helminths and the impact on the development of type 2 diabetes

Ruiter, K. de

Citation
Ruiter, K. de. (2019, March 26). *Immune modulation by helminths and the impact on the development of type 2 diabetes*. Retrieved from https://hdl.handle.net/1887/70477

Version:	Not Applicable (or Unknown)
License:	Leiden University Non-exclusive license
Downloaded from:	https://hdl.handle.net/1887/70477

Note: To cite this publication please use the final published version (if applicable).

Cover Page

Universiteit Leiden

The handle http://hdl.handle.net/1887/70477 holds various files of this Leiden University dissertation.

Author: Ruiter, K. de
Title: Immune modulation by helminths and the impact on the development of type 2 diabetes
Issue Date: 2019-03-26

IMMUNE MODULATION BY HELMINTHS AND THE IMPACT ON THE DEVELOPMENT OF TYPE 2 DIABETES

IMMUNE MODULATION BY HELMINTHS AND THE IMPACT ON THE DEVELOPMENT OF TYPE 2 DIABETES

Proefschrift

ter verkrijging van
de graad van Doctor aan de Universiteit Leiden,
op gezag van Rector Magnificus prof.mr. C.J.J.M. Stolker,
volgens besluit van het College voor Promoties
te verdedigen op dinsdag 26 maart 2019
klokke 15.00 uur

door

Karin de Ruiter
geboren te Renkum in 1988

ISBN: 978-94-6182-936-8

© 2019 Karin de Ruiter

The work presented in this thesis was performed at the Department of Parasitology, at the Leiden University Medical Center, in collaboration with the Department of Parasitology at the Faculty of Medicine of University of Indonesia, Jakarta.

The studies described in this thesis were financially supported by The Royal Netherlands Academy of Arts and Science (KNAW).

Cover design and artwork: Evelien Jagtman (www.evelienjagtman.com)

Layout and Printing: Off Page, Amsterdam (www.offpage.nl)

Promotores

Prof. Dr. M. Yazdanbakhsh
Prof. Dr. T. Supali (Universitas Indonesia, Jakarta, Indonesia)

Co-promotor

Dr. B. Guigas

Leden promotiecommissie

Prof. Dr. P.C.N. Rensen
Prof. Dr. M.J. Jager
Prof. Dr. C.H. Hokke
Prof. Dr. A.G.M. Tielens (Utrecht University)
Dr. J. Hendriks (The Janssen Pharmaceutical Companies of Johnson & Johnson)

TABLE OF CONTENTS

1

GENERAL INTRODUCTION

Adapted from: Helminths, Hygiene Hypothesis and Type 2 Diabetes

Karin de Ruiter*, Dicky L. Tahapary*, Erliyani Sartono, Pradana Soewondo,
Taniawati Supali, Johannes W.A. Smit and Maria Yazdanbakhsh

*Both authors contributed equally

Parasite Immunology (2017)

A SHORT INTRODUCTION TO HELMINTHS

Helminths, or parasitic worms, are multicellular organisms and represent one of the most prevalent infectious agents affecting nearly one-third of the population worldwide (1). Helminth infections are widely distributed in tropical and subtropical regions, primarily in rural areas where sanitation is poor. Soil-transmitted helminths (STHs) (main species: *Ascaris lumbricoides*, *Trichuris trichiura*, hookworm) represent the most common species infecting humans, followed by schistosomes and filarial nematodes (1). Helminths have varied life cycles, and routes of infection can vary from direct penetration (schistosomes, hookworms), entrance via a mosquito bite (filarial worms) or through ingestion (*A. lumbricoides, T. trichiura*). Also the location of adult worms within the human body differs from the peripheral blood (schistosomes), the lymphatics (filarial worms), the intestine (STHs), or other tissues.

It was estimated that 1.45 billion people worldwide were infected with at least one species of STHs in 2010, with the majority of infections and highest burden occurring in Asia (2). When expressing the burden of helminth infections in disability-adjusted life years (DALYs), 5.2 million DALYs were attributable to STHs, 3.3 million to schistosomiasis and 2.8 million to lymphatic filariasis, meaning that helminths contribute, to the greatest extent, to the total burden of neglected tropical diseases (26 million DALYs) (2, 3). Despite this worldwide burden and presumed helminth-associated morbidities such as malnutrition, poor growth, cognitive deficits and anaemia among children with heavy and chronic STH infections (4, 5), most infections are often clinically asymptomatic and mortality due to STHs is rare (6). Interestingly, a recent analysis of the Cochrane database demonstrated that mass treatment of all children in endemic areas does not improve average nutritional status, haemoglobin, cognition, school performance or survival, although it might have nutritional benefits among helminth-infected children (7).

The high prevalence of helminth infections, and its chronic and often asymptomatic nature of infection therefore suggests a long evolutionary co-adaptation between helminths and their human host. Indeed, there seems to be an immunological interaction between helminths and their host in which helminths polarize the immune system towards a strong type 2 immune response that is believed to be associated with tissue repair (8), as well as establishment of a regulatory network, which can contribute to the control of overt immune responses to allow longer term survival of the parasite while restricting inflammation that might otherwise lead to pathology (9).

HELMINTH-ASSOCIATED TH2 RESPONSES AND IMMUNE REGULATORY NETWORK

Helminth parasites are strong inducers of type 2 immunity which involves activation and expansion of $CD4^+$ T helper 2 (Th2) cells producing the cytokines interleukin (IL)-4, IL-5, IL-9, IL-10 and IL-13, systemic and localized eosinophilia, expansion of basophils and mast cells, goblet-cell hyperplasia and the production of IgE (10). Moreover, the presence of

alternatively activated macrophages (AAMs), induced by IL-4 and/or IL-13, is a characteristic feature of the polarized Th2 response (11). The type 2 response is host protective by controlling the number of parasites through direct killing or expulsion, and inducing tissue repair, necessary to protect against the damage caused by tissue-migrating helminths (12).

Cellular immune hyporesponsiveness in individuals infected with helminths was first observed in the 1970s, when lymphocytes isolated from subjects chronically infected with *Schistosoma mansoni* showed a diminished proliferative response upon stimulation with schistosome antigens (13). Subsequently, several human studies demonstrated that chronic helminth infections, such as schistosomiasis and filariasis, result in parasite-antigen-specific immune suppression (14-17). As the responsiveness is restored after anthelmintic treatment (18-22), a causal relationship between the presence of helminths and suppression of the immune system was considered likely (23). This T-cell hyporesponsiveness is thought to be mediated by a helminth-induced regulatory network involving regulatory T cells (Tregs) and their associated regulatory cytokines IL-10 and transforming growth factor (TGF)-β (14, 24). Tregs, the subset of T cells that maintains self-tolerance in humans (23), can dampen both Th1 and Th2 cell activation (9) and can be activated during many infections, such as parasitic, viral, fungal and bacterial infections (25). Several studies in animal models and humans show that helminth infections are associated with increased Treg frequencies and/or functional capacity (26-28). Moreover, the finding that mice were cleared of parasites after the administration of antibodies to Treg surface markers (GITR and CD25) supported the concept that the induction of Tregs is part of the helminths' own survival strategy (29).

T-cell hyporesponsiveness, as observed in helminth-infected populations, is not restricted to parasite antigens but extends to bystander antigens, such as vaccines, allergens or autoantigens (9). This "spillover suppression" seems to be present particularly with increasing intensity of infection (30) and has several consequences, one of them being that infected subjects develop a regulatory network which helps to control inappropriate inflammation. Indeed, areas where helminths are endemic have been associated with a reduced prevalence of immunopathologies such as Th2-mediated allergic-diseases (reviewed in (6, 31, 32)), and Th1-mediated autoimmune diseases (33, 34).

HELMINTHS AND TYPE 2 DIABETES: AN INVERSE ASSOCIATION?

There has been an alarming increase in the worldwide burden of diabetes, especially in low- to middle-income countries (35). Rapid socioeconomic development in these countries has led to a shift in dietary habits and infrastructure that promotes overnutrition and decreased physical activity, ultimately increasing the risk for type 2 diabetes (T2D) (36). Obesity-induced chronic low-grade inflammation has been shown to be a key feature in the development of insulin resistance (IR; a decrease in insulin-stimulated glucose uptake), which is a strong predictor for the development of T2D (37, 38). Initiation of inflammation in

obesity involves inflammation of visceral adipose tissue and the liver, as well as the release of free fatty acids, which then promote systemic inflammation, reflected by increased levels of pro-inflammatory cytokines (37). As helminths can skew the immune system towards an anti-inflammatory profile, it is possible that the inflammation leading to IR is decreased, which would translate into a protective role of helminths in the development of T2D. This hypothesis is supported by the notion that there is little overlap between the proportion of children per country requiring preventive chemotherapy for STH and the prevalence of diabetes (39, 40). However, it should be noted that potential confounding factors such as relative wealth, diet and physical activity are likely to play a role in this observation.

Interestingly, a number of epidemiological studies in different populations, listed in Figure 1, have reported an inverse association between helminths and metabolic diseases (Reviewed in more detail in (41)), and a recent meta-analysis showed that individuals with a previous or current helminth infection were 50% less likely to manifest metabolic dysfunction (hyperglycaemia, T2D, metabolic syndrome or insulin resistance) compared to those uninfected (OR 0.50; 95% CI 0.38-0.66) (42). Moreover, it was shown by a study in Indonesia that subjects with a current STH infection had a lower BMI and lower levels of

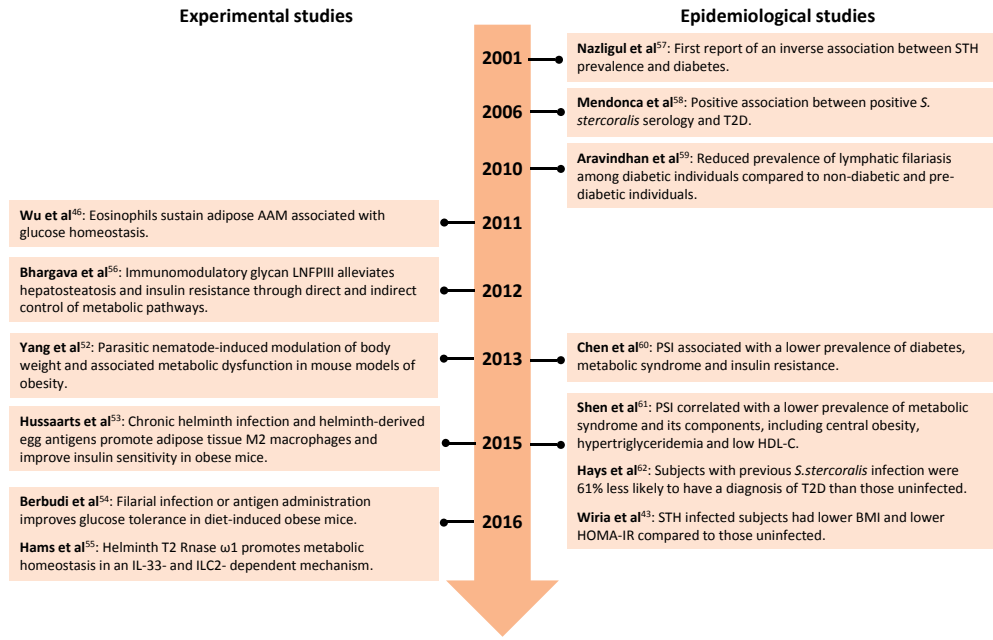

Figure 1. Overview of experimental and epidemiological landmark studies investigating the association between helminth infections or administration of helminth-derived molecules and metabolic outcomes. (AAM, alternatively activated macrophage; ILC2, innate lymphoid type 2 cells; T2D, type 2 diabetes; STH, soil-transmitted helminths; PSI, previous schistosome infection; HDL-C, high-density lipoprotein cholesterol; BMI, body mass index; HOMA-IR, homeostatic model assessment of insulin resistance).

HOMA-IR, indicating that STH-infected subjects were more insulin sensitive compared to uninfected subjects (43). A significant negative association was found between the number of helminth species a subject was infected with and HOMA-IR, even after adjustment for age, sex and BMI (43). However, cross-sectional studies provide no information on the causal relationship between helminths and metabolic diseases and therefore longitudinal studies are needed.

HELMINTHS' IMMUNOMODULATORY EFFECTS ASSOCIATED WITH IMPROVED METABOLIC HOMEOSTASIS

A number of landmark studies have provided evidence for the beneficial effects of helminths and helminth-derived molecules on metabolic homeostasis (**Figure 1**), and shed light on the immunomodulatory mechanisms that could explain the link between helminths and T2D. It was demonstrated that the maintenance of AAMs in white adipose tissue (WAT), necessary to maintain glucose homeostasis partly through secretion of IL-10 (44, 45), depends on the presence of IL-4 secreting eosinophils (46). Helminth infections promote WAT eosinophilia (46) and this accumulation is highly dependent on type 2 cytokines, particularly IL-5 (47-49). Innate lymphoid type 2 cells (ILC2s) are widely distributed in tissues, including WAT, lack antigen-specific receptors and are capable of producing type-2 cytokines in response to alarmins such as IL-25 and IL-33 (50). By functional deletion of these cells it was shown that ILC2s are required to sustain eosinophils and AAMs in WAT as they are the major source of IL-5 and IL-13 (51). These findings indicate that the presence of eosinophils, AAMs and ILC2 immune cells in WAT have beneficial effects on obesity-induced inflammation and improve glucose homeostasis in obese mice.

Recent studies have provided further evidence by demonstrating that the type 2 environment induced by infection with *Nippostrongylus brasiliensis* (52), *S. mansoni* (53) or the filarial nematode *Litomosoides sigmodontis* (54) improves glucose tolerance and insulin sensitivity in diet-induced obese mice. In addition, similar insulin-sensitizing effects have been attributed to the administration of helminth-derived (egg) antigens (53-55). Despite the different experimental models used, increased numbers of eosinophils and AAMs in WAT of helminth-infected HFD-fed mice are consistently found (52-54). By infecting eosinophil-deficient mice, it was shown that the improvement in glucose tolerance by *L. sigmodontis* infection depended on eosinophils (54). As expected, infection induced Th2 cytokine responses (IL-4, IL-5, IL-13) in WAT with IL-4 being the key cytokine consistently upregulated after infection.

In addition, *S. mansoni*-soluble egg antigen (SEA) (53), *S. mansoni* egg-derived omega-1 (ω1) (55) and *L. sigmodontis* antigen (54) administration enhanced the number of group 2 innate lymphoid cells (ILC2s) in WAT and resulted in slightly increased IL-5 (not IL-13) production (53). Recently, Hams et al. showed that ω1 induces the release of IL-33, a potent inducer of ILC2s, from adipocytes in both mice and humans (55). In the absence of ILC2s, ω1 failed to induce the infiltration of eosinophils and AAMs in WAT and was

unable to improve glucose tolerance in obese mice (55). This indicates a causative role of ILC2s in alteration of the immune cell environment in WAT.

Taken together, these findings show that in experimental animal models, helminths influence metabolic homeostasis, at least partly, by changing the immune cell composition in the adipose tissue (**Figure 2**). Whereas obesity-induced, chronic low-grade inflammation is characterized by the accumulation of $CD8^+$ T cells, $CD4^+$ Th1 cells, CAMs, B cells and mast cells in the adipose tissue, chronic helminth infections or helminth-derived molecules induce increased numbers of $CD4^+$ Th2 cells, eosinophils, AAMs, Tregs and ILC2s, dampening the inflammation and improving glucose tolerance.

SCOPE AND OUTLINE OF THIS THESIS

Although previous studies strongly suggest that there is an association between helminth infections and metabolic homeostasis, the causality of this relationship in humans has not been demonstrated as yet. Therefore, the main objective of this thesis is to improve the understanding of the role of helminth infections in the development of insulin resistance, hence T2D, and to gain insight into the immunological mechanisms underlying this possible association.

To this end, we initiated a large scale cluster randomized controlled trial (RCT), described in **Chapter 2**, assessing the effect of anthelmintic treatment on insulin resistance and other metabolic, as well as immunological parameters, in a rural area of Indonesia.

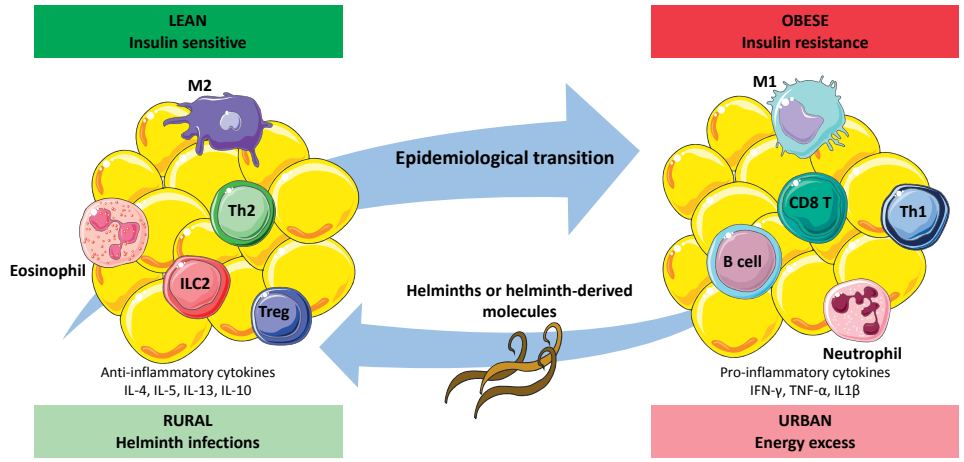

Figure 2. The effects of helminths and obesity on the immune cell composition in adipose tissue. Along with epidemiological transition, the prevalence of obesity is higher and exposure to helminth infections is lower in urban areas compared to rural areas. With obesity, the immune cell composition in the adipose tissue shifts towards a Th1 and pro-inflammatory profile associated with insulin resistance. Helminths or helminth-derived molecules are thought to prevent and/or reverse this shift by inducing a Th2 and anti-inflammatory immune cell environment, which is associated with insulin sensitivity. AAM, alternatively activated macrophages; CAM, classically activated macrophages.

This area is endemic for STH and has been previously reported to have a low prevalence of insulin resistance and T2D.

In **chapter 3**, we analyze the outcomes of this RCT with respect to the effects of anthelmintic treatment on STH prevalence, adiposity, insulin resistance and Th2 responses (e.g. eosinophil counts and total IgE levels).

Omega-1 (ω1) is a glycoprotein that was previously identified as the major immunomodulatory component in *S. mansoni*-soluble egg antigen (SEA) and in **chapter 4**, we study the effects of plant-produced recombinant ω1 treatment on whole-body glucose homeostasis and insulin sensitivity in a mouse model of diet-induced obesity. To investigate whether ω1 has a beneficial effect on metabolic homeostasis and the underlying mechanisms, we perform in-depth metabolic profiling and analyze the immune cell composition of metabolic organs.

Whereas field studies in endemic areas may be complicated by logistic challenges, there is no substitute for real-life biological settings of infection and it provides opportunities to study the underlying immunological processes that might explain the possible beneficial effects of helminth infections. **Chapter 5** describes the method that was developed to study granulocyte activation by flow cytometry in the field with only basic laboratory infrastructure. This method is applied in our RCT conducted in Indonesia in order to study the effect of anthelmintic treatment on eosinophil and neutrophil activation by assessing activation markers, the responsiveness to stimuli and circulating levels of eosinophil granule proteins, the outcomes of which are described in **chapter 6**.

Chapter 7 describes the effect of anthelmintic treatment on Th2-mediated responses in a large scale RCT in Indonesia. It measures two different components of the Th2 mediated response, namely IgE and IL-5 response to a mitogen, PHA.

To fully understand immune modulation by helminths and identify specific cells that might be important in this process, we applied mass cytometry in **chapter 8**, allowing high-resolution dissection of the cellular composition of the immune system by the simultaneous measurement of 37 cellular markers at a single-cell level. The effects of deworming on type 2 and regulatory immune responses are studied by performing unbiased immune profiling of Indonesian adults before and after anthelmintic treatment.

Finally, **chapter 9** summarizes the main findings presented in this thesis and provides directions for future research towards understanding the link between helminth infections, their immunomodulatory effects and inflammatory diseases such as T2D.

REFERENCES

1. Hotez PJ, Brindley PJ, Bethony JM, King CH, Pearce EJ, Jacobson J. Helminth infections: the great neglected tropical diseases. The Journal of clinical investigation 2008; 118(4): 1311-21.
2. Pullan RL, Smith JL, Jasrasaria R, Brooker SJ. Global numbers of infection and disease burden of soil transmitted helminth infections in 2010. Parasit Vectors 2014; 7: 37.
3. Global Atlas of Helminth Infections. http://wwwthiswormyworldorg/worms/global-burden.
4. Bethony J, Brooker S, Albonico M, et al. Soil-transmitted helminth infections: ascariasis, trichuriasis, and hookworm. Lancet 2006; 367(9521): 1521-32.
5. de Silva NR. Impact of mass chemotherapy on the morbidity due to soil-transmitted nematodes. Acta Trop 2003; 86(2-3): 197-214.
6. Wammes LJ, Mpairwe H, Elliott AM, Yazdanbakhsh M. Helminth therapy or elimination: epidemiological, immunological, and clinical considerations. The Lancet Infectious diseases 2014; 14(11): 1150-62.
7. Taylor-Robinson DC, Maayan N, Soares-Weiser K, Donegan S, Garner P. Deworming drugs for soil-transmitted intestinal worms in children: effects on nutritional indicators, haemoglobin, and school performance. The Cochrane database of systematic reviews 2015; 7: CD000371.
8. Chen F, Liu Z, Wu W, et al. An essential role for TH2-type responses in limiting acute tissue damage during experimental helminth infection. Nat Med 2012; 18(2): 260-6.
9. Maizels RM, Yazdanbakhsh M. Immune regulation by helminth parasites: cellular and molecular mechanisms. Nature reviews Immunology 2003; 3(9): 733-44.
10. Allen JE, Maizels RM. Diversity and dialogue in immunity to helminths. Nat Rev Immunol 2011; 11(6): 375-88.
11. Jenkins SJ, Allen JE. Similarity and diversity in macrophage activation by nematodes, trematodes, and cestodes. J Biomed Biotechnol 2010; 2010: 262609.
12. Allen JE, Sutherland TE. Host protective roles of type 2 immunity: parasite killing and tissue repair, flip sides of the same coin. Semin Immunol 2014; 26(4): 329-40.
13. Ottesen EA, Hiatt RA, Cheever AW, Sotomayor ZR, Neva FA. The acquisition and loss of antigen-specific cellular immune responsiveness in acute and chronic schistosomiasis in man. Clin Exp Immunol 1978; 33(1): 37-47.
14. King CL, Mahanty S, Kumaraswami V, et al. Cytokine control of parasite-specific anergy in human lymphatic filariasis. Preferential induction of a regulatory T helper type 2 lymphocyte subset. The Journal of clinical investigation 1993; 92(4): 1667-73.
15. Yazdanbakhsh M, Paxton WA, Kruize YC, et al. T cell responsiveness correlates differentially with antibody isotype levels in clinical and asymptomatic filariasis. J Infect Dis 1993; 167(4): 925-31.
16. Grogan JL, Kremsner PG, Deelder AM, Yazdanbakhsh M. Antigen-specific proliferation and interferon-gamma and interleukin-5 production are down-regulated during Schistosoma haematobium infection. The Journal of infectious diseases 1998; 177(5): 1433-7.
17. Piessens WF, McGreevy PB, Piessens PW, et al. Immune responses in human infections with Brugia malayi: specific cellular unresponsiveness to filarial antigens. The Journal of clinical investigation 1980; 65(1): 172-9.
18. Piessens WF, Ratiwayanto S, Piessens PW, et al. Effect of treatment with diethylcarbamazine on immune responses to filarial antigens in patients infected with Brugia malayi. Acta Trop 1981; 38(3): 227-34.
19. Colley DG, Barsoum IS, Dahawi HS, Gamil F, Habib M, el Alamy MA. Immune responses and immunoregulation in relation to human schistosomiasis in Egypt. III. Immunity and longitudinal studies of in vitro responsiveness after treatment. Trans R Soc Trop Med Hyg 1986; 80(6): 952-7.
20. Grogan JL, Kremsner PG, Deelder AM, Yazdanbakhsh M. Elevated proliferation and interleukin-4 release from CD4+ cells after chemotherapy in human Schistosoma haematobium infection. Eur J Immunol 1996; 26(6): 1365-70.
21. Sartono E, Kruize YC, Kurniawan A, et al. Elevated cellular immune responses and interferon-gamma release after long-term diethylcarbamazine treatment of patients

with human lymphatic filariasis. J Infect Dis 1995; 171(6): 1683-7.
22. Wammes LJ, Hamid F, Wiria AE, et al. Community deworming alleviates geohelminth-induced immune hyporesponsiveness. Proceedings of the National Academy of Sciences of the United States of America 2016; 113(44): 12526-31.
23. McSorley HJ, Maizels RM. Helminth infections and host immune regulation. Clin Microbiol Rev 2012; 25(4): 585-608.
24. Turner JD, Jackson JA, Faulkner H, et al. Intensity of intestinal infection with multiple worm species is related to regulatory cytokine output and immune hyporesponsiveness. J Infect Dis 2008; 197(8): 1204-12.
25. Belkaid Y. Regulatory T cells and infection: a dangerous necessity. Nat Rev Immunol 2007; 7(11): 875-88.
26. Maizels RM, Smith KA. Regulatory T cells in infection. Adv Immunol 2011; 112: 73-136.
27. Metenou S, Nutman TB. Regulatory T cell subsets in filarial infection and their function. Front Immunol 2013; 4: 305.
28. Watanabe K, Mwinzi PN, Black CL, et al. T regulatory cell levels decrease in people infected with Schistosoma mansoni on effective treatment. The American journal of tropical medicine and hygiene 2007; 77(4): 676-82.
29. Taylor MD, LeGoff L, Harris A, Malone E, Allen JE, Maizels RM. Removal of regulatory T cell activity reverses hyporesponsiveness and leads to filarial parasite clearance in vivo. J Immunol 2005; 174(8): 4924-33.
30. Smits HH, Hammad H, van Nimwegen M, et al. Protective effect of Schistosoma mansoni infection on allergic airway inflammation depends on the intensity and chronicity of infection. J Allergy Clin Immunol 2007; 120(4): 932-40.
31. Leonardi-Bee J, Pritchard D, Britton J. Asthma and current intestinal parasite infection: systematic review and meta-analysis. Am J Respir Crit Care Med 2006; 174(5): 514-23.
32. Flohr C, Quinnell RJ, Britton J. Do helminth parasites protect against atopy and allergic disease? Clin Exp Allergy 2009; 39(1): 20-32.
33. Fleming JO, Cook TD. Multiple sclerosis and the hygiene hypothesis. Neurology 2006; 67(11): 2085-6.
34. Correale J, Farez M. Association between parasite infection and immune responses in multiple sclerosis. Annals of neurology 2007; 61(2): 97-108.
35. Collaboration NCDRF. Worldwide trends in diabetes since 1980: a pooled analysis of 751 population-based studies with 4.4 million participants. Lancet 2016; 387(10027): 1513-30.
36. Hu FB. Globalization of diabetes: the role of diet, lifestyle, and genes. Diabetes care 2011; 34(6): 1249-57.
37. de Luca C, Olefsky JM. Inflammation and insulin resistance. FEBS Lett 2008; 582(1): 97-105.
38. Shoelson SE, Lee J, Goldfine AB. Inflammation and insulin resistance. The Journal of clinical investigation 2006; 116(7): 1793-801.
39. Federation ID. International Diabetes Federation: IDF Diabetes Atlas, 7th edn. . 2015.
40. http://www.who.int/mediacentre/factsheets/fs366/en/.
41. de Ruiter K, Tahapary DL, Sartono E, et al. Helminths, hygiene hypothesis and type 2 diabetes. Parasite immunology 2017; 39(5).
42. Tracey EF, McDermott RA, McDonald MI. Do worms protect against the metabolic syndrome? A systematic review and meta-analysis. Diabetes Res Clin Pract 2016; 120: 209-20.
43. Wiria AE, Hamid F, Wammes LJ, et al. Infection with Soil-Transmitted Helminths Is Associated with Increased Insulin Sensitivity. PloS one 2015; 10(6): e0127746.
44. Chawla A, Nguyen KD, Goh YP. Macrophage-mediated inflammation in metabolic disease. Nature reviews Immunology 2011; 11(11): 738-49.
45. Lumeng CN, Bodzin JL, Saltiel AR. Obesity induces a phenotypic switch in adipose tissue macrophage polarization. The Journal of clinical investigation 2007; 117(1): 175-84.
46. Wu D, Molofsky AB, Liang HE, et al. Eosinophils sustain adipose alternatively activated macrophages associated with glucose homeostasis. Science 2011; 332(6026): 243-7.
47. Mould AW, Matthaei KI, Young IG, Foster PS. Relationship between interleukin-5 and eotaxin in regulating blood and tissue eosinophilia in mice. The Journal of clinical investigation 1997; 99(5): 1064-71.
48. Kopf M, Brombacher F, Hodgkin PD, et al. IL-5-deficient mice have a developmental defect in CD5+ B-1 cells and lack eosinophilia but have normal antibody and cytotoxic T cell responses. Immunity 1996; 4(1): 15-24.

49. Foster PS, Hogan SP, Ramsay AJ, Matthaei KI, Young IG. Interleukin 5 deficiency abolishes eosinophilia, airways hyperreactivity, and lung damage in a mouse asthma model. J Exp Med 1996; 183(1): 195-201.
50. Licona-Limon P, Kim LK, Palm NW, Flavell RA. TH2, allergy and group 2 innate lymphoid cells. Nat Immunol 2013; 14(6): 536-42.
51. Molofsky AB, Nussbaum JC, Liang HE, et al. Innate lymphoid type 2 cells sustain visceral adipose tissue eosinophils and alternatively activated macrophages. J Exp Med 2013; 210(3): 535-49.
52. Yang Z, Grinchuk V, Smith A, et al. Parasitic nematode-induced modulation of body weight and associated metabolic dysfunction in mouse models of obesity. Infection and immunity 2013; 81(6): 1905-14.
53. Hussaarts L, Garcia-Tardon N, van Beek L, et al. Chronic helminth infection and helminth-derived egg antigens promote adipose tissue M2 macrophages and improve insulin sensitivity in obese mice. FASEB journal : official publication of the Federation of American Societies for Experimental Biology 2015; 29(7): 3027-39.
54. Berbudi A, Surendar J, Ajendra J, et al. Filarial Infection or Antigen Administration Improves Glucose Tolerance in Diet-Induced Obese Mice. J Innate Immun 2016; 8(6).
55. Hams E, Bermingham R, Wurlod FA, et al. The helminth T2 RNase omega1 promotes metabolic homeostasis in an IL-33- and group 2 innate lymphoid cell-dependent mechanism. FASEB journal : official publication of the Federation of American Societies for Experimental Biology 2016; 30(2): 824-35.
56. Bhargava P, Li C, Stanya KJ, et al. Immunomodulatory glycan LNFPIII alleviates hepatosteatosis and insulin resistance through direct and indirect control of metabolic pathways. Nat Med 2012; 18(11): 1665-72.
57. Nazligul Y, Sabuncu T, Ozbilge H. Is there a predisposition to intestinal parasitosis in diabetic patients? Diabetes care 2001; 24(8): 1503-4.
58. Mendonca SC, Goncalves-Pires Mdo R, Rodrigues RM, Ferreira A, Jr., Costa-Cruz JM. Is there an association between positive Strongyloides stercoralis serology and diabetes mellitus? Acta tropica 2006; 99(1): 102-5.
59. Aravindhan V, Mohan V, Surendar J, et al. Decreased prevalence of lymphatic filariasis among diabetic subjects associated with a diminished pro-inflammatory cytokine response (CURES 83). PLoS neglected tropical diseases 2010; 4(6): e707.
60. Chen Y, Lu J, Huang Y, et al. Association of previous schistosome infection with diabetes and metabolic syndrome: a cross-sectional study in rural China. The Journal of clinical endocrinology and metabolism 2013; 98(2): E283-7.
61. Shen SW, Lu Y, Li F, et al. The potential long-term effect of previous schistosome infection reduces the risk of metabolic syndrome among Chinese men. Parasite immunology 2015; 37(7): 333-9.
62. Hays R, Esterman A, Giacomin P, Loukas A, McDermott R. Does Strongyloides stercoralis infection protect against type 2 diabetes in humans? Evidence from Australian Aboriginal adults. Diabetes research and clinical practice 2015; 107(3): 355-61.

2

HELMINTH INFECTIONS AND TYPE 2 DIABETES: A CLUSTER-RANDOMIZED PLACEBO CONTROLLED SUGARSPIN TRIAL IN NANGAPANDA, FLORES, INDONESIA

Dicky L. Tahapary*, Karin de Ruiter*, Ivonne Martin, Lisette van Lieshout, Bruno Guigas, Pradana Soewondo, Yenny Djuardi, Aprillianto E. Wiria, Oleg A. Mayboroda, Jeanine J. Houwing-Duistermaat, Hengki Tasman, Erliyani Sartono, Maria Yazdanbakhsh, Johannes W.A. Smit# and Taniawati Supali#

*,# Equal contribution

BMC Infectious Diseases (2015)

ABSTRACT

Background

Insulin resistance is a strong predictor of the development of type 2 diabetes mellitus. Chronic helminth infections might protect against insulin resistance via a caloric restriction state and indirectly via T-helper-2 polarization of the immune system. Therefore, the elimination of helminths might remove this beneficial effect on insulin resistance.

Methods/Design

To determine whether soil-transmitted helminth infections are associated with a better whole-body insulin sensitivity and whether this protection is reversible by anthelmintic treatment, a household-based cluster-randomized, double blind, placebo-controlled trial was conducted in the area of Nangapanda on Flores Island, Indonesia, an area endemic for soil-transmitted helminth infections. The trial incorporates three monthly treatment with albendazole or matching placebo for one year, whereby each treatment round consists of three consecutive days of supervised drug intake. The presence of soil-transmitted helminths will be evaluated in faeces using microscopy and/or PCR. The primary outcome of the study will be changes in insulin resistance as assessed by HOMA-IR, while the secondary outcomes will be changes in body mass index, waist circumference, fasting plasma glucose, 2h-glucose levels after oral glucose tolerance test, HbA1c, serum lipid levels, immunological parameters, and efficacy of anthelmintic treatment.

Discussion

The study will provide data on the effect of helminth infections on insulin resistance. It will assess the relationship between helminth infection status and immune responses as well as metabolic parameters, allowing the establishment of a link between inflammation and whole-body metabolic homeostasis. In addition, it will give information on anthelmintic treatment efficacy and effectiveness.

Trial registration

This study has been approved by the ethical committee of Faculty of Medicine Universitas Indonesia (ref: 549/H2.F1/ETIK/2013), and has been filed by the ethics committee of Leiden University Medical Center, clinical trial number: ISRCTN75636394. The study is reported in accordance with the CONSORT guidelines for cluster-randomised trials.

BACKGROUND

The number of people with diabetes mellitus is increasing worldwide (1-3). At present, 8.3% of adults (382 million people) have diabetes mellitus (4) and Asia is a major site of this rapidly emerging epidemic (5). In many Asian countries, including Indonesia, rapid socio-economic development has led to a shift in infrastructure, technology and introduction of Western style diets, which promotes overnutrition and sedentary lifestyles (5-8). These changes have already led to an increasing prevalence of diabetes mellitus in Indonesia (9-12).

A strong predictor for the development of type 2 diabetes mellitus (DM2) is insulin resistance (13,14), which is caused by complex disturbances in multiple biological systems. There is now abundant evidence that inflammation (15) plays a role in the development of DM2, in addition to the more established relationship between an altered energy balance resulting from excess consumption of high-energy foods and/or decreased physical activity. In DM2 subjects, chronic low-grade inflammation is a common feature (15) which results, at least in part, from the activation of inflammatory pathways by fatty acids in multiple organs (16-18). However, the fundamental molecular mechanisms are still incompletely understood (19).

In developing countries, infectious pressure might be one particular modifier of insulin resistance. Helminth infections, which are still endemic in many low to middle income countries, may therefore affect whole-body and tissue-specific insulin sensitivity owing to their immunomodulatory properties (20). Previous studies have shown that helminth infections can adopt an immune evasion strategy by inducing regulatory T cells (21-26). Hereby helminth infections may decrease systemic inflammation and subsequently the development of inflammatory diseases, including DM2 (27-30). Studies examining the relationship between helminth infections and DM2 in both humans (31,32) and murine modelss (33,34) support this hypothesis. At a molecular level, mTOR, a serine/threonine protein kinase located downstream of insulin signalling, plays an essential role in immune cell energy metabolism and function (35,36). Furthermore, it has been shown that STAT6 signalling downstream of IL-4, as well as Th2 responses induced by helminths, improve glucose metabolism and insulin signalling (33,37). Intriguingly, in humans, immune intervention with IL-1 receptor antagonist (Anakinra) has also been shown to influence glucose metabolism (38).

Helminths are also known to reduce energy intake and thereby change the energy balance (39), which may be beneficial in terms of insulin resistance (39,40). Helminths may therefore both directly improve insulin sensitivity via a caloric restriction state and indirectly via Th2 activation. It appears, the immune system which has evolved with helminths (41) and under conditions of low energy intake, seems to be out of balance in situations of nutritional overload and decreasing exposure to parasites (23,42). In line with the proposed beneficial effects of helminth infections on glucose metabolism, our previous unpublished cross sectional study in Flores Island, Indonesia, has shown that

subjects infected with intestinal helminths have a significantly lower insulin resistance as expressed by HOMA-IR.

Although aforementioned studies strongly suggest that there is an association between helminth infections, systemic inflammation and glucose metabolism, the causality in these relationships has not been demonstrated as yet. Therefore, we have initiated a large scale cluster randomized controlled trial (RCT) with the aim to assess the effect of anthelmintic treatment on insulin resistance, the hypothesis being that reduction of worm load to undetectable levels will lead to a higher degree of insulin resistance. While study outcomes will be analysed at the individual participant level, a household cluster randomization was chosen to minimise contamination between treatment groups and therefore reinfection of treated individuals.

STUDY DESIGN

Study area

The study area is located in Nangapanda, a sub-district of the Ende District of Flores Island, Indonesia (43,44). Nangapanda is a semi-urban coastal area with a population of approximately 22.000 people being divided over 29 villages. Our study area includes three of these villages (Ndeturea, Ndorurea 1, Ndorurea, with a total population of 3698 people, from which most of the adult population are farmers. Previous studies have shown that this area is endemic for soil-transmitted helminth (STH) infections (45). A detailed map of the study area has been published (43).

Trial design

The study is designed as a household-based cluster-randomized, double-blind trial with two arms. In one arm treatment is given with albendazole (single dose of 400 mg) on 3 consecutive days, while the other arm consists of matching placebo treatment (both albendazole and placebo are manufactured by PT Indofarma Pharmaceutical, Bandung, Indonesia). The treatment is provided every three months for a period of 1 year (total 4 rounds) to all household members except children below 2 years of age, while subjects aged 16 or above will undergo clinical and laboratory examination. Subjects with active treatment for diabetes mellitus, serious concomitant disease and pregnancy will be excluded.

The population was randomised by JWAS and JJH using computer aided block randomization at household level, utilizing Random Allocation Software to assign treatment groups. Both study investigators and patients are blinded for treatment codes. The treatment code will be unblinded when all data needed for analysis are cleaned and entered into the database. An additional randomization was performed in a subgroup of individuals, who will undergo an oral glucose tolerance test and immunological studies in order to study glucose metabolism and immune mechanisms in more detail. For this subgroup, we aimed to select one subject per household and stratified by age group

(16-36 years of age, 36-56 years of age, and >56 years of age) to ensure that sufficient numbers of all age groups are participating. Randomization was based on households.

Well trained community workers were recruited and trained to distribute the drugs. These workers were also trained to assist during clinical examination and sample collection and were involved in health promotion within the population. Community workers and research team members will directly supervise the study participants while taking the study medication, and will collect empty drug canisters at each visit to confirm compliance. Furthermore, assessment of side effects will take place during these visits and migration and death will be noted. Adverse events spontaneously reported by the patient or observed by the investigators, will be monitored throughout the study. After completion of the study, the whole study population will be treated with a single dose of albendazole (400 mg) for 3 consecutive days.

Outcomes

As this study aims to assess the effect of anthelmintic treatment on whole-body insulin sensitivity, our primary outcome is a change in insulin resistance as assessed by HOMA-IR between both treatment arms after one year of treatment. Secondary outcomes are changes in body mass index and waist circumference, fasting plasma glucose, 2h-glucose levels after oral glucose tolerance test, HbA1c, serum lipid levels, immunological parameters, and efficacy of anthelmintic treatment.

Sample size

Sample size is calculated according to intention to treat analysis in which we will need 1580 subjects in total. Based on our previous study (45) we assume that the average household size is 4 and that around 20% will be lost to follow up after one year. We use a significance level of 5% and a power of 80%. Correlations within households are taken into account by using the correction factor 1 + (m-1) ICC, with m being the household size and ICC the intra-class correlation. The sample size is computed for a difference in mean between the two treatment groups of 0.18 and an ICC of 0.1.

For the subgroup of individuals undergoing an oral glucose tolerance test, a sample size of 335 subjects in total is calculated assuming that around 20% will be lost to follow up after one year and using a significance level of 5% and a power of 80%. The sample size is computed for a difference in mean of 10.3 mg/dL and a standard deviation of glucose level of 30 mg/dL.

METHODS

Sample collection

At baseline all eligible subjects, aged 16 and above will be invited to visit the examination centre after an overnight fasting and to provide stool, blood and first morning urine

samples. During this visit, participant's education level and profession will be registered. After 1 year of treatment, follow-up sample collection will take place as shown in Table 1.

Clinical anthropometry assessment

Anthropometric measurements of body weight, height, waist and hip circumference are obtained using the National Heart, Lung, and Blood Institute (NHLBI) practical guidelines. To measure body weight a flat scale for mobile use (SECA Model 876, Seca Gmbh Co, Hamburg, Germany) is used, while a portable stadiometer (SECA Model 213, Seca Gmbh Co, Hamburg, Germany) is used to measure height. Waist and hip circumference are measured using ergonomic circumference measuring tape (SECA Model 201, Seca Gmbh Co, Hamburg, Germany). In addition, body fat composition is measured using a Tanita body composition analyser (TBF-300A, Tanita Corp, Tokyo, Japan). Three blood pressure measurements (left arm, sitting upright position, after resting 5 minutes) are taken from each subject, using a digital sphygmomanometer (HEM-7200, Omron Healthcare Co, Ltd, Kyoto, Japan), and calibrated using a Riester nova-presameterH-Desk model mercury sphygmomanometer (Gerhard Glufke Rudolf Riester GmbH & Co, Jungingen, Germany) and a 3MTM LittmannH Classic II S.E. Stethoscope (3M, St. Paul, Minnesota, USA). The average of three systolic/diastolic blood pressure measurements will be used for analysis.

Parasitological examination

To assess intestinal helminth infection, stool containers are distributed and collected by health workers. Stool samples are examined by the Kato Katz method (46) for identification and quantification of STH eggs using 2 slides for each sample. An aliquot of the fresh stool samples is frozen at -20°C in the field and subsequently at -80°C in laboratories of the Departments of Parasitology at Leiden University Medical Center, Leiden, The Netherlands and Faculty of Medicine Universitas Indonesia, Jakarta, Indonesia for DNA extraction (43). Part of the stool sample will be saved for potential future analysis of the microbiome.

Table 1. Study schedule of the Sugarspin project

		3 monthly treatment				
Outcome	Baseline	1st	2nd	3rd	4th	1 year follow up
Clinical Anthropometry	X					X
Parasitological examination	X					X
Metabolic parameters	X					X
Immunological parameters	X					X
Assessment of side effects		X	X	X	X	X

DNA isolation and helminth real-time PCR

DNA isolation from stool will be performed as described elsewhere (43), with some minor modifications. Real-time PCR will be performed to detect the presence of *A. duodenale*, *N. americanus* (hookworm), *A. lumbricoides* and *T. trichiura* using a method described previously (43) with some modifications.

Blood collection

Peripheral blood is collected into EDTA and SST Vacutainers (BD, Franklin Lakes, NJ, USA). Giemsa-stained peripheral blood smear is prepared to evaluate neutrophil and eosinophil count. In a subset of the study population, additional blood is collected in PAXgene Blood RNA Tubes (PreAnalytiX GmbH, Hombrechtikon, Switzerland) and Sodium Heparin Vacutainers (BD). Blood collected in PAXgene Blood RNA Tubes will be used to study RNA expression profiles, while blood collected in Sodium Heparin Vacutainers will be used for detailed immunological measurements as described below (section Immunological methods). All samples deriving from EDTA and SST Vacutainers (serum, plasma, cell pellet and whole blood) and all PAXgene Blood RNA Tubes are kept at -20°C at the Field Clinical Research Centre (FCRC) and will be sent on dry ice to the University's laboratory for storage at -80°C.

Metabolic parameters

Fasting blood glucose is measured in capillary blood using Breeze®2 glucose meters (Bayer Health Care LLC, Basel, Switzerland). An oral glucose tolerance test is performed in a subset of the study population according to the WHO protocol (47,48). Glucose levels are measured in capillary blood using Breeze®2 glucose meters after overnight fasting and 2 hours after ingesting 75g of anhydrous glucose dissolved in 200 cc of water. Insulin, HbA1c and lipid profiles will be measured in an internationally accredited laboratory. HOMA-IR, a well-validated measure of insulin resistance will be calculated to estimate insulin resistance (49).

Immunological methods

The immunological parameters that will be studied are 1) Total IgE levels as one of the markers of a Th2 response and its relation to metabolic parameters, 2) Circulating pro- and anti-inflammatory cytokines in order to study their relationship to metabolic parameters, 3) Antigen specific IgE and IgG to *Ascaris lumbricoides* to monitor antibody responses to one of the helminths studied as a marker of changing immune responses as a result of anthelmintic treatment, 4) Granulocyte (neutrophil and eosinophil) frequencies and their activation to assess whether granulocytes, in particular eosinophils which are associated with a Th2 response, are linked to helminth infections and metabolic parameters, 5) Peripheral blood mononuclear cells (PBMC) subset analysis and polarisation by flow cytometry in order to assess the relationship between immune cell frequencies (T cell

subsets, B cell subsets, monocyte subsets, NK cells and myeloid suppressor cells) in situ as well as after activation and metabolic parameters.

Total IgE

Total IgE will be measured using ELISA with rabbit anti-human IgE antibodies (Dako, Glostrup, Denmark) and goat anti-human IgE biotinylated antibodies (Vector Laboratories, Burlingame, CA, USA) as capture and detection antibodies, as described previously (43). The World Health Organization standard of human serum IgE was used as a reference (National Institute for Biological Standards and Control). The results will be expressed in International Units (IU).

Circulating cytokines

Pro- and anti-inflammatory cytokines (TNFα, IFNγ, IL-1, IL-6, IL-10, TGFβ) will be measured in serum samples using cytokines kit with high sensitivity.

Ascaris-specific IgE

Ascaris antigen will be prepared from *Ascaris lumbricoides* worms as described previously (50). Maxisorp plates (Thermo Fisher Scientific, Roskilde, Denmark) will be coated overnight with 5 µg/ml *Ascaris* antigen in 0.1 M carbonate buffer (pH 9.6). Plates will be blocked for 1 hour with PBS containing 2% bovine serum albumin. Samples will be diluted 1/60 in 0.1 M Tris-HCl containing 0.05% Tween-20 and incubated overnight together with a pool of positive standard plasma containing 1 x 10^6 arbitrary units (AU) parasite specific IgE. After a washing step, goat anti-human IgE biotinylated antibodies (Vector) will be incubated followed by streptavidin-HRP (Sanquin, Amsterdam, the Netherlands). The color is developed by adding 3,3',5,5' tetramethylbenzidine (TMB) (KPL, Gaithersburg, MD, USA). The reaction will be stopped by adding 1.8 M H_2SO_4 and absorbance will be read at 450 nm in an automated plate reader.

Ascaris-specific IgG isotypes

Maxisorp plates will be coated with *Ascaris* antigen as described for *Ascaris* specific IgE above. Blocking will be done using PBS containing 5% bovine serum albumin. Samples will be diluted 1/1000, 1/10, 1/5 or 1/25 for IgG1, IgG2, IgG3 and IgG4 respectively, and a pool of positive standard plasma containing 1 x 10^6 arbitrary units (AU) parasite specific IgG isotypes will be included in each plate. After overnight incubation, HRP-labelled anti human IgG isotypes (Sanquin) in PBS 0.05% Tween-20 will be added for 4 hours incubation at 37^0C using the following dilutions: 1/3000 for anti IgG1 (HP6188) and anti IgG4 (HP6196); 1/1000 for anti IgG2 (HP6014) and anti IgG3 (HP6095). TMB substrate will be used to develop the color and the reaction will be stopped as described above.

Whole blood stimulation and fixed granulocyte cryopreservation

To study the expression of activation markers on granulocytes, 600 µl of heparinised venous blood is divided over 3 polystyrene tubes (200 µl/tube). After a pre-incubation of 5 minutes in a 37°C waterbath, a 5 minutes stimulation at 37°C is performed with N-Formyl-Met-Leu-Phe (FMLP, 10^{-5} M; Sigma, Saint Louis, MO, USA) or eotaxin (10^{-7} M; R&D systems, Abingdon, UK). Subsequently, 4 ml of FACS lysing solution (BD) is added and after an incubation period of 15 minutes at room temperature the red blood cells are lysed while white blood cells, including granulocytes, become fixed. Cells are washed with RPMI 1640 containing 10% heat-inactivated FCS and then resuspended in RPMI 1640 containing 10% of heat-inactivated foetal calf serum (FCS) and 10% dimethyl sulfoxyde (DMSO). Cryovials containing the cell suspension are placed at -80°C for minimum of 4 hours, followed by storage in liquid nitrogen until further analysis.

PBMC cryopreservation

Peripheral blood mononuclear cells (PBMCs) are isolated from heparinised venous blood using Ficoll density gradient centrifugation within 12 hours after blood collection. After isolation, cells are cryopreserved in RPMI 1640 containing 20% of FCS and 10% DMSO. Cryovials containing the cell suspension are transferred to a freezing unit which is placed in a -80°C freezer for minimum of 4 hours. Subsequently, vials are stored in liquid nitrogen until analysis.

Metabolomics for metabolic profiling

Urine samples and blood samples from heparinized blood are kept at -20^0C at the FCRC and subsequently stored at -80^0C at the University's laboratory for possible future metabolomics measurements. The exploratory metabolomics analysis will be performed by 1H-NMR and LC-MS metabolomics, a combination of NMR and LC-MS proposed for this study provides a comprehensive coverage of metabolome and as such increases the probability of finding physiologically meaningful associations within the data.

Data management and statistical analyses

A centrally accessible database designed in Microsoft Access is established and the data is entered by well-trained data entry personnel. Descriptive data will be summarized for continuous variables as mean +/- SD for normally distributed data and median (range) for non-normally distributed data. Categorical data will be expressed as proportions.

The effect of anthelmintic treatment on insulin resistance (HOMA-IR) as our primary outcome will be assessed using an intention to treat approach after 1 year of treatment using mixed models to account for the correlation within households, in which relevant confounders (including age, gender, BMI, village) are entered. The characterization of immune responses to helminth infections and systemic inflammation will be assessed by measuring cytokine profiles. Moreover, for these analyses multilevel modelling will be

used and the use of longitudinal data will take repeated measurement into account (51). The mediation of helminth's effects on insulin resistance via immune responses will also be assessed.

Ethical approval, trial registration and consent

This study has been approved by The Health Research Ethical Committee, Faculty of Medicine, Universitas Indonesia Cipto Mangunkusumo Hospital, Jakarta, Indonesia (reference number:549/H2.F1/ETIK/2013). It has also been filed by the ethics committee of Leiden University Medical Center and is registered as a clinical trial ref: ISRCTN75636394 (http://www.controlled-trials.com/isrctn/pf/75636394). The local health authorities have been informed about this study and have given their approval and support. The study, its benefits and risks are explained to the population and consent forms are distributed to be signed by the subjects who are willing to participate in this study. They are informed that they can withdraw from the study at any time, for any reasons and without any consequences.

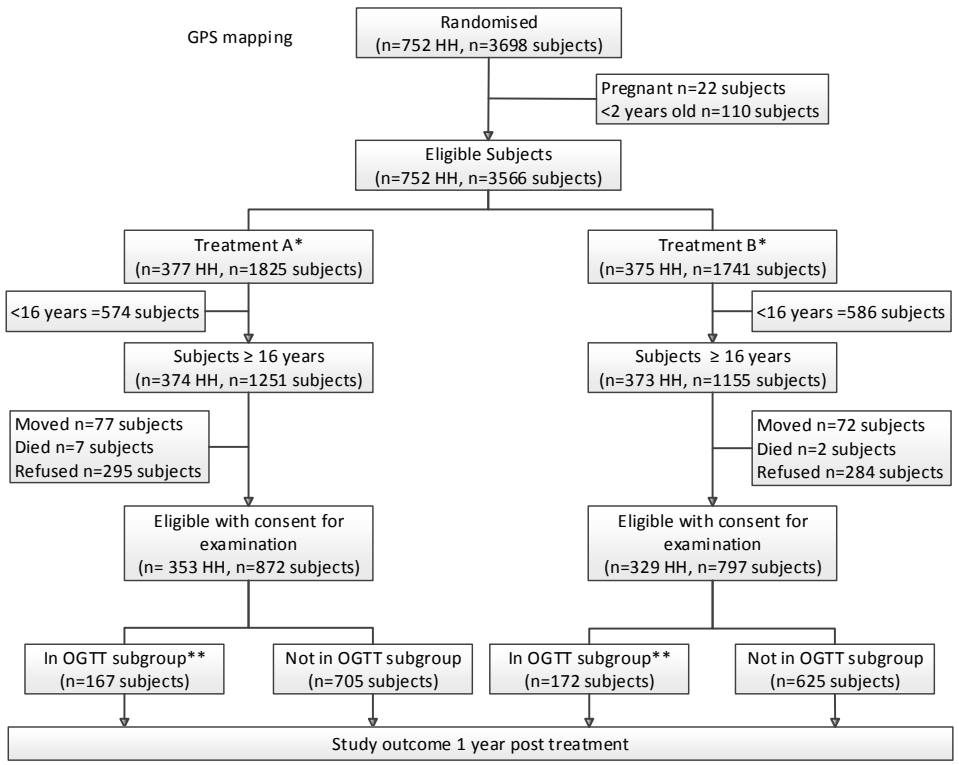

*Households were assigned to three monthly treatment with albendazole or placebo for 1 year
**For the oral glucose tolerance test (OGTT) and immunological studies, a random selection was made and 339 individuals were invited to participate.

Figure 1. Flow diagram of the Sugarspin project.

Description of the population recruited

So far, the study has provided the following data (Figure 1). At baseline, a total of 3698 individuals were registered in 752 households. Of the 2428 subjects aged 16 years or older, 1669 subjects were eligible with consent for examination. For the oral glucose tolerance test and immunological studies 339 subjects were randomly selected and gave approval.

Figure 2 shows the age pyramid of both the total population in the study area and the study population. In the study population farming and fishing are the traditional source of income, while some individuals engage in jobs at government offices or in the private sector (Figure 3). A similar distribution is seen in the total population. The education level of the majority of subjects in the study population is elementary school (33%), followed by senior high school (22%), and junior high school (16%), while 11% has college or university degrees. Moreover, 18% of the subjects is illiterate, either not educated at all or dropped out from elementary school (Figure 4). A similar distribution of education levels is seen in the total population.

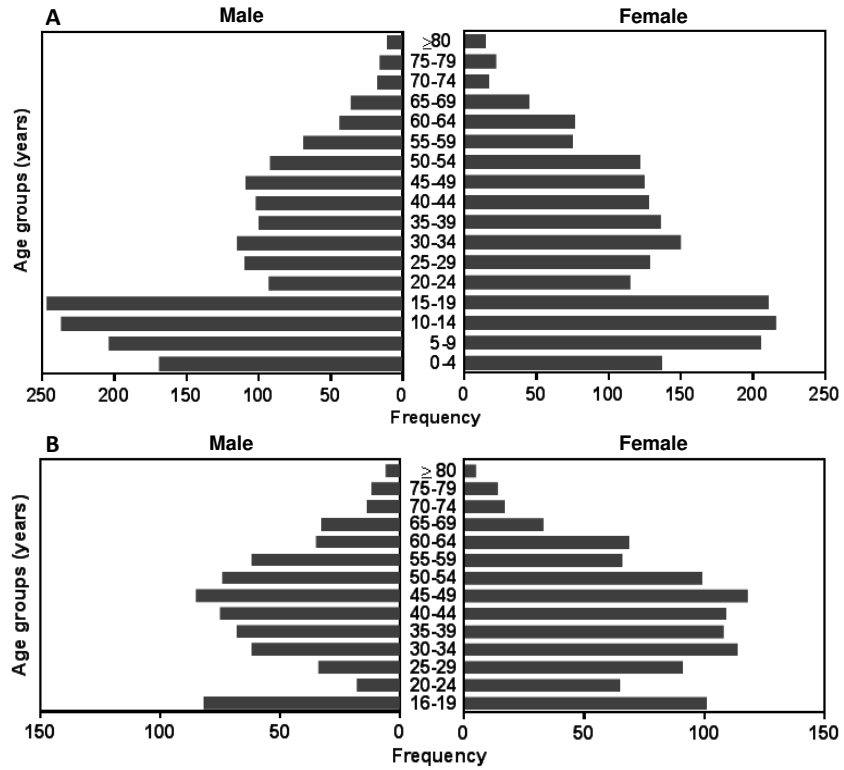

Figure 2. Age pyramid. Age pyramid of all individuals living in the study area in Nangapanda, Flores island, Indonesia (n=3698 subjects, 52% female) (*A*), and of study participants (n=1669 subjects, 60% female) (*B*).

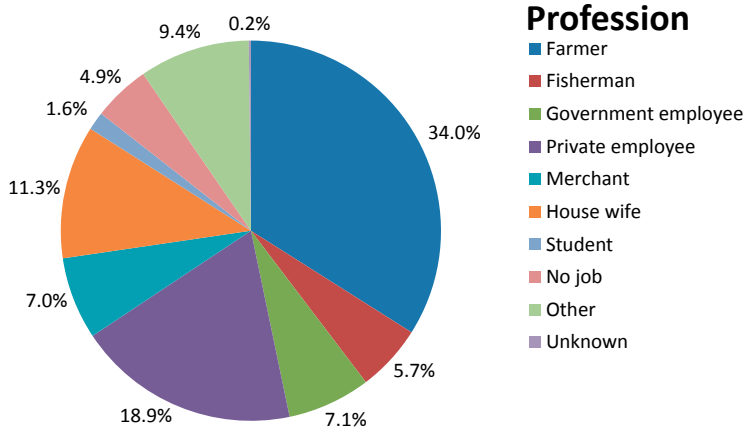

Figure 3. Job distribution. At baseline, profession was assessed for study participants (n=1669 subjects).

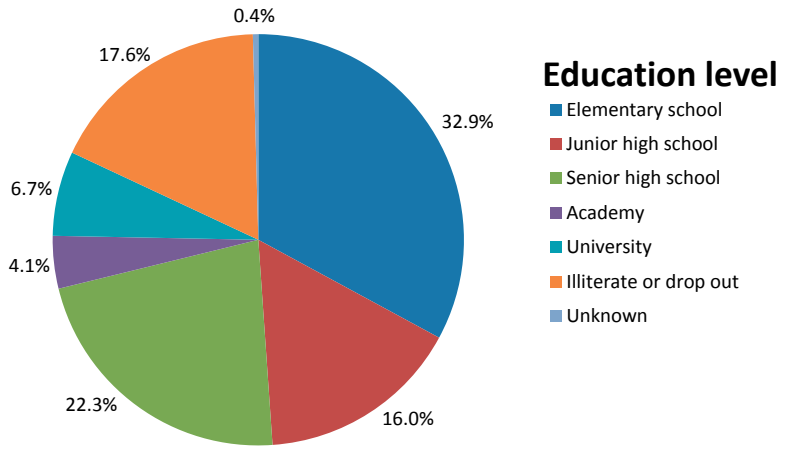

Figure 4. Education level. At baseline, education level was assessed for study participants (n=1669 subjects).

DISCUSSION

The SUGARSPIN trial is the first and currently the only longitudinal study investigating the effects of anthelmintic treatment on whole-body insulin sensitivity. This placebo-controlled trial enables us for the first time to investigate the causal relationship between helminth infections, systemic inflammation and glucose metabolism in humans. In addition, this study will provide data on anthelmintic treatment efficacy and effectiveness in a large population in a developing country like Indonesia.

ACKNOWLEDGEMENTS

This study is funded by The Royal Netherlands Academy of Arts and Science (KNAW), Ref 57-SPIN3-JRP and Universitas Indonesia (Research Grant BOPTN 2742/H2.R12/HKP.05.00/2013.). The authors thank The Indonesian Directorate General of Higher Education (DIKTI) for providing scholarship to two PhD candidates involved in this project; Bernadus Idu as the head of sub district Nangapanda for his support; Yusuf Gedu, Husni Abdullah, Suparti as the head of village Ndeturea, Ndorurea 1 and Ndorurea respectively; Dr. Helda Sihotang and Dr Agus Tobing; all health workers in Nangapanda's Community Health Centre; Octavia as the responsible person for data entry; all local field workers; the UI team (Sudirman, Suwarto, Yosi Destani, Eka S Mulyawan, Clara C. Djimandjaja, Femmy Pical, Rospita Maylasari, Difa Stefanie, Sovia N. Linda, Budi Prasetyo) and Yvonne Kruize. Most of all, thanks to all inhabitants of Nangapanda.

REFERENCES

1. Guariguata L, Whiting DR, Hambleton I, Beagley J, Linnenkamp U, Shaw JE: Global estimates of diabetes prevalence for 2013 and projections for 2035. *Diabetes Res Clin Pract* 2014, 103: 137-149.
2. Guariguata L: By the numbers: new estimates from the IDF Diabetes Atlas Update for 2012. *Diabetes Res Clin Pract* 2012, 98: 524-525.
3. Shaw JE, Sicree RA, Zimmet PZ: Global estimates of the prevalence of diabetes for 2010 and 2030. *Diabetes Res Clin Pract* 2010, 87: 4-14.
4. International Diabetes Federation. *IDF Diabetes Atlas.* 6th ed. Brussels, Belgium: International Diabetes Federation; 2013.
5. Chan JC, Malik V, Jia W, Kadowaki T, Yajnik CS, Yoon KH *et al.*: Diabetes in Asia: epidemiology, risk factors, and pathophysiology. *JAMA* 2009, 301: 2129-2140.
6. Chan JC: Diabetes in Asia: from understanding to action. *Ann Acad Med Singapore* 2008, 37: 903-905.
7. Ramachandran A, Snehalatha C, Shetty AS, Nanditha A: Trends in prevalence of diabetes in Asian countries. *World J Diabetes* 2012, 3: 110-117.
8. Soewondo P, Ferrario A, Tahapary DL: Challenges in diabetes management in Indonesia: a literature review. *Global Health* 2013, 9: 63.
9. Badan Penelitian dan Pengembangan Kesehatan KKRI. Riset Kesehatan Dasar (Riskesdas) 2013. 2013. http://www.litbang.depkes.go.id/sites/download/rkd2013/Laporan_Riskesdas2013.PDF. Accessed 28 January 2015
10. Mihardja L, Soetrisno U, Soegondo S: Prevalence and clinical profile of diabetes mellitus in productive aged urban Indonesians. *J Diabetes Investig* 2014, 5: 507-512.
11. Mihardja L, Delima, Manz HS, Ghani L, Soegondo S: Prevalence and determinants of diabetes mellitus and impaired glucose tolerance in Indonesia (a part of basic health research/Riskesdas). *Acta Med Indones* 2009, 41: 169-174.
12. Pramono LA, Setiati S, Soewondo P, Subekti I, Adisasmita A, Kodim N *et al.*: Prevalence and predictors of undiagnosed diabetes mellitus in Indonesia. *Acta Med Indones* 2010, 42: 216-223.
13. Kim CH, Kim HK, Kim EH, Bae SJ, Park JY: Relative contributions of insulin resistance and beta-cell dysfunction to the development of Type 2 diabetes in Koreans. *Diabet Med* 2013, 30: 1075-1079.
14. Reddy KJ, Singh M, Bangit JR, Batsell RR: The role of insulin resistance in the pathogenesis of atherosclerotic cardiovascular disease: an updated review. *J Cardiovasc Med (Hagerstown)* 2010, 11: 633-647.
15. Calle MC, Fernandez ML: Inflammation and type 2 diabetes. *Diabetes Metab* 2012, 38: 183-191.
16. Cruz NG, Sousa LP, Sousa MO, Pietrani NT, Fernandes AP, Gomes KB: The linkage between inflammation and Type 2 diabetes mellitus. *Diabetes Res Clin Pract* 2013, 99: 85-92.
17. Donath MY, Shoelson SE: Type 2 diabetes as an inflammatory disease. *Nat Rev Immunol* 2011, 11: 98-107.
18. Garcia C, Feve B, Ferre P, Halimi S, Baizri H, Bordier L *et al.*: Diabetes and inflammation: fundamental aspects and clinical implications. *Diabetes Metab* 2010, 36: 327-338.
19. Aroor AR, McKarns S, Demarco VG, Jia G, Sowers JR: Maladaptive immune and inflammatory pathways lead to cardiovascular insulin resistance. *Metabolism* 2013, 62: 1543-1552.
20. Wiria AE, Djuardi Y, Supali T, Sartono E, Yazdanbakhsh M: Helminth infection in populations undergoing epidemiological transition: a friend or foe? *Semin Immunopathol* 2012, 34: 889-901.
21. MacDonald AS, Maizels RM: Alarming dendritic cells for Th2 induction. *J Exp Med* 2008, 205: 13-17.
22. Harn DA, McDonald J, Atochina O, Da'dara AA: Modulation of host immune responses by helminth glycans. *Immunol Rev* 2009, 230: 247-257.
23. van RE, Hartgers FC, Yazdanbakhsh M: Chronic helminth infections induce immunomodulation: consequences and mechanisms. *Immunobiology* 2007, 212: 475-490.
24. Everts B, Smits HH, Hokke CH, Yazdanbakhsh M: Helminths and dendritic cells: sensing and regulating via pattern recognition receptors, Th2 and Treg responses. *Eur J Immunol* 2010, 40: 1525-1537.
25. Schramm G, Haas H: Th2 immune response against Schistosoma mansoni infection. *Microbes Infect* 2010, 12: 881-888.
26. Wammes LJ, Hamid F, Wiria AE, de GB, Sartono E, Maizels RM *et al.*: Regulatory T cells in human geohelminth infection suppress immune responses to BCG and Plasmodium falciparum. *Eur J Immunol* 2010, 40: 437-442.
27. Wammes LJ, Mpairwe H, Elliott AM, Yazdanbakhsh M: Helminth therapy or elimination: epidemiological, immunological, and clinical considerations. *Lancet Infect Dis* 2014.
28. Wiria AE, Sartono E, Supali T, Yazdanbakhsh M: Helminth infections, type-2 immune response, and metabolic syndrome. *PLoS Pathog* 2014, 10: e1004140.
29. van den Biggelaar AH, van RR, Rodrigues LC, Lell B, Deelder AM, Kremsner PG *et al.*: Decreased atopy in children infected with Schistosoma haematobium: a role for parasite-induced interleukin-10. *Lancet* 2000, 356: 1723-1727.
30. Smits HH, Hammad H, van NM, Soullie T, Willart MA, Lievers E *et al.*: Protective effect of Schistosoma mansoni infection on allergic airway inflammation depends on the intensity and chronicity of infection. *J Allergy Clin Immunol* 2007, 120: 932-940.
31. Aravindhan V, Mohan V, Surendar J, Muralidhara RM, Pavankumar N, Deepa M *et al.*: Decreased prevalence of lymphatic filariasis among diabetic subjects associated with a diminished pro-inflammatory cytokine response (CURES 83). *PLoS Negl Trop Dis* 2010, 4: e707.
32. Chen Y, Lu J, Huang Y, Wang T, Xu Y, Xu M *et al.*: Association of previous schistosome infection with diabetes and metabolic syndrome: a cross-sectional study in rural China. *J Clin Endocrinol Metab* 2013, 98: E283-E287.
33. Wu D, Molofsky AB, Liang HE, Ricardo-Gonzalez RR, Jouihan HA, Bando JK *et al.*: Eosinophils sustain adipose alternatively activated macrophages associated with glucose homeostasis. *Science* 2011, 332: 243-247.
34. Yang Z, Grinchuk V, Smith A, Qin B, Bohl JA, Sun R *et al.*: Parasitic nematode-induced modulation of body weight and associated metabolic dysfunction in mouse models of obesity. *Infect Immun* 2013, 81: 1905-1914.
35. Fox CJ, Hammerman PS, Thompson CB: Fuel feeds function: energy metabolism and the T-cell response. *Nat Rev Immunol* 2005, 5: 844-852.
36. Pearce EL, Walsh MC, Cejas PJ, Harms GM, Shen H, Wang LS *et al.*: Enhancing CD8 T-cell memory by modulating fatty acid metabolism. *Nature* 2009, 460: 103-107.
37. Ricardo-Gonzalez RR, Red EA, Odegaard JI, Jouihan H, Morel CR, Heredia JE *et al.*: IL-4/STAT6 immune axis regulates peripheral nutrient metabolism and insulin sensitivity. *Proc Natl Acad Sci U S A* 2010, 107: 22617-22622.
38. van Asseldonk EJ, Stienstra R, Koenen TB, Joosten LA, Netea MG, Tack CJ: Treatment with Anakinra improves disposition index but not insulin sensitivity in nondiabetic subjects with the metabolic syndrome: a randomized, double-blind, placebo-controlled study. *J Clin Endocrinol Metab* 2011, 96: 2119-2126.
39. Papier K, Williams GM, Luceres-Catubig R, Ahmed F, Olveda RM, McManus DP *et al.*: Childhood malnutrition and parasitic helminth interactions. *Clin Infect Dis* 2014, 59: 234-243.
40. Alderman H, Konde-Lule J, Sebuliba I, Bundy D, Hall A: Effect on weight gain of routinely giving albendazole to preschool children during child health days in Uganda: cluster randomised controlled trial. *BMJ* 2006, 333: 122.
41. Jackson JA, Friberg IM, Little S, Bradley JE: Review series on helminths, immune modulation and the hygiene hypothesis: immunity against helminths and immunological phenomena in modern human populations: coevolutionary legacies? *Immunology* 2009, 126: 18-27.
42. Maizels RM, Yazdanbakhsh M: Immune regulation by helminth parasites: cellular and molecular mechanisms. *Nat Rev Immunol* 2003, 3: 733-744.
43. Wiria AE, Prasetyani MA, Hamid F, Wammes LJ, Lell B, Ariawan I *et al.*: Does treatment of intestinal helminth infections influence malaria? Background and methodology of a longitudinal study of

clinical, parasitological and immunological parameters in Nangapanda, Flores, Indonesia (ImmunoSPIN Study). *BMC Infect Dis* 2010, 10: 77.

44. Hamid F, Wiria AE, Wammes LJ, Kaisar MM, Lell B, Ariawan I *et al.*: A longitudinal study of allergy and intestinal helminth infections in semi urban and rural areas of Flores, Indonesia (ImmunoSPIN Study). *BMC Infect Dis* 2011, 11: 83.
45. Wiria AE, Hamid F, Wammes LJ, Kaisar MM, May L, Prasetyani MA *et al.*: The effect of three-monthly albendazole treatment on malarial parasitemia and allergy: a household-based cluster-randomized, double-blind, placebo-controlled trial. *PLoS One* 2013, 8: e57899.
46. World Health Organization. *Bench aids for the diagnosis of intestinal parasites*. Geneva: World Health Organization; 1994.
47. World Health Organization. *Definition and diagnosis of diabetes mellitus and intermediate hyperglycemia : report of a WHO/IDF consultation.* Geneva : WHO Document Production Services; 2006.
48. World Health Organization. Diabetes mellitus : report of a WHO Study Group. *World Health Organ Tech Rep Ser* 1985, 727: 1-113.
49. Wallace TM, Levy JC, Matthews DR: Use and abuse of HOMA modeling. *Diabetes Care* 2004, 27: 1487-1495.
50. van RE, Wuhrer M, Wahyuni S, Retra K, Deelder AM, Tielens AG *et al.*: Antibody responses to Ascaris-derived proteins and glycolipids: the role of phosphorylcholine. *Parasite Immunol* 2006, 28: 363-371.
51. Uh HW, Hartgers FC, Yazdanbakhsh M, Houwing-Duistermaat JJ: Evaluation of regression methods when immunological measurements are constrained by detection limits. *BMC Immunol* 2008, 9: 59.

3

EFFECT OF ANTHELMINTIC TREATMENT ON INSULIN RESISTANCE: A CLUSTER-RANDOMIZED, PLACEBO-CONTROLLED TRIAL IN INDONESIA

Dicky L. Tahapary*, Karin de Ruiter*, Ivonne Martin, Eric A.T. Brienen, Lisette van Lieshout, Christa M. Cobbaert, Pradana Soewondo, Yenny Djuardi, Aprillianto E. Wiria, Jeanine J. Houwing-Duistermaat, Erliyani Sartono, Johannes W.A. Smit#, Maria Yazdanbakhsh# and Taniawati Supali#

*,# Equal contribution

Clinical Infectious Diseases (2017)

ABSTRACT

Background

Emerging evidence suggests that helminth infections are associated with lower insulin resistance (IR). Current deworming programs might remove this helminth-associated protective effect. Therefore, we evaluated the anthelmintic treatment effect on changes in IR.

Methods

We conducted a double-blind, household-cluster-randomized, placebo-controlled clinical trial on Flores island, Indonesia, an area endemic for soil-transmitted helminths (STHs). All subjects received four rounds of albendazole or matching placebo with 3-month intervals, for 3 consecutive days. The primary outcome was the change in homeostatic model assessment of IR (HOMA-IR) in those aged >16 years. An intention-to-treat analysis was performed involving all subjects and ad hoc in the helminth-infected subjects.

Results

We examined 797 (in 329 households) and 872 (in 353 households) subjects, who were assigned randomly into the albendazole and placebo arm, respectively. Albendazole was associated with a significant reduction in STH prevalence, total Immunoglobulin E (IgE) and eosinophil count. Whereas albendazole had no effect on IR (estimated treatment effect, 0.006 (95% confidence interval, -.010 – .021), *P* = .48) at the community level, it was associated with a significant increase in IR (estimated treatment effect, 0.031 (95% confidence interval, .004 – .059), *P* = .04) (*P* value for interaction = .01) among helminth-infected subjects as detected by microscopy. Pathway analysis suggested that this might in part be due to an increased body mass index or a reduced eosinophil count.

Conclusions

Anthelmintic treatment reduces STH prevalence, total IgE and eosinophil count but has no effect on IR at the community level. In helminth-infected subjects, treatment significantly increases IR, highlighting the need for metabolic health monitoring with ongoing deworming programs.

Clinical Trial Registration

ISRCTN 75636394.

INTRODUCTION

The increasing prevalence of type 2 diabetes mellitus (DM2) is a major health concern worldwide, in particular in low- and middle-income countries (1). Rapid socioeconomic development in these countries has led to a shift in dietary habits and infrastructure that promotes overnutrition and decreased physical activity (2), ultimately increasing the risk for DM2. DM2 is characterized by increased insulin resistance (IR). Although the pathophysiology of DM2 is complex and involves several defects (3), there is evidence that in addition to an altered energy balance, chronic low-grade systemic inflammation plays a key role, linking the immune system and the impairment in metabolic homeostasis (4).

Helminth infections, which are still endemic in many low- and middle-income countries (5), are associated with skewed immune responses toward type 2 and regulatory immune responses (6). This may lead to a decreased systemic inflammation and consequently increased whole-body and tissue-specific insulin sensitivity (7). In addition, helminths are associated with a lower body mass index (BMI) (8), which may be beneficial in terms of IR. Helminths may therefore improve insulin sensitivity via immunological and non-immunological pathways (6, 9, 10).

Interleukin 4 (11) and interleukin 10 (12), key cytokines in helminth infections, have been shown to regulate peripheral nutrient metabolism and insulin sensitivity (11). Recent studies in animal models of diet-induced obesity (13-17) have also shown that helminth infections (13, 15-17) and helminth-derived molecules (14, 16-18) can increase insulin sensitivity through direct and indirect control of metabolic pathways (18). Furthermore, several population-based studies have reported a lower DM2 risk in subjects with previous (19, 20) or current (21, 22) chronic helminth infections. In a previous study on Flores island in Indonesia, we reported that chronic soil-transmitted helminth (STH) infections were associated with lower whole-body IR, independent of BMI (8).

However, all human studies performed so far have been cross-sectional, preventing any insight on a causal relation between helminth infections and IR. Therefore, we performed a cluster-randomized controlled trial of anthelmintic treatment in an area endemic for STHs, studying the hypothesis that a reduction of helminth infections will lead to a higher degree of IR.

METHODS

Study Overview

We conducted a household-based, cluster-randomized, double-blind trial in 3 villages in Nangapanda, Ende, Flores island, Indonesia. The trial was approved by the ethics committee of Faculty of Medicine, Universitas Indonesia (FKUI), filed by the ethics committee of Leiden University Medical Center (LUMC), and registered as a clinical trial (http://www.isrctn.com/ISRCTN75636394). The protocol was published previously (23).

Participants

All subjects in the study area, except children <2 years of age and pregnant women, were included in the trial to avoid cross-contamination between household members. Subjects aged ≥16 years underwent clinical and laboratory examination, excluding subjects with active treatment for diabetes mellitus and serious concomitant diseases.

Study Design and Treatments

After obtaining written informed consent, the population was randomized by household blocks using random allocation software for assignment to treatment. Both study investigators and participants were blinded for the treatment code. After randomization, all study subjects received a tablet of albendazole (400 mg) or matching placebo (both manufactured by PT Indofarma Pharmaceutical, Bandung, Indonesia) for 3 consecutive days with direct supervision. This treatment regimen was given 4 times with 3-month intervals (weeks 9-10, 21-22, 33-34, and 45-46). Clinical measurements, as well as blood and stool sample collection, were performed during the first 8 weeks before the start of the drug administration (baseline or t=0) and 6 weeks after the last drug administration (follow-up or t=52 weeks) (Supplementary Figure 1). After completion of the study, the whole study population was treated with a tablet of albendazole (400 mg) for 3 consecutive days.

Study Procedures and Outcomes

All clinical measurements and blood sample collections were performed after an overnight fast. Detailed information on study procedures are available in the Supplementary Appendix. In brief, body weight, height, waist circumference, and hip circumference were measured, from which BMI and waist-to-hip-ratio were calculated. Fasting blood glucose was determined in capillary blood. All sera, plasma, whole blood, and stool samples were frozen at −20°C and subsequently stored at −80°C. Insulin, hemoglobin A1c (HbA1c), total cholesterol, high-density lipoprotein cholesterol (HDL-C), triglycerides and high-sensitivity C-reactive protein (hs-CRP) were measured pairwise (baseline and follow-up) in the same analytical runs at the LUMC. A Giemsa-stained peripheral thin blood smear was read at FKUI to assess the differential white blood cell count, resulting in a relative percentage of basophils, eosinophils, neutrophils, lymphocytes and monocytes. Total immunoglobulin E (IgE) was measured at LUMC as described previously (24).

Fresh stool samples were examined by microscopy using the Kato-Katz method to detect STHs (hookworm, *Ascaris lumbricoides,* and *Trichuris trichiura*). Multiplex real-time polymerase chain reaction (PCR) was performed to simultaneously detect the presence of hookworm (*Ancylostoma duodenale, Necator americanus*), *A. lumbricoides, T. trichiura,* and *Strongyloides stercoralis*. Stool samples were considered positive by PCR when cycle threshold (Ct) values were <50, and further grouped into 3 categories: Ct <30, 30 to <35, and ≥35 representing a high, moderate and low DNA load, respectively (25).

Primary outcome was IR, assessed using the homeostatic model assessment of IR (HOMA-IR), a well-validated measure of whole body IR in humans (HOMA-IR = fasting serum insulin x fasting glucose / 22.5) (26). Secondary outcomes included BMI, waist circumference, fasting blood glucose, HbA1c, lipid levels, total IgE, eosinophil count, hs-CRP and prevalence of STHs as assessed by microscopy and stool PCR. Adverse events reported by subjects or observed by the investigators were monitored during the trial.

Statistical Analysis

The sample size was calculated according to intention-to-treat analysis. Based on our previous study (27), we assumed that the average household size is 4 and that around 20% of participants would be lost to follow-up after one year. We used a significance level of 5% and a power of 80%. Correlations within households were taken into account by using the correction factor $1+(m-1)$ ICC, with m being the household size and ICC the intra-class correlation. The sample size was calculated to aim at a difference in mean HOMA-IR between the 2 treatment groups of 0.18 and an ICC of 0.1, indicating 1580 subjects in total.

For continuous variables, normally distributed data were summarized as mean and standard deviation (SD), whereas non-normally distributed data (HOMA-IR, insulin, hs-CRP, total IgE and eosinophil count) were summarized as geometric mean and 95% confidence interval (CI), and log-transformed for analyses. HOMA-IR and hsCRP were log transformed as $\log_{10}(1+(\text{value}))$. Categorical data were expressed as proportions.

The effect of anthelmintic treatment on HOMA-IR was assessed at community level using an intention-to-treat approach, using mixed models to account for the correlation within households. As an ad hoc analysis, we stratified by infection status by including helminth infection status (no infection, any infection) at baseline and its interaction with treatment into the model. We also stratified by the number of helminth species a subject was infected with, by including the number of helminth species (no infection, single infection, multiple infection) at baseline and its interaction with treatment into the model. Two random effects were used: To model clustering within households, a random household specific intercept was used, and to model correlation within subjects, random subject-specific intercept was used. Parameter estimates for treatment effect and 95% CIs were reported. The reported *P* values were obtained using a likelihood ratio test comparing the model with and without the treatment effect. We used the same model for secondary outcomes. For the binary outcome (helminth infection status), a logistic model was used with random household effects and random subject effects. All models were fitted using the lme4 package (R software).

RESULTS

Between 1 April 2014 and 3 June 2014, we initially included 752 households with 3566 subjects in the trial. Randomization resulted in 1825 subjects assigned to placebo and 1741

subjects to albendazole (377 and 375 households, respectively). The overall trial profile is shown in Figure 1, with a total of 1669 subjects aged ≥16 years who were examined at baseline (872 subjects (353 households) and 797 subjects (329 households) in the placebo and the albendazole groups, respectively). Baseline characteristics were similar between both treatment arms (Table 1).

The overall loss to follow-up, from baseline to 52 weeks, was 18.9%. The main reason for loss to follow-up was permanent or temporary movement out of the village for

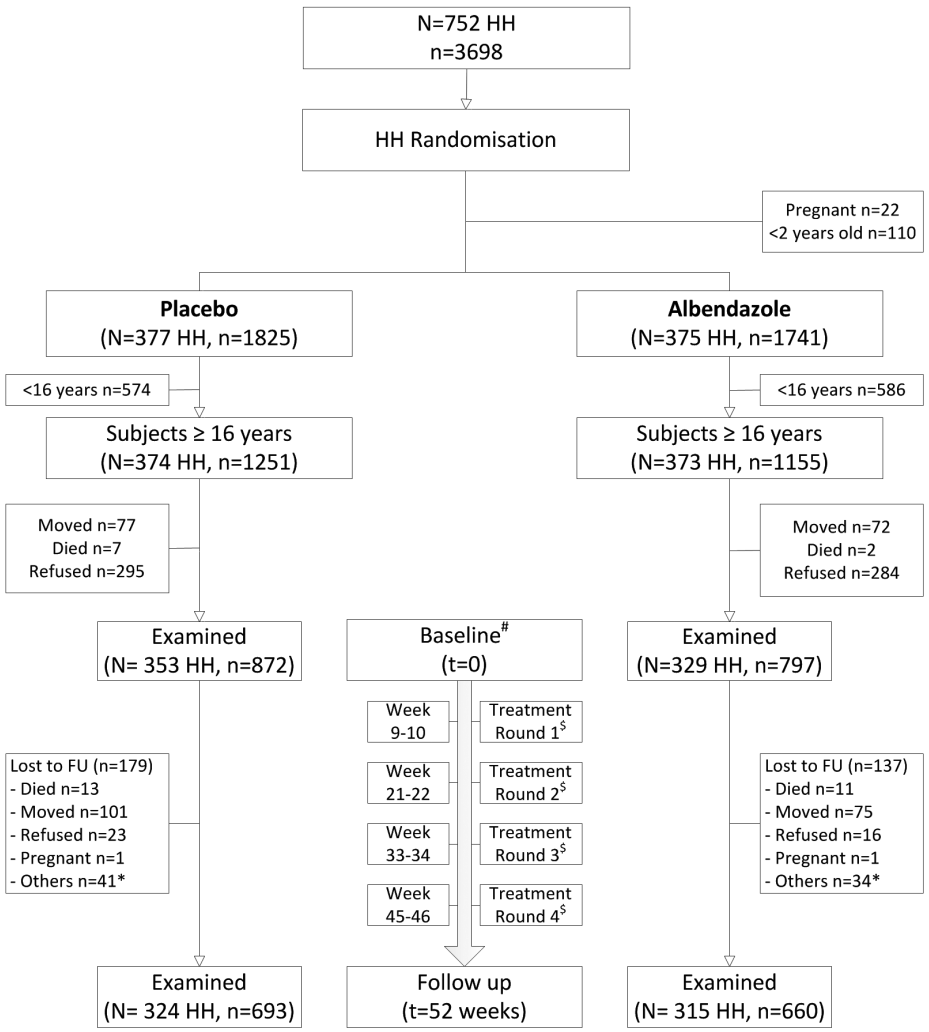

Figure 1. Trial profile. #Baseline data (t=0) were collected during the first 8 weeks before the start of the drug administration. $Single dose of albendazole or matching placebo was given for 3 consecutive days to all household members, except children <2 years of age and pregnant women. *Other reasons of lost to follow-up were harvesting crops, working on funeral ceremonies, severely ill, hospitalized, and nursing mother. Abbreviations: HH, households; FU, follow-up.

Table 1. Baseline characteristics of the study population

Characteristic	No.	Placebo	No.	Albendazole
Age, y, mean (SD)	872	42.5 (15.7)	797	42.5 (15.7)
Sex, female, No. (%)	872	534 (61.2)	797	478 (60.0)
Body mass index, kg/m2, mean (SD)	860	22.4 (4.2)	790	22.4 (4.0)
Waist circumference, cm, mean (SD)				
Female	532	76.5 (12.6)	476	77.0 (12.6)
Male	333	76.5 (11.6)	317	76.6 (11.3)
Waist-to-hip-ratio, mean (SD)				
Female	507	0.88 (0.07)	473	0.89 (0.08)
Male	317	0.94 (0.07)	315	0.94 (0.07)
Systolic BP, mmHg, mean (SD)	871	129.3 (23.4)	765	129.5 (23.8)
Diastolic BP, mmHg, mean (SD)	871	76.4 (12.1)	765	76.5 (12.1)
Total cholesterol, mmol/L, mean, (SD)	836	4.9 (1.1)	764	4. 9 (1.1)
HDL cholesterol, mmol/L, mean, (SD)				
Female	517	1.3 (0.4)	457	1.3 (0.4)
Male	319	1.1 (0.3)	307	1.1 (0.3)
LDL cholesterol, mmol/L, mean, (SD)	836	3.0 (0.9)	763	3.0 (0.9)
Triglycerides, mmol/L, mean, (SD)	836	1.4 (0.7)	764	1.5 (0.7)
HbA1c[a], mmol/mol, mean (SD)	715	32.5 (9.0)	683	32.3 (8.5)
Fasting blood glucose, mmol, mean, (SD)	836	5.5 (1.6)	768	5. 5 (1.6)
Fasting Insulin, mU/L, GM (95%CI)	836	3.5 (3.2 – 3.7)	768	3.5 (3.3 – 3.8)
HOMA-IR, GM (95%CI)	836	1.09 (1.02 – 1.15)	768	1.08 (1.01 – 1.14)
hs-CRP, mg/L, GM (95%CI)	836	1.26 (1.16 – 1.36)	764	1.26 (1.16 – 1.37)
Total IgE, IU/mL, GM (95%CI)	835	557.2 (498.1 – 623.3)	766	601.6 (534.8 – 676.7)
Eosinophil count, %, GM (95%CI)	829	5.9 (5.6 – 6.1)	763	6.1 (5.8 – 6.4)
Helminth infection by microscopy, No. (%)	655	283 (43.2)	602	251 (41.7)
Single		185 (28.2)		160 (26.6)
Multiple		98 (15.0)		91 (15.1)
Helminth infection by PCR, No. (%)	783	425 (54.3)	710	393 (55.4)
Single		256 (32.7)		252 (35.5)
Multiple		169 (21.6)		141 (19.9)

Abbreviations: BP, blood pressure; CI, confidence interval; GM, geometric mean; HDL, high-density lipoprotein; HbA1c, hemoglobin A1c; HOMA-IR, homeostasis model assessment for insulin resistance; hs-CRP, high-sensitivity C-reactive protein; IgE, immunoglobulin E; LDL, low-density lipoprotein; PCR, polymerase chain reaction; SD, standard deviation. [a]After excluding subjects with unidentified hemoglobinopathy on the Tosoh G8 high-performance liquid chromatography analyzer (13.9% [116/831] in the placebo group and 10.5% [80/763] in the albendazole group).

employment or study. Those who moved out and refused to come for follow-up were younger in comparison to the whole population. There were no significant differences between both treatment arms in terms of loss to follow-up (Supplementary Table 1). With respect to compliance, 87.9% (1189/1353) of the subjects took the maximum of 12 tablets (87.0% (574/660) vs 88.7% (615/693) in the albendazole and the placebo groups, respectively). We collected stool samples from 92.0% (1535/1669) of the subjects at baseline and 89.9% (1217/1353) of the subjects at follow-up. Data to calculate HOMA-IR

were available for 1604 subjects at baseline, and for 1272 subjects at follow-up. Sixteen subjects who were receiving active treatment for DM2 were excluded from analysis.

Effect of Treatment at the Community Level

Albendazole treatment reduced the percentage of subjects with any helminth infection as assessed by either microscopy (from 41.7% (251/602) to 5.6% (27/486) in the albendazole arm vs 43.2% (283/655) to 34.4% (181/526) in the placebo arm; $P < .0001$) or PCR (from 55.4% (393/710) to 11.3% (62/550) in the albendazole arm vs 54.3% (425/783) to 46.8% (278/594) in the placebo arm; $P < .0001$). The highest reduction was seen for hookworm, followed by *A. lumbricoides* and *T. trichiura* infection (Figure 2). When assessing the infection intensity in categories based on PCR, albendazole treatment resulted in a reduction in intensity across these 3 helminth species with the least effect on *T. trichiura* infection (Figure 2B). *S. stercoralis* prevalence, which was already low, was eliminated in the albendazole group (Supplementary Table 2).

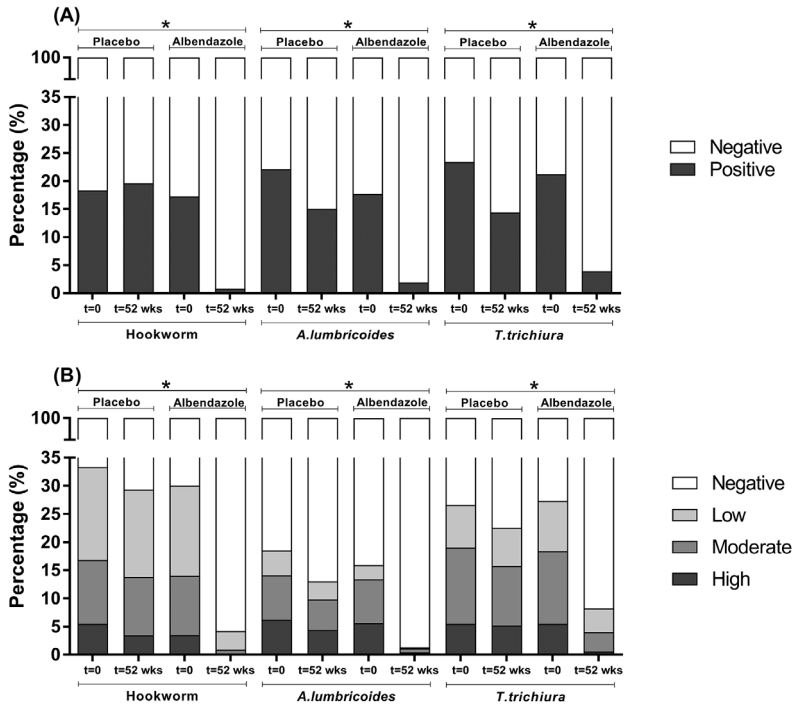

Figure 2. The effect of albendazole treatment on the prevalence and intensity of soil-transmitted helminths. Percentage of hookworm-, *Ascaris lumbricoides*-, and *Trichuris trichiura*-infected subjects at baseline (t=0) and following treatment (t=52 weeks), in the placebo and albendazole treatment arms, as detected by microscopy (n=1011; *A*) and polymerase chain reaction (n=1144; *B*). Albendazole treatment was associated with a significant reduction of hookworm, *A. lumbricoides* and *T. trichiura*. *P* values were calculated using a logistic model with random household effects and random subject effects. **P* <.0001.

At the community level, neither HOMA-IR nor BMI, waist circumference, fasting blood glucose, HbA1c, total cholesterol, HDL-C, LDL-C, triglycerides, or hs-CRP were found to be affected by albendazole treatment (Table 2). However, the significant reduction of infection prevalence and intensity by albendazole treatment was accompanied by a significant decrease in total IgE level (estimated treatment effect, -0.066 (95% CI, -.094 – -.037); $P < .0001$) and eosinophil count (-0.057 (95% CI, -.086 – -.028); $P = .0001$) (Table 2).

Effect of Treatment in STH-infected Subjects

Next, the effect of treatment was assessed only in those who were infected with helminths at baseline, as detected by microscopy. Albendazole treatment resulted in a significant increase in HOMA-IR (0.031 (95% CI, .004 – .059); $P = .04$) (Figure 3A). This effect was greater in comparison to subjects without helminth infections at baseline ($P = .01$ for the interaction between helminth infection status at baseline and treatment). Moreover, with an increasing number of helminth species infecting a subject at baseline, there was a gradual increase in HOMA-IR after treatment. Thus, whereas we saw no significant effect of treatment among those with no infection (-0.013 (95% CI, -.035 – .010); $P = .28$) or those infected with single species (0.017 (95% CI, -.017 – .050); $P = .34$), treatment in those infected with multiple helminth species resulted in a significantly higher HOMA-IR (0.061 [95% CI, .015 – .106]; $P = .02$; P value for interaction = .005) (Figure 3A). These effects were also reflected for BMI (Figure 3B), eosinophil count (Figure 3C), and total IgE level (Figure 3D), but not for HbA1c, total cholesterol, HDL-C, LDL-C, triglycerides or hs-CRP level. Pathway analysis showed that adjustment for BMI and eosinophil count, but not total IgE level, attenuated the treatment effect on HOMA-IR among helminth-infected subjects (Supplementary Table 3).

When using PCR to detect STH infection, a significant increase of HOMA-IR was observed only among subjects who were infected with multiple helminth species at baseline (Supplementary Figure 2A). A significant increase of BMI was also observed in these subjects (Supplementary Figure 2B). The group of subjects infected with multiple helminth species had a significantly higher infection intensity in comparison to the group of subjects infected with single helminth species (Supplementary Table 4).

Adverse Events

Adverse events were reported in 3.9% (31/797) and 2.6% (23/872) of subjects in the albendazole and the placebo groups, respectively. Abdominal pain was the most commonly reported complaint (35% (11/31) vs 13% (3/23) in the albendazole and the placebo groups, respectively). Other commonly reported complaints were diarrhea and nausea, which were similar in both treatment arms.

Table 2. Effect of albendazole treatment on primary and secondary outcomes at the community level

		Placebo		Albendazole			
Outcome	Parameter	Baseline	Follow-up	Baseline	Follow-up	Treatment Effect (95%CI)	*P* value
Insulin resistance	HOMA-IR	1.09 (1.02 – 1.15) n=836	1.16 (1.09 – 1.24) n=659	1.08 (1.01 – 1.14) n=768	1.17 (1.13 – 1.25) n=635	0.006 (-.010 – .021)	.48
Glucose-related	Fasting blood glucose (mmol)	5.49 (1.61) n=836	5.47 (1.09) n=650	5.45 (1.58) n=768	5.52 (1.49) n=634	0.018 (-.105 – .142)	.77
	Fasting insulin (mU/L)	3.5 (3.2 – 3.7) n=836	3.8 (3.5 – 4.1) n=646	3.5 (3.3 – 3.8) n=768	3.9 (3.6 -4.2) n=628	0.006 (-.032 – .043)	.77
	HbA1c (mmol/mol)	32.5 (9.0) n=715	32.7 (7.4) n=564	32.3 (8.5) n=683	32.7 (8.4) n=556	0.051 (-.350 – .452)	.80
Adiposity-related	Body mass index (kg/m^2)	22.4 (4.2) n=860	22.8 (4.2) n=690	22.4 (4.0) n=790	22.9 (4.1) n=659	0.104 (-.011 – .220)	.08
	Waist circumference (cm)	76.5 (12.2) n=865	77.2 (11.5) n=692	76.8 (12.1) n=793	77.4 (11.1) n=657	-0.229 (-.855 – .397)	.47
Lipid-related	Total cholesterol (mmol/L)	4.9 (1.0) n=836	5.0 (1.1) n=659	4.9 (1.1) n=764	5.0 (1.1) n=632	-0.031 (-.098 – .035)	.35
	HDL-C (mmol/L)	1.2 (0.3) n=836	1.3 (0.3) n=659	1.2 (0.3) n=764	1.3 (0.4) n=632	-0.008 (-.031 – .016)	.52
	LDL-C (mmol/L)	3.0 (0.9) n=836	3.1 (0.9) n=658	3.0 (0.9) n=763	3.1 (1.0) n=631	-0.032 (-.089 – .024)	.26
	Triglycerides (mmol/L)	1.4 (0.7) n=836	1.5 (0.7) n=659	1.5 (0.7) n=764	1.5 (0.7) n=632	-0.003 (-.023 – .090)	.25
Immune-related	Total IgE (IU/mL)	557.2 (498.1 – 623.3) n=835	441.8 (386.7 – 504.7) n=651	601.6 (534.8 – 676.7) n=766	399.0 (347.9 – 457.7) n=628	-0.066 (-.094 – -.037)	<.0001
	Eosinophil count (%)	5.9 (5.6 – 6.1) n=829	5.9 (5.6 – 6.1) n=641	6.1 (5.8 – 6.4) n=763	5.2 (5.0 -5.5) n=619	-0.057 (-.086 – -.028)	.0001
	hs-CRP (mg/L)	1.26 (1.16 – 1.36) n=836	1.30 (1.19 – 1.42) n=659	1.26 (1.16 – 1.37) n=764	1.34 (1.23 – 1.46) n=632	0.010 (-.017 – -.038)	.46

The estimated treatment effect after 12-months of follow-up for HOMA-IR and other glucose-related parameters, adiposity, lipid, and immunological parameters at community level is displayed with corresponding 95% CI. The estimated treatment effects were obtained by mixed models and *P* values are indicated. HOMA-IR, fasting insulin, total IgE, eosinophil count and hs-CRP were log transformed.

Abbreviations: CI, confidence interval; HbA1c, hemoglobin A1c; HDL-C, high-density lipoprotein cholesterol; HOMA-IR, homeostatic model assessment for insulin resistance; hs-CRP, high sensitivity C-Reactive Protein. IgE, Immunoglobulin E; LDL-C, low-density lipoprotein cholesterol.

DISCUSSION

Here, we report the first cluster-randomized trial in humans investigating the causal relationship between helminth infections and whole-body IR in an area endemic for STHs. We found that after 12 months of follow-up, 4 rounds of anthelmintic treatment with 3-month intervals did not lead to an increase in IR or other parameters such as BMI, waist circumference, fasting blood glucose, HbA1c, serum lipid levels and hs-CRP at the community level, when all participants irrespective of their helminth status were included in the analysis. This despite the fact that the prevalence and infection intensity of STHs, as well as their associated type 2 immune responses, measured by total IgE and eosinophil count, were significantly reduced in albendazole-treated subjects.

When considering helminth-infected subjects, we observed that albendazole treatment resulted in a significant increase of IR among helminth-infected subjects when infection was detected by microscopy. Moreover, the effect of treatment on IR was stronger in those infected with multiple STH species at baseline compared to those with a single STH infection. We observed a similar pattern of the treatment effect on BMI. Even though significant, it is important to note that the magnitude of the effect of 1 year of deworming

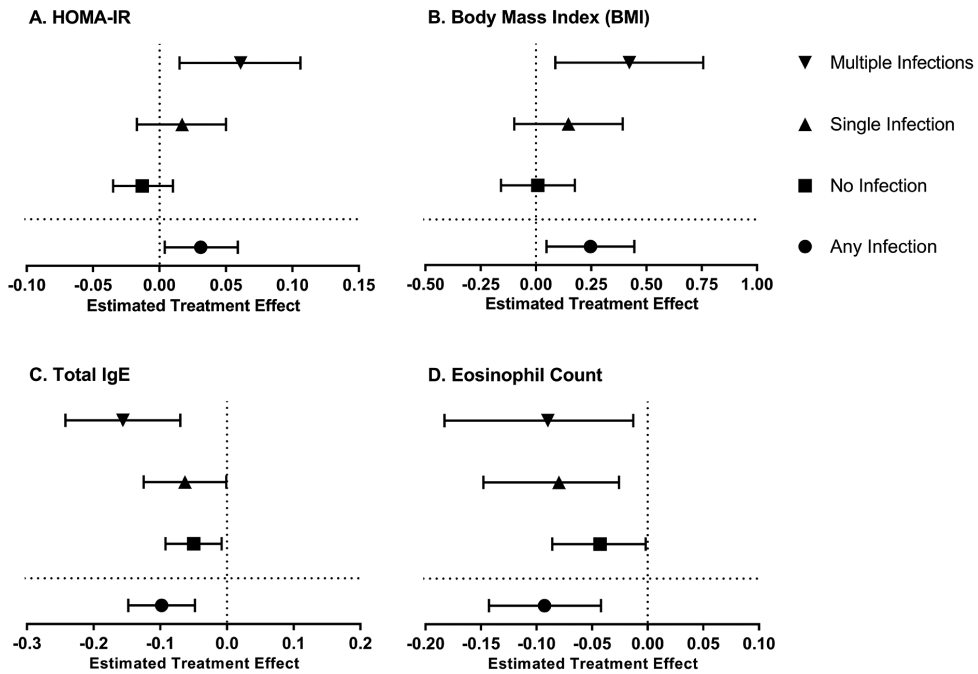

Figure 3. Effect of albendazole treatment on homeostatic model assessment for insulin resistance (HOMA-IR), body mass index (BMI), total immunoglobulin E (IgE), and eosinophil count, stratified by the number of helminth species carried by infected subjects at baseline as detected by microscopy. Effect of albendazole treatment on HOMA-IR (n = 1211; *A*), BMI (n = 1233; *B*), total IgE (n = 1209; *C*), and eosinophil count (n = 1200; *D*), stratified by the number of helminth species infecting subjects at baseline, as detected by microscopy. The estimated treatment effects are displayed with the corresponding 95% confidence interval. Circle, infected with at least 1 helminth species; square, no infection; triangle, infected with 1 helminth species; inverse triangle, infected with >1 helminth species.

on IR was modest. The effect of deworming in increasing IR seemed to be partly mediated through an increase in BMI, as adjustment for BMI, a strong predictor of IR (28), attenuated the treatment effect on IR. Similar to BMI, eosinophil count and total IgE were significantly decreased in helminth-infected subjects, and this was stronger in those with multiple helminth infections. The possible importance of eosinophils in IR, shown in animal models (13, 14, 16, 17) and in 1 epidemiological study (29), is also seen in our study as correction for eosinophil count reduced the treatment effect on IR.

When infection was assessed by PCR, which, in comparison to the Kato-Katz method, has a better ability to detect low-intensity infections that may be clinically less relevant (25), we only observed a significant increase in IR in the group of subjects who were infected with multiple helminth species at baseline. The infection intensity (DNA load) in this group of subjects was significantly higher than in those infected with a single STH species. Albendazole treatment led to a strong reduction of infection intensity in those

infected with multiple STH species, which might explain the significant increase in IR following albendazole treatment.

The observed modest increase of IR after treatment among helminth-infected subjects, as detected by microscopy, could also contribute to the lack of a significant effect of albendazole treatment on IR at the community level. Two recent meta-analyses on deworming in children support this notion as they show that although a mass deworming approach, thus irrespective of helminth infection status, resulted in no change in weight gain, targeted anthelmintic treatment of infected children resulted in a significant weight gain (30, 31).

However, several other explanations for the absence of a treatment effect on IR at the community level need to be considered. Although our study design was successful in lowering STH infection prevalence and its associated Th2 responses, it is possible that longer treatment and follow-up would show stronger effects. It is also possible that both immune and non-immune-related effects of helminths on IR are not only associated with current helminth infections (8) but also with exposure to helminth infections in the past and therefore sustained (13, 19). The causal relationship between helminth infection and IR, as found in the subgroup of infected subjects, might have a relatively small contribution to the multifactorial pathogenesis of IR (28). Therefore, longer follow-up studies involving assessment of other more established factors, such as diet and physical activity (28), will be needed to investigate this.

The use of PCR in our study, in addition to microscopy for detection of helminths, has helped us realize that the burden of infections, in terms of the number of helminth species as well as the infection intensity (DNA load), might influence the effect of anthelmintic treatment on IR. Deworming in subjects with increasing burden of infections resulted in an increasing change in IR. In addition, treatment of uninfected subjects, as assessed by either microscopy or PCR, did not influence IR, which suggests that an undetectable or a low level of helminth infection might be irrelevant for IR. The question whether a high burden of helminth infection causes different modulating effects on the immune system or energy balance, remains to be answered.

In conclusion, intensive anthelmintic treatment in an STH-endemic area significantly reduces both the STH infection prevalence and intensity, as well as its related type 2 responses. This treatment does not lead to an increase of whole-body IR at the community level, but it does increase IR among those with a microscopy-detected STH infection. Studies are needed to determine the long term metabolic consequences of anthelmintic treatment in communities where STHs are highly prevalent. However, in terms of policy, countries implementing helminth control programs need to be aware that this may exacerbate or accelerate the deterioration in metabolic health, and that education and prevention strategies for noncommunicable diseases such as DM2 need to go hand in hand with infectious disease control measures.

ACKNOWLEDGEMENTS

The authors thank all study participants in Nangapanda, Ende, Flores, Indonesia; all local government and health officers in Nangapanda who supported this project; all field workers from Universitas Indonesia and Nangapanda; Alison Elliott and Bruno Guigas for reading the manuscript critically; Yvonne Kruize, Angga M. Fuady, and all colleagues at the Department of Parasitology, LUMC for their technical support; and the Indonesian Directorate General of Higher Education (DIKTI) for providing scholarships to 2 PhD candidates involved in this project.

REFERENCES

1. Collaboration NCDRF. Worldwide trends in diabetes since 1980: a pooled analysis of 751 population-based studies with 4.4 million participants. Lancet 2016; 387(10027): 1513-30.
2. Hu FB. Globalization of diabetes: the role of diet, lifestyle, and genes. Diabetes Care 2011; 34(6): 1249-57.
3. Defronzo RA. Banting Lecture. From the triumvirate to the ominous octet: a new paradigm for the treatment of type 2 diabetes mellitus. Diabetes 2009; 58(4): 773-95.
4. Hotamisligil GS. Inflammation and metabolic disorders. Nature 2006; 444(7121): 860-7.
5. Hotez PJ, Brindley PJ, Bethony JM, King CH, Pearce EJ, Jacobson J. Helminth infections: the great neglected tropical diseases. The Journal of clinical investigation 2008; 118(4): 1311-21.
6. Wammes LJ, Mpairwe H, Elliott AM, Yazdanbakhsh M. Helminth therapy or elimination: epidemiological, immunological, and clinical considerations. The Lancet Infectious diseases 2014; 14(11): 1150-62.
7. de Ruiter K, Tahapary DL, Sartono E, et al. Helminths, hygiene hypothesis and type 2 diabetes. Parasite Immunol 2016.
8. Wiria AE, Hamid F, Wammes LJ, et al. Infection with Soil-Transmitted Helminths Is Associated with Increased Insulin Sensitivity. PLoS One 2015; 10(6): e0127746.
9. Wiria AE, Sartono E, Supali T, Yazdanbakhsh M. Helminth infections, type-2 immune response, and metabolic syndrome. PLoS pathogens 2014; 10(7): e1004140.
10. Berbudi A, Ajendra J, Wardani AP, Hoerauf A, Hubner MP. Parasitic helminths and their beneficial impact on type 1 and type 2 diabetes. Diabetes Metab Res Rev 2015.
11. Ricardo-Gonzalez RR, Red Eagle A, Odegaard JI, et al. IL-4/STAT6 immune axis regulates peripheral nutrient metabolism and insulin sensitivity. Proc Natl Acad Sci U S A 2010; 107(52): 22617-22.
12. Hong EG, Ko HJ, Cho YR, et al. Interleukin-10 prevents diet-induced insulin resistance by attenuating macrophage and cytokine response in skeletal muscle. Diabetes 2009; 58(11): 2525-35.
13. Wu D, Molofsky AB, Liang HE, et al. Eosinophils sustain adipose alternatively activated macrophages associated with glucose homeostasis. Science 2011; 332(6026): 243-7.
14. Hams E, Bermingham R, Wurlod FA, et al. The helminth T2 RNase omega1 promotes metabolic homeostasis in an IL-33- and group 2 innate lymphoid cell-dependent mechanism. FASEB journal : official publication of the Federation of American Societies for Experimental Biology 2016; 30(2): 824-35.
15. Yang Z, Grinchuk V, Smith A, et al. Parasitic nematode-induced modulation of body weight and associated metabolic dysfunction in mouse models of obesity. Infection and immunity 2013; 81(6): 1905-14.
16. Hussaarts L, Garcia-Tardon N, van Beek L, et al. Chronic helminth infection and helminth-derived egg antigens promote adipose tissue M2 macrophages and improve insulin sensitivity in obese mice. FASEB journal : official publication of the Federation of American Societies for Experimental Biology 2015; 29(7): 3027-39.
17. Berbudi A, Surendar J, Ajendra J, et al. Filarial Infection or Antigen Administration Improves Glucose Tolerance in Diet-Induced Obese Mice. J Innate Immun 2016; 8(6).
18. Bhargava P, Li C, Stanya KJ, et al. Immunomodulatory glycan LNFPIII alleviates hepatosteatosis and insulin resistance through direct and indirect control of metabolic pathways. Nat Med 2012; 18(11): 1665-72.
19. Chen Y, Lu J, Huang Y, et al. Association of previous schistosome infection with diabetes and metabolic syndrome: a cross-sectional study in rural China. The Journal of clinical endocrinology and metabolism 2013; 98(2): E283-7.
20. Shen SW, Lu Y, Li F, et al. The potential long-term effect of previous schistosome infection reduces the risk of metabolic syndrome among Chinese men. Parasite immunology 2015; 37(7): 333-9.
21. Aravindhan V, Mohan V, Surendar J, et al. Decreased prevalence of lymphatic filariasis among diabetic subjects associated with a diminished pro-inflammatory cytokine response (CURES 83). PLoS neglected tropical diseases 2010; 4(6): e707.
22. Hays R, Esterman A, Giacomin P, Loukas A, McDermott R. Does Strongyloides stercoralis

infection protect against type 2 diabetes in humans? Evidence from Australian Aboriginal adults. Diabetes research and clinical practice 2015; 107(3): 355-61.
23. Tahapary DL, de Ruiter K, Martin I, et al. Helminth infections and type 2 diabetes: a cluster-randomized placebo controlled SUGARSPIN trial in Nangapanda, Flores, Indonesia. BMC Infect Dis 2015; 15: 133.
24. Wiria AE, Prasetyani MA, Hamid F, et al. Does treatment of intestinal helminth infections influence malaria? Background and methodology of a longitudinal study of clinical, parasitological and immunological parameters in Nangapanda, Flores, Indonesia (ImmunoSPIN Study). BMC Infect Dis 2010; 10: 77.
25. Arndt MB, John-Stewart G, Richardson BA, et al. Impact of helminth diagnostic test performance on estimation of risk factors and outcomes in HIV-positive adults. PLoS One 2013; 8(12): e81915.
26. Wallace TM, Levy JC, Matthews DR. Use and abuse of HOMA modeling. Diabetes Care 2004; 27(6): 1487-95.
27. Wiria AE, Hamid F, Wammes LJ, et al. The effect of three-monthly albendazole treatment on malarial parasitemia and allergy: a household-based cluster-randomized, double-blind, placebo-controlled trial. PLoS One 2013; 8(3): e57899.
28. Riserus U, Arnlov J, Berglund L. Long-term predictors of insulin resistance: role of lifestyle and metabolic factors in middle-aged men. Diabetes Care 2007; 30(11): 2928-33.
29. Zhu L, Su T, Xu M, et al. Eosinophil inversely associates with type 2 diabetes and insulin resistance in Chinese adults. PloS one 2013; 8(7): e67613.
30. Welch VA, Ghogomu E, Hossain A, et al. Mass deworming to improve developmental health and wellbeing of children in low-income and middle-income countries: a systematic review and network meta-analysis. Lancet Glob Health 2017; 5(1): e40-e50.
31. Taylor-Robinson DC, Maayan N, Soares-Weiser K, Donegan S, Garner P. Deworming drugs for soil-transmitted intestinal worms in children: effects on nutritional indicators, haemoglobin, and school performance. The Cochrane database of systematic reviews 2015; 7: CD000371.

SUPPLEMENTARY APPENDIX

Supplementary Methods

Study Procedures

All clinical measurements and blood sample collections were performed after an overnight fast. Anthropometric measurements of body weight (SECA Model 876, Seca Gmbh Co, Hamburg, Germany), height (SECA Model 213, Seca Gmbh Co, Hamburg, Germany), waist and hip circumference (SECA Model 201, Seca Gmbh Co, Hamburg, Germany) were obtained using the National Heart, Lung, and Blood Institute (NHLBI) practical guidelines by a team of trained researchers. BMI was calculated as weight in kg divided by square of height in meter, while Waist Hip Ratio (WHR) was calculated as waist circumference divided by hip circumference. Three blood pressure measurements (left arm, sitting upright position, after resting 5 minutes) were taken from each subject, using a digital sphygmomanometer (HEM-7200, Omron Healthcare Co, Ltd, Kyoto, Japan). The average of all three measurements was used for analysis.

Fasting blood glucose was measured in capillary blood using Breeze®2 glucose meters (Bayer Health Care LLC, Basel, Switzerland). All sera, plasma and whole blood samples were frozen at −20°C in the field study centre and subsequently stored at −80°C at the Department of Parasitology of FKUI and LUMC. Insulin, HbA1c, total cholesterol, high-density lipoprotein (HDL)-cholesterol, triglycerides and high-sensitive C-reactive protein (hsCRP) were measured pairwise (baseline and follow-up) in the same analytical runs at the Department of Clinical Chemistry and Laboratory Medicine at LUMC, which is ISO 15189:2012 accredited. Accuracy of test results is periodically and independently verified in EQA-schemes organized by the Dutch EQA-organization, the SKML.

Serum insulin concentrations were determined by a solid-phase, enzyme-labeled chemiluminescent immunometric assay (Siemens IMMULITE 2000XPi). The measuring range of the insulin assay was 2–300 mU/L (CV_a <7% at all levels). IR was assessed by HOMA-IR, a well-validated measure of whole body IR in humans (HOMA-IR = fasting serum insulin x fasting glucose / 22.5) (26). HbA1c was measured using a cation-exchange chromatography (IC)-based high performance liquid chromatogtaphy (HPLC) assay (Tosoh G8 HPLC Analyzer, from Tosoh Corporation, Tokyo, Japan and distributed through Sysmex in the Netherlands), with a measuring range of 20–125 mmol/mol Hb (CV_a<5% at all levels). Test results are in accordance to the IFCC Reference Measurement System for HbA1c. The non-porous ion exchange HPLC-column and four-steps buffer gradient enables a clear separation of HbA1c from other fractions and haemoglobin variants such as HbC, HbD and HbS. As these variants can be detected, the software automatically corrects the HbA1c results for these variants. However, other variants which may typically be present in non-Caucasian populations, are not detected and lead to inaccurate HbA1c results. Therefore, all chromatograms were visually inspected by experienced technicians in order to detect the unidentified Hb-variants. HbA1c results from unidentified Hb-variants were excluded as these test results were inaccurate.

Total cholesterol, HDL-cholesterol and triglycerides assays were based on enzymatic colorimetric methods (Modular P analyzers, Roche Diagnostics, Mannheim, Germany). The measuring range of total cholesterol, HDL-cholesterol and triglycerides were 0.08–20.7 mmol/L (CV_a<2%), 0.08–3.10 mmol/L (CV_a<2%) and 0.05–11.4 mmol/L (CV_a<5%), respectively. Lipid test results are standardized to internationally recognized CDC Reference Measurement Systems. Low-density lipoprotein (LDL)-cholesterol (in mmol/L) was calculated using The Friedewald formula, (LDL-chol, mmol/L) = (Total chol) - (HDL-chol) - (0.456 X (TG)). A latex-enhanced immunoturbidimetric method was used to measure hs-CRP on Roche Modular P-instrumentation, the measuring range being 0.1–20.0 mg/L. hs-CRP test results are ERM-DA470k/IFCC standardized.

A Giemsa-stained peripheral thin blood smear was read at the Department of Clinical Pathology, FKUI to assess differential white blood cell count, resulting in a relative percentage of basophils, eosinophils, neutrophils, lymphocytes and monocytes. Total IgE was measured at the Department of Parasitology, LUMC using ELISA with rabbit anti-human IgE antibody (Ab) (Dako, Glostrup, Denmark) as capture Ab and goat anti-human IgE biotinylated Ab (Vector Laboratories, Burlingname, CA, USA) as detection Ab (24).

Fresh stool samples were examined by the Kato Katz method to identify and quantify STH (hookworm, *Ascaris lumbricoides* and *Trichuris trichiura*) eggs using 2 slides for each sample. Aliquots of fresh stool samples were frozen at −20°C in the field study centre and subsequently at −80°C at the Department of Parasitology of FKUI and LUMC for DNA extraction. Stool DNA isolation and real-time PCR were performed pairwise (baseline and follow-up). DNA isolation from stool was performed as described elsewhere (24), with an additional step of bead beating (1800 rpm for 3 minutes) inside the Fastprep-96™ system to optimize DNA extraction. Multiplex real-time PCR was performed to simultaneously detect the presence of hookworm (*Ancylostoma duodenale*, *Necator americanus*), *A. lumbricoides*, *T. trichiura* and *Strongyloides stercoralis* using a method described previously(24) with some modifications, adding the *T. trichiura* primers and probe, and combining the fluorescence of *A. duodenale* and *N. americanus* as one reading of hookworm. Stool samples were considered positive by PCR when cycle threshold (Ct) values were below 50. Positive Ct values were further grouped into 3 categories: Ct<30, 30≤Ct<35 and Ct≥35 representing a high, moderate and low DNA load, respectively (25), An additional grouping was made based on the number of different STH species that subjects were infected with: no infection, single infection (one of the four STHs: hookworm, *A.lumbricoides*, *T.trichiura*, *S.stercoralis*) and multiple infections (more than one of these STHs).

SUPPLEMENTAL DATA

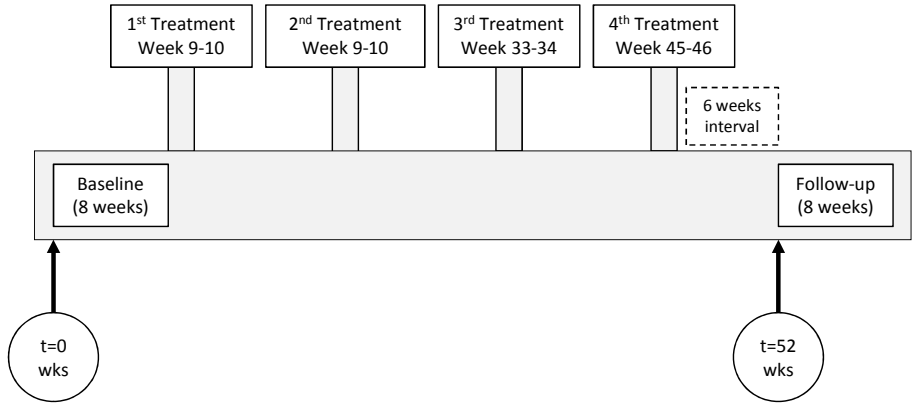

Supplementary Figure S1. Trial time frame. Baseline data (t=0) were collected during the first 8 weeks before the start of the drug administration. Treatment regimen was given 4 times with three month time intervals (week 9-10, 21-22, 33-34, and 45-46). Follow-up data (t=52 weeks) were collected 6 weeks after the last treatment round.

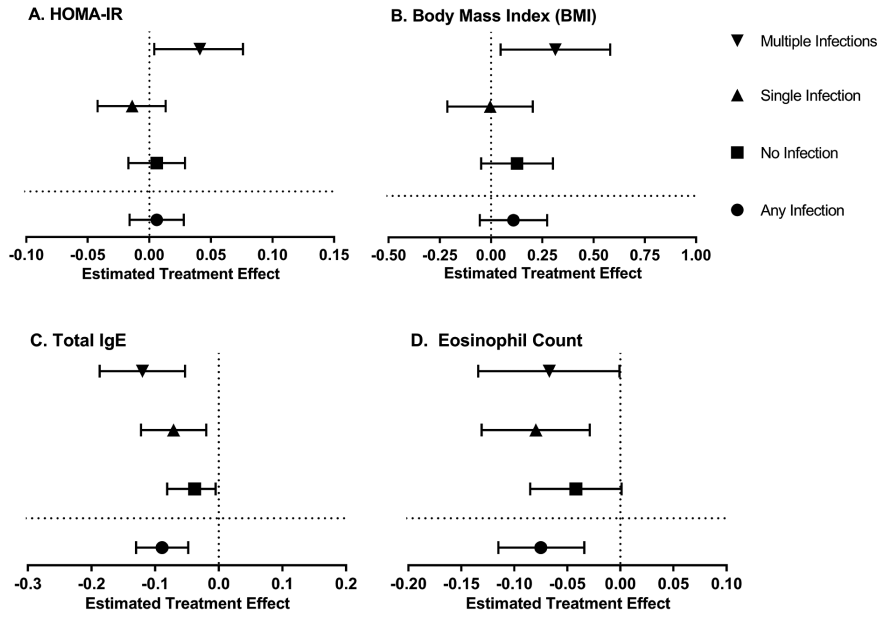

Supplementary Figure S2. Effect of albendazole treatment on HOMA-IR, BMI, total IgE and eosinophil count stratified by the number of helminth species carried by infected subjects at baseline as detected by PCR. Effect of albendazole treatment on HOMA-IR (n= 1433; *A*), BMI (n= 1464; *B*), total IgE (n=1430; *C*), and eosinophil count (n=1422; *D*) stratified by the number of helminth species infecting subjects at baseline, as detected by PCR. The estimated treatment effects are displayed with corresponding 95% confidence interval. Circle, infected with at least 1 helminth species; square, no infection; triangle, infected with 1 helminth species; inverse triangle, infected with >1 helminth species.

Supplementary table S1. Summary of subjects lost to follow-up

	Died		Moved		Refused		Other Reasons		Total Lost to Follow Up	
	Pla	Alb	Pla	Alb	Pla	Alb	Pla	Alb	Pla	Alb
Subjects	13	11	101	75	23	16	42	35	179	137
(n, %)*	(1.5)	(1.4)	(11.5)	(9.4)	(2.6)	(2.0)	(4.8)	(4.4)	(20.5)	(17.2)
Age	56.8	63.1	29.7	29.5	36.6	39.9	42.4	39.7	35.5	36.0
(mean, SD)	(10.1)	(10.7)	(14.1)	(14.0)	(13.9)	(13.8)	(17.2)	(41.1)	(16.5)	(17.1)
Sex (male)	10/13	6/11	40/101	34/75	14/23	11/16	22/42	19/35	86/179	70/137
(n/N, %)	(77)	(55)	(40)	(45)	(61)	(69)	(52)	(54)	(48.0)	(51.1)

*% was calculated from all subjects in each treatment arm (placebo n=872, albendazole n=797).
Abbreviations: Pla, Placebo; Alb, Albendazole.

Supplementary table S2. Effect of albendazole treatment on infection intensity detected by PCR

		Baseline (t=0)		Follow-Up (t=52 weeks)	
Type of STH	Infection Intensity*	Placebo n=594	Albendazole n=550	Placebo n=594	Albendazole n=550
Hookworm	Negative	396 (66.7)	385 (70.0)	420 (70.7)	527 (95.8)
n (%)	Low	98 (16.5)	88 (16)	92 (15.5)	18 (3.3)
	Moderate	67 (11.3)	58 (10.5)	62 (10.4)	5 (0.9)
	High	33 (5.5)	19 (3.5)	20 (3.4)	0 (0.0)
A. lumbricoides	Negative	484 (81.5)	462 (84.0)	517 (87.0)	543 (98.7)
n (%)	Low	26 (4.4)	14 (2.5)	19 (3.2)	1 (0.2)
	Moderate	47 (7.9)	43 (7.8)	32 (5.4)	4 (0.7)
	High	37 (6.2)	31 (5.6)	26 (4.4)	2 (0.4)
T. trichiura	Negative	436 (73.4)	400 (72.7)	460 (77.4)	505 (91.8)
n (%)	Low	45 (7.6)	49 (8.9)	40 (6.7)	23 (4.2)
	Moderate	80 (13.5)	71 (12.9)	63 (10.6)	19 (3.5)
	High	33 (5.5)	30 (5.5)	31 (5.2)	3 (0.5)
S. stercoralis	Negative	588 (99.0)	547 (99.5)	589 (99.1)	550 (100.0)
n (%)	Low	3 (0.5)	1 (0.2)	3 (0.5)	0 (0.0)
	Moderate	2 (0.3)	1 (0.2)	1 (0.2)	0 (0.0)
	High	1 (0.2)	1 (0.2)	1 (0.2)	0 (0.0)

*Ct value of 50 indicates no infection (negative). Ct values <50 were further grouped into 3 categories: Ct<30, 30≤Ct<35 and Ct≥35 representing a high, moderate and low DNA load, respectively.
Abbreviations: Ct=Cycle threshold.

Supplementary table S3. Pathway analysis of the treatment effect on insulin resistance in helminth-infected subjects as detected by microscopy

Model	Estimated Treatment Effect (95%CI), *P* value
Unadjusted	0.031 (0.004 – 0.059), p=0.04
Adjusted for BMI changes	0.025 (-0.001 – 0.051), p=0.10
Adjusted for total IgE changes	0.030 (0.002 – 0.057), p=0.06
Adjusted for eosinophil count changes	0.026 (-0.002 – 0.053), p=0.13
Adjusted for BMI and eosinophil changes	0.020 (-0.007 – 0.046), p=0.23

Abbreviations: BMI=Body Mass Index, IgE= Immunoglobulin E.

Supplementary table S4A. Comparison of baseline infection intensity in subjects infected with single and multiple helminth species as detected by PCR

Helminth species	Single (n=491) [Ct value, mean (SD)]	Multiple (n=296) [Ct value, mean (SD)]	Mean differences (95%CI), *P* value*
Hookworm	35.9 (4.0), n=259	34.3 (4.4), n=226	-1.6 (-2.3 – -0.8), p<0.0001
A.lumbricoides	32.9 (3.2), n=75	31.0 (3.7), n=179	-1.9 (-2.9 – -0.9), p<0.0001
T.trichiura	33.7 (2.9), n=156	32.3 (3.3) n=247	-1.4 (-2.0 – -0.8), p<0.0001

This analysis was conducted in subjects analyzed in Figure S1. Infection intensity was assessed using Ct values of PCR, which represent the amount of DNA in the stool sample. The lower the Ct value, the higher the amount of DNA. Number of subjects with *S.stercoralis* was very low (one within the single infection group and nine within the multiple infection group). *Independent t-test.

Supplementary table S4B. Comparison of baseline infection intensity in subjects infected with single and multiple helminth species as detected by microscopy

Helminth species	Single (n=334) [epg, median (IQR), n]	Multiple (n=180) [epg, median (IQR), n]	*P* value*
Hookworm	96 (48 – 267), n=108	138 (72 – 474), n=108	0.087
A.lumbricoides	360 (72 – 1596), n=103	1980 (432 – 6264), n=143	<0.001
T.trichiura	36 (12 – 120), n=123	84 (36 – 261), n=152	<0.001

This analysis was conducted in subjects analyzed in Figure 3. Infection intensity was assessed using the number of egg per gram of stool sample (epg) from Kato Katz method. *Independent-samples Mann Whitney U Test.

4

THE *SCHISTOSOMA MANSONI* GLYCOPROTEIN OMEGA-1 IMPROVES WHOLE-BODY METABOLIC HOMEOSTASIS INDEPENDENT OF ITS TH2 POLARIZING CAPACITY

Hendrik J.P. van der Zande, Karin de Ruiter, Michael Gonzalez, Ruud Wilbers, Mariska van Huizen, Kim van Noort, Frank Otto, Cornelis H. Hokke, Arjen Schots, P'ng Loke, Maria Yazdanbakhsh and Bruno Guigas

Thesis Chapter

ABSTRACT

Type 2 immunity is involved in the maintenance of metabolic homeostasis and its disruption during obesity promotes chronic low-grade inflammation. Helminth parasites are the strongest natural inducers of type 2 immunity and we previously reported that infection with *Schistosoma mansoni* or treatment with a mixture of soluble egg antigens (SEA) both improved whole-body metabolic homeostasis in insulin-resistant obese mice. In the present study, we investigated the effects of two plant-produced glycosylation variants of omega-1, a glycoprotein present in SEA that has been shown to trigger dendritic cell-mediated Th2 polarization by a glycan-dependent mechanism, on whole-body metabolic homeostasis. We showed that both recombinant omega-1 glycovariants decreased fat mass and improved whole-body metabolic homeostasis in obese mice, an effect associated with increased adipose tissue Th2 cells, eosinophils and alternatively-activated macrophages. In the liver, omega-1 did not affect hepatic steatosis but increased IL-13-expressing Th2 cells and expression of fibrotic gene markers. Remarkably, the metabolic effects of omega-1 were still observed in obese STAT6-/- mice, although the Th2-mediated immune response was completely abolished. Omega-1 did not affect locomotor activity or energy expenditure but inhibited food intake in both WT and STAT6-/- mice. Altogether, we conclude that the improvement of metabolic homeostasis by omega-1 is independent of its Th2-inducing capacity and may be explained by brain-mediated inhibition of food intake and/or immune-independent direct interaction of omega-1 with metabolic cells.

INTRODUCTION

Obesity is associated with chronic low-grade inflammation in metabolic tissues (1). This so-called meta-inflammation plays a prominent role in the etiology of insulin resistance and type 2 diabetes (1-4), and is notably associated with increased numbers of pro-inflammatory macrophages in white adipose tissue (WAT) (5), liver (6, 7) and skeletal muscle (8, 9). In WAT, these macrophages mainly originate from newly-recruited blood monocytes that differentiate into pro-inflammatory, classically-activated macrophages (CAMs) upon entering the inflammatory milieu (5) and/or being activated by elevated local concentration of free fatty acids (10). These pro-inflammatory macrophages produce cytokines, such as tumor necrosis factor alpha (TNF-α) and interleukin 1-beta (IL-1β), which directly inhibit canonical insulin signaling (as reviewed in (2)) and contribute to tissue-specific insulin resistance and whole-body metabolic dysfunction. In the liver, activation of Kupffer cells, the resident macrophages (11), promote the recruitment of pro-inflammatory monocytes (6) and neutrophils (12) which trigger hepatic inflammation and insulin resistance through the production of pro-inflammatory cytokines and elastase, respectively (6, 11-13). While obese adipose tissue is thus characterized by pro-inflammatory type 1 cytokines, a type 2 cytokine environment is present in metabolic tissues under homeostatic, insulin sensitive conditions. Indeed, type 2 innate lymphoid cells (ILC2s) and T helper 2 (Th2) cells produce the type 2 cytokines IL-4, IL-5 and IL-13 in healthy adipose tissue and sustain a WAT eosinophils and alternatively activated macrophages (AAM) axis that is largely driven by eosinophil-produced IL-4 (14, 15). According to the current paradigm, AAMs are the final effector cells of this type 2 immune response that sustain insulin sensitivity through underlying molecular mechanism(s) that are still largely unknown.

Parasitic helminths are the strongest natural inducers of type 2 immunity (16). Interestingly, soil-transmitted helminth infection was reported to be associated with higher insulin sensitivity in humans (17), suggesting that helminth-induced type 2 immunity could protect against metabolic disorders. Moreover, both the short-lived rodent helminth *Nippostrongylus brasiliensis* and human *Schistosoma mansoni* improved insulin sensitivity and glucose tolerance in high-fat diet (HFD)-induced obese mice, an effect associated with strong WAT eosinophilia (15, 18). We also showed that chronic treatment with *S. mansoni* soluble egg antigens (SEA) promoted eosinophilia, T-helper 2 cells (Th2), type 2 cytokines expression and AAMs in WAT, and improved whole-body metabolic homeostasis (18).

SEA drives DC-mediated Th2 skewing at least partly through glycosylated molecules ((19), and reviewed in (20)). More specifically, an unknown Dectin-1/2-ligand in SEA (21, 22) and the T2 RNAse glycoprotein omega-1 (ω1; (23, 24)) have been shown to drive Th2 skewing. We have previously reported that ω1 is internalized by human DCs through an interaction between its glycans and the mannose receptor, and promotes Th2 skewing through interfering with protein synthesis (24). Interestingly, acute treatment of HFD-fed obese mice with human embryonic kidney 293 (HEK-293)-produced recombinant ω1 was recently shown to decrease body weight and improve whole-body glucose tolerance

through an IL-33-ILC2-axis (25). In this study, the metabolic effect of ω1 was reported to be glycan-dependent, yet we have previously shown that glycans on HEK-293-produced ω1 differ significantly from *S. mansoni* native ω1 (23, 24). Notably, HEK-293-produced ω1 glycans did not express the immunogenic Lewis-X (Le^X) motifs present on native ω1, but rather expressed LDN-F (24), a glycan motif with similar C-type lectin-binding properties as Le^X. However, as *S. mansoni* expresses an abundance of complex and unique glycans that modulate host immunity (as reviewed in (26)), it is critical to produce recombinant immunomodulatory molecules that harbour as similar glycosylation pattern as possible to the native ones. By exploiting the flexible N-glycosylation machinery of *Nicotiana benthamiana* plants, we successfully produced large amounts of recombinant ω1 carrying a terminal single branch Le^X-motif (pLe^X-ω1), a carbohydrate structure found on native ω1, making this glyco-engineered molecule more potent in Th2 skewing than the wild-type plant-glycosylated recombinant ω1 (pWT-ω1) (27). In the present study, we therefore investigate the effects and underlying mechanisms of these two plant-produced recombinant ω1 molecules on whole-body metabolic homeostasis in HFD-fed obese mice. Remarkably, treatment with both molecules improved the metabolic homeostasis of obese mice, an effect independent from the Th2 response but associated with a significant reduction in food intake. This raises the possibility that these glycoproteins can modulate the neuro-immunological axis involved in the control of feeding behaviour in mice.

MATERIALS AND METHODS

Animals, diet and treatment

All mouse experiments were performed in accordance with the Guide for the Care and Use of Laboratory Animals of the Institute for Laboratory Animal Research and have received approval from the university Ethical Review Boards (Leiden University Medical Center, Leiden, The Netherlands; DEC12199). 8-10 week-old male C57BL/6J mice (Charles River, L'Arbresle, France) were housed in a temperature-controlled room with a 12 hour light-dark cycle. Throughout the experiment, food and tap water were available *ad libitum*. Mice were fed a high-fat diet (HFD, 45% energy derived from fat, D12451, Research Diets) or a low-fat diet (LFD, 10% energy derived from fat, D12450B, Research Diets, Wijk bij Duurstede, The Netherlands) for 12 weeks, followed by group randomization according to body weight, fat mass, and fasting plasma glucose levels.

Recombinant omega-1 was produced in either wild-type (pWT-ω1) or Le^X-glyco-engineered *N. benthamiana* plants (pLe^X-ω1), as described previously (27). Recombinant pWT/pLe^X-ω1 (50 µg) and vehicle control (sterile-filtered 0.9% phosphate-buffered saline) were injected intraperitoneally every 3 days for 4 weeks, in four independent experiments. Short-term effects of pWT/pLe^X-ω1 were assessed in LFD- or HFD-fed mice treated every 2 days with 50 µg pWT/pLe^X-ω1 for one week. Dose-dependent effects of pLe^X-ω1 treatment were investigated by treating HFD-fed mice with 10, 25 or 50 µg of pLe^X-ω1 every 3 days for 4 weeks.

To investigate the role of type 2 immunity in the immunometabolic effects of pLe^X-ω1, 8-10 weeks-old male wild-type (WT) and *Stat6*$^{-/-}$ mice on C57BL/6J background (The Jackson Laboratory, Bar Harbor, ME, USA) were randomized based on body weight and fasting blood glucose levels, and either put on a HFD (60% energy derived from fat; D12492; Research Diets, New Brunswick, NJ, USA) or LFD (10% energy derived from fat; D12450J; Research Diets) for 10 weeks. To exclude effects of genotype-dependent microbiota differences on metabolic and immunological outcomes, the beddings of LFD- and HFD-fed WT and *Stat6*$^{-/-}$ mice were frequently mixed within similar diet groups throughout the run-in period. After 10 weeks, HFD-fed mice were randomized as described above and treated i.p. every 3 days for 4 weeks with 50 µg pLe^X-ω1 or vehicle-control.

Body composition and indirect calorimetry

Body composition was measured by MRI using an EchoMRI (Echo Medical Systems, Houston, TX, USA). Groups of 4-8 mice with free access to food and water were subjected to individual indirect calorimetric measurements during the initiation of the treatment with recombinant ω1 for a period of 7 consecutive days using a Comprehensive Laboratory Animal Monitoring System (Columbus Instruments, Columbus, OH, USA). Before the start of the measurements, single-housed animals were acclimated to the cages for a period of 48 h. Feeding behaviour was assessed by real-time food intake. Oxygen consumption and carbon dioxide production were measured at 15-min intervals. Energy expenditure (EE) was calculated and normalized for lean body mass (LBM), as previously described (18). Spontaneous locomotor activity was determined by the measurement of beam breaks.

At sacrifice, visceral white adipose tissue (epididymal; eWAT), subcutaneous white adipose tissue (inguinal; iWAT), supraclavicular brown adipose tissue (BAT) and liver were weighed and collected for further processing.

Plasma analysis

Blood samples were collected from the tail tip of 4h-fasted mice (food removed at 9 am) using chilled paraoxon-coated capillaries. Blood glucose level was determined using a Glucometer (Accu-Check; Roche Diagnostics, Almere, The Netherlands) and plasma insulin level was measured using a commercial kit according to the instructions of the manufacturer (Chrystal Chem, Zaandam, The Netherlands). The homeostatic model assessment of insulin resistance (HOMA-IR) adapted to mice was calculated as ((glucose (mg/dl)*0.055) × (insulin (ng/ml) × 172.1))/3857 and used as a surrogate measure of whole-body insulin resistance (28). The plasma concentrations of alanine aminotransferase (ALAT) was measured using a Reflotron® kit (Roche diagnostics) using a pool of plasma samples from each group (n = 4-6 mice per group) in 2 separate experiments.

Glucose and insulin tolerance tests

Whole-body insulin sensitivity was determined by an i.p. insulin tolerance test (ipITT) at week 1 or week 3 of treatment, as described previously (18). In short, after an initial blood

collection (t = 0), an i.p. bolus of insulin (1 U/kg (lean) body mass of insulin (NOVORAPID, Novo Nordisk, Alphen aan den Rijn, Netherlands)) was administered to 4h-fasted mice. Blood glucose was measured by tail bleeding at 20, 40, 60, and 90 min after insulin administration using a Glucometer.

Whole-body glucose tolerance was assessed by an i.p. glucose tolerance test at week 3 of treatment, as previously reported (18). After an initial blood collection (t = 0), a glucose load (2 g/kg total body weight of D-Glucose (Sigma-Aldrich, Zwijndrecht, The Netherlands)) was administered to 6h-fasted mice, and blood glucose was measured by tail bleeding at 20, 40, 60, and 90 min after glucose administration using a Glucometer. In addition, blood was collected at t = 20 minutes post glucose injection for assessing glucose-induced insulin secretion.

Isolation of stromal vascular fraction from adipose tissue

Epididymal adipose tissues were collected at sacrifice after a one minute perfusion with PBS through the heart left ventricle and digested as described previously (18). In short, collected tissues were digested for 1 h at 37°C in HEPES buffer (pH 7.4) containing 0.5 g/L collagenase type I from *Clostridium histolyticum* (Sigma-Aldrich) and 2% (w/v) dialyzed bovine serum albumin (BSA, fraction V; Sigma-Aldrich). The disaggregated adipose tissue was passed through a 100 µm cell strainer that was washed with PBS supplemented with 2.5 mM EDTA and 5% FCS. After centrifugation (350 x g, 10 minutes at room temperature), the supernatant was discarded and the pellet was treated with erythrocyte lysis buffer. The cells were next washed with PBS supplemented with 2.5 mM EDTA and 5% FCS, and counted manually.

Isolation of leukocytes from liver tissue

Livers were collected and digested as described previously (18). In short, livers were minced and digested for 45 minutes at 37°C in RPMI 1640 + Glutamax (Life Technologies, Bleiswijk, The Netherlands) containing 1 mg/mL collagenase type IV from *Clostridium histolyticum*, 2000 U/mL DNase (both Sigma-Aldrich) and 1 mM $CaCl_2$. The digested liver tissues were passed through a 100 µm cell strainer that was washed with PBS/EDTA/FCS. Following centrifugation (530 x g, 10 minutes at 4°C), the supernatant was discarded, after which the pellet was resuspended in PBS/EDTA/FCS and centrifuged at 50 x g to pellet hepatocytes (3 minutes at 4°C). Next, supernatants were collected and pelleted (530 x g, 10 minutes at 4°C). The cell pellet was first treated with erythrocyte lysis buffer and next washed with PBS/EDTA/FCS. $CD45^+$ leukocytes were isolated using LS columns and CD45 MicroBeads (35 µL beads per liver, Miltenyi Biotec) according to manufacturer's protocol and counted manually.

Processing of isolated immune cells for flow cytometry

For analysis of macrophage and lymphocyte subsets, both WAT stromal vascular cells and liver leukocytes were stained with the live/dead marker Aqua (Invitrogen), fixed with

either 1.9% paraformaldehyde (Sigma-Aldrich) or the eBioscience™ Intracellular fixation and permeabilization kit (Invitrogen), and stored in FACS buffer (PBS, 0.02% sodium azide, 0.5% FCS) at 4°C in the dark until subsequent analysis. For analysis of cytokine production, isolated cells were cultured for 4 hours in culture medium in the presence of 100 ng/mL phorbol myristate acetate, 1 µg/mL ionomycin and 10 µg/mL Brefeldin A (all from Sigma-Aldrich). After culture, cells were washed with PBS, stained with Aqua, and fixed as described above.

Flow cytometry

For analysis of CD4 T cells and innate lymphoid cell (ILC) subsets, SVF cells were stained with antibodies against B220 (RA3-6B2), CD11b (M1/70), CD3 (17A2), CD4 (GK1.5), NK1.1 (PK136) and Thy1.2 (53-2.1; eBioscience, San Diego, CA, USA), and CD11c (HL3) and GR-1 (RB6-8C5; both BD Biosciences, San Jose, CA, USA). For analysis of ILC2s, antibodies against CD25 (PC61.5; eBioscience), T1/ST2 conjugated to biotin (DJ8; MD Bioscience) and streptavidin-APC (BD Biosciences) as second staining were additionally included.

CD4 T cell subsets and cytokine production by ILCs were analyzed following permeabilization with either 0.5% saponin (Sigma-Aldrich) or eBioscience™ Intracellular fixation and permeabilization kit. Subsets were identified using antibodies against CD11b, CD11c, GR-1, B220, NK1.1, CD3, CD45, CD4, Thy1.2, IL-4 (11B11), IL-13 (eBio13A), Foxp3 (FJK-16s; all eBioscience), IL-5 (TRFK5) and IFN-γ (XMG1.2; both Biolegend).

For analysis of macrophages, eosinophils, monocytes and neutrophils, cells were permeabilized as described above. Cells were then incubated with an antibody against YM1 conjugated to biotin (polyclonal; R&D Systems, Minneapolis, MN, USA), washed, and stained with streptavidin-PerCP (BD Biosciences), and antibodies directed against CD45, CD11b, CD11c (HL3 (BD Biosciences) or N418 (Biolegend)), F4/80 (BM8; eBioscience or Biolegend), SiglecF (E50-2440; BD Biosciences), and Ly6C (HK1.4; Biolegend).

All cells were stained and measured within 4 days post fixation. Flow cytometry was performed using a FACSCanto or LSR-II (both BD Biosciences), and gates were set according to Fluorescence Minus One (FMO) controls. Representative gating schemes are shown in Figure S1.

RNA purification and qRT-PCR

RNA was extracted from snap-frozen adipose tissue samples (~20 mg) using Tripure RNA Isolation reagent (Roche Diagnostics, Almere, The Netherlands). Total RNA (1 µg) was reverse transcribed and quantitative real-time PCR was then performed with SYBR Green Core Kit on a MyIQ thermal cycler (Bio-Rad) using specific primers sets (available on request). mRNA expression was normalized to ribosomal protein, large, P0 (RplP0) mRNA content and expressed as fold change compared to LFD-fed mice using the ΔΔCT method.

Hepatic triglyceride content

Liver lipids were extracted as previously described (29). Briefly, small liver samples were homogenized in ice-cold methanol. After centrifugation, lipids were extracted by addition of 1800 µl CH3OH:CHCl3 (1:3 v/v) to 45 µl homogenate, followed by vigorous vortexing and phase separation by centrifugation (14,000 rpm; 15 min at RT). The organic phase was dried and dissolved in 2% Triton X-100 in water. Triglycerides concentrations were measured using a commercially available enzymatic kit (Instruchemie, Delfzijl, the Netherlands) and expressed as nanomoles per mg protein, which was determined using the Bradford protein assay kit (Sigma-Aldrich).

Histological analysis

A piece of liver was fixed in 4% paraformaldehyde (PFA; Sigma-Aldrich), paraffin-embedded, sectioned at 4 µm and stained with Hematoxilin and Eosin (H&E), or Sirius Red to visualize collagen. Six fields at 20x magnification (total area 1.68 mm^2) were used for the analysis of hepatic steatosis in H&E-stained sections. On Sirius Red-stained sections, fibrosis was scored on 10 fields at 40x magnification (total area 1.23 mm^2) as absent (score 0), present in the perisinusoidal or periportal area (score 1), present in the perisinusoidal and periportal (score 2), bridging fibrosis (score 3) or cirrhosis (score 4) as described elsewhere (30).

Statistical analysis

All data are presented as mean ± standard error of the mean (SEM). Statistical analysis was performed using GraphPad Prism version 7.04 for Windows (GraphPad Software, La Jolla, CA, USA) with ordinary one-way analysis of variance (ANOVA) followed by Bonferroni post-hoc test. Differences between groups were considered statistically significant at $P < 0.05$.

RESULTS

Plant-produced recombinant omega-1 glycovariants reduce body weight and improve whole-body metabolic homeostasis in obese mice

To study the effects of recombinant ω1 glycovariants on whole-body metabolic homeostasis, C57BL/6J mice were fed a LFD or HFD for 12 weeks and next treated biweekly with intraperitoneal injections of 50 µg pWT-ω1, pLe^X-ω1 or PBS (vehicle-control) for 4 weeks. Both ω1 glycovariants induced a rapid and gradual body weight loss in HFD-fed mice (Fig. 1A-B), which was exclusively due to a decrease in fat mass (Fig. 1C) whereas lean mass was not affected (Fig. 1D). pWT/pLe^X-ω1 significantly reduced epididymal white adipose tissue (eWAT) mass but had no effect on liver, subcutaneous white adipose tissue (iWAT) and brown adipose tissue (BAT) masses (Fig. 1E). Using metabolic cages, we found that both ω1 glycovariants induced a significant decrease in cumulative food intake during

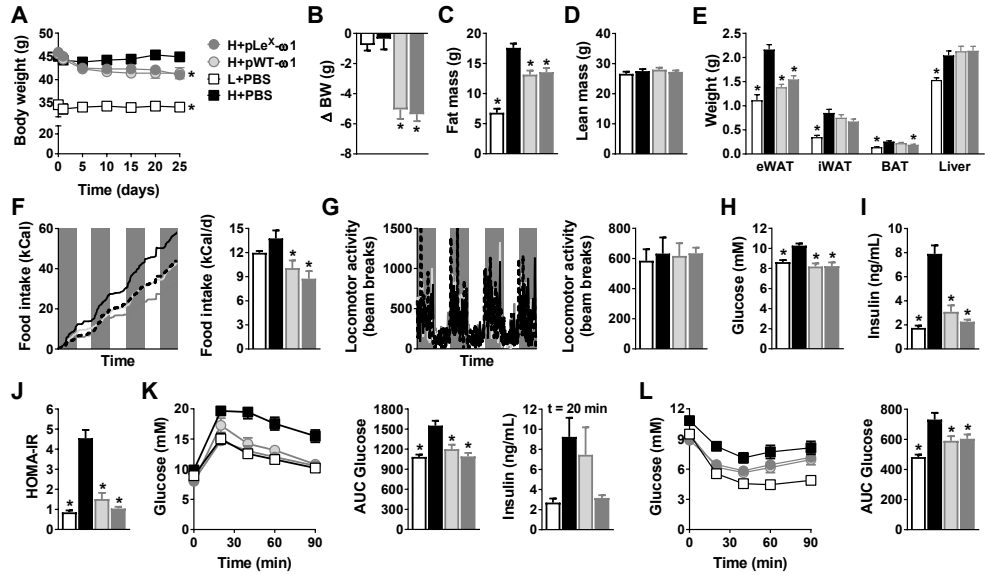

Figure 1. Plant-produced recombinant ω1 glycovariants reduce body weight, visceral fat mass and food intake in diet-induced obese mice. Mice were fed a LFD or a HFD for 12 weeks, after which they were treated i.p. with PBS, or 50 µg pWT-ω1 or pLe^X-ω1 once every 3 days for a period of 4 weeks. Body weight was monitored throughout the experimental period (*A-B*). Body composition (*C-D*) and weight of epididymal WAT (eWAT), inguinal WAT (iWAT), instrascapular brown adipose tissue (BAT) and the liver (*E*) were measured after 4 weeks of treatment. Food intake was assessed using fully automated single-housed metabolic cages during the first week of treatment (*F*). Locomotor activity was determined by measuring by beam breaks (*G*). Blood glucose (*H*) and plasma insulin levels (*I*) were determined in 4h-fasted mice during week 4 of treatment and HOMA-IR was calculated (*J*). An i.p. glucose tolerance test (2 g/kg body weight) was performed in 6h-fasted mice at week 3 of treatment. Blood glucose levels were measured at the indicated time points and the AUC of the glucose excursion curve was calculated (*K*). Blood was also collected for determination of glucose-induced insulin secretion at t = 20 minutes post glucose injection (*K*). An i.p. insulin tolerance test (1U/kg lean body mass) was performed in 4h-fasted mice at week 3 of treatment. Blood glucose levels were measured at the indicated time points and the area under the curve (AUC) of the glucose excursion curve was calculated (*L*). Data shown are a pool of 2 (D) or 4 (A-E, H-L) independent experiments. Results are expressed as means ± SEM. * *P*<0.05 *vs* HFD (n = 12-20 animals per group in A-E, K-L, and 4-13 animals per group in F-J).

the experimental period (Fig. 1F). Consequently, mean daily energy intake was reduced to the same extent while locomotor activity was not affected (Fig. 1G).

We next investigated the effects of pWT/pLe^X-ω1 on whole-body metabolic homeostasis. As expected, HFD-feeding increased fasting blood glucose, plasma insulin and homeostatic model assessment of insulin resistance (HOMA-IR) as compared to LFD-fed mice (Fig. 1H-J). Remarkably, treatment with both ω1 glycovariants for 4 weeks significantly reduced blood glucose and insulin in obese mice to the levels of LFD-fed lean mice (Fig. 1H-I). As a result, HOMA-IR was significantly reduced in ω1-treated mice, indicating a better insulin sensitivity with a trend towards a stronger effect induced by

the recombinant molecule harbouring single branch Le^X (Fig. 1J). Congruent with these data, we observed a significant improvement in whole-body glucose tolerance (Fig. 1K) and insulin sensitivity (Fig. 1L) in both pWT and pLe^X-ω1-treated obese mice. Of note, the effects of these two ω1 glycovariants on plasma metabolic parameters and whole-body insulin sensitivity were already observed after one week of treatment, although there was only marginal impact on body weight and fat mass at this time point (Fig. S2). Furthermore, the improvement of metabolic homeostasis was found to be dose-dependent, at least for pLe^X-ω1 (Fig. S3). Altogether, these data show that both recombinant ω1 glycovariants improve whole-body metabolic homeostasis in insulin-resistant obese mice.

Omega-1 glycovariants increase adipose tissue Th2 cells, eosinophils and alternatively-activated macrophages, but not ILC2s

An ILC2-eosinophil-AAM axis contributes to the maintenance of adipose tissue insulin sensitivity in homeostatic conditions and is disrupted during obesity (14, 15). To investigate whether the beneficial metabolic effects induced by ω1 glycovariants could be due to an increase in these type 2 immune cells, we isolated the stromal vascular fraction (SVF) from eWAT and analysed the immune cell composition by flow cytometry (Fig. S1). We found that both ω1 glycovariants markedly increased WAT CD4 T cells, with pWT-ω1 being more potent than pLe^X-ω1, while total ILCs were unaffected (Fig. 2A). Interestingly, *ex vivo* restimulation revealed a specific increase in IL-4/5/13-expressing Th2 cells, while the other CD4 T cell subsets, *i.e.* regulatory T cells (Treg) and Th1 cells, were not affected (Fig. 2B). In addition, we confirmed that HFD reduced WAT IL-5$^+$/IL-13$^+$ ILC2s, as previously reported (14), an effect that was even further pronounced with ω1 glycovariants (Fig. 2C).

The type 2 cytokines IL-5 and IL-13 produced by either ILC2s and/or Th2 cells have been reported to maintain WAT eosinophils (14). Congruent with our data on Th2 cells, we found a potent increase in WAT eosinophils upon ω1 treatment that was of similar extent for both glycovariants (Fig. 2D). Finally, both pWT-ω1 and pLe^X-ω1 increased WAT Ym1$^+$ AAMs while the pro-inflammatory CD11c$^+$ macrophages were not affected, shifting the balance of cell polarization towards a M2/M(IL-4)-like phenotype (Fig. 2E-H). A similar immune response was already observed after one week of treatment with ω1 glycovariants (Fig. S4) and appears to be dose-dependent (Fig. S5).

Omega-1 glycovariants do not induce WAT beiging

Although the concept was recently challenged (31), AAMs have been suggested to trigger WAT beiging through production of catecholamines, thereby increasing energy expenditure (32-34). Since WAT AAMs were significantly increased in ω1-treated obese mice, we investigated whether the ω1 glycovariants could induce WAT beiging and therefore enhance adaptive thermogenesis and energy expenditure. We found that the recombinant molecules neither increased *Ucp1* or other beiging gene markers mRNA expression in both epididymal and subcutaneous (inguinal) fat pads (Fig. 3A-B), nor

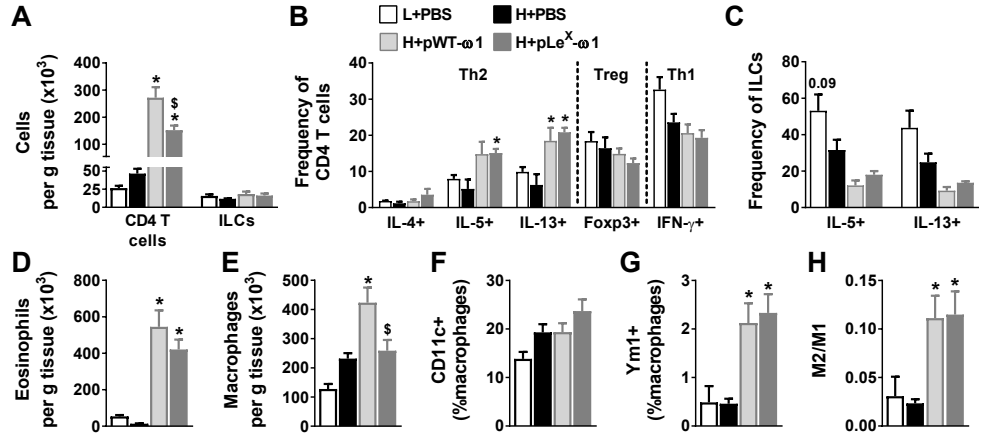

Figure 2. **ω1 glycovariants increase WAT Th2 cells, eosinophils and AAM, without affecting ILCs.** Mice were fed a LFD or a HFD and were treated with PBS or pWT/pLe^X-ω1 as described in the legend of Figure 1. At sacrifice (week 4 of treatment), eWAT was collected and the stromal vascular fraction (SVF) was isolated. Following fixation and permeabilization, SVF cells were stained and analyzed by flow cytometry. The complete gating strategy is shown in Figure S1. Numbers per gram tissue CD4 T cells, ILCs (*A*), eosinophils (*D*) and macrophages (*E*) were determined. Intracellular cytokine production was analyzed after 4h stimulation with PMA and ionomycin in the presence of Brefeldin A. CD4 T cells were identified as Aqua$^-$CD45$^+$Thy1.2$^+$Lineage$^+$CD4$^+$ cells, and ILCs were identified as Aqua$^-$CD45$^+$Thy1.2$^+$Lineage$^-$CD3$^-$CD4$^-$ cells, in which the lineage cocktail included antibodies against CD11b, CD11c, B220, GR-1, NK1.1 and CD3. Frequencies of CD4 T helper subsets (*B*) and cytokine-expressing ILCs (*C*) were determined. Percentages of CD11c$^+$Ym1$^-$ (M1-like; *F*) and CD11c$^-$Ym1$^+$ (M2-like; *G*) in macrophages. Using the percentages of M1-like and M2-like macrophages, M2/M1 ratios were calculated (*H*). Data shown are a pool of at least three independent experiments, except for C and E, which are a representative experiment of at least two independent experiments. Results are expressed as means ± SEM. * P<0.05 *vs* HFD, $ P<0.05 *vs* pWT-ω1 (n = 6-19 animals per group in A-B, D, F-I, and 3-9 animals per group in C and E).

the whole-body energy expenditure measured in metabolic cages (Fig. 3C), indicating that ω1 does not induce canonical or non-canonical WAT beiging in our conditions.

STAT6-mediated type 2 immunity is not required for the effects of pLe^X-ω1 on metabolic homeostasis

Induction of AAM polarization is a classical feature of type 2 immunity which usually occurs through IL-4/IL-13 receptor-mediated signalling and requires the transcription factor STAT6 (35, 36). In order to assess whether type 2 immunity is required for the metabolic effects of ω1, we therefore used Stat6-deficient mice. As expected, while pLe^X-ω1 increased WAT Th2 cells and AAMs in WT mice, this specific type 2 immune response was abrogated in Stat6$^{-/-}$ mice (Fig. 4A-B). However, treatment with pLe^X-ω1 still reduced body weight (Fig. 4C) and food intake (Fig. 4D) in Stat6$^{-/-}$ obese mice to the same extent as in WT mice. In addition, while pLe^X-ω1 did not significantly affect fasting blood glucose levels, both insulin levels and HOMA-IR were markedly decreased in both genotypes (Fig. 4E-G).

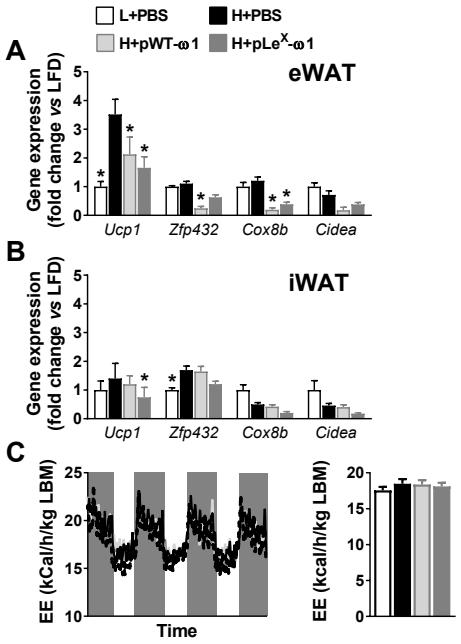

Figure 3. **ω1 glycovariants do not induce WAT beiging.** Mice were fed a LFD or a HFD and were treated with PBS or pWT/pLe^{X}-ω1 as described in the legend of Figure 1. At sacrifice, mRNA expression in eWAT (*A*) and iWAT (*B*) of the indicated genes was quantified by RT-PCR and expressed relative to the *RplP0* gene as fold difference compared to the LFD-fed mice. Energy expenditure, corrected for lean body mass, was measured using fully automated single-housed metabolic cages during the first week of treatment (*C*). Data shown are a pool of two independent experiments. Results are expressed as means ± SEM. * $P<0.05$ *vs* HFD (n = 4-10 animals per group).

Moreover, the improvements in whole-body glucose tolerance (Fig. 4H-I) and insulin sensitivity (Fig. 4J) was still observed in Stat6$^{-/-}$ mice, indicating that pLe^{X}-ω1 restored metabolic homeostasis in obese mice independent of its Th2-inducing capacity.

Omega-1 glycovariants do not affect hepatic steatosis, but increase fibrotic gene markers and liver damage

Similar to WAT, maintenance of hepatic insulin sensitivity is also associated with type 2 immunity (37). On the other hand, obesity-driven activation of Kupffer cells increases the recruitment of pro-inflammatory monocytes and triggers hepatic insulin resistance (2, 11). In our conditions, while pWT/pLe^{X}-ω1 increased Th2 cells in the liver, we surprisingly did not find alternative activation of Kupffer cells (Fig. 5A-D). Instead, the ω1 glycovariants increased the number of CD11c^{+} pro-inflammatory Kupffer cells (Fig. 5E-F) and newly recruited monocytes (Fig. 5G). However, ω1 glycovariants did not affect hepatic steatosis, as assessed by histomorphologic assessment of hematoxylin and eosin (H&E)-stained liver sections (Fig. 5H-I) and tissue triglycerides content (Fig. 5J).

In addition to ectopic lipid deposition in the liver during NAFLD, increased inflammation, hepatocyte damage and fibrosis may characterize progression towards non-alcoholic steatohepatitis (NASH) (38). IL-13 has recently also been implicated to play a role in the development of liver fibrosis (39, 40), hence we investigated whether ω1 glycovariants affect liver fibrosis. pLe^{X}-ω1 significantly increased fibrotic gene marker expression (Fig. 5K), while no clinical fibrosis was detected (Fig. 5L). However, we observed an increase in circulating alanine transaminase levels (Fig. 5M), which indicates enhanced liver damage.

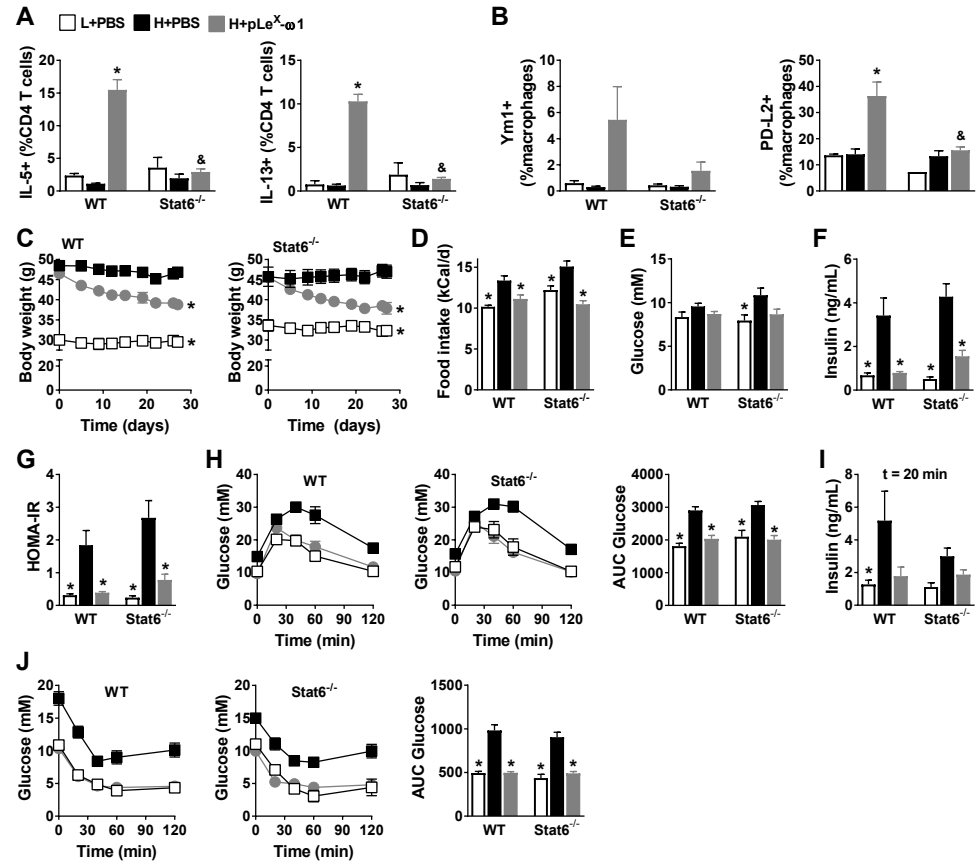

Figure 4. **STAT6 is not required for metabolic effects of pLe^{X}-ω1.** WT and Stat6-/- mice on a C57BL/6J background were fed a LFD or a HFD for 12 weeks before 4 weeks of biweekly intraperitoneal injections with PBS or 50 µg pLe^{X}-ω1. At the end of the experiment (week 4 of treatment), eWAT was collected, processed and analyzed as described in the legend of Figure 2. The frequencies of cytokine-expressing CD4 T cells were determined (*A*). Abundances of Ym1^{+} or PD-L2^{+} (M2-like) macrophages (*B*) were determined. Body weight (*C*) and food intake (*D*) was monitored throughout the experimental period. Blood glucose (*E*) and plasma insulin levels (*F*) were determined and HOMA-IR (*G*) was calculated as described in the legend of Figure 1. An i.p. glucose tolerance test (2 g/kg body weight; *H-I*) and i.p. insulin tolerance test (1U/kg body weight; *J*) were performed as described in the legend of Figure 1. Results are expressed as means ± SEM. *$P<0.05$ *vs* HFD, & $P<0.05$ *vs* WT (n = 3-5 animals per group for all measurements).

To investigate the role of type 2 immunity in the pro-fibrotic effects of pLe^{X}-ω1, we used Stat6-deficient mice. As expected, the increase in liver IL-13^{+} Th2 cells in response to pLe^{X}-ω1 was markedly reduced in Stat6-deficient mice (Fig. 5N). In line with this data, the increase in hepatic IL-13 gene expression induced by pLe^{X}-ω1 was also significantly reduced in obese Stat6$^{-/-}$ mice as compared to WT (Fig. 5O). Although pLe^{X}-ω1 still induced expression of fibrotic gene markers in Stat6-deficient mice, there was a marked decrease in expression as compared to WT mice (Fig. 5O), suggesting that recombinant

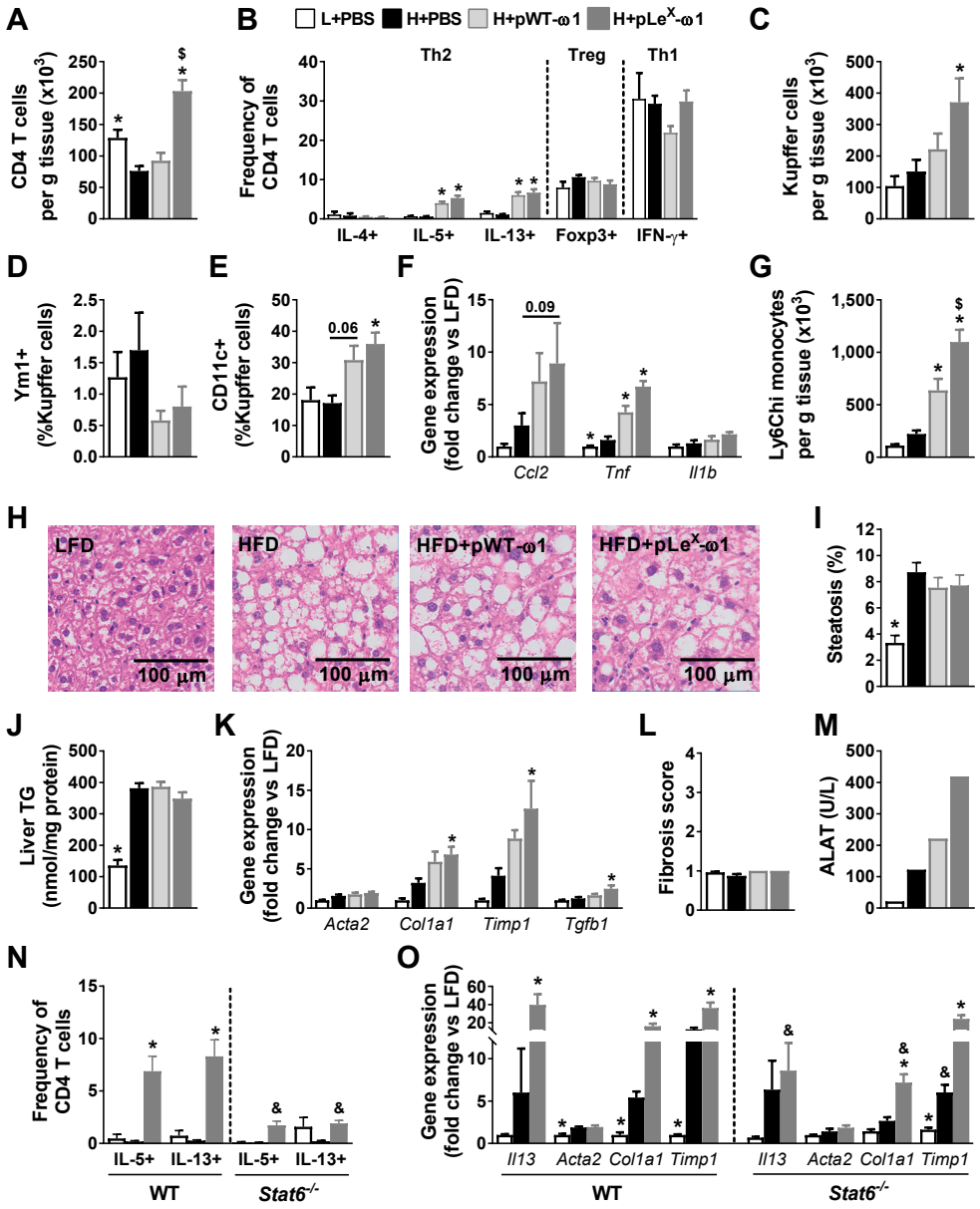

Figure 5. ω1 glycovariants do not affect hepatic steatosis, but increase fibrotic gene markers and liver damage. Mice were fed a LFD or a HFD and were treated with PBS or pWT/pLe^{X}-ω1 as described in the legend of Figure 1. At sacrifice, a small piece of liver was immediately snap-frozen for qPCR and liver lipid content analyses, and another piece was used for H&E staining. From the remaining liver, CD45^{+} liver cells were isolated and analyzed by flow cytometry. The cell numbers per gram tissue and abundances of CD4 T cells (*A*) and T helper subsets (*B*), Kupffer cells (*C*), macrophage phenotypes (*D-E*) and Ly6C^{hi} monocytes (*G*) were determined. mRNA expression of the indicated genes was analysed as described in the legend of figure 3 (*F*). H&E slides of the liver (*H*) were used for determining hepatic steatosis (*I*). Liver triglycerides were determined (*J*). mRNA expression of the indicated genes was analysed as described in the legend of Figure 3 (*K*). Sirius Red-stained sections were scored for fibrosis (*L*). Plasma alanine aminotransferase levels (*M*) were determined. WT and Stat6-/- mice were fed a LFD or a HFD and were treated as described in the legend of Figure 4. Frequencies of IL-5/IL-13-expressing CD4 T cells were determined (*N*). mRNA expression of the indicated genes was analysed as described in the legend of figure 3 (*O*). Data shown are a pool of at least two independent experiments, except for N-O. Results are expressed as means ± SEM. * $P<0.05$ *vs* HFD, $ $P<0.05$ *vs* pWT-ω1 (n 5=18 animals per group in A-M, and 3-5 animals per group in N-O).

ω1 induces fibrotic gene markers at least partly through type 2 immunity. Taken together, these results show that recombinant ω1 glycovariants improve whole-body metabolic homeostasis independent of their Th2 inducing capacity, while simultaneously inducing early markers of mild hepatic fibrosis.

DISCUSSION

Type 2 immunity is involved in the maintenance of metabolic homeostasis and its disruption during obesity promotes chronic low-grade inflammation, associated with insulin resistance (1). Since helminths induce type 2 immunity, the association between helminths and their potential effects on insulin sensitivity and glucose homeostasis has gained increasing attention (41), accompanied by the search for single helminth-derived molecules that are capable of driving the type 2 immune response (20). The glycoprotein omega-1, a T2 ribonuclease which is secreted from *S. mansoni* eggs, has previously been identified as the major immunomodulatory component in SEA (23, 24) and was shown to condition dendritic cells to prime Th2 responses, as least partly through its glycan-mediated uptake and intracellular RNase activity (24). Here, we report that two plant-produced recombinant ω1 glycovariants induced a rapid and sustained reduction in body weight and improved HOMA-IR, whole-body insulin sensitivity and glucose tolerance in obese mice. Although both ω1 glycovariants induced a strong type 2 immune response in WAT, characterized by a significant increase in Th2 cells, eosinophils and AAMs, the beneficial effect on metabolic homeostasis was still present in Stat6-deficient obese mice, indicating that improvements of insulin sensitivity and glucose tolerance occurred independently of the Th2-inducing capacity of ω1. These findings indicate that helminth derived molecules may act through multiple distinct pathways that can improve metabolic homeostasis. Interestingly, a trend for a stronger effect on insulin sensitivity was observed with pLe^{X}–ω1, whose glycans resemble the ones of native helminth ω1 the most, whereas the improvement of glucose tolerance was similar to pWT–ω1.

A recent study from Hams et al. reported that acute treatment of HFD-fed obese mice with HEK-293-produced recombinant ω1 induced long-lasting weight loss, and improved glucose tolerance by a mechanism involving IL-33-mediated increase in WAT ILC2s and adipose beiging (25). However, in contrast to this finding, we only observed a slight increase in IL-33 expression in eWAT (data not shown) and no increase in WAT

ILC2s after either one, or four weeks of treatment with plant-produced ω1 glycovariants. Moreover, we did not find any evidence of WAT beiging in both eWAT and iWAT from obese mice treated with ω1 glycovariants. Importantly, it should be noted that despite similar RNase activities when compared to native ω1 (27), the recombinant ω1 produced by HEK-293 cells and the glyco-engineered ones from tobacco plants harbor significantly different N-glycosylation patterns (23, 24). Finally, on top of differences in treatment regimen (2 injections in 4 days *versus* bi-weekly injection for 4 weeks in our study), it is worth mentioning that in Hams et al. the effects of HEK-produced ω1 were compared to the effects of ovalbumin (25), which is an immunomodulatory molecule by itself, differing significantly from our experimental condition where a neutral vehicle (PBS) was used as control.

Both ω1 glycovariants were found to induce a type 2 immune response in WAT, characterized by a significant increase in Th2 cells, eosinophils and AAMs. In our study, as previously described for SEA (18), the ω1-induced increase in type 2 cytokines was shown to be clearly derived from $CD4^+$ T cells, not ILC2s. Our data indicate that both pWT–ω1 and pLe^X–ω1 require Th2 cells, rather than ILC2s to induce WAT eosinophilia and AAM polarization. It was previously shown that pLe^X–ω1, compared to pWT-ω1, induced a stronger Th2 polarization *in vivo* using a footpad immunization model in mice (27). In our conditions, both glycovariants induced a similar increase in the percentage of Th2 cells in metabolic tissue from obese mice, whereas pLe^X–ω1 increased total $CD4^+$ T cells to a greater extent in the liver and to a lesser extent in WAT when compared to pWT-ω1. Altogether, this suggests that the glycosylation pattern of ω1 might induce tissue-specific differences in total Th2 cells.

In the liver, ω1 glycovariants increased IL-13-producing Th2 cells but, unlike SEA (18), promoted CD11c expression in Kupffer cells while not affecting the expression of Ym1, suggesting that macrophages are rather polarized towards a pro-inflammatory state. Of note, ω1 glycovariants also increased hepatic expression of fibrotic gene markers and circulating ALAT levels, both indicating increased liver damage. Interestingly, the pLe^X–ω1-induced increase in liver IL-13^+ Th2 cells and hepatic IL-13 gene expression were markedly reduced in Stat6-deficient mice, which was accompanied by a decreased expression of fibrotic gene markers. Collectively, these findings confirmed previous studies in which IL-13 was shown to play a role in the development of liver fibrosis (39, 40).

As the type 2 immune response seems not to be significantly involved in the beneficial metabolic effects of ω1, the question of the underlying mechanism(s) remains. Interestingly, we found that treatment with both ω1 glycovariants significantly reduced food intake, with a trend for pLe^X–ω1 being more potent than pWT–ω1. Furthermore, this anorexigenic effect of ω1, which was not observed previously when mice were chronically infected with *S. mansoni* or treated with SEA (18), was dose-dependent (already detectable at a concentration of 10 µg) and also present in Stat6-deficient mice. Altogether, these findings lead us to the hypothesis that the beneficial metabolic effects of ω1 might be mediated through a reduction in food intake, rather than an increase in type 2 immune

cells. Of note, in the study from Hams et al. using HEK-produced ω1, the authors claimed that treatment with this recombinant molecule in obese mice did not significantly affect food intake, but unfortunately these crucial data were not shown (25).

Since both locomotor activity and lean body mass were not affected by ω1, we also conclude that the reduced food intake was not related to wasting or illness (as reviewed in (42)). In order to assess the contribution of reduced food intake to the metabolic benefits of recombinant ω1, paired-feeding could be used in future studies. In addition, in search for underlying mechanisms, it will be important to study the biodistribution of ω1 using labeled molecules, notably to investigate whether the molecules can be detected in brain areas known to be involved in the control of food intake, such as the hypothalamus (43). In line with this, it would be interesting to assess the effect of ω1 on the hypothalamic expression of anorexigenic (e.g. POMC, CART) and orexigenic (e.g. NPY, AgRP) peptides.

In conclusion, our work has revealed that the improvement of metabolic homeostasis in insulin-resistant obese mice by plant-produced recombinant ω1 glycovariants is independent of their Th2-inducing capacities.

Our current hypotheses are that the beneficial metabolic effects of ω1 could be explained by brain-mediated food intake and/or immune-independent direct interaction of ω1 with metabolic cells. Further studies are undoubtedly required to unravel these underlying mechanisms. Of note, with regards to the therapeutic potential of ω1 as treatment for metabolic disorders, it is important to cautiously underline that recombinant ω1 induced early markers of mild hepatic fibrosis, by a mechanism partly mediated through ω1-induced type 2 immunity.

REFERENCES

1. Donath MY, Shoelson SE. Type 2 diabetes as an inflammatory disease. Nat Rev Immunol 2011; 11(2): 98-107.
2. Lackey DE, Olefsky JM. Regulation of metabolism by the innate immune system. Nat Rev Endocrinol 2016; 12(1): 15-28.
3. Heilbronn LK, Campbell LV. Adipose tissue macrophages, low grade inflammation and insulin resistance in human obesity. Curr Pharm Des 2008; 14(12): 1225-30.
4. Kolb H, Mandrup-Poulsen T. The global diabetes epidemic as a consequence of lifestyle-induced low-grade inflammation. Diabetologia 2010; 53(1): 10-20.
5. Lumeng CN, DelProposto JB, Westcott DJ, Saltiel AR. Phenotypic switching of adipose tissue macrophages with obesity is generated by spatiotemporal differences in macrophage subtypes. Diabetes 2008; 57(12): 3239-46.
6. Obstfeld AE, Sugaru E, Thearle M, et al. C-C chemokine receptor 2 (CCR2) regulates the hepatic recruitment of myeloid cells that promote obesity-induced hepatic steatosis. Diabetes 2010; 59(4): 916-25.
7. Morinaga H, Mayoral R, Heinrichsdorff J, et al. Characterization of distinct subpopulations of hepatic macrophages in HFD/obese mice. Diabetes 2015; 64(4): 1120-30.
8. Fink LN, Oberbach A, Costford SR, et al. Expression of anti-inflammatory macrophage genes within skeletal muscle correlates with insulin sensitivity in human obesity and type 2 diabetes. Diabetologia 2013; 56(7): 1623-8.
9. Fink LN, Costford SR, Lee YS, et al. Pro-inflammatory macrophages increase in skeletal muscle of high fat-fed mice and correlate with metabolic risk markers in humans. Obesity (Silver Spring) 2014; 22(3): 747-57.
10. Kratz M, Coats BR, Hisert KB, et al. Metabolic dysfunction drives a mechanistically distinct proinflammatory phenotype in adipose tissue macrophages. Cell Metab 2014; 20(4): 614-25.
11. Lanthier N, Molendi-Coste O, Horsmans Y, van Rooijen N, Cani PD, Leclercq IA. Kupffer cell activation is a causal factor for hepatic insulin resistance. Am J Physiol Gastrointest Liver Physiol 2010; 298(1): G107-16.
12. Talukdar S, Oh DY, Bandyopadhyay G, et al. Neutrophils mediate insulin resistance in mice fed a high-fat diet through secreted elastase. Nat Med 2012; 18(9): 1407-12.
13. Cai D, Yuan M, Frantz DF, et al. Local and systemic insulin resistance resulting from hepatic activation of IKK-beta and NF-kappaB. Nat Med 2005; 11(2): 183-90.
14. Molofsky AB, Nussbaum JC, Liang HE, et al. Innate lymphoid type 2 cells sustain visceral adipose tissue eosinophils and alternatively activated macrophages. J Exp Med 2013; 210(3): 535-49.
15. Wu D, Molofsky AB, Liang HE, et al. Eosinophils sustain adipose alternatively activated macrophages associated with glucose homeostasis. Science 2011; 332(6026): 243-7.
16. Maizels RM, Yazdanbakhsh M. Immune regulation by helminth parasites: cellular and molecular mechanisms. Nature reviews Immunology 2003; 3(9): 733-44.
17. Wiria AE, Hamid F, Wammes LJ, et al. Infection with Soil-Transmitted Helminths Is Associated with Increased Insulin Sensitivity. PLoS One 2015; 10(6): e0127746.
18. Hussaarts L, Garcia-Tardon N, van Beek L, et al. Chronic helminth infection and helminth-derived egg antigens promote adipose tissue M2 macrophages and improve insulin sensitivity in obese mice. FASEB journal : official publication of the Federation of American Societies for Experimental Biology 2015; 29(7): 3027-39.
19. Okano M, Satoskar AR, Nishizaki K, Abe M, Harn DA, Jr. Induction of Th2 responses and IgE is largely due to carbohydrates functioning as adjuvants on Schistosoma mansoni egg antigens. J Immunol 1999; 163(12): 6712-7.
20. Hussaarts L, Yazdanbakhsh M, Guigas B. Priming dendritic cells for th2 polarization: lessons learned from helminths and implications for metabolic disorders. Front Immunol 2014; 5: 499.
21. Ritter M, Gross O, Kays S, et al. Schistosoma mansoni triggers Dectin-2, which activates the Nlrp3 inflammasome and alters adaptive immune responses. Proc Natl Acad Sci U S A 2010; 107(47): 20459-64.
22. Kaisar MMM, Ritter M, Del Fresno C, et al. Dectin-1/2-induced autocrine PGE2 signaling licenses dendritic cells to prime Th2 responses. PLoS Biol 2018; 16(4): e2005504.
23. Everts B, Perona-Wright G, Smits HH, et al. Omega-1, a glycoprotein secreted by Schistosoma mansoni eggs, drives Th2 responses. J Exp Med 2009; 206(8): 1673-80.
24. Everts B, Hussaarts L, Driessen NN, et al. Schistosome-derived omega-1 drives Th2 polarization by suppressing protein synthesis following internalization by the mannose receptor. J Exp Med 2012; 209(10): 1753-67, S1.
25. Hams E, Bermingham R, Wurlod FA, et al. The helminth T2 RNase omega1 promotes metabolic homeostasis in an IL-33- and group 2 innate lymphoid cell-dependent mechanism. FASEB journal : official publication of the Federation of American Societies for Experimental Biology 2016; 30(2): 824-35.
26. Hokke CH, Yazdanbakhsh M. Schistosome glycans and innate immunity. Parasite Immunol 2005; 27(7-8): 257-64.
27. Wilbers RH, Westerhof LB, van Noort K, et al. Production and glyco-engineering of immunomodulatory helminth glycoproteins in plants. Sci Rep 2017; 7: 45910.
28. Lee S, Muniyappa R, Yan X, et al. Comparison between surrogate indexes of insulin sensitivity and resistance and hyperinsulinemic euglycemic clamp estimates in mice. Am J Physiol Endocrinol Metab 2008; 294(2): E261-70.
29. Geerling JJ, Boon MR, van der Zon GC, et al. Metformin lowers plasma triglycerides by promoting VLDL-triglyceride clearance by brown adipose tissue in mice. Diabetes 2014; 63(3): 880-91.
30. Kleiner DE, Brunt EM, Van Natta M, et al. Design and validation of a histological scoring system for nonalcoholic fatty liver disease. Hepatology 2005; 41(6): 1313-21.
31. Fischer K, Ruiz HH, Jhun K, et al. Alternatively activated macrophages do not synthesize catecholamines or contribute to adipose tissue adaptive thermogenesis. Nat Med 2017; 23(5): 623-30.
32. Nguyen KD, Qiu Y, Cui X, et al. Alternatively activated macrophages produce catecholamines to sustain adaptive thermogenesis. Nature 2011; 480(7375): 104-8.
33. Qiu Y, Nguyen KD, Odegaard JI, et al. Eosinophils and type 2 cytokine signaling in macrophages orchestrate development of functional beige fat. Cell 2014; 157(6): 1292-308.
34. Lee MW, Odegaard JI, Mukundan L, et al. Activated type 2 innate lymphoid cells regulate beige fat biogenesis. Cell 2015; 160(1-2): 74-87.
35. Loke P, Allison JP. PD-L1 and PD-L2 are differentially regulated by Th1 and Th2 cells. Proc Natl Acad Sci U S A 2003; 100(9): 5336-41.
36. Huber S, Hoffmann R, Muskens F, Voehringer D. Alternatively activated macrophages inhibit T-cell proliferation by Stat6-dependent expression of PD-L2. Blood 2010; 116(17): 3311-20.
37. Ricardo-Gonzalez RR, Red Eagle A, Odegaard JI, et al. IL-4/STAT6 immune axis regulates peripheral nutrient metabolism and insulin sensitivity. Proc Natl Acad Sci U S A 2010; 107(52): 22617-22.
38. Koyama Y, Brenner DA. Liver inflammation and fibrosis. J Clin Invest 2017; 127(1): 55-64.
39. Gieseck RL, 3rd, Ramalingam TR, Hart KM, et al. Interleukin-13 Activates Distinct Cellular Pathways Leading to Ductular Reaction, Steatosis, and Fibrosis. Immunity 2016; 45(1): 145-58.
40. Hart KM, Fabre T, Sciurba JC, et al. Type 2 immunity is protective in metabolic disease but exacerbates NAFLD collaboratively with TGF-beta. Sci Transl Med 2017; 9(396).
41. de Ruiter K, Tahapary DL, Sartono E, et al. Helminths, hygiene hypothesis and type 2 diabetes. Parasite immunology 2017; 39(5).
42. Morton GJ, Meek TH, Schwartz MW. Neurobiology of food intake in health and disease. Nat Rev Neurosci 2014; 15(6): 367-78.
43. Li Z, Yi CX, Katiraei S, et al. Butyrate reduces appetite and activates brown adipose tissue via the gut-brain neural circuit. Gut 2018; 67(7): 1269-79.

SUPPLEMENTAL DATA

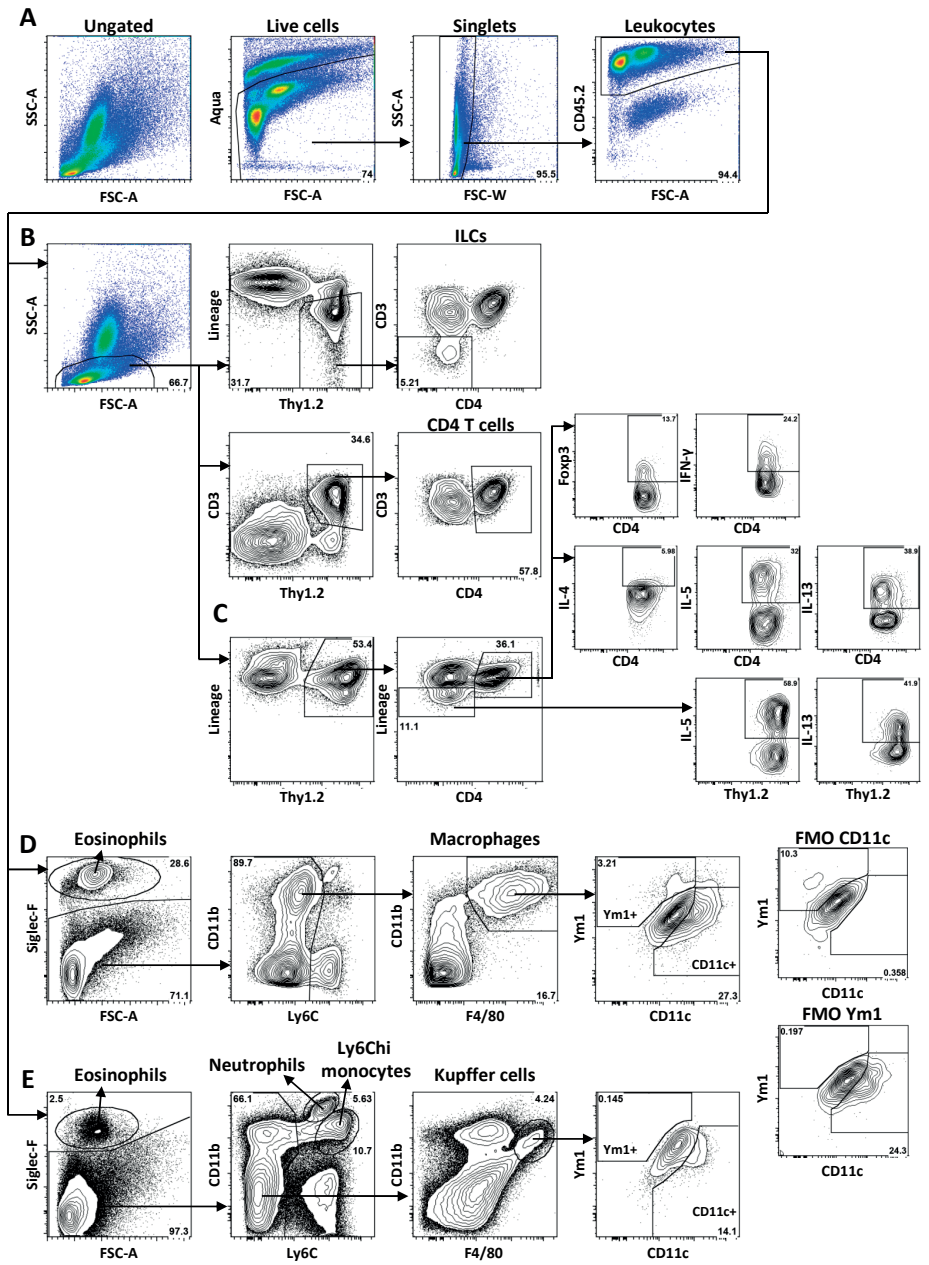

Supplementary Figure S1. Gating strategies. Isolated cells were pre-gated on Aqua$^-$CD45$^+$ single cells (*A*). The gating strategy for analysis of ILCs, CD4 T cells (*B*), CD4 T helper subsets and intracellular cytokine expression (*C*) is shown. Here, the lineage channel includes antibodies against CD11b, CD11c, B220, GR-1, NK1.1 and CD3. Representative samples were chosen from eWAT samples; gating strategies for lymphocyte subsets were similar in liver samples. The gating strategy is shown for eosinophils, CD11c$^+$Ym1$^-$ M1-like macrophages and CD11c$^-$Ym1$^+$ M2-like macrophages in eWAT, including Fluorescence Minus One (FMO) controls for CD11c and Ym1 (*D*). The gating strategy for liver eosinophils, neutrophils, Ly6Chi monocytes, CD11c$^+$Ym1$^-$ Kupffer cells and CD11c$^-$Ym1$^+$ Kupffer cells is shown (*E*).

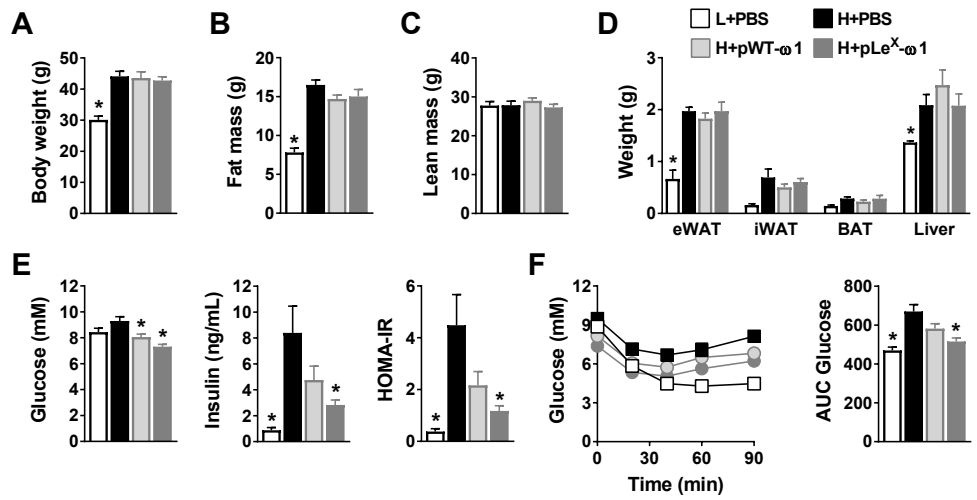

Supplementary Figure S2. ω1 glycovariants improve whole-body insulin sensitivity after one week of treatment, without affecting body composition. Mice were fed a LFD or a HFD for 12 weeks, after which they were treated i.p. with PBS or 50 µg pWT/pLe^X-ω1 once every 2 days for 1 week. Body weight was monitored throughout the experimental period (*A*). Body composition (*B-C*) and weights of different fat pads and the liver (*D*) were measured after 1 week of treatment. Blood glucose and plasma insulin levels were determined and HOMA-IR was calculated as described in the legend of Figure 1 (*E*). An i.p. insulin tolerance test was performed as described in the legend of Figure 1 (*F*). Results are expressed as means ± SEM. * $P<0.05$ *vs* HFD (n = 4-9 animals per group in A-E).

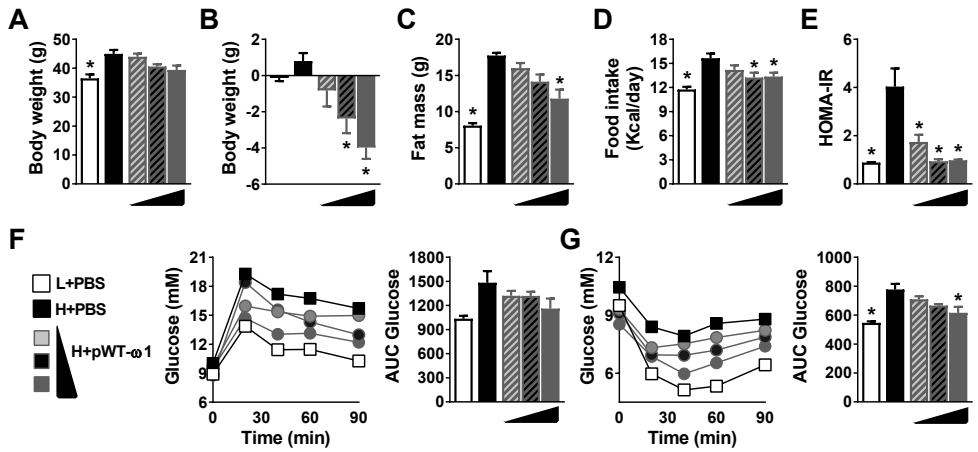

Supplementary Figure S3. pLe^{X}-ω1 improves whole-body insulin sensitivity and glucose tolerance in a dose-dependent manner. Mice were fed a LFD or a HFD and were treated i.p. with PBS or 10 µg, 25 µg or 50 µg pLe^{X}-ω1 every three days for four weeks. Body weight (*A-B*) and body composition (*C*) were determined after four weeks of treatment. Food intake was monitored throughout the treatment period (*D*). Blood glucose (*E*) and plasma insulin levels (*F*) were determined and HOMA-IR (*G*) was calculated as described in the legend of Figure 1. An i.p. glucose tolerance test (2 g/kg body weight; *H-I*) and i.p. insulin tolerance test (1U/kg lean body mass; *J*) were performed as described in the legend of Figure 1. Results are expressed as means ± SEM. * *P*<0.05 *vs* HFD (n = 3-4 animals per group).

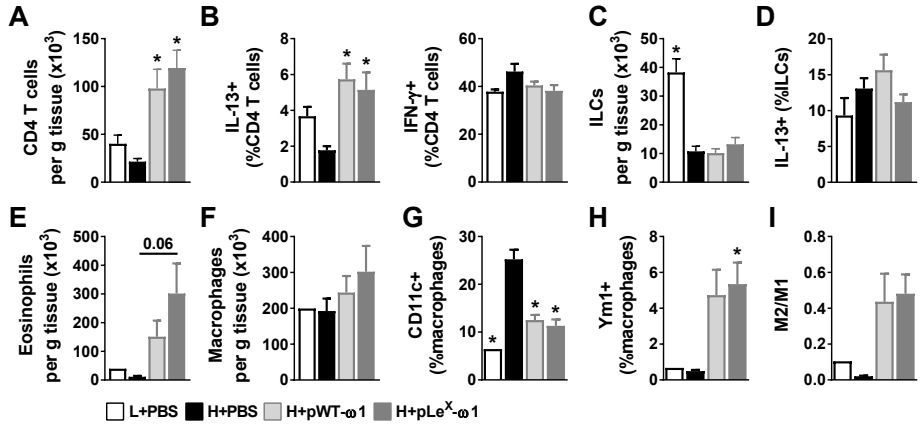

Supplementary Figure S4. ω1 glycovariants increase WAT type 2 immune cells after one week of treatment. Mice were fed a LFD or a HFD and treated with PBS or pWT/pLe^{X}-ω1 as described in the legend of Figure S2. At the end of the experiment, eWAT was collected, processed and analyzed as described in the legend of Figure 2. The numbers per gram tissue of CD4 T cells (*A*) and the frequencies of intracellular cytokine producing CD4 T cells (*B*) were determined. Numbers per gram tissue of ILCs were assessed (*J*), and frequencies of intracellular cytokine producing ILCs were determined (*D*). Cell numbers per gram tissue of eosinophils (*E*) and macrophages (*F*), and percentages of CD11c^{+}Ym1^{-} (M1-like; *G*) and CD11c^{-}Ym1^{+} (M2-like; *H*) in macrophages were determined. The M2 over M1 ratios were calculated (*I*). Results are expressed as means ± SEM. * *P*<0.05 *vs* HFD (n = 1-6 animals per group).

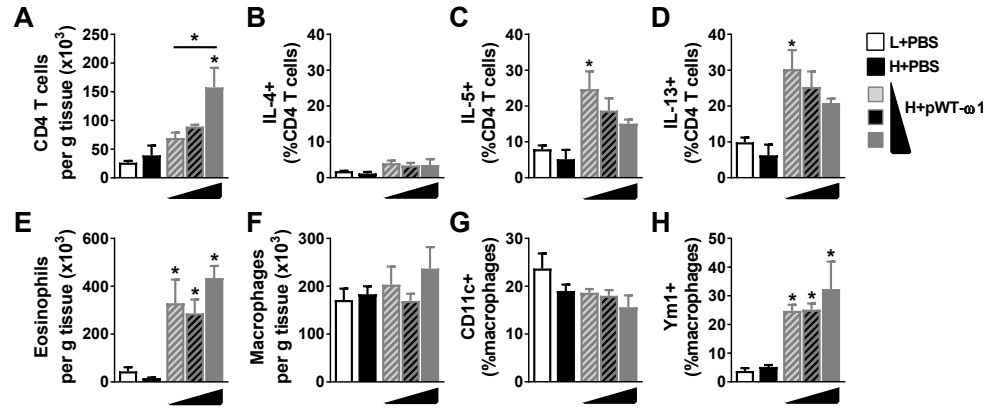

Supplementary Figure S5. pLe^{X}-ω1 increases WAT type 2 immune cells in a dose-dependent manner. Mice were fed a LFD or a HFD and were treated with PBS or pLe^{X}-ω1 as described in the legend of Figure S3. At the end of the experiment, eWAT was collected, processed and analysed as described in the legend of Figure 2. The numbers per gram tissue of CD4 T cells (*E*), and the frequencies of intracellular cytokine producing CD4 T cells (*B-D*) were determined. Numbers per gram tissue of eosinophils (*E*) and macrophages (*F*), and macrophages phenotypes (*G-H*) were assessed. Results are expressed as means ± SEM. * *P*<0.05 *vs* HFD or as indicated (n = 3-4 animals per group).

Supplementary table S1. Primer sequences for qRT-PCR

Gene	Accession number	Forward primer	Reverse primer
Acta2	NM_007392.3	AGCCATCTTTCATTGGGATGG	CCCCTGACAGGACGTTGTTA
Ccl2	NM_011333.3	TCAGCCAGATGCAGTTAACGCCC	GCTTCTTTGGGACACCTGCTGCT
Cidea	NM_007702	CTCGGCTGTCTCAATGTCAA	CCGCATAGACCAGGAACTGT
Col1a1	NM_007742.3	GAGAGGTGAACAAGGTCCCG	AAACCTCTCTCGCCTCTTGC
Cox8b	NM_007751.3	GACCCCGAGAATCATGCCAA	CCTGCTCCACGGCGGAA
Il1b	NM_008361	GACCCCAAAAGATGAAGGGCT	ATGTGCTGCTGCGAGATTTG
Rplp0	NM_007475	TCTGGAGGGTGTCCGCAACG	GCCAGGACGCGCTTGTACCC
Tgfb1	NM_011577	GCTGAACCAAGGAGACGGAA	ATGTCATGGATGGTGCCCAG
Timp1	NM_001044384	TCGGACCTGGTCATAAGGGC	GCTTTCCATGACTGGGGTGT
Tnfa	NM_013693	GTCCCCAAAGGGATGAGAAG	CACTTGGTGGTTTGCTACGA
Ucp1	NM_009463	TCAGGATTGGCCTCTACGAC	TGCATTCTGACCTTCACGAC
Zfp423	NM_033327.2	TTCACAGTCTTCGTCCAGGC	AGATTTTGTCCTCCTGCCCG

5

A FIELD-APPLICABLE METHOD FOR FLOW CYTOMETRIC ANALYSIS OF GRANULOCYTE ACTIVATION: CRYOPRESERVATION OF FIXED GRANULOCYTES

Karin de Ruiter, Selma van Staveren, Bart Hilvering, Edward Knol, Nienke Vrisekoop, Leo Koenderman and Maria Yazdanbakhsh

Cytometry Part A (2018)

ABSTRACT

Upon activation granulocytes upregulate several adhesion molecules (CD11b) and granule proteins (CD35, CD66b) and shed surface L-selectin (CD62L). These changes in expression, as assessed by flow cytometry, can be used as markers for activation. Whereas these markers are usually studied in fresh blood samples, a new method is required when samples are collected at a field site with no direct access to a flow cytometer. Therefore, we developed and tested a field-applicable method in which fixed leukocytes were cryopreserved. Using this method, the intensity of granulocyte activation markers was compared to samples that were either stained fresh, or fixed prior to staining but not cryopreserved. In addition, the response to an in vitro stimulation with fMLF was determined. While we observed differences in marker intensities when comparing fresh and fixed granulocytes, similar intensities were found between fixed cells that had been cryopreserved and fixed cells that did not undergo cryopreservation. Although fixation using FACS lysing solution might lead to membrane permeabilization, activation markers, and the responsiveness to fMLF or eotaxin could still be clearly measured. This method will, therefore, enable future studies of granulocyte activation in settings with limited resources and will allow simultaneous analysis of samples collected at different time points.

INTRODUCTION

Granulocytes form a class of innate effector cells and consist of eosinophils, neutrophils, and basophils, all characterized by the presence of lobulated nuclei and secretory granules in their cytoplasm. Upon inflammation, granulocytes are recruited from the circulation to the site of tissue injury or infection, where they become activated and exert their effector functions. To adhere to the endothelium, granulocytes express L-selectin (CD62L), and several selectin ligands which mediate "rolling" along the vessel endothelium (1, 2). This is followed by firm adhesion to and transmigration through endothelial cells, which is mainly mediated by the integrins Mac1 (CD11b/CD18) and VLA4 (CD49d/CD29, only expressed by eosinophils and basophils) (1, 2).

In addition to adhesion molecules, surface expression of proteins normally residing inside granule membranes can be used as markers for degranulation and, therefore, activation (3). Relevant are complement receptor 1 (CD35), mediating binding and phagocytosis of C3b coated particles and immune complexes, present in secretory vesicles, and CEACAM-8 (CD66b) which is present in specific granules (3).

Whereas neutrophils demonstrate a rapid upregulation of CD11b, CD35 and CD66b after in vitro activation with inflammatory agonists such as *N*-Formyl-Met-Leu-Phe (fMLF), the level of CD62L reduces as a result of stimulation-induced shedding (4, 5). Similarly, eosinophils respond to the chemokine eotaxin (amongst others) by upregulating CD11b and shedding their CD62L (6, 7). Therefore, quantification of these markers by flow cytometry can be used as read-out for the activation state and responsiveness of the cells for inflammatory mediators (4, 5, 8-14).

To study the expression of activation markers on granulocytes by flow cytometry, the use of lysed whole blood is preferred over cell isolation techniques as the latter could lead to nonspecific activation (15). In addition, purification procedures often require more time and a larger volume of blood compared to using whole blood. Therefore, total leukocytes are usually analysed by multicolour flow cytometry after staining whole blood with fluorescently-labelled antibodies followed by multiple gating (4, 5, 16). Whereas this method is suitable for laboratories with direct access to flow cytometers, circumstances are different when blood is collected at a field site with only basic laboratory infrastructure. Hence, a novel method is required in which samples can be collected in a setting with limited resources and stored for long time periods until analysis in a fully equipped laboratory.

Fixation methods are often used to preserve cells and studies have successfully demonstrated the applicability of granulocyte fixation prior to staining (8, 10, 17). However, fixation can modify cell morphology as measured by forward scatter (FSC) and side scatter (SSC) of leukocytes (8, 17-19). Fixation may also affect granulocyte cell membrane permeability (18-20) and can affect antigen epitopes and, thereby, their interaction with the monoclonal antibodies (9). This requires careful evaluation of each antigen-antibody combination.

As the cryopreservation of freshly isolated granulocytes has been proven difficult because of high susceptibility to damage during the cryopreservation method (21), cryopreservation of fixed lysed whole blood samples might be a suitable method for long-term storage. This would allow sample collection at the field site requiring only pipettes, a centrifuge and a -80°C freezer, followed by transport to a central laboratory for flow cytometric analysis. Moreover, long-term storage allows researchers to analyse samples collected at different time points simultaneously.

Nemes et al. previously provided proof-of-principle that cryopreservation leads to accurate quantification of cell subsets (granulocytes, lymphocytes, monocytes, T cells and B cells) by flow cytometry in fixed whole blood samples (17). Our study tested the hypothesis that also granulocyte activation can be determined in such samples by comparing the expression of granulocyte activation markers on samples that were either fresh (no fixation), fixed prior to staining, or fixed and cryopreserved prior to staining. In addition, we set out experiments to measure the response of granulocytes to an in vitro stimulation with fMLF (neutrophils or basophils) or eotaxin (CCL11; eosinophils) in cells fixed and cryopreserved after activation.

The applicability of cryopreservation of fixed cells was subsequently tested in a controlled laboratory model of acute inflammation (22) and in a field study in Flores, Indonesia (23). We now show that cryopreservation of fixed total leukocyte populations allows the determination of activated granulocytes, either activated by chemokines in vitro or by inflammation in vivo.

MATERIALS & METHODS

Sample preparation

Venous blood of three healthy volunteers was collected in sodium heparin vacutainers (BD Biosciences, Franklin Lakes, NJ, USA) and handled within 30 minutes. Different methods were compared, depicted in Figure 1, and for each method 2 polystyrene round-bottom tubes containing 200 µL of blood per donor were pre-incubated for 5 min in a 37°C waterbath, followed by a 5 min-stimulation at 37°C with fMLF (10^{-5} M; Sigma, Saint Louis, MO, USA) or left unstimulated. Subsequently, samples were subjected to the following treatments: (1) Erythrocyte lysis using lysing buffer consisting of 155 mM NH_4Cl and 10 mM Na_2EDTA, with a pH of 7.0 and osmolarity of 298-305. Cells were transferred to ice and to each sample 900 µL lysing buffer was added. Cells were centrifuged at 1600 rpm for 5 min and washed with first 500 µL lysis buffer, followed by washing and resuspension in FACS buffer (PBS complemented with 0.5% BSA and 2 mM EDTA) and directly stained. (2) Erythrocyte lysis and leukocyte fixation using FACS lysing solution (BD Biosciences, #349202) for 15 min at room temperature. Following the recommended procedures, the FACS lysing solution (stock solution 10x) was diluted, and 4 mL of the diluted reagent was used for each whole blood sample. After lysis the cells were centrifuged, washed with RPMI 1640 containing 10% heat-inactivated foetal calf serum (FCS), centrifuged again and

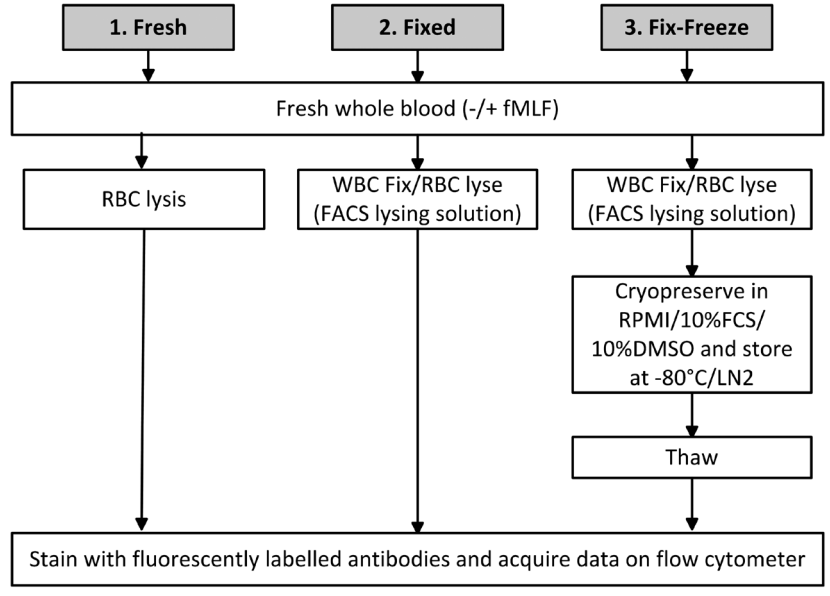

Figure 1. Experiment overview.

finally resuspended in FACS buffer and stored (<8 hrs) at 4°C until staining. (3) Erythrocyte lysis and leukocyte fixation using FACS lysing solution as described above (Treatment 2). Following lysis, cells were washed with 10% FCS/RPMI and resuspended in 10% FCS/10% dimethyl sulfoxide (DMSO)/RPMI. Cryovials containing the cell suspension were placed at -80°C. The cryopreserved fixed cells were thawed on the bench and subsequently transferred to 5 ml polystyrene round-bottom tubes containing 1 mL 10% FCS/RPMI. After centrifugation at 1600 RPM for 5 min, cells were resuspended in FACS buffer and stored (<2 hrs) at 4°C until staining. In the results section, Treatments 1, 2 and 3 will be referred to as "Fresh", "Fixed" and "Fix & Freeze", respectively.

Cryopreservation of fixed leukocytes (Treatment 3), was applied in a clinical trial conducted in a rural area at Flores island in Indonesia to study the effect of soil-transmitted helminth infections on granulocyte activation. This SUGARSPIN trial was approved by the ethics committee of Faculty of Medicine, Universitas Indonesia (FKUI), filed by the ethics committee of Leiden University Medical Center (LUMC), and registered as a clinical trial (http://www.isrctn.com/ISRCTN75636394). The study protocol was published previously (23). Blood samples were collected after obtaining written consent and processed according to Treatment 3, with the only difference that cells were stored in liquid nitrogen after placement at -80°C for a minimum of 4 hours. In addition to the stimulation with fMLF described above, whole blood was stimulated for 5 min at 37°C with eotaxin (CCL11; 10^{-7} M, R&D systems, Abingdon, UK) to study in vitro eosinophil activation.

Neutrophil subset identification after LPS challenge

To assess whether neutrophil activation can also be detected after using the method of fixation and cryopreservation following in vivo stimulation, cells from a large endotoxin trial (NCT02629874 at www.clinicaltrials.gov) were used. In short, healthy male volunteers were enrolled after screening and were prehydrated. U.S. Reference *E. coli* endotoxin (Lot Ec-5; Centre for Biologic Evaluation and Research, U.S. Food and Drug Administration, Bethesda, MD, USA) was used in this study. Endotoxin was reconstituted in 5 mL saline and injected as a single intravenous bolus (2 ng/kg) during 1 min at t = 0. The study protocol was approved by the Ethics Committee of the Radboud University Nijmegen Medical Centre and complies with the Declaration of Helsinki and Good Clinical Practice guidelines. Subjects gave written informed consent.

At t = 180 min, blood samples, anticoagulated with sodium heparin, were taken from the arterial catheter. The blood samples were processed according to Treatments 1 and 3 described above. For Treatment 3, cells were first stored at -30°C for 8 days for operational reasons (no -80°C freezer at sampling site), before they were transferred to -80°C.

Flow cytometric analysis

Irrespective of the method used, cells were counted by microscopy after erythrocyte lysis and 500.000 leukocytes were transferred to a 96-well V-bottom microplate and incubated for 30 min at 4°C with anti-CD35-FITC (E11, Biolegend, San Diego, USA), anti-CD66b-PerCP/Cy5.5 (G10F5, Biolegend), anti-CD193-PE (5e, Biolegend), anti-CD16-PE/CF594 (3G8, BD Biosciences), anti-CD69-PE/Cy5 (FN50, Biolegend), anti-CD3/CD19/CD20/CD56-APC (UCHT1, HIB19, 2H7, 5.1H11, Biolegend), anti-CD11b-APC/eF780 (ICRF44, eBioscience Inc., San Diego, USA), anti-CD203c-BV421 (NP4D6, Biolegend), anti-CD14-BV510 (M5E2, Biolegend) and anti-CD62L-BV605 (DREG-56, BD Biosciences). Cells collected after LPS challenge were stained with anti-CD16-Pacific Orange (3G8, Beckman Coulter) and CD62L-BV650 (DREG-56, Biolegend). Compensation beads (BD Biosciences) were stained with each antibody separately and run before acquisition to calculate the compensation matrix using BD Facs Diva flow cytometry software.

As we aimed to compare three methods, all samples were measured on the same day and stained with the same antibody mix, with exception of the samples that were collected in the endotoxin clinical trial or as part of the SUGARSPIN study. Cells were measured on a LSR Fortessa flow cytometer (BD Biosciences), equipped with 405, 488, 561 and 640 lasers. Data were analysed with FlowJo software (Treestar Inc., Ashland, OR, USA) and median fluorescence intensity (MFI) data are displayed. Representative gating schemes are shown in Supplementary Figure S1. Although neutrophils and eosinophils clearly differ in their FSC/SSC properties, we used the expression of CD193 (in fresh samples) or the autofluorescent signal (in fixed samples) to gate eosinophils. Neutrophils were gated based on their FSC/SSC properties and subsequently separated from monocytes based on their $CD14^{-}/CD11b^{+}$ expression. Basophils were gated based on their expression of CD193 and CD203c and lack of the lineage markers CD3, CD19, CD20 and CD56.

Statistical analysis

Data analysis was performed using GraphPad Prism version 7 for Windows (Graphpad Software, San Diego, CA, USA) and this software was also used to make graphs. Paired t test was used to assess the effect of fMLF stimulation on the expression of activation markers in neutrophils and basophils. The effect of stimulation on markers expressed by neutrophils, eosinophils and basophils from samples collected in a field study was tested using Wilcoxon matched-pairs signed rank test. P values ≤ 0.05 were considered statistically significant.

RESULTS

Fixation leads to changes in FSC/SSC profiles

After fixation, granulocytes displayed different forward scatter/ side scatter (FSC/SSC) profiles compared to fresh cells suggesting a change in morphology (Figure 2). Eosinophils showed a shift in FSC and became more autofluorescent after fixation (Supplementary Figure S2). No increase in autofluorescence was observed for neutrophils (data not shown). After fixation, neutrophils exhibited a lower SSC signal, resulting in an overlap between neutrophils and monocytes. The amount of overlap increased after freeze-thawing, and it was, therefore, important to add a monocyte marker (e.g. CD14) and/or a specific neutrophil marker (e.g. CD66b) to the panel to be able to discriminate between these cell types. Except for neutrophils, fixed leukocytes that had been cryopreserved displayed similar FSC-SSC properties compared to fixed cells that did not undergo cryopreservation.

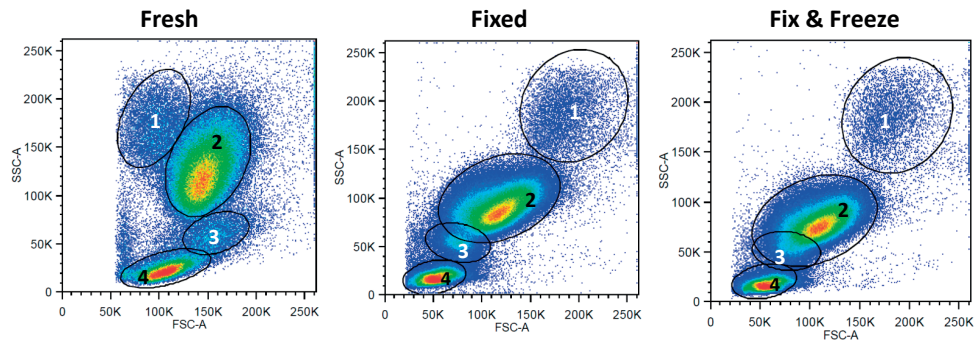

Figure 2. FSC/SSC properties of granulocytes. Numbers indicate different cell populations: (1) eosinophils, (2) neutrophils, (3) monocytes and (4) lymphocytes. After fixation, eosinophils change in FSC/SSC and monocytes and neutrophils show overlap in FSC/SSC properties. This overlap is further amplified after freeze-thawing the cells. Basophils overlap with lymphocytes in FSC/SSC properties.

Neutrophils

Cellular activation and responsiveness to fMLF can be measured by activation markers after fixation and cryopreservation

We observed changes in marker intensities when comparing fresh and fixed unstimulated neutrophils (Figure 3, Table 1). The measured intensities of CD11b, CD35 and CD66b were elevated after fixation when compared to fresh cells, whereas the detected intensity of CD62L on neutrophils was lower after fixation compared to fresh cells. These changes were consistent in all three donors. No major differences in the marker intensities were observed when fixed neutrophils that had been cryopreserved were compared to fixed cells that did not undergo cryopreservation (Figure 3), indicating that the observed differences with fresh cells are a consequence of fixation, and are not caused by the process of freeze-thawing.

To assess whether it is possible to detect activation of neutrophils after fixation and cryopreservation, we measured the levels of activation markers in samples that were incubated with and without fMLF. Despite the changes in marker intensities that were described above, fMLF activation could still further increase the expression of measured activation markers in fixed and cryopreserved neutrophils (Figure 3, Table 1). The detected responsiveness of CD35 and CD11b to fMLF was similar in fresh and fixed neutrophils, irrespective of freezing. Regarding CD66b, we observed an increased expression after stimulation with fMLF in fresh neutrophils as well as fixed cells. However, in fixed cells, the increase in CD66b expression was rather weak compared to fresh cells, indicating that CD66b might not be suitable for studying functional capacity of neutrophils in terms of responding to a stimulus when this field applicable method is used. CD62L is shed from the membrane upon activation, and despite the overall lower intensity of CD62L in fixed neutrophils, we could still observe this response after activation with fMLF.

Three neutrophil subsets can be identified based on CD16 and CD62L expression after fixation and cryopreservation

The experiments described above relied on the in vitro activation of leukocytes by fMLF. We next studied leukocyte subsets that have been described in fresh cells following

Table 1. Expression of CD11b, CD35, CD66b and CD62L on neutrophils and the response to fMLF.

Neutrophils	Fresh Mean MFI (SD)		Fixed Mean MFI (SD)		Fix & Freeze Mean MFI (SD)	
	Medium	fMLF	Medium	fMLF	Medium	fMLF
CD11b	164 (20)	857 (124)	1175 (101)	1758 (222)	1525 (132)	2154 (186)
CD35	788 (92)	4054 (921)	1113 (160)	3729 (832)	1399 (99)	3981 (845)
CD66b	337 (25)	909 (113)	518 (62)	583 (18)	590 (74)	720 (17)
CD62L	5304 (753)	261 (49)	1216 (108)	169 (8)	1118 (41)	156 (8)

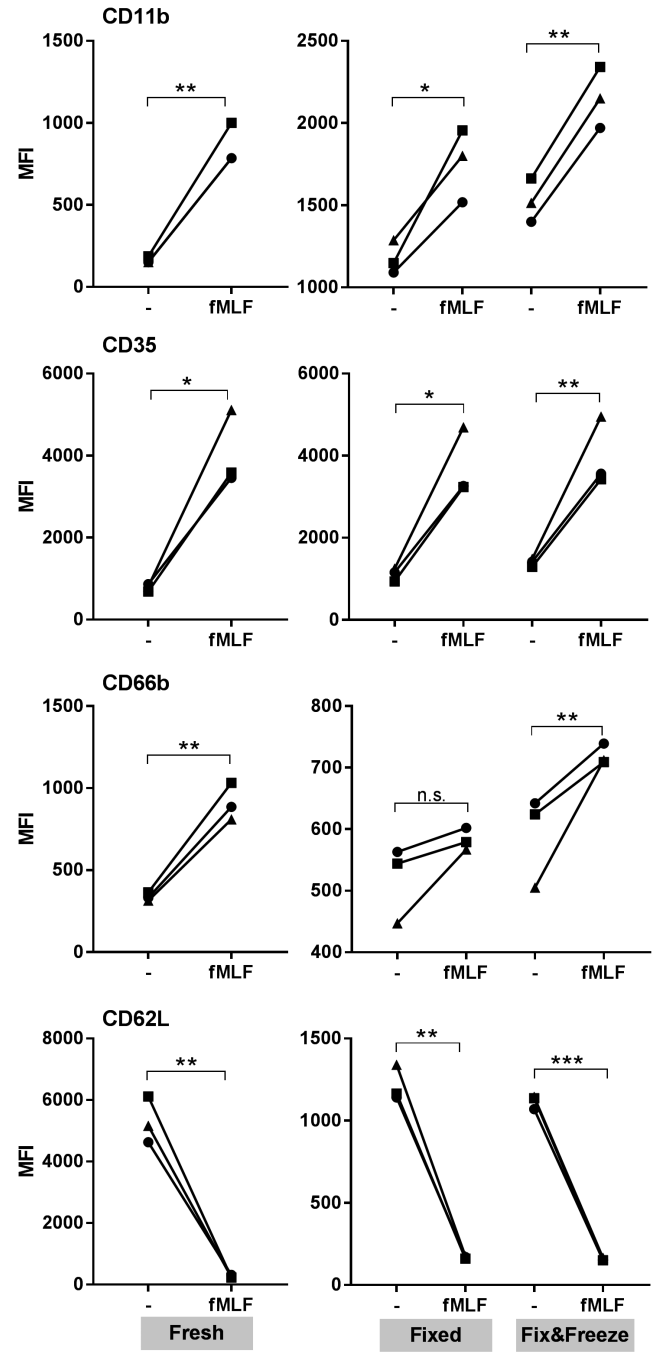

Figure 3. Expression of CD11b, CD35, CD66b and CD62L on neutrophils and the response to fMLF. Median fluorescent intensity (MFI) of markers on neutrophils left unstimulated and stimulated with fMLF. Neutrophils were stained either fresh (Fresh), after fixation (Fixed) or after being fixed, cryopreserved and thawed (Fix & Freeze). Symbols (circle, triangle, square) represent three different donors. *indicates analysis with paired *t* test. *, $P \leq 0.05$. **, $P \leq 0.01$. ***, $P \leq 0.001$. n.s., not significant.

in vivo stimulation by a systemic pro-inflammatory stimulus, LPS. Thus, since CD62L intensities were found to be decreased after fixation, we assessed whether we would still be able to identify the three different neutrophil subsets that were previously described on fresh cells (22). Although both CD16 and CD62L intensities were lower after fixation and cryopreservation, we were able to identify the three different neutrophil subsets (1- $CD16^{bright}CD62L^{bright}$; 2- $CD16^{dim}CD62L^{bright}$; 3- $CD16^{bright}CD62L^{dim}$) based on expression of these two markers (Supplementary Figure S3).

Eosinophils and Basophils

The intensities of all eosinophil markers studied (CD193, CD66b, CD35, CD11b, CD62L and CD69) were similar between fixed eosinophils that had been cryopreserved and fixed cells that did not undergo cryopreservation (Figure 4). However, similar to the situation with neutrophils, differences were observed in the intensities of activation markers for eosinophils when comparing fresh and fixed cells. The measured intensities of CD35 and CD66b were slightly higher after fixation, while the intensity of CD11b was strongly increased and CD62L detection was lower in fixed compared to fresh cells.

Basophils also respond to fMLF (24) and the intensity of CD11b, CD35 and CD203c was increased after stimulation (Supplementary Figure S4, Table S1). Like the expression of these markers in unstimulated cells, the responsiveness to fMLF was similar between fresh, fixed and cryopreserved cells.

Field study application

The aim of this study was to set up a method to assess granulocyte activation and responsiveness in a field study with limited laboratory equipment. After testing the method to fix and cryopreserve leukocytes for flow cytometric analysis, this method was applied in a clinical trial in a rural area in Indonesia (23). Blood samples from 300 subjects were processed according to the method described and stored in liquid nitrogen for up to two years until analysis. Figures 5 and 6 and Supplementary Figure S5 show representative samples collected during this study. Even after long-term storage we could measure the expression of activation markers on neutrophils (Figure 5A), eosinophils (Figure 6A) and basophils (Supplementary Figure S5A). Moreover, the response of neutrophils and basophils to fMLF evoked in samples in the field was clearly present (Figure 5B, Supplementary Figure S5B, Table S2). To study the responsiveness of eosinophils, we stimulated whole blood with eotaxin and observed an increased intensity of CD35 and CD11b when compared to unstimulated cells (Figure 6B, Table S2). Although not compared to fresh cells, this shows that the activation effect in eosinophils can be measured after fixation and cryopreservation.

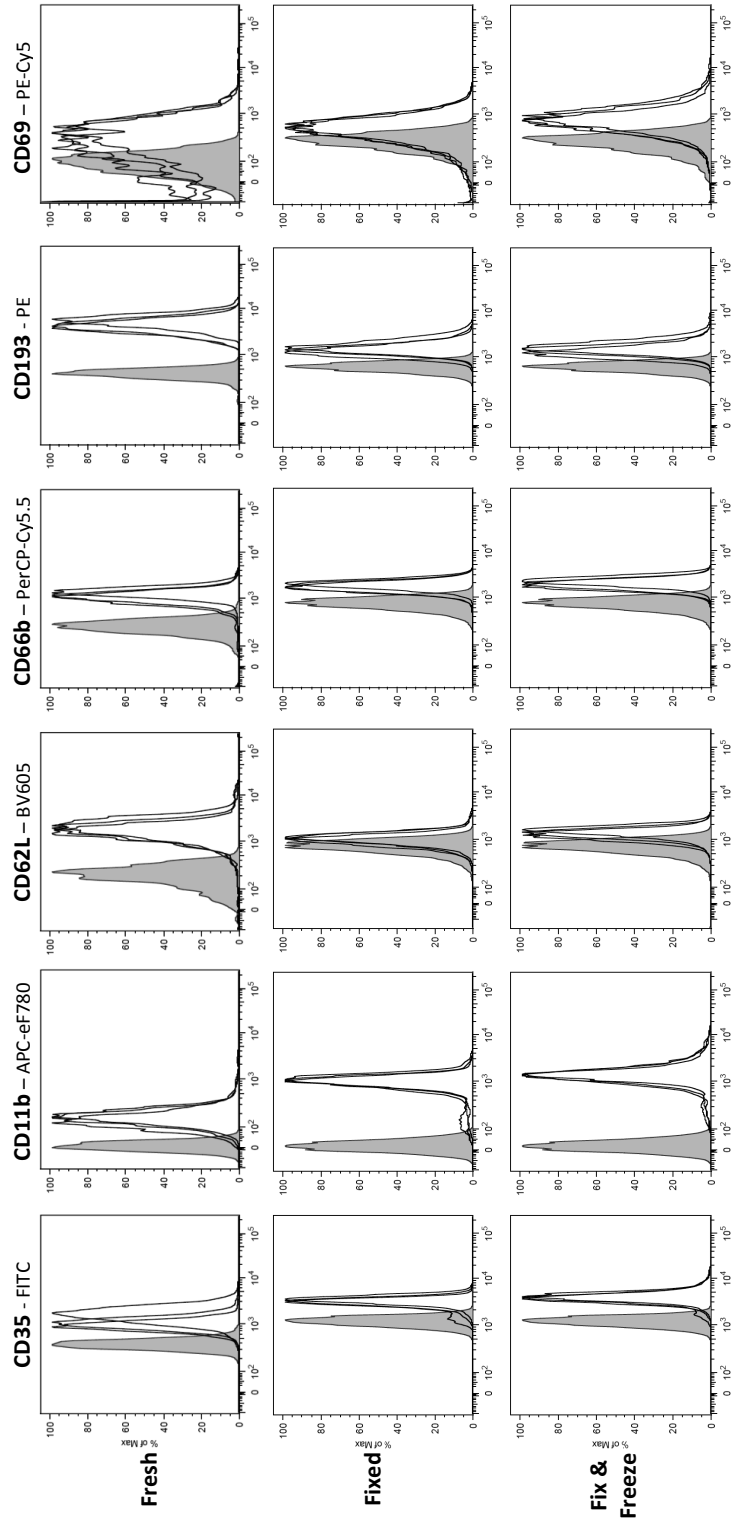

Figure 4. Expression of CD35, CD11b, CD62L, CD66b, CD193 and CD69 on eosinophils. Grey histograms represent unstained eosinophils while the black lines represent three different donors. Cells were stained either fresh (Fresh), after fixation (Fixed) or after being fixed, cryopreserved and thawed (Fix & Freeze).

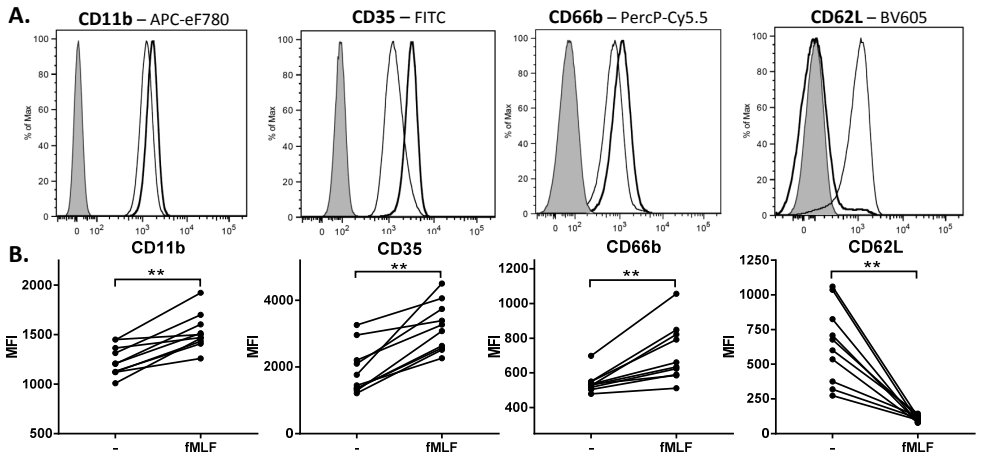

Figure 5. Expression of CD11b, CD35, CD66b and CD62L on neutrophils collected in a field study. Samples were cryopreserved for 2 years in liquid nitrogen. (*A*) Histograms of a representative sample, filled lines display unstained neutrophils, the thin black lines unstimulated cells and the thick black lines fMLF-stimulated cells. (*B*) Median fluorescent intensity (MFI) of markers in neutrophils from 10 representative donors left unstimulated and stimulated with fMLF. Means and standard deviations are shown in Supplementary Table S2. *indicates analysis with Wilcoxon matched-pairs signed rank test. **, $P \leq 0.01$.

DISCUSSION

Here, we show that the activation status of neutrophils, eosinophils, and basophils and their responsiveness to stimuli such as fMLF and eotaxin, can be studied in whole-blood samples that were lysed, fixed and cryopreserved. Previously, Nemes et al. showed that cryopreservation of fixed leukocytes provides for an accurate quantification of cell subsets based on the expression of lineage-specific markers (CD66b, CD14, CD3, CD19, CD16), as analysed by flow cytometry (17). However, they had not tested whether the method was also suitable for assessing the activation status of granulocytes. We show that cryopreservation of granulocytes allows detection of activation of granulocytes in vitro in response to fMLF and eotaxin, as well as activation in vivo during acute inflammation evoked by experimental endotoxemia in healthy volunteers. It will now be possible to measure differences in innate immune responses at field sites where no flow cytometers are available for direct analysis.

Cryopreservation of fixed granulocytes induces some differences in cellular characteristics that preclude direct comparison with analysis of fresh cells. For instance, the differences detected in FSC/SSC profiles of granulocytes and marker intensities between cryopreserved and fresh cells were mainly caused by fixation. The increased intensity of CD11b, CD35 and CD66b in fixed neutrophils might be a consequence of fixation-induced membrane permeabilization, potentially leading to intracellular staining in the granules (19, 20). This is particularly relevant for markers normally residing in the granular

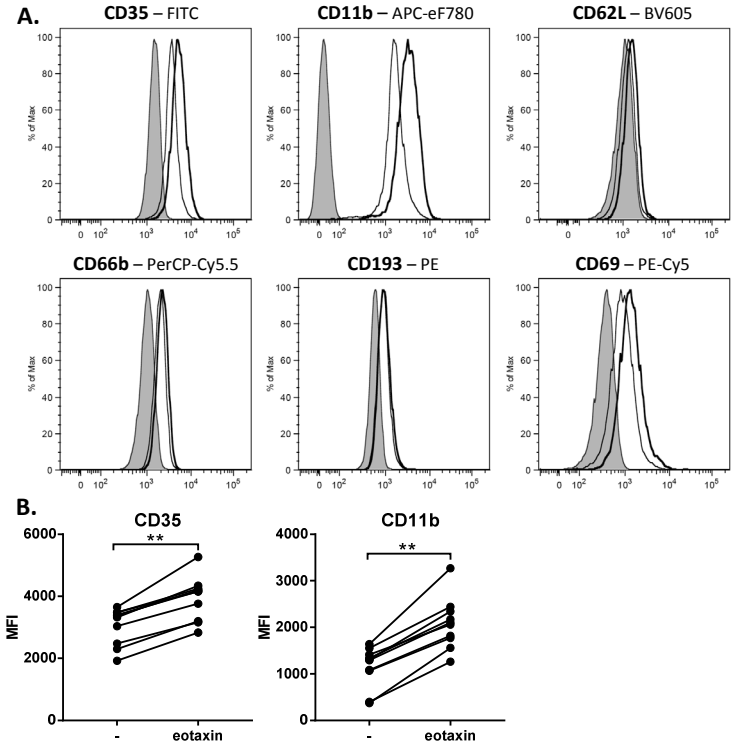

Figure 6. Expression of CD35, CD11b, CD62L, CD66b, CD193 and CD69 on eosinophils collected in a field study. Samples were cryopreserved for 2 years in liquid nitrogen. (*A*) Histograms of a representative sample, filled lines represent unstained eosinophils, the thin black lines unstimulated cells and the thick black lines eotaxin-stimulated cells. (*B*) Median fluorescent intensity (MFI) of CD35 and CD11b in eosinophils from 10 donors left unstimulated and stimulated with eotaxin. Means and standard deviations are shown in Supplementary Table S2. *indicates analysis with Wilcoxon matched-pairs signed rank test. **, $P \leq 0.01$.

compartment, which become expressed upon degranulation. Only 5% of the total cellular content of the CD11b-CD18 (Mac-1) complexes in unstimulated neutrophils is expressed on the plasma membrane, whereas 95% colocalized with specific granules and secretory vesicles (25). Therefore, the increased intensity of CD11b in fixed versus fresh neutrophils might reflect some staining of the intracellular pool of CD11b molecules. Importantly, despite the putative membrane permeability caused by fixation, we could still observe a significant effect of fMLF in neutrophils (in particular for CD35, CD11b and CD62L) and basophils (in particular for CD203c, CD35 and CD11b), and of eotaxin in eosinophils (in particular for CD35 and CD11b). This activation effect was also clearly present in samples collected in the field which had been cryopreserved for up to two years.

Hamblin et al. observed no intracellular leukocyte staining of p8,14 (expressed in all circulating monocytes and neutrophils) nor DNA staining after fixation with 0.4%

formaldehyde (8). This suggests that different fixation methods might have different effects in terms of cell permeabilization. However, the use of FACS lysing solution is a quick and easy method and, therefore, suitable to be used in the field.

We also observed that eosinophils became more autofluorescent after fixation and it is, therefore, difficult to determine in eosinophils whether the differences in marker intensity between fresh and fixed cells are a result of cell membrane permeabilization, affected antigen epitopes, or increased autofluorescence. The effect of autofluorescence on the intensity of a certain marker depended on the fluorescent channel being used, as we observed no shift in the channel used to detect APC/eF780. CD193 (chemokine receptor CCR3 / eotaxin receptor) is a well-known marker for eosinophils and we observed a lower detection of CD193 in fixed compared to fresh eosinophils. Combined with an increased autofluorescent signal in the PE-channel, we recommend not to use CD193 as single eosinophil marker when analysing fixed, cryopreserved granulocytes. CD193 functioned well as a basophil marker, irrespective of fixation (26, 27). For similar reasons, we advise to use a CD62L antibody with a different fluorophore than BV605, or to increase the amount of antibody when staining fixed eosinophils to be able to detect CD62L.

In summary, these results demonstrate that fixation and cryopreservation of lysed whole blood samples can be applied at field sites with limited laboratory infrastructure. We showed that the activation status of granulocytes and responsiveness to fMLF or eotaxin could be measured after cryopreservation, allowing to measure changes in the innate immune response in patients. This will enable future studies of granulocyte activation in settings with limited resources and allows the parallel analysis of samples collected at different time points and at different sites.

REFERENCES

1. Rosenberg HF, Dyer KD, Foster PS. Eosinophils: changing perspectives in health and disease. Nature reviews Immunology 2013; 13(1): 9-22.
2. Kolaczkowska E, Kubes P. Neutrophil recruitment and function in health and inflammation. Nature reviews Immunology 2013; 13(3): 159-75.
3. Cowland JB, Borregaard N. Granulopoiesis and granules of human neutrophils. Immunol Rev 2016; 273(1): 11-28.
4. Mann BS, Chung KF. Blood neutrophil activation markers in severe asthma: lack of inhibition by prednisolone therapy. Respir Res 2006; 7: 59.
5. Berends C, Hoekstra MO, Dijkhuizen B, de Monchy JG, Gerritsen J, Kauffman HF. Expression of CD35 (CR1) and CD11b (CR3) on circulating neutrophils and eosinophils from allergic asthmatic children. Clinical and experimental allergy: journal of the British Society for Allergy and Clinical Immunology 1993; 23(11): 926-33.
6. Santamaria LF, Palacios JM, Beleta J. Inhibition of eotaxin-mediated human eosinophil activation and migration by the selective cyclic nucleotide phosphodiesterase type 4 inhibitor rolipram. British journal of pharmacology 1997; 121(6): 1150-4.
7. Tenscher K, Metzner B, Schopf E, Norgauer J, Czech W. Recombinant human eotaxin induces oxygen radical production, Ca(2+)-mobilization, actin reorganization, and CD11b upregulation in human eosinophils via a pertussis toxin-sensitive heterotrimeric guanine nucleotide-binding protein. Blood 1996; 88(8): 3195-9.
8. Hamblin A, Taylor M, Bernhagen J, et al. A method of preparing blood leucocytes for flow cytometry which prevents upregulation of leucocyte integrins. Journal of immunological methods 1992; 146(2): 219-28.
9. Finn A, Rebuck N. Measurement of adhesion molecule expression on neutrophils and fixation. Journal of immunological methods 1994; 171(2): 267-70.
10. Torsteinsdottir I, Arvidson NG, Hallgren R, Hakansson L. Enhanced expression of integrins and CD66b on peripheral blood neutrophils and eosinophils in patients with rheumatoid arthritis, and the effect of glucocorticoids. Scand J Immunol 1999; 50(4): 433-9.
11. Mawhorter SD, Stephany DA, Ottesen EA, Nutman TB. Identification of surface molecules associated with physiologic activation of eosinophils. Application of whole-blood flow cytometry to eosinophils. Journal of immunology (Baltimore, Md: 1950) 1996; 156(12): 4851-8.
12. Chiba T, Kamada Y, Saito N, et al. RANTES and eotaxin enhance CD11b and CD18 expression on eosinophils from allergic patients with eosinophilia in the application of whole Blood flow cytometry analysis. Int Arch Allergy Immunol 2005; 137 Suppl 1: 12-6.
13. Yoon J, Terada A, Kita H. CD66b regulates adhesion and activation of human eosinophils. Journal of immunology (Baltimore, Md: 1950) 2007; 179(12): 8454-62.
14. Zhao L, Xu S, Fjaertoft G, Pauksen K, Hakansson L, Venge P. An enzyme-linked immunosorbent assay for human carcinoembryonic antigen-related cell adhesion molecule 8, a biological marker of granulocyte activities in vivo. Journal of immunological methods 2004; 293(1-2): 207-14.
15. Kuijpers TW, Tool AT, van der Schoot CE, et al. Membrane surface antigen expression on neutrophils: a reappraisal of the use of surface markers for neutrophil activation. Blood 1991; 78(4): 1105-11.
16. Fujiwara RT, Cancado GG, Freitas PA, et al. Necator americanus infection: a possible cause of altered dendritic cell differentiation and eosinophil profile in chronically infected individuals. PLoS neglected tropical diseases 2009; 3(3): e399.
17. Nemes E, Kagina BM, Smit E, et al. Differential leukocyte counting and immunophenotyping in cryopreserved ex vivo whole blood. Cytometry Part A : the journal of the International Society for Analytical Cytology 2015; 87(2): 157-65.
18. Carulli G, Sbrana S, Azzara A, et al. Detection of eosinophils in whole blood samples by flow cytometry. Cytometry 1998; 34(6): 272-9.
19. Tiirikainen MI. Evaluation of red blood cell lysing solutions for the detection of intracellular antigens by flow cytometry. Cytometry 1995; 20(4): 341-8.

20. Vuorte J, Jansson SE, Repo H. Evaluation of red blood cell lysing solutions in the study of neutrophil oxidative burst by the DCFH assay. Cytometry 2001; 43(4): 290-6.
21. Vian AM, Higgins AZ. Membrane permeability of the human granulocyte to water, dimethyl sulfoxide, glycerol, propylene glycol and ethylene glycol. Cryobiology 2014; 68(1): 35-42.
22. Pillay J, Kamp VM, van Hoffen E, et al. A subset of neutrophils in human systemic inflammation inhibits T cell responses through Mac-1. The Journal of clinical investigation 2012; 122(1): 327-36.
23. Tahapary DL, de Ruiter K, Martin I, et al. Helminth infections and type 2 diabetes: a cluster-randomized placebo controlled SUGARSPIN trial in Nangapanda, Flores, Indonesia. BMC infectious diseases 2015; 15: 133.
24. Chirumbolo S, Vella A, Ortolani R, et al. Differential response of human basophil activation markers: a multi-parameter flow cytometry approach. Clin Mol Allergy 2008; 6: 12.
25. Sengelov H, Kjeldsen L, Diamond MS, Springer TA, Borregaard N. Subcellular localization and dynamics of Mac-1 (alpha m beta 2) in human neutrophils. The Journal of clinical investigation 1993; 92(3): 1467-76.
26. Hausmann OV, Gentinetta T, Fux M, Ducrest S, Pichler WJ, Dahinden CA. Robust expression of CCR3 as a single basophil selection marker in flow cytometry. Allergy 2011; 66(1): 85-91.
27. Uguccioni M, Mackay CR, Ochensberger B, et al. High expression of the chemokine receptor CCR3 in human blood basophils. Role in activation by eotaxin, MCP-4, and other chemokines. The Journal of clinical investigation 1997; 100(5): 1137-43.

SUPPLEMENTAL DATA

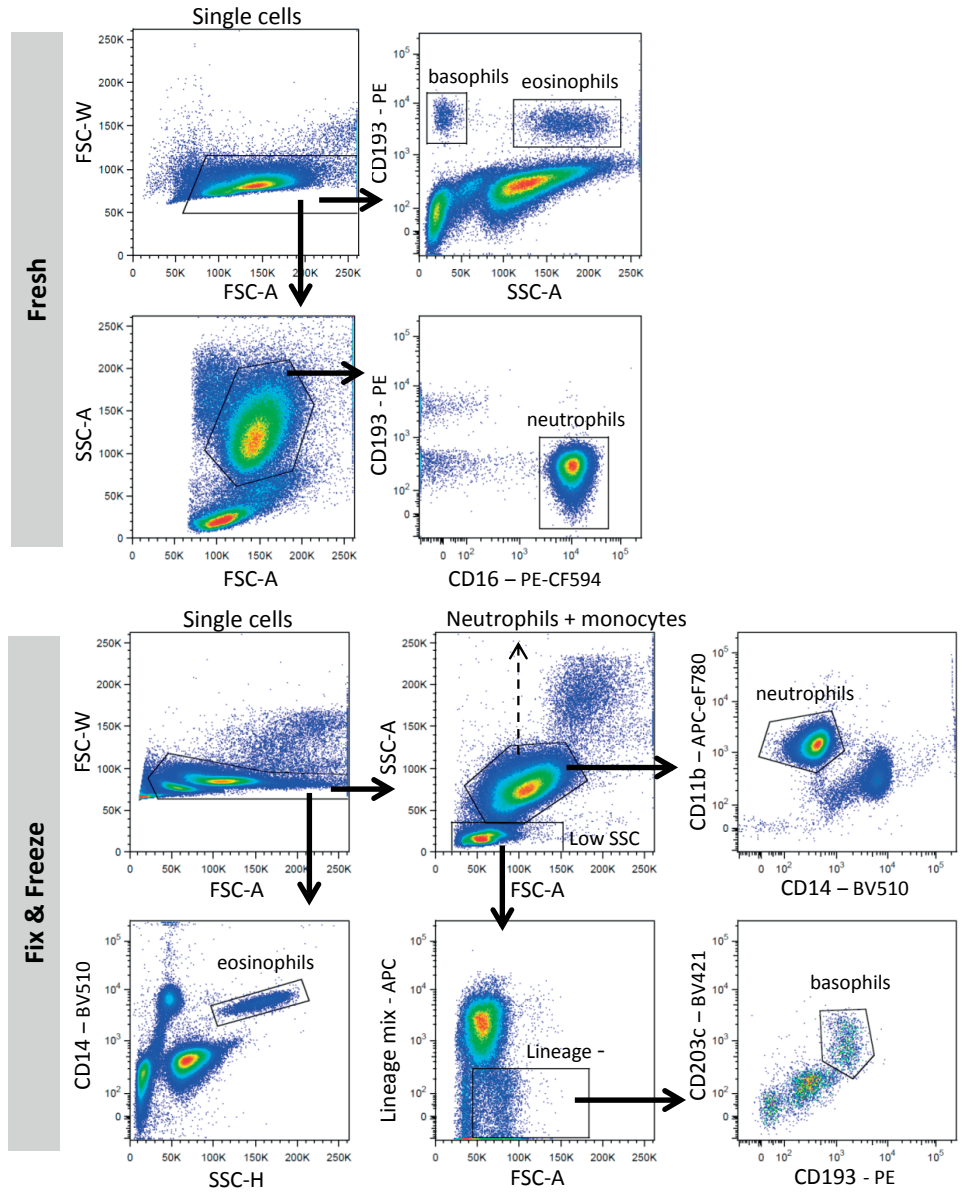

Supplementary Figure S1. Gating strategies. The gating strategy for the analysis of eosinophils, neutrophils and basophils in a representative fresh sample (upper panel) and fixed-cryopreserved sample (lower panel) is shown.

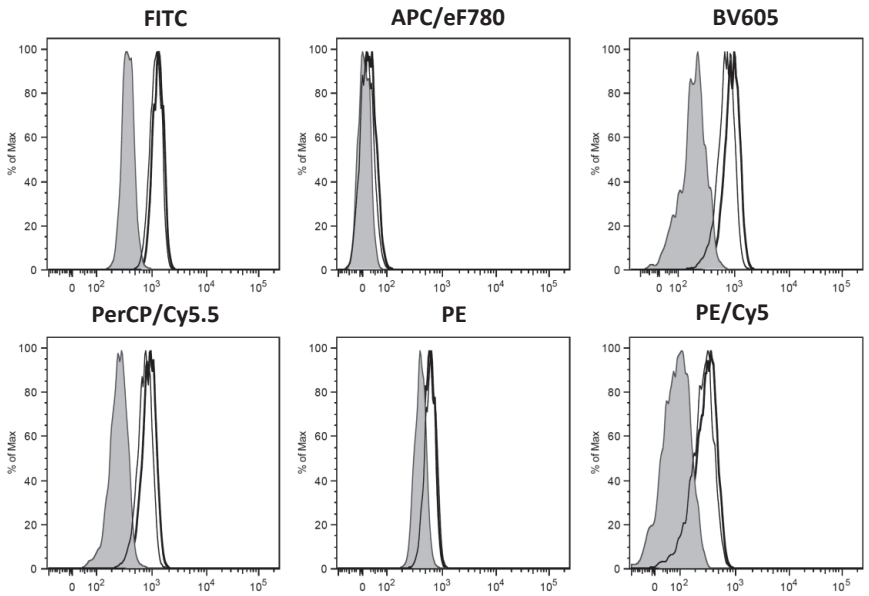

Supplementary Figure S2. Increased autofluorescence of eosinophils after fixation. The filled lines represent fresh, non-fixed, unstained eosinophils, while the thin black lines display fixed unstained cells that did not undergo cryopreservation and the thick black lines fixed, unstained cells after cryopreservation.

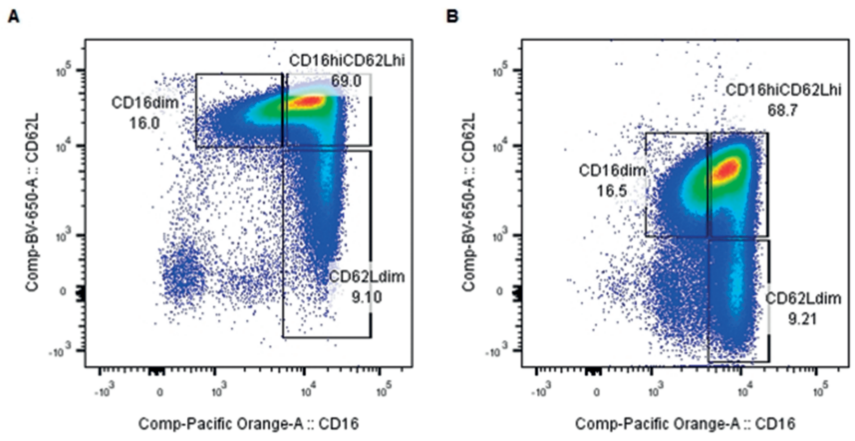

Supplementary Figure S3. Expression of CD203c, CD11b and CD35 on basophils and the response to fMLF. (*A*) Median fluorescent intensity (MFI) of markers on basophils left unstimulated and stimulated with fMLF. (*B*) The response of basophils to fMLF expressed as the difference in MFI between stimulated and unstimulated cells. The symbols (circle, triangle, square) represent three different donors. Means and standard deviations are shown in Supplementary Table S1. Data analysed with paired *t* test. n.s., not significant.

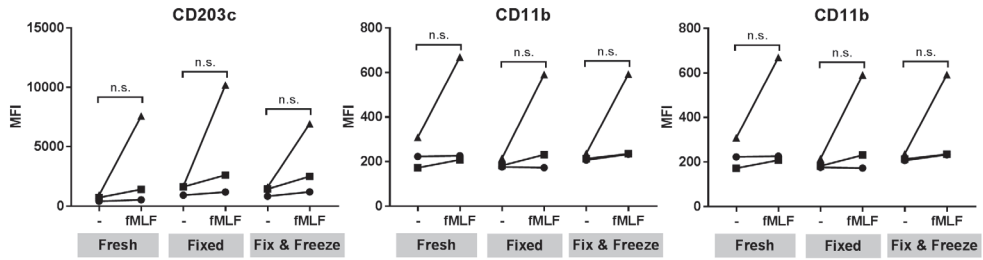

Supplementary Figure S4. CD16/CD62L expression of neutrophils that were activated in vivo in response to intravenous LPS infusion. Two extra neutrophil subsets (CD16^{dim}CD62L^{hi} and CD16^{hi}CD62L^{dim}) can be identified in both (*A*) fresh and (*B*) fixed and cryopreserved cells.

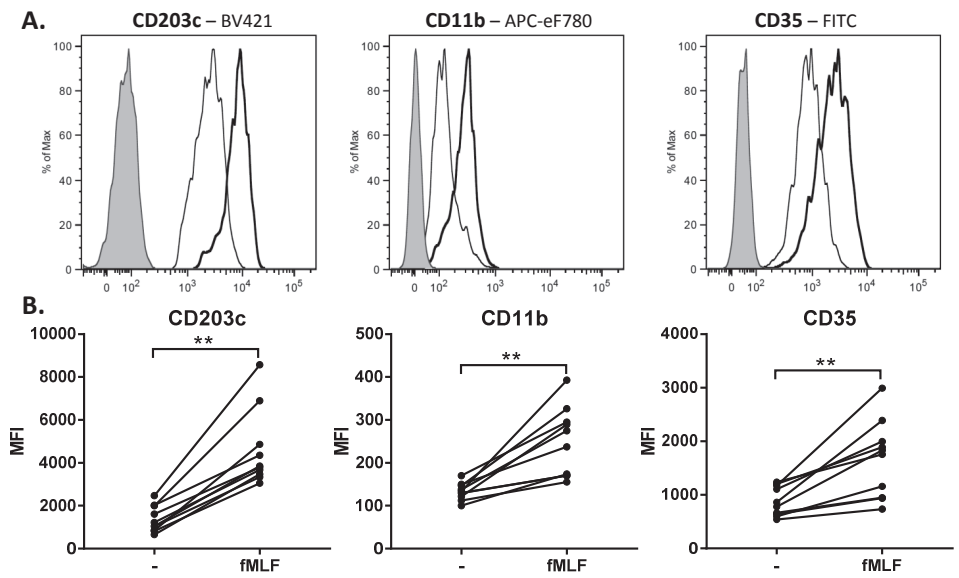

Supplementary Figure S5. Expression of CD203c, CD11b and CD35 on basophils collected in a field study. Samples were cryopreserved for 2 years in liquid nitrogen. (*A*) Histograms of a representative sample, filled lines display a fluorescence-minus-one (FMO) sample, the thin black line unstimulated cells and the thick black line fMLF-stimulated cells. (*B*) Median fluorescent intensity (MFI) of markers in basophils from 10 donors left unstimulated and stimulated with fMLF. Means and standard deviations are shown in Supplementary Table S2. *indicates analysis with Wilcoxon matched-pairs signed rank test. **, $P \leq 0.01$.

Supplementary table S1. Expression of CD203c, CD11b and CD35 on basophils and the response to fMLF.

	Fresh Mean MFI (SD)		Fixed Mean MFI (SD)		Fix & Freeze Mean MFI (SD)	
Basophils	Medium	fMLF	Medium	fMLF	Medium	fMLF
CD203c	682 (260)	3172 (3844)	1397 (417)	4661 (4840)	1288 (401)	3542 (3007)
CD11b	234 (69)	368 (261)	191 (21)	332 (226)	219 (15)	353 (207)
CD35	582 (148)	1361 (1122)	886 (157)	1618 (938)	888 (157)	1538 (779)

Supplementary table S2. Expression of activation markers on neutrophils, eosinophils and basophils from 10 representative donors collected in a field study presented as mean MFI and standard deviation.

Neutrophils	Medium	fMLF
CD11b	1237 (151)	1527 (181)
CD35	1895 (728)	3203 (735)
CD66b	543 (59)	713 (164)
CD62L	641 (278)	105 (23)
Eosinophils	**Medium**	**Eotaxin**
CD35	3044 (596)	3933 (714)
CD11b	1147 (438)	2079 (550)
Basophils	**Medium**	**fMLF**
CD203c	1374 (615)	4587 (1779)
CD11b	133 (20)	249 (80)
CD35	880 (275)	1663 (718)

6

THE EFFECT OF HELMINTHS ON GRANULOCYTE ACTIVATION: A CLUSTER-RANDOMIZED PLACEBO-CONTROLLED TRIAL IN INDONESIA

Karin de Ruiter, Dicky L. Tahapary, Erliyani Sartono, Thomas B. Nutman, Johannes W.A. Smit, Leo Koenderman, Taniawati Supali and Maria Yazdanbakhsh

The Journal of Infectious Diseases (2018) [Epub ahead of print]

ABSTRACT

Background

Eosinophils are a prominent cell type in the host response to helminths, and some evidence suggests that neutrophils might also play a role. However, little is known about the activation status of these granulocytes during helminth infection.

Methods

We analysed the expression of eosinophil and neutrophil activation markers in peripheral blood by flow cytometry, and measured serum levels of eosinophil granule proteins in 300 subjects residing in an area endemic for soil-transmitted helminths (STH). The data generated are on samples before and after 1 year of 3-monthly albendazole treatment.

Results

Anthelmintic treatment significantly reduced the prevalence of STH. While eosinophil numbers were significantly higher in STH-infected subjects compared to those uninfected and significantly decreased following albendazole treatment, there was no effect exerted by the helminths on either eosinophil nor neutrophil activation. Although at baseline, eosinophil granule protein levels were not different between STH-infected and uninfected subjects, treatment significantly reduced the levels of eosinophil-derived neurotoxin (EDN) in those infected at baseline.

Conclusions

These results show that besides decreasing eosinophil numbers, anthelmintic treatment does not significantly change the activation status of eosinophils, nor of neutrophils, and the only effect seen was a reduction on circulating levels of EDN.

Clinical trial registration

http://www.isrctn.com/ISRCTN75636394

INTRODUCTION

Eosinophilia is a well-known hallmark of helminth infections. While these bone marrow-derived, innate cells reside primarily in the tissues where they can survive up to two weeks (1), elevated frequencies are found in peripheral blood during helminth infections and, to a lesser extent, in allergic diseases. Although in vitro, eosinophils have been shown to be able to kill helminths (2-5), their role during helminth infections remains uncertain, as in vivo depletion of eosinophils has shown inconclusive results regarding their protective efficacy (6), and helminths such as *Trichinella* larvae, appear to benefit from the presence of eosinophils (7, 8). Furthermore, eosinophils are increasingly being recognized as cells that contribute to tissue, metabolic and immune homeostasis (9). Adipose tissue eosinophils for example, play a crucial role in maintaining insulin sensitivity through the secretion of the cytokines IL-4 and IL-13 (10).

Whereas increased eosinophil concentrations are characteristic of helminth infections, it is the activation status of these cells that drives the eosinophil mediated effects (11). Eosinophils can exist in different states of activation, and this is reflected by the expression of certain surface markers and by the increased serum levels of eosinophil-specific granule proteins. Upon recruitment to inflammatory sites, eosinophils alter the expression of a number of surface molecules that are involved in tethering, rolling along and adhesion to endothelial cells, followed by trans-endothelial migration into the tissue (12). The presence of these surface molecules (e.g. CD11b, CD35, CD69, CD66b and CD62L) on peripheral blood eosinophils is a useful indicator of cellular activation, during both helminth infections (13-15) and allergic diseases (16-19). Moreover, eosinophils respond to eotaxin, a chemokine responsible for eosinophil recruitment into tissues, by upregulating CD11b and shedding CD62L (20, 21).

Upon eosinophil degranulation, cytotoxic proteins including major basic protein (MBP), eosinophil cationic protein (ECP), eosinophil-derived neurotoxin (EDN) and eosinophil peroxidase (EPO) are released from secondary granules, and increased serum levels of these granule proteins are also considered to be a measure of eosinophil activation (19).

While neutrophils are known primarily for their potent anti-bacterial properties through the secretion of their granule proteins such as myeloperoxidase (MPO), they have also been shown to kill helminth larvae (22-24), and levels of MPO were significantly elevated in subjects infected with *Strongyloides stercoralis* (25) indicating that neutrophils can also become activated during helminth infections. Similar to eosinophils, neutrophil activation is associated with the upregulation of several surface molecules including CD11b, CD35, CD66b and the shedding of CD62L (16, 18). Although the expression of these markers and their upregulation or shedding in response to *N*-Formyl-Met-Leu-Phe (fMLF) have been used as a very sensitive measure of neutrophil (pre-)activation in patients with allergic asthma (16-18), it has never been studied in the context of helminth infections.

In this study, we assessed the effect of helminth infections on the activation status and responsiveness of both eosinophils and neutrophils. Although previous work has shown

that helminth infections are associated with increased eosinophil activation by assessing either activation markers (13-15) or eosinophil granule proteins (11, 25-28), these studies often had a cross-sectional design, a relatively small sample size, and did not assess eosinophil responsiveness. To this end, we measured the expression of eosinophil and neutrophil activation markers by flow cytometry, both ex vivo and after in vitro stimulation, in subjects infected with soil-transmitted helminths (STH), before and after 1 year of anthelmintic treatment. In addition, serum levels of eosinophil granule proteins were assessed. This study is part of a large cluster-randomized, placebo-controlled trial (29) and therefore the first placebo-controlled trial investigating the effect of helminths on granulocyte activation.

METHODS

Study design

This report describes a nested study within the SugarSPIN trial (29), a household-based cluster-randomized double-blind trial that was conducted in Nangapanda, Ende district of Flores Island (East Nusa Tenggara), Indonesia. After randomisation, all study subjects received either a single tablet of albendazole (400 mg) or matching placebo (tablets from PT Indopharma Pharmaceutical, Bandung, Indonesia) for three consecutive days under direct supervision from the research team members. This treatment regimen was given every three months for a total of four rounds (maximum of 12 tablets in total), between May 2014 and February 2015.

Although the study was aimed at subjects aged 16 and above, all subjects in the study area, except children below 2 years of age and pregnant women, were included in the trial to avoid cross-contamination between household members. Subjects aged 16 and above underwent clinical and laboratory examination, excluding subjects with active treatment for diabetes mellitus and serious concomitant diseases. Written informed consent was obtained from participants prior to the study. The study was approved by the ethics committee of the Faculty of Medicine, Universitas Indonesia (FKUI) (ref: 549/H2·F1/ETIK/2013), and filed by the ethics committee of Leiden University Medical Center (LUMC), the Netherlands. The trial is registered as a clinical trial (Ref: ISRCTN75636394).

Study population

The randomization for the total study was based on 752 households comprising 3698 individuals, resulting in 1825 (377 houses) and 1741 (375 houses) subjects in the placebo and albendazole group, respectively (Supplementary Figure S1). An additional randomization was performed on the 2406 subjects aged 16 and above, in order to study immune mechanisms in more detail (29). For this subgroup, we aimed to select one subject per household and stratified by age group (16-36 years, 36-56 years, and >56 years) to ensure that sufficient numbers of all groups were represented. Randomization was based on households. This resulted in a total of 300 subjects who were included for

immunological studies (152 subjects on placebo and 148 subjects in albendazole group) and randomly selected, paired samples from 195 subjects were subsequently used for flow cytometric analysis.

We also collected venous blood of 9 healthy volunteers which had not been exposed to helminth infections, hereafter referred to as "Europeans". We used the whole blood samples for flow cytometric analysis to assess granulocyte phenotype and response in naïve subjects.

Parasitological examination

Fresh stool samples were frozen at -20°C in the field centre and subsequently at -80°C at the Department of Parasitology of FKUI. Stool DNA isolation and real-time PCR were performed pairwise (baseline and follow-up). DNA isolation from stool was performed as described elsewhere (30, 31). Multiplex real-time polymerase chain reaction (PCR) was performed to simultaneously detect the presence of hookworm (*Ancylostoma duodenale*, *Necator americanus*), *Ascaris lumbricoides*, *Trichuris trichiura*, and *Strongyloides stercoralis*, using a method described previously (30). Stool samples were considered positive by PCR when cycle threshold (Ct) values were <50. Since the prevalence of *S. stercoralis* at baseline appeared to be very low (1.4% (4/284)), this species was not included in the analysis.

Sample collection

Blood samples were collected and processed as previously described (29, 32). Briefly, from each subject 3 polystyrene tubes containing 200 µL of heparinised venous blood were pre-incubated for 5 minutes in a 37°C waterbath, followed by a 5 minute-stimulation at 37°C with fMLF (10^{-5} M; Sigma, Saint Louis, MO, USA) or eotaxin (10^{-7} M; R&D systems, Abingdon, UK) or left unstimulated. While both Indonesian and European blood samples were stimulated with fMLF, stimulation with eotaxin was only applied to Indonesian samples. Subsequently, 4 mL of FACS lysing solution (BD Biosciences) was added and after an incubation period of 15 minutes at room temperature, cells were washed with RPMI 1640 containing 10% heat-inactivated foetal calf serum (FCS) and resuspended in RPMI 1640 containing 10% FCS and 10% dimethyl sulfoxyde (DMSO). Cryovials containing the cell suspension were placed at -80°C for a minimum of 4 hours, followed by storage in liquid nitrogen until analysis.

Flow cytometry of granulocyte surface markers

While flow cytometric analysis of the samples was randomly divided over multiple measurement days, all samples belonging to one individual were thawed, stained and measured pairwise (baseline and follow-up) on the same day. After thawing, cells were washed in RPMI 1640 containing 10% FCS and resuspended in FACS buffer (PBS supplemented with 0.5% BSA and 2 mM EDTA). Cells were counted using microscopy and 500.000 white blood cells were stained for 30 minutes at 4°C with anti-CD35-FITC (E11,

Biolegend), anti-CD66b-PerCP/Cy5.5 (G10F5, Biolegend), anti-CD193-PE (5e, Biolegend), anti-CD16-PE/CF594 (3G8, BD Biosciences), anti-CD69-PE/Cy5 (FN50, Biolegend), anti-CD274-PE/Cy7 (MIH1, eBioscience), anti-CD3/CD19/CD20/CD56-APC (UCHT1, HIB19, 2H7, 5.1H11, Biolegend), anti-CD11b-APC/eF780 (ICRF44, eBioscience), anti-CD203c-BV421 (NP4D6, Biolegend), anti-CD14-BV510 (M5E2, Biolegend), anti-CD62L-BV605 (DREG-56, BD Biosciences). Antibody dilutions can be found in Supplementary Table S1. For each antibody, a fluorescence-minus-one (FMO) control sample was included using pooled cells from different subjects. Cells were acquired on a LSR Fortessa flow cytometer (BD Biosciences) and before each measurement a performance run was conducted with cytometer setup and tracking (CS&T) beads (BD Biosciences). Data was analysed in FlowJo software (version 9.9.3) and median fluorescence intensity (MFI) data are displayed. Representative gating schemes to select eosinophil and neutrophils are shown in Supplementary Figure S2. As all cells of each sample were acquired, the absolute number of eosinophils and neutrophils which was analysed, would differ per sample.

After gating all leukocyte populations (eosinophils, neutrophils, basophils, monocytes, lymphocytes), percentages of eosinophils and neutrophils were calculated relative to the total amount of white blood cells. The absolute eosinophil count (AEC) reflects the number of eosinophils in 200 µl blood, and was calculated using the proportion of eosinophils and the white blood cell count after thawing.

As described previously (32), the detection of CD62L on eosinophils was impaired as a result of fixation and this marker was therefore not included in the analysis as activation marker for eosinophils.

Serum eosinophil granule proteins

The serum concentrations of eosinophil granule proteins, MBP, ECP, EDN and EPO were measured in a suspension array assay in multiplex as previously described (33). As the levels of EPO were below the limit of detection of 6 ng/ml in every sample, this protein was excluded from analysis. Eosinophil granule proteins were measured in the total subgroup selected for immunological studies (300 and 258 subjects at baseline and follow up, respectively). In 5/558 samples, one of the proteins could not be detected while in 1/558 samples, neither MBP, ECP, nor EDN could be detected.

Statistical analysis

For continuous variables, normally distributed data were presented as mean and standard deviation, while non-normally distributed data (eosinophil count, total IgE, eosinophil granule proteins and eosinophil activation markers) were presented as geometric mean and 95% confidence interval, and log-transformed for analyses. Categorical data such as infection prevalence were expressed as proportions. Comparisons between STH-infected and uninfected subjects at baseline were performed with Student's *t* test. Comparisons between Indonesian STH-infected, Indonesian uninfected and European subjects were

performed with ANOVA followed by Tukey's multiple comparisons test. ANOVA followed by a Dunnett's multiple comparison test was used to test granulocyte counts after stratifying subjects by helminth species. To determine the relationship between serum levels of eosinophil granular proteins and eosinophil counts Spearman's rank correlation was used. Paired *t* tests were performed to assess the responsiveness of granulocytes to eotaxin or fMLF. *P* values < .05 were considered statistically significant.

The effect of anthelmintic treatment on eosinophil counts, eosinophil granule proteins and eosinophil activation markers was assessed using an intention-to-treat approach, applying mixed models to account for the correlation within households. Two random effects were used: to model clustering within households a random household specific intercept was used and to model correlation within subjects random subject-specific intercept was used. Parameter estimates for treatment effect and 95% CIs were reported. The reported *p* values were obtained using a likelihood ratio test comparing the model with and without the treatment effect. For the binary outcome (helminth infection status), a logistic model was used with random household effects and random subject effects. All models were fitted using the lme4 package (R software).

RESULTS

Study population

At baseline, 300 subjects were included for immunological studies (152 subjects and 148 subjects in the placebo and the albendazole group respectively) (Supplementary Figure S1). The loss to follow up was 14% which was mainly due to movement out of the village. Baseline characteristics of the study participants are shown in Table 1, while details of a subset of the study population (n=195), used to study granulocyte activation markers by flow cytometry can be found in Supplementary Table S1.

At baseline 59.2% (168/284) of the individuals were infected with one or more helminth species, with hookworm infection being the most prevalent. In all subjects treated with albendazole in the SugarSPIN trial, the prevalence of helminth infection was 55.4% before, and 11.3% after treatment (30). Similar to this result, we observed that albendazole treatment reduced the percentage of subjects with any helminth (55.9% (80/143) to 9.2% (11/120) in the albendazole arm vs 62.4% (88/141) to 51.2% (62/121) in the placebo arm, *P* < .0001). The highest reduction was seen for hookworm, followed by *A. lumbricoides* and *T. trichiura* infection (Supplementary Figure S3).

Granulocyte counts in peripheral blood

At baseline, the frequency of eosinophils in whole blood was significantly higher in infected subjects compared to non-infected subjects (Geomean (95% CI), STH+ 7.0 (6.3-7.8)% vs STH- 5.5 (4.7-6.5)%, *P* = .01) (Figure 1A). Irrespective of coinfection with other helminths, subjects infected with hookworm showed the highest eosinophil counts (7.9 (6.9-8.9)%) (Figure 1A). As observed in the whole SugarSPIN trial (34), anthelmintic

Table 1. Baseline characteristics of the study population.

	n	Placebo	n	Albendazole
Age (mean in years, SD)	151	46.7 (13.4)	148	46.2 (16.2)
Sex (female, n, %)	151	100 (66.2)	148	86 (58.1)
BMI (kg/m^2) (mean, SD)	149	23.1 (4.2)	147	22.5 (4.2)
Total IgE (IU/mL) (GM, 95% CI)	150	663 (506-870)	148	672 (514-878)
Eosinophil count* (GM, 95% CI)	148	5.5 (4.9-6.2)	146	6.1 (5.5-6.8)
MBP (ng/mL) (GM, 95% CI)	150	978 (859-1154)	147	969 (830-1132)
ECP (ng/mL) (GM, 95% CI)	150	908 (756-1124)	147	935 (786-1111)
EDN (ng/mL) (GM, 95% CI)	149	346 (295-408)	147	380 (326-442)
Helminth infection by PCR (n,%)	141	88 (62.4)	143	80 (55.9)
A. lumbricoides	141	36 (25.5)	143	22 (15.4)
Hookworm	141	62 (44.0)	143	53 (37.1)
T. trichuris	141	50 (35.5)	143	36 (25.2)

*Determined by using a Giemsa-stained peripheral thin blood smear. Abbreviations: BMI body mass index; ECP eosinophil cationic protein; EDN eosinophil-derived neurotoxin; GM geometric mean; IgE immunoglobulin; MBP major basic protein; PCR polymerase chain reaction; SD standard deviation.

treatment effectively reduced eosinophil counts, especially in those infected with helminths at baseline (Estimated treatment effect (95% CI), -0.187 (-0.258 – -0.117), P = .01) (Figure 1C). Neutrophil counts did not differ between uninfected and infected subjects at baseline (P = 0.59, Figure 1B). Interestingly, albendazole treatment significantly increased the frequency of neutrophils in peripheral blood in those who were infected with helminths at baseline (0.041 (0.017 – 0.066), P < .01) (Figure 1D). While Europeans exhibited significantly lower eosinophil frequencies (Geomean (95% CI), 1.9 (0.9-3.7)%) compared to Indonesians, irrespective of current helminth infections, similar frequencies of neutrophils were observed (53 (45-62)%).

Eosinophil activation status and responsiveness

At baseline, the intensity of the eosinophil activation markers CD11b, CD35, CD66b and CD69 was similar in STH-infected and uninfected subjects (Table 2). Albendazole treatment did not influence the expression of these markers (Table 3). Neither at community level, nor when analysing subjects with helminth infection as baseline. The comparison with Europeans revealed a lower intensity of CD35 in Indonesian subjects, both STH-infected and uninfected, while other markers did not differ (Table 2).

Whole blood stimulated with eotaxin or fMLF was used to assess the responsiveness of eosinophils. The intensity of CD11b, CD35, CD66b and CD69 on eotaxin- or fMLF-stimulated eosinophils did not differ between uninfected subjects and those infected with helminths at baseline (Supplementary Figure S4 A-B). Moreover, albendazole treatment did not affect the responsiveness (data not shown). Interestingly, not all individuals responded to eotaxin or fMLF by upregulating the activation markers. In half of the subjects, there

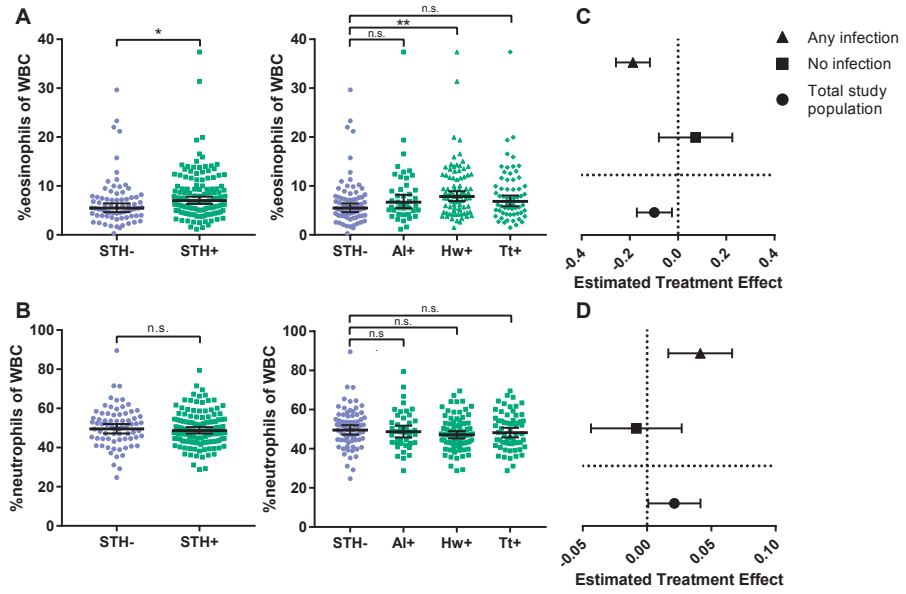

Figure 1. Granulocyte counts. Percentage of eosinophils (*A*) and neutrophils (*B*) relative to the total number of white blood cells (WBC). Counts at baseline are shown displaying geomeans and corresponding 95% confidence intervals (STH- n=73, STH+ n=118, Al+ n=42, Hw+ n=81, Tt+ n=61). The effect of anthelmintic treatment eosinophil (*C*) and neutrophil (*D*) counts is displayed with the corresponding 95% confidence intervals (n=195). Differences between STH- and STH+ subjects were tested with Student's *t* test. Differences between STH-, Al+, Hw+ and Tt+ subjects were tested with ANOVA followed by a Dunnett's multiple comparison test. Treatment effect was assessed using mixed models (see Methods). *P <.05; **P <.01; n.s. not significant; STH Soil-transmitted helminths; Al *A. lumbricoides*; Hw Hookworm; Tt *T. trichuria*.

Table 2. Expression of granulocyte activation markers at baseline.

	STH- (n=73)	STH+ (n=118)	EU (n=9)
Eosinophils			
CD11b	1444 (1337-1559)	1376 (1297-1459)	1700 (1551-1864)
CD35	3269 (3144-3435)	3254 (3150-3360)	3915 (3688-4155)[a,b]
CD66b	2100 (2031-2172)	2055 (2004-2108)	2046 (1825-2295)
CD69	783 (735-834)	772 (737-809)	677 (632-725)
Neutrophils			
CD11b	1151 (1107-1196)	1172 (1141-1203)	1387 (1238-1554)[a,b]
CD35	1571 (1457-1695)	1618 (1519-1722)	1413 (1101-1816)
CD66b	581 (553-609)	592 (568-617)	590 (532-654)
CD62L	748 (676-827)	788 (726-856)	1358 (1262-1462)[a,b]

Geomean of MFI and corresponding 95% confidence intervals are shown. [a] P <.05 analysed using ANOVA Tukey statistical test for comparison with Indonesian STH- subjects. [b] P <.05 analysed using ANOVA Tukey statistical test for comparison with Indonesian STH+ subjects. STH soil-transmitted helminths.

Table 3. The effect of anthelmintic treatment on granulocyte activation markers.

	All (n=195)	STH- (n=73)	STH+ (n=118)
Eosinophils	Estimated treatment effect (95% CI), p value		
CD11b	0.024 (-0.010-0.058), p=0.18	0.012 (-0.045-0.069), p=0.69	0.039 (-0.005-0.082), p=0.09
CD35	0.009 (-0.006-0.024), p=0.23	0.008 (-0.018-0.034), p=0.54	0.015 (-0.004-0.034), p=0.13
CD66b	0.003 (-0.008-0.014), p=0.55	0.004 (-0.016-0.024), p=0.73	0.007 (-0.007-0.020), p=0.32
CD69	-0.016 (-0.038-0.007), p=0.19	-0.029 (-0.067-0.009), p=0.14	0.003 (-0.026-0.031), p=0.86
Neutrophils			
CD11b	0.003 (-0.018-0.023), p=0.81	0.021 (-0.014-0.055), p=0.25	-0.007 (-0.032-0.018), p=0.60
CD35	-0.010 (-0.041-0.021), p=0.53	0.001 (-0.058-0.061), p=0.96	-0.010 (-0.045-0.025), p=0.59
CD66b	0.015 (-0.002-0.032), p=0.09	0.023 (-0.006-0.052), p=0.12	0.010 (-0.012-0.032), p=0.39
CD62L	0.029 (-0.029-0.087), p=0.33	0.053 (-0.041-0.146), p=0.27	-0.009 (-0.082-0.065), p=0.82

Treatment effect was assessed using mixed models (see Methods). Estimated treatment effects are displayed with the corresponding 95% confidence intervals. *P* values were obtained using a likelihood ratio test comparing the model with and without the treatment effect. STH soil-transmitted helminths.

was an increase in the MFI of the activation markers whereas in the other half the MFI of markers decreased after stimulation (Supplementary Figure S4 C-D). Of note, in those who had a low intensity of markers before stimulation, the expression of the markers went up whereas the opposite was seen in subjects who had a high marker expression (Supplementary Figure S4 C-D). However, this observation could not be associated with the infection status, since in both infected and uninfected subjects the same was seen. In Europeans, most subjects responded to fMLF by upregulating the activation markers, also reflected in a stronger responsiveness (Supplementary Figures S4 B).

Neutrophil activation status and responsiveness

We found no difference in the expression levels of neutrophil activation markers (CD11b, CD35, CD66b, CD62L) between STH-infected and uninfected subjects at baseline (Table 2), and treatment did not alter the intensity of these markers (Table 3). When compared to Europeans, levels of both CD11b and CD62L were lower in Indonesians, irrespective of their current infection status (Table 2). Although neutrophils strongly responded to fMLF by upregulating CD11b, CD35 and CD66b, while shedding CD62L, the responsiveness was similar in all subjects, irrespective of their helminth infection status (Supplementary

Figure S5). Albendazole treatment did not affect neutrophil responsiveness (data not shown). When neutrophils in Europeans were considered, the responsiveness was more marked compared to Indonesians (Supplementary Figure S5).

Eosinophil granule proteins

Serum levels of MBP, ECP and EDN were similar in STH-infected and uninfected subjects at baseline (Geomean, (95% CI), MBP, STH+ 979 (864-1156) ng/ml vs STH- 910 (766-1063) ng/ml, *P* = .52; ECP, STH+ 892 (748-1077) ng/ml vs STH- 920 (764-1129) ng/ml, *P* = .82; EDN, STH+ 362 (313-423) ng/ml vs STH- 353 (297-419) ng/ml, *P* = .83) (Figure 2A). No relation was found between protein concentrations and different helminth species or the total number of helminth species a subject was infected with (data not shown). Levels of EDN correlated with absolute eosinophil counts (AEC) at baseline (r=0.54, *P* < .01), however, the correlation coefficient for MBP, although statistically significant, was weak (MBP: r = 0.27, *P* < .01) and when considering ECP no correlation could be found with eosinophil counts (ECP: r = 0.03, *P* = .69) (Supplementary Figure S6). Albendazole treatment decreased the level of MBP (Estimated treatment effect (95% CI), -0.070 (-0.124 – -0.015), *P* = .01) and EDN (-0.060 (-0.121 – 0.0002), *P* = .05),

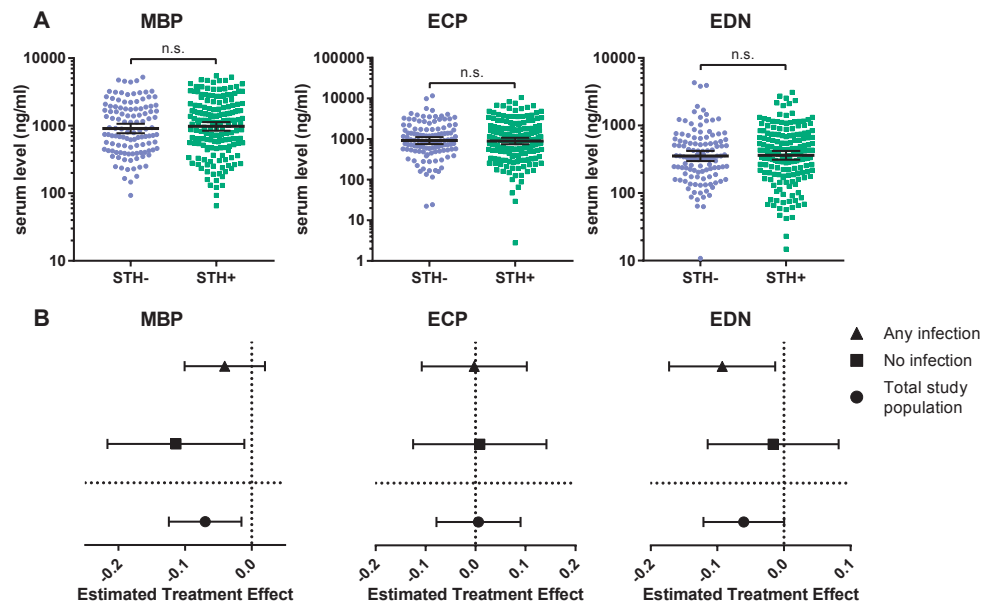

Figure 2. Eosinophil granule proteins. Major basic protein (MBP), eosinophil cationic protein (ECP) and eosinophil derived neurotoxin (EDN) concentrations in serum at baseline (*A*) and the effect of albendazole treatment (*B*) are shown. Lines represent geomeans and corresponding 95% confidence intervals (STH- n=116, STH+ n=168 (*A*)). The effect of anthelmintic treatment is displayed with the corresponding 95% confidence intervals (n=299 (*B*)). Differences between STH- and STH+ subjects were tested with Student's *t* test. Treatment effect was assessed using mixed models (see Methods). n.s. not significant; STH Soil-transmitted helminths.

whereas the level of ECP did not change (0.006 (-0.078-0.090), *P* = .93) at community level (Figure 2B). When analysing those infected with helminths at baseline, EDN levels significantly decreased after treatment (-0.093 (-0.172 – -0.013), *P* = .02).

DISCUSSION

Eosinophil numbers are associated with helminth infections. We hypothesized that not only eosinophil numbers, but also their activation status would be affected by the presence of helminths. As a measure of activation, a range of activation markers in peripheral blood eosinophils and neutrophils were assessed, as well as the responsiveness to stimulation. In addition, circulating levels of eosinophil granule proteins were measured as a marker for the activation status of eosinophils, not only in blood but also in tissues. This study was nested within a cluster-randomized, double-blind placebo-controlled trial, conducted in a rural area in Indonesia (29). To our knowledge, this is the first placebo-controlled trial studying the effect of helminth infections on granulocyte activation and derives strength from its design and large sample size.

Although the number of eosinophils was higher in STH-infected compared to uninfected subjects and decreased significantly after albendazole treatment, the intensities of eosinophil, as well as neutrophil, activation markers were not affected by helminths and did not change upon anthelmintic treatment. This is in contrast to what has been reported (11, 13-15, 25-28). Previously, Mawhorter et al. showed an elevated percentage of CD69, CD66 and CD81 positive eosinophils in 18 subjects recruited in the USA, infected with one or more species of seven helminths, and found CD66 to be decreased in the five subjects that were followed after short term anthelmintic treatment (13). In a study conducted in Brazil, the observation that the frequency of $CD23^{+}$ eosinophils was increased while that of $CD62L^{+}$ cells was decreased in subjects infected with *Schistosoma mansoni*, led to the conclusion that eosinophils were chronically activated during infection (15). However, this conflicted with a lower frequency of $CD69^{+}$ eosinophils, indicating little early activation of eosinophils (15). In another study in Brazil, Fujiwara et al. demonstrated a highly activated state of eosinophils in subjects infected with hookworms compared to uninfected individuals (14). None of these studies, in contrast to ours, included uninfected subjects from the endemic regions. Moreover, they included a relatively small number of study subjects (varying from 23 to 35 individuals), and perhaps more importantly, the antibody staining was directly performed on fresh blood. As we were limited by the infrastructure at the field study site with no direct access to a flow cytometer, we developed a method to analyse granulocyte activation markers in cryopreserved, fixed whole blood (32). As previously described, it was observed that marker intensities varied when comparing fresh and fixed granulocytes, most likely due to intracellular staining and increased eosinophil autofluorescence as a consequence of fixation (32). However, we showed that the responsiveness to stimuli could still be clearly measured after fixation. Nevertheless, it is possible that the use of fresh cells allows smaller differences to be detected.

By taking along European subjects, we could compare the results with naïve eosinophils and neutrophils from individuals with lower exposure to microorganisms and helminths. The eosinophils from Indonesians had a lower expression of the activation marker CD35 and a lower responsiveness to fMLF. With respect to neutrophils, there was an interesting observation that both CD62L and CD11b showed a lower expression in Indonesians. While lower CD11b on neutrophils from Indonesians would indicate a lower activation status of these cells, the lower expression of CD62L, which is shed by activated neutrophils, would suggest a higher activation status of neutrophils in Indonesians, contradicting the CD11b data. However, the loss of CD62L has also been associated with aged neutrophils (35) and therefore, it is possible that in Indonesia, the higher exposure of the granulocytes to microbes or inflammation, results in more aged granulocytes with lower responsiveness. Indeed, this is supported by the lower activation of neutrophils from Indonesian subjects by fMLF compared to the response of neutrophils from Europeans. However, future studies are needed to clarify this further.

Whereas the expression of activation markers was assessed in circulating eosinophils, mature eosinophils are predominantly tissue dwelling cells and serum levels of eosinophil granule proteins are thought to be an indirect measure of degranulation in the tissues. MBP, being stored in the core of secondary granules is the most abundant protein and its release is toxic to helminths (1). EDN and ECP, also known as RNase 2 and RNase 3 respectively, both have ribonuclease activity and can be found in the granule matrix (1). Whereas ECP is cytotoxic to helminth larvae, EDN seems to be less efficient in killing helminths (2). In contrast to our hypothesis, we observed no differences in the levels of eosinophil granule proteins between helminth infected and uninfected subjects. It should be noted that the study area was highly endemic for STH infections (36) and perhaps exposure to an environment contaminated with parasite eggs or infective larvae can lead to altered eosinophil homeostasis and maturity/activation, thereby masking the potential difference between currently infected and uninfected subjects.

Elevated eosinophil cationic protein levels have previously been described in subjects infected with filaria (*Onchocerca volvulus* (26), *Loa Loa* (37), *Wuchereria bancrofti* (26)), soil-transmitted helminths (*A. lumbricoides* (27), hookworm (27), and *S. stercoralis* (25)) and *S. mansoni* (26, 28). Whereas most studies had a cross-sectional design, two reports described a significant decline in granular protein levels in subjects infected with *S. mansoni* or *S. stercoralis*, respectively, after anthelmintic treatment, indicating a decrease in eosinophil degranulation (25, 28). In our study, albendazole treatment significantly decreased EDN levels in subjects that were infected at baseline, whereas the levels of MBP and ECP did not change. Out of the three proteins, EDN also showed the strongest correlation with the number of eosinophils at baseline and therefore its decrease is likely to reflect the decrease in eosinophil numbers after treatment.

The aim of this study was to investigate the effect of soil-transmitted helminths on granulocyte activation. Based on our results, we can conclude that helminths affect eosinophil numbers in the circulation, but the activation status and responsiveness of

these cells is similar between infected and uninfected subjects, and was not influenced by anthelmintic treatment. The same applies to neutrophils. However, this study should be repeated in an endemic setting with access to a flow cytometer that would allow the analysis of fresh granulocytes to assess activation of these cells, as fixing cells might not allow subtle differences to be detected between helminth infected and uninfected or before and after treatment.

ACKNOWLEDGEMENTS

The authors would like to thank all study participants and field workers in Nangapanda, Ende, Flores, Indonesia; Samatha Bandapalle for performing the eosinophil granule protein suspension array assay at the Laboratory of Parasitic Diseases at the National Institutes of Health, Bethesda, MD, US; and Dr. E.F. Knol (Laboratory of Translational Immunology, Dept. of Dermatology and Allergology, University Medical Center Utrecht) for his initial help with the study.

REFERENCES

1. Ravin KA, Loy M. The Eosinophil in Infection. Clin Rev Allergy Immunol 2016; 50(2): 214-27.
2. McLaren DJ, McKean JR, Olsson I, Venges P, Kay AB. Morphological studies on the killing of schistosomula of Schistosoma mansoni by human eosinophil and neutrophil cationic proteins in vitro. Parasite immunology 1981; 3(4): 359-73.
3. Ackerman SJ, Gleich GJ, Loegering DA, Richardson BA, Butterworth AE. Comparative toxicity of purified human eosinophil granule cationic proteins for schistosomula of Schistosoma mansoni. The American journal of tropical medicine and hygiene 1985; 34(4): 735-45.
4. Hamann KJ, Barker RL, Loegering DA, Gleich GJ. Comparative toxicity of purified human eosinophil granule proteins for newborn larvae of Trichinella spiralis. J Parasitol 1987; 73(3): 523-9.
5. Hamann KJ, Gleich GJ, Checkel JL, Loegering DA, McCall JW, Barker RL. In vitro killing of microfilariae of Brugia pahangi and Brugia malayi by eosinophil granule proteins. Journal of immunology (Baltimore, Md : 1950) 1990; 144(8): 3166-73.
6. Klion AD, Nutman TB. The role of eosinophils in host defense against helminth parasites. The Journal of allergy and clinical immunology 2004; 113(1): 30-7.
7. Huang L, Gebreselassie NG, Gagliardo LF, et al. Eosinophil-derived IL-10 supports chronic nematode infection. Journal of immunology (Baltimore, Md : 1950) 2014; 193(8): 4178-87.
8. Huang L, Beiting DP, Gebreselassie NG, et al. Eosinophils and IL-4 Support Nematode Growth Coincident with an Innate Response to Tissue Injury. PLoS pathogens 2015; 11(12): e1005347.
9. Weller PF, Spencer LA. Functions of tissue-resident eosinophils. Nature reviews Immunology 2017; 17(12): 746-60.
10. Wu D, Molofsky AB, Liang HE, et al. Eosinophils sustain adipose alternatively activated macrophages associated with glucose homeostasis. Science (New York, NY) 2011; 332(6026): 243-7.
11. Gazzinelli-Guimaraes PH, Bonne-Annee S, Fujiwara RT, Santiago HC, Nutman TB. Allergic Sensitization Underlies Hyperreactive Antigen-Specific CD4+ T Cell Responses in Coincident Filarial Infection. Journal of immunology (Baltimore, Md: 1950) 2016; 197(7): 2772-9.
12. Rosenberg HF, Dyer KD, Foster PS. Eosinophils: changing perspectives in health and disease. Nature reviews Immunology 2013; 13(1): 9-22.
13. Mawhorter SD, Stephany DA, Ottesen EA, Nutman TB. Identification of surface molecules associated with physiologic activation of eosinophils. Application of whole-blood flow cytometry to eosinophils. Journal of immunology (Baltimore, Md: 1950) 1996; 156(12): 4851-8.
14. Fujiwara RT, Cancado GG, Freitas PA, et al. Necator americanus infection: a possible cause of altered dendritic cell differentiation and eosinophil profile in chronically infected individuals. PLoS neglected tropical diseases 2009; 3(3): e399.
15. Silveira-Lemos D, Teixeira-Carvalho A, Martins-Filho OA, Oliveira LF, Correa-Oliveira R. High expression of co-stimulatory and adhesion molecules are observed on eosinophils during human Schistosoma mansoni infection. Memorias do Instituto Oswaldo Cruz 2006; 101 Suppl 1: 345-51.
16. Berends C, Hoekstra MO, Dijkhuizen B, de Monchy JG, Gerritsen J, Kauffman HF. Expression of CD35 (CR1) and CD11b (CR3) on circulating neutrophils and eosinophils from allergic asthmatic children. Clinical and experimental allergy: journal of the British Society for Allergy and Clinical Immunology 1993; 23(11): 926-33.
17. in 't Veen JC, Grootendorst DC, Bel EH, et al. CD11b and L-selectin expression on eosinophils and neutrophils in blood and induced sputum of patients with asthma compared with normal subjects. Clinical and experimental allergy: journal of the British Society for Allergy and Clinical Immunology 1998; 28(5): 606-15.
18. Mann BS, Chung KF. Blood neutrophil activation markers in severe asthma: lack of inhibition by prednisolone therapy. Respir Res 2006; 7: 59.
19. Metcalfe DD, Pawankar R, Ackerman SJ, et al. Biomarkers of the involvement of mast cells, basophils and eosinophils in

asthma and allergic diseases. World Allergy Organ J 2016; 9: 7.
20. Santamaria LF, Palacios JM, Beleta J. Inhibition of eotaxin-mediated human eosinophil activation and migration by the selective cyclic nucleotide phosphodiesterase type 4 inhibitor rolipram. British journal of pharmacology 1997; 121(6): 1150-4.
21. Tenscher K, Metzner B, Schopf E, Norgauer J, Czech W. Recombinant human eotaxin induces oxygen radical production, Ca(2+)-mobilization, actin reorganization, and CD11b upregulation in human eosinophils via a pertussis toxin-sensitive heterotrimeric guanine nucleotide-binding protein. Blood 1996; 88(8): 3195-9.
22. O'Connell AE, Hess JA, Santiago GA, et al. Major basic protein from eosinophils and myeloperoxidase from neutrophils are required for protective immunity to Strongyloides stercoralis in mice. Infection and immunity 2011; 79(7): 2770-8.
23. Buys J, Wever R, Ruitenberg EJ. Myeloperoxidase is more efficient than eosinophil peroxidase in the in vitro killing of newborn larvae of Trichinella spiralis. Immunology 1984; 51(3): 601-7.
24. Jong EC, Mahmoud AA, Klebanoff SJ. Peroxidase-mediated toxicity to schistosomula of Schistosoma mansoni. Journal of immunology (Baltimore, Md : 1950) 1981; 126(2): 468-71.
25. Rajamanickam A, Munisankar S, Bhootra Y, Dolla CK, Nutman TB, Babu S. Elevated Systemic Levels of Eosinophil, Neutrophil, and Mast Cell Granular Proteins in Strongyloides Stercoralis Infection that Diminish following Treatment. Frontiers in immunology 2018; 9: 207.
26. Tischendorf FW, Brattig NW, Buttner DW, Pieper A, Lintzel M. Serum levels of eosinophil cationic protein, eosinophil-derived neurotoxin and myeloperoxidase in infections with filariae and schistosomes. Acta tropica 1996; 62(3): 171-82.
27. Tischendorf FW, Brattig NW, Lintzel M, et al. Eosinophil granule proteins in serum and urine of patients with helminth infections and atopic dermatitis. Tropical medicine & international health : TM & IH 2000; 5(12): 898-905.
28. Reimert CM, Tukahebwa EM, Kabatereine NB, Dunne DW, Vennervald BJ. Assessment of Schistosoma mansoni induced intestinal inflammation by means of eosinophil cationic protein, eosinophil protein X and myeloperoxidase before and after treatment with praziquantel. Acta tropica 2008; 105(3): 253-9.
29. Tahapary DL, de Ruiter K, Martin I, et al. Helminth infections and type 2 diabetes: a cluster-randomized placebo controlled SUGARSPIN trial in Nangapanda, Flores, Indonesia. BMC infectious diseases 2015; 15: 133.
30. Tahapary DL, de Ruiter K, Martin I, et al. Effect of Anthelmintic Treatment on Insulin Resistance: A Cluster-Randomized, Placebo-Controlled Trial in Indonesia. Clin Infect Dis 2017; 65(5): 764-71.
31. Kaisar MMM, Brienen EAT, Djuardi Y, et al. Improved diagnosis of Trichuris trichiura by using a bead-beating procedure on ethanol preserved stool samples prior to DNA isolation and the performance of multiplex real-time PCR for intestinal parasites. Parasitology 2017; 144(7): 965-74.
32. de Ruiter K, van Staveren S, Hilvering B, et al. A field-applicable method for flow cytometric analysis of granulocyte activation: Cryopreservation of fixed granulocytes. Cytometry Part A : the journal of the International Society for Analytical Cytology 2018.
33. Makiya MA, Herrick JA, Khoury P, Prussin CP, Nutman TB, Klion AD. Development of a suspension array assay in multiplex for the simultaneous measurement of serum levels of four eosinophil granule proteins. Journal of immunological methods 2014; 411: 11-22.
34. de Ruiter K, Tahapary DL, Sartono E, et al. Helminths, hygiene hypothesis and type 2 diabetes. Parasite immunology 2017; 39(5).
35. Van Eeden SF, Bicknell S, Walker BA, Hogg JC. Polymorphonuclear leukocytes L-selectin expression decreases as they age in circulation. Am J Physiol 1997; 272(1 Pt 2): H401-8.
36. Wiria AE, Hamid F, Wammes LJ, et al. The effect of three-monthly albendazole treatment on malarial parasitemia and allergy: a household-based cluster-randomized, double-blind, placebo-controlled trial. PloS one 2013; 8(3): e57899.
37. Herrick JA, Metenou S, Makiya MA, et al. Eosinophil-associated processes underlie differences in clinical presentation of loiasis between temporary residents and those indigenous to Loa-endemic areas. Clin Infect Dis 2015; 60(1): 55-63.

SUPPLEMENTAL DATA

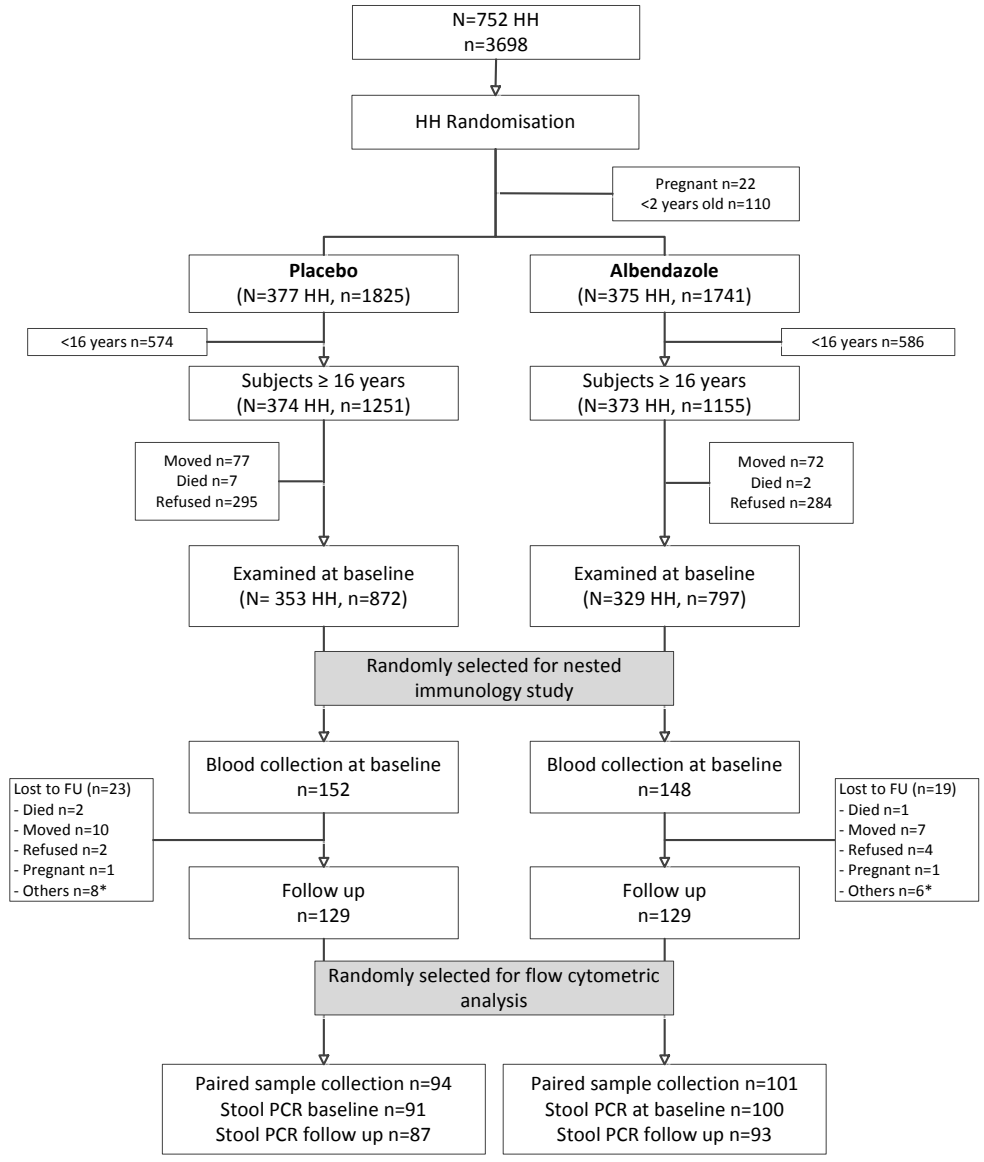

*Other reasons of lost to follow-up were harvesting crops, working on funeral ceremonies, severely ill, hospitalized, nursing mother, etc

Supplementary Figure S1. Consort diagram.

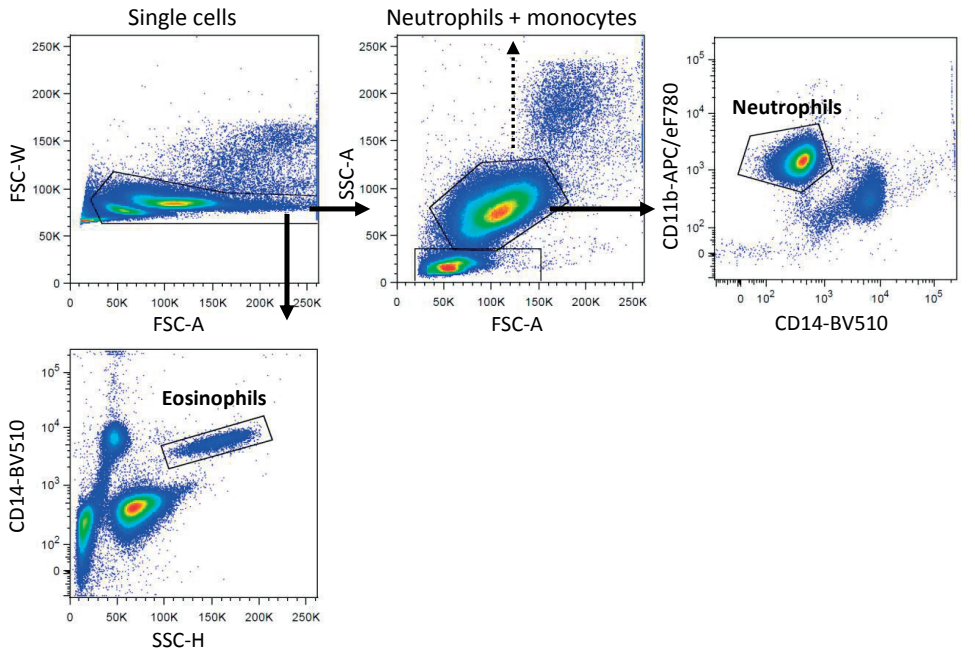

Supplementary Figure S2. FlowJo gating strategy of eosinophils and neutrophils. Eosinophils were selected from single cells and subsequently gated on autofluorescence (CD14-BV510/SSC-H plot). Neutrophils were selected from single cells, then distinguished from monocytes based on their CD11b and CD14 staining.

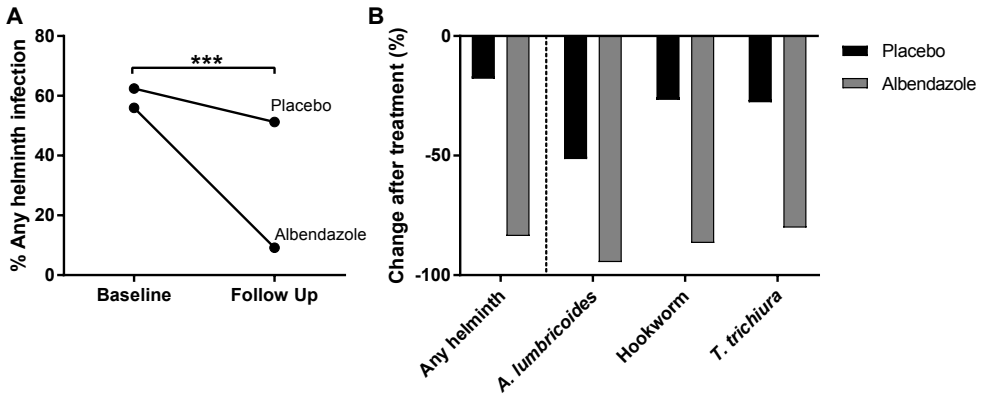

Supplementary Figure S3. The effect of albendazole treatment on the prevalence of soil-transmitted helminths. Percentage of helminth-infected subjects at baseline and following treatment, in placebo (n=141) and albendazole (n=143) treatment arms, as detected by PCR (*A*). Statistical analysis by a logistic model with random household effects and random subject effects; ****P* <.001. Fold change in infection prevalence stratified by helminth species (*B*).

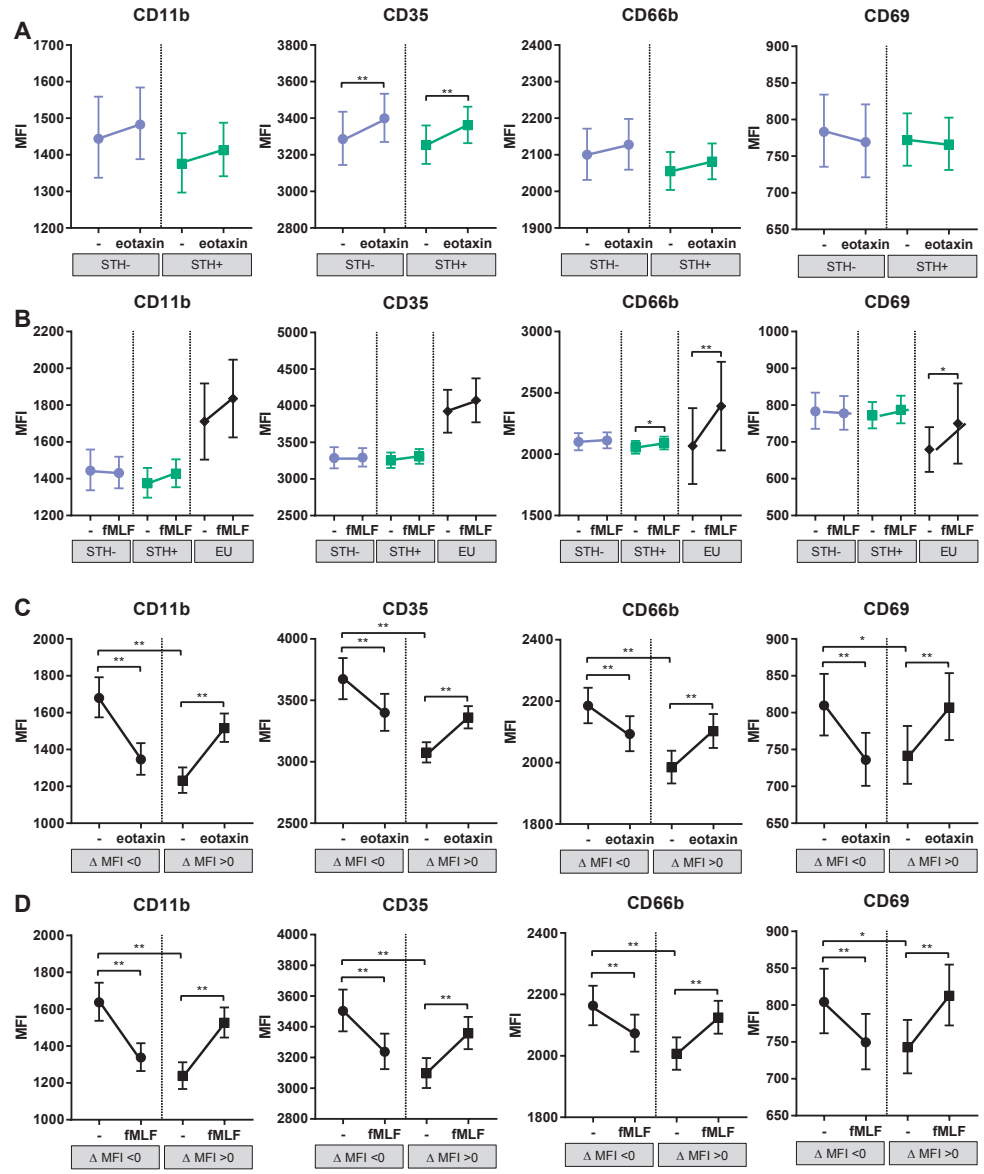

Supplementary Figure S4. Eosinophil responsiveness to eotaxin and fMLF. Median fluorescent intensity (MFI) of CD11b, CD35, CD66b and CD69 of eosinophils left unstimulated (-) and after stimulation with eotaxin (*A, C*) or fMLF (*B, D*). Indonesian subjects were either stratified by helminth infection (*A,B*; STH- (n=73) vs STH+ (n=118)) or by responsiveness (*C,D*; ΔMFI <0 vs ΔMFI >0). Europeans were not included in D, as most responded to fMLF. Geomeans and corresponding 95% confidence intervals are shown. Differences between before and after stimulation were tested with paired *t* tests. Differences between ΔMFI <0 and ΔMFI >0 before stimulation were tested by unpaired *t* tests. **P* <.05; ***P* <.01; n.s. not significant; STH Soil-transmitted helminths.

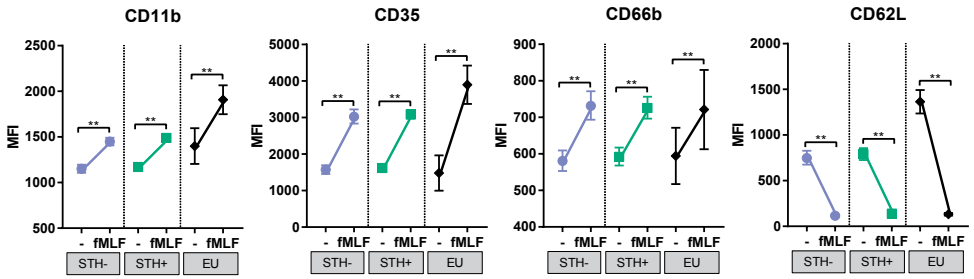

Supplementary Figure S5. Neutrophil responsiveness. Median fluorescent intensity (MFI) of CD11b, CD35, CD66b and CD62L of neutrophils left unstimulated (-) and after stimulation with fMLF. Indonesian subjects were stratified by helminth infection (STH- (n=73) vs STH+ (n=118)). Geomeans and corresponding 95% confidence intervals are shown. Differences between before and after stimulation were tested with paired *t* tests. ***P* <.01.

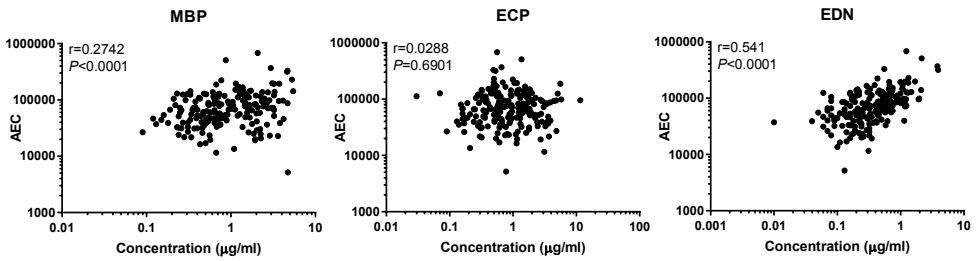

Supplementary Figure S6. Association between eosinophil granule proteins and eosinophil counts. Major basic protein (MBP), eosinophil cationic protein (ECP) and eosinophil derived neurotoxin (EDN) concentrations in serum at baseline and their association with absolute eosinophil counts (AEC). Spearman's rank correlation was used for statistical analysis (n=195).

Supplementary table S1. Antibody panel used for flow cytometry

Fluorochrome	Specificity	Clone	Vendor	Cat.no.	Dilution	Stock conc. (µg/mL)
FITC	CD35	E11	Biolegend	333404	300x	200
PerCP-Cy5.5	CD66b	G10F5	Biolegend	305107	100x	50
PE	CD193	5e8	Biolegend	310705	100x	100
PE-CF594	CD16	3G8	BD Biosciences	562320	4000x	100
PE-Cy5	CD69	FN50	Biolegend	310907	50x	20
PE-Cy7	CD274	MIH1	eBioscience	25-5983-41	80x	50
APC	CD3, CD19, CD20, CD56	UCHT1, HIB19, 2H7, 5.1H11	Biolegend	363601	150x	5, 6.25, 1.5, 17.5
APC-eF780	CD11b	ICRF44	eBioscience	47-0118-41	100x	50
BV421	CD203c	NP4D6	Biolegend	324611	100x	25
BV510	CD14	M5E2	Biolegend	301841	100x	150
BV605	CD62L	DREG-56	BD Biosciences	562720	100x	50

Supplementary table S2. Baseline characteristics of a subset of the study population, used to study granulocyte activation markers by flow cytometry.

	n	Placebo	n	Albendazole
Age (mean in years, SD)	94	48.6 (12.4)	101	47.4 (15.6)
Sex (female, n, %)	94	64 (68.1)	101	58 (57.4)
BMI (kg/m^2) (mean, SD)	93	23.3 (4.2)	100	22.5 (4.4)
Total IgE (IU/mL) (GM, 95% CI)	94	547 (376-794)	101	572 (410-797)
Eosinophil count (GM, 95% CI)	94	6.3 (5.6-7.1)	101	6.5 (5.6-7.5)
MBP (ng/mL) (GM, 95% CI)	93	816 (691-1010)	101	966 (814-1146)
ECP (ng/mL) (GM, 95% CI)	93	758 (610-981)	101	836 (698-1000)
EDN (ng/mL) (GM, 95% CI)	92	403 (238-352)	101	376 (316-448)
Eosinophil activation markers				
CD11b (GM, 95% CI)	94	1451 (1362-1547)	101	1366 (1276-1462)
CD35	94	3270 (3155-3391)	101	3267 (3147-3391)
CD66b	94	2103 (2047-2160)	101	2046 (1988-2105)
CD69	94	791 (752-833)	101	762 (723-804)
Neutrophil activation markers				
CD11b (GM, 95% CI)	94	1188 (1155-1222)	101	1143 (1107-1181)
CD35	94	1679 (1107-1181)	101	1532 (1436-1635)
CD66b	94	601 (576-628)	101	577 (552-602)
CD62L	94	747 (678-823)	101	794 (729-864)
Helminth infection by PCR (n,%)	91	63 (69.2)	100	55 (55.0)
A. lumbricoides	91	26 (28.6)	100	16 (16.0)
Hookworm	91	44 (48.4)	100	37 (37.0)
T. trichuris	91	34 (37.4)	100	27 (27.0)

Abbreviations: BMI body mass index; ECP eosinophil cationic protein; EDN eosinophil-derived neurotoxin; GM geometric mean; IgE immunoglobulin; MBP major basic protein; PCR polymerase chain reaction; SD standard deviation.

7

THE EFFECT OF THREE-MONTHLY ALBENDAZOLE TREATMENT ON TH2 RESPONSES: DIFFERENTIAL EFFECTS ON IGE AND IL-5

Karin de Ruiter*, Dicky L. Tahapary*, Linda J. Wammes, Apprillianto E. Wiria, Firdaus Hamid, Lisette van Lieshout, Johannes W.A. Smit, Jeanine J. Houwing-Duistermaat, Erliyani Sartono, Taniawati Supali and Maria Yazdanbakhsh

*Both authors contributed equally

Parasite Immunology (2017)

ABSTRACT

Helminth parasites induce a strong Th2 response, characterized by high levels of IgE and elevated signature cytokines such as IL-5. As many global deworming programs are underway, there is concern that this might lead to emergence of Th1-mediated pathologies when the counterbalancing helminth-induced Th2 response is absent. Therefore, we assessed the effect of deworming on Th2-mediated responses in a household-clustered randomized controlled trial in Indonesia. Total plasma IgE and whole-blood IL-5 responses to mitogen phytohaemagglutinin (PHA) were measured in 1494 and 682 subjects, respectively, at baseline, 9 and 21 months after three-monthly single-dose treatment with albendazole or placebo. Anthelmintic treatment did not result in complete removal of helminth infections in the community. However, treatment significantly decreased IgE levels in albendazole- compared to placebo-treated subjects. IL-5 responses to PHA were not significantly affected by anthelmintic treatment and tended to increase in albendazole-treated subjects, indicating that intensive treatment of helminth parasites has different outcomes on B-cell (IgE levels) and T-cell (IL-5) responses. The data shows that 2 years of deworming can have differential effects on responses typified as Th2-mediated, which needs to be taken into account when examining the impact of helminths on noncommunicable diseases.

INTRODUCTION

Amongst helminth parasites, soil-transmitted helminths (STHs) which reside in the gut, are most prevalent. More than 1.5 billion people are infected with STHs worldwide, and infections are widely distributed in tropical and subtropical countries (1). Important STHs include *Ascaris lumbricoides*, *Trichiuris trichiura* and hookworm (*Ancylostoma duodenale* and *Necator americanus*).

Helminth parasites are the most potent natural stimuli for T helper 2 (Th2) responses, characterized by Th2 cytokines (IL-4, IL-5 and IL-13), eosinophilia and high levels of IgE antibodies. Whereas IL-5 regulates eosinophilia, IL-4 and IL-13 promote IgE production by inducing B-cell switching to IgE-producing cells.

Th2 responses do not solely protect against helminth infections but also play an important role in the development of various inflammatory diseases, where an imbalance between Th1/Th2 cell responses and their regulation can lead to pathogenesis. Studies in animal models and in humans have indicated that helminths might play a protective role in the development of allergies, autoimmunities and inflammatory bowel disease (2). Moreover, recent in vivo studies showed that helminth infections might protect against insulin resistance as helminth-induced Th2 responses were associated with improved glucose metabolism and insulin signalling in mice (3-6). This has raised concern regarding the implementation of deworming programs, which might lead to emergence of Th1-mediated pathologies. The immunological consequences of deworming should therefore be examined in detail, given that Th2 responses consist of multiple arms.

To this end, we analysed the immunological data obtained from a household-based cluster-randomized double-blind placebo-controlled trial of three-monthly single-dose albendazole treatment in an area where STHs are highly endemic (7). This study describes the effect of anthelmintic treatment on two different components of the Th2 response, namely total IgE levels and total IL-5 production in response to a polyclonal stimulation (phytohemagglutinin, PHA).

MATERIALS AND METHODS

Study design

This report describes a nested study within the ImmunoSPIN trial (8, 9). The trial was conducted in 2 villages, Nangapanda and Anaranda, in Ende district, Flores Island, Indonesia. In 2008, the double-blind placebo-controlled trial of 2 year duration was initiated by randomizing all households to receive either a single dose of 400 mg albendazole or a matching placebo every 3 months over a 2-year study period (tablets from PT Indofarma Pharmaceutical, Bandung, Indonesia). Treatment allocation was based on household to minimize the risk of cross-contamination and therefore reinfection of treated individuals. Treatment was provided to all household members older than 2 years of age, except for pregnant women. Drug intake was observed by field workers. The study was approved by the Ethical Committee of the Medical Faculty, University of Indonesia, Jakarta (ref: 194/

PT02.FK/Etik/2006) and has been filed by the ethics committee of the Leiden University Medical Center, The Netherlands. The trial was registered as clinical trial (ISRCTN83830814). Informed consent or parental consent was obtained from all participants.

Study population

The randomization for the total study was based on 954 households comprising of 4004 individuals in the 2 villages, resulting in 2022 (481 houses) and 1982 (473 houses) subjects in the placebo and albendazole group, respectively, as described before (7). The current study included 1762 (363 houses) and 1731 (362 houses) subjects in the placebo and albendazole group in the village of Nangapanda, respectively (Supplementary Figure S1). At baseline, blood samples from 2349 subjects were collected to analyse total IgE levels and after inclusion of subjects with at least one follow-up blood sample, 1494 subjects were included at baseline, corresponding to 753 placebo- and 741 albendazole-treated individuals.

To study immunological responses, 250 households were randomly selected and individuals older than 4 years of age were invited for morning venous blood sampling and assessment of anthropometric parameters. This resulted in the inclusion of 882 individuals, of which 858 provided sufficient blood samples for whole-blood cultures. After inclusion of subjects with at least baseline and one follow-up blood sample, we ended up with 682 subjects at baseline, corresponding to 374 placebo- and 308 albendazole-treated individuals (Supplementary Figure S1). As this is a nested immunology study, 86% (584 of 682) of the subjects were also part of the group of 1494 subjects included for the analysis of IgE levels.

Parasitological examination

Yearly stool samples were collected in order to examine the effect of treatment on helminth prevalence. *T. trichiura* was detected by microscopy after formol-ether concentration and 18S-based multiplex real-time PCR was used for the specific amplification and detection of hookworm (*A. duodenale, N. americanus), A. lumbricoides*, and *S. stercoralis* DNA, as described previously (9). PCR output was expressed as the cycle threshold (Ct) reflecting the load of parasite specific DNA in the sample tested. Parasite specific DNA loads of *A. duodenale*, *N.americanus* and *A.lumbricoides* were categorized as low load (Ct≥30) and high load (Ct<30), irrespective of infection with *T. trichiura* of which only microscopy data were available. A subject was defined to have a heavy infection when a high DNA load (Ct<30) was measured for either hookworm or *A. lumbricoides*, whereas a light infection refers to subjects with low DNA loads (Ct≥30) for both of these helminth species, including subjects that are helminth negative.

Plasma IgE

The levels of total IgE were measured by ELISA in Jakarta as described previously (9). The results are expressed in International Units (IU/ml).

Whole blood culture and IL-5 measurements

Whole blood was stimulated in vitro as described before (9, 10). Cultures were stimulated for 72h to detect adaptive responses to phytohaemagglutinin (PHA, 2 µg/ml, Wellcome Diagnostics, Darford, UK) and unstimulated control wells were included. Due to budget restrictions, we could only measure one Th2 cytokine and opted for IL-5. Supernatants were stored at -20°C until IL-5 was quantified using Luminex cytokine kits (Biosource, Camarillo, USA) on a Liquichip 200® Workstation (Qiagen, Venlo, The Netherlands) equipped with Liquichip analyzer software (Qiagen, Venlo, The Netherlands). Cytokine levels that fell below the assay's detectable range were replaced by half of the detection limit provided by the manufacturer.

Statistical analysis

The total IgE and cytokine data were log-transformed to obtain a normally distributed variable. Cross-sectional comparisons between groups at baseline were tested with Student's *t* test. To assess treatment effects, generalized linear mixed models were used with addition of three random effects, namely a random household-specific intercept to model clustering within households and a random subject-specific intercept and slope to model correlation within subjects, as previously described (10). Parameter estimates for treatment effects at 9 and 21 months and 95% confidence intervals are reported, as well as interaction *P* values when a subgroup analysis was performed. The reported *P* values are obtained using likelihood ratio tests by comparing the model with and without the treatment effect. All models were fitted using the lme4 package (11). The analysis was intention to treat, and involved all participants as assigned randomly at the start of the trial.

RESULTS

Study population

Baseline characteristics of the study participants are shown in Table 1. At baseline, 84.8% of the individuals were infected with one or more helminth species, with hookworm infections being the most prevalent (73.1% of total). At baseline, total IgE levels and IL-5 production in response to PHA were similar in both treatment arms. The consort diagram of the study is shown in Supplementary Figure S1. Subjects were included in the analysis when data from baseline and at least one of the two follow-up time points were available.

Effect of albendazole treatment on helminth prevalence

Similar to the major study (7), subset analysis in this study revealed that intensive treatment with albendazole resulted in a reduction in STHs both after 9 (percentage infected: 49.9% for albendazole vs. 80.5% for placebo) and after 21 months of treatment (39.9% for albendazole vs. 75.4% for placebo; Figure 1A). Albendazole had the largest effect on hookworm (from 74.4% at baseline to 29.0% at 9 months and 20.7% at 21 months of

Table 1. Baseline characteristics of the study population

	N	Placebo	N	Albendazole
Age (mean in years, SD)	753	32.2 (18.7)	741	32.4 (19.0)
Sex (female, n, % of total)	753	459 (61.0)	741	445 (60.0)
BMI > 19 years old (mean, SD)	490	22.5 (4.0)	486	21.9 (3.7)
Z score of BMI ≤ 19 years old (mean, SD)	254	-1.17 (1.17)	235	-1.27 (1.18)
Parasite infection (n, %)				
Helminth (any *spp*)	421	357 (84.8)	426	361 (84.7)
Hookworm[1]	439	315 (71.8)	438	326 (74.4)
N. americanus	439	310 (70.6)	438	324 (74.0)
A. duodenale	439	27 (6.2)	438	23 (5.3)
A. lumbricoides[1]	439	154 (35.1)	438	146 (33.3)
T. trichiura[2]	558	144 (25.8)	541	150 (20.2)
Total IgE (IU/ml [GM, 95 CI])	753	1372 (1239-1519)	741	1340 (1210-1485)
Interleukin-5 production in response to PHA (pg/ml [median, IQR])	374	511 (287-777)	308	490 (291-808)

[1]diagnosed by PCR, [2]diagnosed by microscopy

treatment) compared to placebo (from 71.8% to 66.7% to 62.1% respectively). This was followed by *A. lumbricoides* (albendazole from 33.3%, to 14.5% and 10.1%; placebo from 35.1% to 33.6% and 32.1%), while the effect on *T. Trichiura* was much less pronounced (albendazole from 27.7%, to 22.0% and 18.2%; placebo from 25.8%, to 30.0% and 25.9%).

Baseline IgE levels

Baseline analysis of total IgE in subjects with light and heavy infections, as defined in Materials and Methods (section Parasitological examination), revealed that higher infection intensity was associated with significantly elevated IgE levels (light infection: 809 (695-940) IU/ml (GM, 95 CI), heavy infection: 1544 (1376-1732) IU/ml, *P*<.001) (Table S1). Polyclonal IgE levels were significantly lower in adults (1185 (1086-1294) IU/ml) compared to children ≤ 19 years (1766 (1561-1999) IU/ml) (*P*<.001), whereas no significant difference was found between males (1307 (1189-1437) IU/ml) and females (1434 (1283-1603) IU/ml) (*P*=.219).

Effect of albendazole treatment on plasma IgE levels

Figure 1B presents the estimated effect of treatment on total IgE levels after 9 and 21 months. Total IgE levels were significantly lower after 9 and 21 months in the albendazole-treated group (estimates (95% CI) at 9 months -0.071 (-0.112 to -0.030), at 21 months -0.060 (-0.099 to -0.020); overall *P* value: P_{time}<.001). When infection was defined as light or heavy based on parasite-specific DNA loads of hookworm and *A. lumbricoides* at baseline, the estimated treatment effect on IgE levels was significant in subjects with a heavy infection at baseline (at 9 months -0.074 (-0.142 to -0.005), at 21 months -0.083 (-0.146 to -0.019); P_{time}=.051). In subjects with light infections, we observed no significant

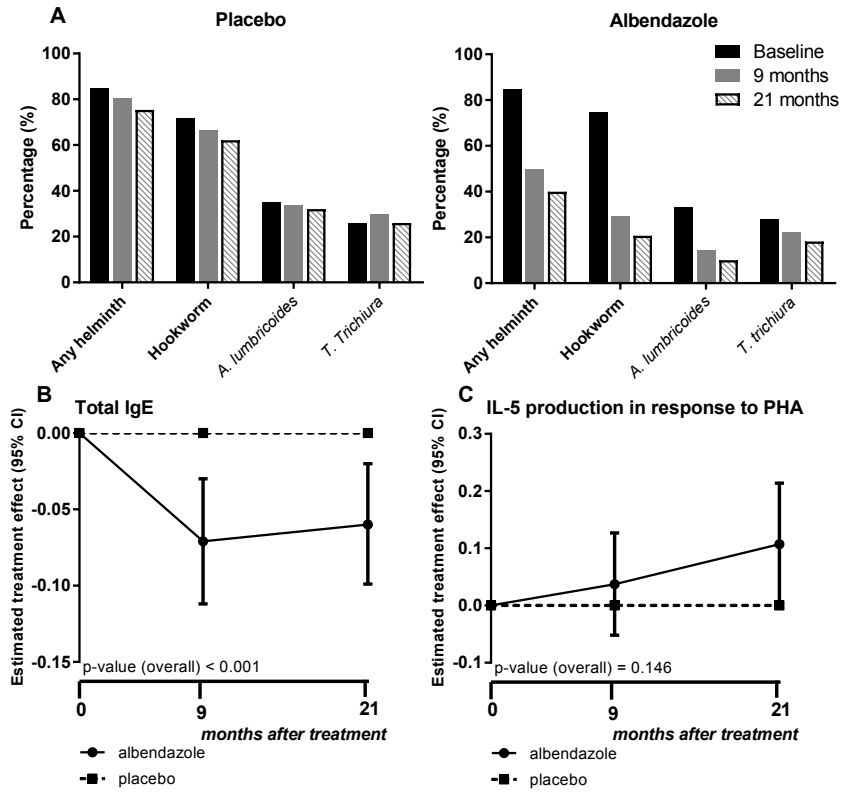

Figure 1. Effect of deworming on the prevalence of helminth infections, total IgE levels and whole blood IL-5 production in response to PHA. A) Percentage of helminth infected subjects in placebo and albendazole treated arms. The estimated effect of albendazole treatment on serum total IgE levels (B) and IL-5 response to PHA in supernatant of 72h-stimulated whole blood cultures (C), is displayed for the 9 and the 21 month time points, with corresponding 95% confidence intervals. The estimates of the treatment effect were obtained by general linear mixed models and overall p-values over time are indicated.

treatment effect on IgE (at 9 months -0.039 (-0.126 to 0.047), at 21 months -0.001 (-0.08 to 0.079); P_{time}=.664; *P* value for interaction=.252), nor in subjects who were uninfected at baseline (at 9 months -0.134 (-0.280 to 0.012), at 21 months -0.040 (-0.078 to 0.158); overall *P* value: P_{time}= .140).

Similar effects of treatment on IgE levels were observed in children (at 9 months -0.069 (-0.134 to 0.004), at 21 months -0.071 (-0.134 to 0.009); P_{time}=.003) and adults (at 9 months -0.070 (-0.120 to -0.021), at 21 months -0.053 (-0.099 to -0.007); P_{time}=.006; *P* value for interaction=.876). Albendazole treatment reduced total IgE to a similar extent in both males (at 9 months -0.038 (-0.102 to 0.025), at 21 months -0.067 (-0.125 to -0.009); P_{time}=.059) and females (at 9 months -0.093 (-0.143 to -0.042), at 21 months -0.055 (-0.103 to -0.007); P_{time}=.001; *P* value for interaction=.349).

Baseline IL-5 production in response to PHA

At baseline, we detected no significant difference in IL-5 levels to PHA between subjects with light (474 (242-775) pg/ml (median, IQR)) and heavy infections (490 (283-801) pg/ml) (*P*=.364) (Table S1). IL-5 responses were significantly lower in adults (472 (258-728) pg/ml) compared to children (534 (319-841) pg/ml) (*P*=.04). When considering gender, significantly higher levels of IL-5 were observed in males (588 (347-884) pg/ml) compared to females (460 (259-698) pg/ml); *P*<.001).

Effect of albendazole treatment on whole blood IL-5 responses to PHA

There was no significant treatment effect on IL-5 production in response to PHA at 9 months (estimates (95% CI), 0.037 (-0.052 to 0.127)). However, we observed significantly elevated levels of IL-5 to PHA at 21 months (0.107 (0.000 to 0.214)). When both time points were taken into account, the overall *P* value over time fell short of statistical significance (P_{time}=.146). IL-5 measured in unstimulated blood revealed no treatment-related differences (data not shown).

Additionally, we observed no effect of treatment on IL-5, nor differences in the treatment effect between subgroups when subjects with light and heavy infections (*P* value for interaction=.850) or children and adults (*P* value for interaction=.998) were analysed separately. In males, treatment did not show a significant effect on the IL-5 response (at 9 months -0.027 (-0.163 to 0.108), at 21 months 0.041 (-0.135 to 0.218); P_{time}=.780), whereas a trend towards an increase in IL-5 response was observed in females (at 9 months 0.086 (-0.031 to 0.203), at 21 months 0.164 (0.018 to 0.311); P_{time}=.192; *P* value for interaction=.316).

DISCUSSION

This is the first time that the effects of long-term placebo-controlled anthelmintic treatment on different components of a helminth-induced Th2 response have been analysed in a whole community. We show a significant decline in plasma IgE levels in albendazole-treated subjects over a period of 21 months compared to placebo-treated subjects. However, whereas both IgE and IL-5 are important products of the helminth-induced Th2 response, IL-5 production by peripheral blood cells in response to PHA was not significantly affected by anthelmintic treatment and rather tended to increase.

It is well known that helminth parasites are potent inducers of IgE production (12-15). So far, only a few longitudinal studies have been performed to study the effect of anthelmintic treatment on polyclonal IgE levels (16-18). In line with our findings, Cooper et al. (14) showed that 1 year of anthelmintic treatment was associated with a significant reduction in total IgE levels in children, suggesting that current STH infections are important determinants of IgE levels. Whereas previous studies only included children below 12 years of age (14, 16), in the current randomized trial, we studied the general population across all ages to show decreases in IgE levels in the whole community irrespective of age.

Overall, the treatment effect on IgE was seen at 9 months, and this effect remained at 21 months and IgE levels did not further decrease. The major effect seen on IgE after 9 months probably reflects the large decrease in prevalence of hookworm and *A. lumbricoides* which was 2.5- and 2.3-fold compared to baseline, respectively, whereas after 21 months, the prevalence of both species decreased 1.4-fold compared to 9 months post-treatment. The lack of further decrease in IgE at 21 months may be due to continued exposure to incoming parasites in a contaminated environment, which would stimulate long-lived IgE plasma cells contributing to sustained IgE antibody production (14, 19).

Given the observed treatment effect on IgE, it would appear that deworming decreases Th2-mediated responses. However, we found no significant effect of treatment on IL-5 in response to PHA and even a trend towards increase at 21 months post-treatment. As described elsewhere in more detail (10), analysis of uninfected subjects showed that treatment had no effect on IL-5 production, ruling out a direct effect of albenzole on immune responses. It has been reported before that IL-5 responses may be suppressed during helminth infections and treatment results in enhanced helminth-specific and unrelated antigen responses (10, 20-22). A study conducted in Kenya showed that in schoolchildren infected with *Schistosoma mansoni*, type 2 cytokine responses including IL-4, IL-5, IL-9 and IL-13, were significantly increased upon stimulation with egg antigen 1 and 2 years post treatment (23). Another study in Gabon showed that specifically IL-5, but neither IL-4 nor IL-13, was downregulated during an active *S. haematobium* infection as only IL-5 responses to worm antigens were increased in subjects who remained free from infection 2 years after helminth clearance, compared to subjects who became reinfected (22). This enhanced cytokine response can be due to either removal of the immunosuppressive effects of active infection or immunological boosting by antigens released from dying parasites (23). Although it is possible that treatment boosts the antigen-specific responses, often also responses to unrelated antigens such as PHA are enhanced by anthelmintic treatment. The latter cannot be explained by helminth antigens boosting specific T-cell responses, unless it is due to cross-reactive antigen responses that are enhanced in these unrelated antigens (10, 21).

As anthelmintic treatment appears to have opposite effects on type 2 cytokine production and total IgE, and IL-4 and IL-13 promote IgE production, this raises the question whether there are IL-4/IL-13 independent pathways of IgE regulation. T-cell-independent IgE^+ B-cell maturation in tissues has been described, suggesting that IgE class switching does not fully depend on Th2 cytokine levels (24). Perhaps IgE memory B cells and/or long-lived IgE plasma cells can maintain the production of IgE via Th2 cytokine-independent pathways, concurrent to Th2 cells becoming hyporesponsive and producing less Th2 cytokines. However, as there is very little data from human studies on IgE memory B cells and the pathways by which IgE is regulated, this remains a speculation.

T follicular helper (Tfh) cells, a subset of $CD4^+$ T cells that migrates to B-cell follicles and induces antibody production by B cells (25), have been described as the dominant source of IL-4 in vivo during infection with *Heligmosomoides polygyrus* (26). In humans,

the frequencies of total and activated peripheral memory Tfh cells were found to be significantly increased during *Schistosoma japonicum* infection (27). Although it is currently unknown what happens to Tfh cell numbers after helminth clearance, decreasing numbers could possibly explain the observed decline in total IgE after treatment, as this would lead to less IL-4 production in B-cell follicles, hence less IgE secretion.

Based on our findings, we could conclude that 2 years of anthelmintic treatment might have differential effects on Th2 responses. IgE responses are elevated in helminth-infected subjects and decline after intensive deworming, whereas IL-5 production by peripheral blood cells seems suppressed in infected subjects and might be reversed after deworming. Both phenomena have separately been reported by others, and here we report the occurrence of both within one community. These differential effects on responses typified as Th2-mediated need to be taken into account when examining the effects of helminths on noncommunicable diseases. The concern that upon deworming, inflammatory diseases such as allergies could increase, might be justified if we look at Th2 cytokines, but not if one considers IgE. However, it is also known that IgE responses during helminth infection are dominated by antibodies that have poor biological activity (28) and therefore a decrease in IgE that is not functional might still be in line with a relative increase in IgE that can trigger mast cell degranulation.

It would be interesting to complement these findings with data on eosinophilia and other Th2 cytokine responses like IL-4 and IL-13, in order to further investigate helminth's immunomodulatory effects on Th2 responses.

ACKNOWLEDGEMENTS

The authors thank the research team from University of Indonesia in Jakarta, the staff from the Puskesmas Primary Health Center Nangapanda, Ende health authorities, the community field workers and most of all the study participants from Nangapanda, Flores, Indonesia.

REFERENCES

1. http://www.who.int/mediacentre/factsheets/fs366/en/.
2. McSorley HJ, Maizels RM. Helminth infections and host immune regulation. Clin Microbiol Rev 2012; 25(4): 585-608.
3. Wu D, Molofsky AB, Liang HE, et al. Eosinophils sustain adipose alternatively activated macrophages associated with glucose homeostasis. Science (New York, NY) 2011; 332(6026): 243-7.
4. Hussaarts L, Garcia-Tardon N, van Beek L, et al. Chronic helminth infection and helminth-derived egg antigens promote adipose tissue M2 macrophages and improve insulin sensitivity in obese mice. FASEB journal : official publication of the Federation of American Societies for Experimental Biology 2015; 29(7): 3027-39.
5. Berbudi A, Surendar J, Ajendra J, et al. Filarial Infection or Antigen Administration Improves Glucose Tolerance in Diet-Induced Obese Mice. J Innate Immun 2016; 8(6).
6. Yang Z, Grinchuk V, Smith A, et al. Parasitic nematode-induced modulation of body weight and associated metabolic dysfunction in mouse models of obesity. Infection and immunity 2013; 81(6): 1905-14.
7. Wiria AE, Hamid F, Wammes LJ, et al. The effect of three-monthly albendazole treatment on malarial parasitemia and allergy: a household-based cluster-randomized, double-blind, placebo-controlled trial. PloS one 2013; 8(3): e57899.
8. Hamid F, Wiria AE, Wammes LJ, et al. A longitudinal study of allergy and intestinal helminth infections in semi urban and rural areas of Flores, Indonesia (ImmunoSPIN Study). BMC infectious diseases 2011; 11: 83.
9. Wiria AE, Prasetyani MA, Hamid F, et al. Does treatment of intestinal helminth infections influence malaria? Background and methodology of a longitudinal study of clinical, parasitological and immunological parameters in Nangapanda, Flores, Indonesia (ImmunoSPIN Study). BMC infectious diseases 2010; 10: 77.
10. Wammes LJ, Hamid F, Wiria AE, et al. Community deworming alleviates geohelminth-induced immune hyporesponsiveness. Proceedings of the National Academy of Sciences of the United States of America 2016; 113(44): 12526-31.
11. R-Forge. lme4 - Mixed-effects models project. 2011.
12. Jarrett EE, Miller HR. Production and activities of IgE in helminth infection. Progress in allergy 1982; 31: 178-233.
13. Alcantara-Neves NM, de SGBG, Veiga RV, et al. Effects of helminth co-infections on atopy, asthma and cytokine production in children living in a poor urban area in Latin America. BMC research notes 2014; 7: 817.
14. Cooper PJ, Alexander N, Moncayo AL, et al. Environmental determinants of total IgE among school children living in the rural Tropics: importance of geohelminth infections and effect of anthelmintic treatment. BMC immunology 2008; 9: 33.
15. Amarasekera M, Gunawardena NK, de Silva NR, Douglass JA, O'Hehir RE, Weerasinghe A. Impact of helminth infection on childhood allergic diseases in an area in transition from high to low infection burden. Asia Pacific allergy 2012; 2(2): 122-8.
16. Hagel I, Lynch NR, Di Prisco MC, Rojas E, Perez M, Alvarez N. Ascaris reinfection of slum children: relation with the IgE response. Clinical and experimental immunology 1993; 94(1): 80-3.
17. Mitre E, Nutman TB. IgE memory: persistence of antigen-specific IgE responses years after treatment of human filarial infections. The Journal of allergy and clinical immunology 2006; 117(4): 939-45.
18. Poirriez J. A three years follow-up of total serum IgE levels in three patients treated for strongyloidiasis. Parasite (Paris, France) 2001; 8(4): 359-62.
19. Wu LC, Zarrin AA. The production and regulation of IgE by the immune system. Nature reviews Immunology 2014; 14(4): 247-59.
20. Cooper PJ, Moncayo AL, Guadalupe I, et al. Repeated treatments with albendazole enhance Th2 responses to Ascaris Lumbricoides, but not to aeroallergens, in children from rural communities in the Tropics. The Journal of infectious diseases 2008; 198(8): 1237-42.

21. Figueiredo CA, Barreto ML, Rodrigues LC, et al. Chronic intestinal helminth infections are associated with immune hyporesponsiveness and induction of a regulatory network. Infection and immunity 2010; 78(7): 3160-7.
22. Grogan JL, Kremsner PG, Deelder AM, Yazdanbakhsh M. Antigen-specific proliferation and interferon-gamma and interleukin-5 production are down-regulated during Schistosoma haematobium infection. The Journal of infectious diseases 1998; 177(5): 1433-7.
23. Wilson S, Jones FM, Kenty LC, et al. Posttreatment changes in cytokines induced by Schistosoma mansoni egg and worm antigens: dissociation of immunity- and morbidity-associated type 2 responses. The Journal of infectious diseases 2014; 209(11): 1792-800.
24. Berkowska MA, Heeringa JJ, Hajdarbegovic E, et al. Human IgE(+) B cells are derived from T cell-dependent and T cell-independent pathways. The Journal of allergy and clinical immunology 2014; 134(3): 688-97.e6.
25. King C. New insights into the differentiation and function of T follicular helper cells. Nature reviews Immunology 2009; 9(11): 757-66.
26. King IL, Mohrs M. IL-4-producing CD4+ T cells in reactive lymph nodes during helminth infection are T follicular helper cells. J Exp Med 2009; 206(5): 1001-7.
27. Chen X, Li W, Zhang Y, et al. Distribution of Peripheral Memory T Follicular Helper Cells in Patients with Schistosomiasis Japonica. PLoS neglected tropical diseases 2015; 9(8): e0004015.
28. Hamid F, Amoah AS, van Ree R, Yazdanbakhsh M. Helminth-induced IgE and protection against allergic disorders. Curr Top Microbiol Immunol 2015; 388: 91-108.

Supplementary Figure S1. Consort diagram. The current study is nested within the ImmunoSPIN trial [8, 9], with a total of 3493 individuals living in the village of Nangapanda. Allocation of placebo and albendazole resulted in 363 and 362 households including 1762 and 1731 subjects, respectively. Subjects were included in the analysis when IgE and/or cytokine data from baseline and at least one of the two follow-up time points were available. While the upper diagram shows the profile with total IgE as outcome, the lower diagram displays the diagram of 250 households that were randomly selected to study immunological responses (IL-5). Availability of parasitological data is indicated at the different time points for treatment arms, numbers reflecting the follow-up of subjects with parasitological data at baseline.

SUPPLEMENTAL DATA

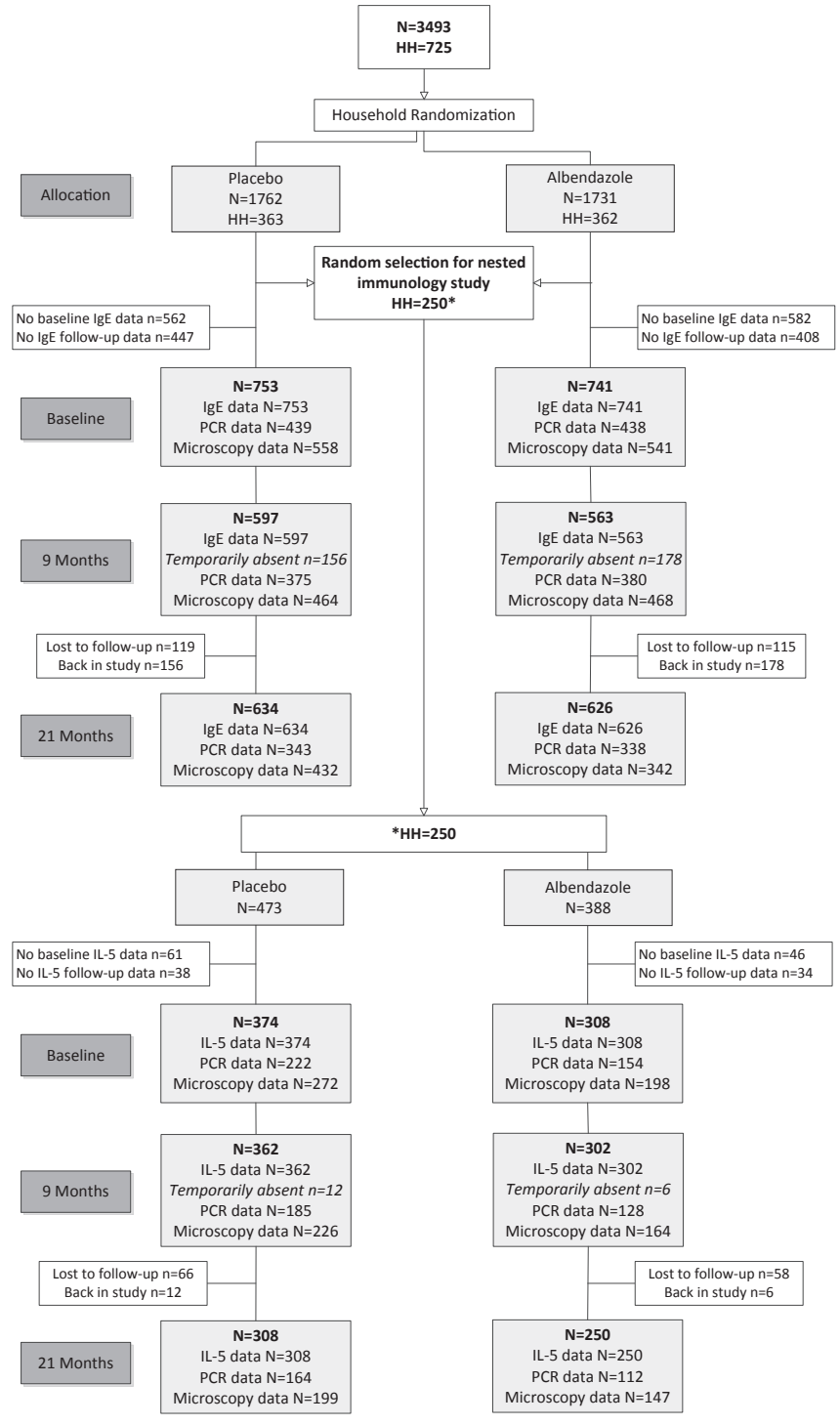

Supplementary table S1. Baseline analysis of total IgE in plasma and total IL-5 production in response to PHA

	N	Total IgE (IU/ml) [GM, 95 CI]	*P* value	N	IL-5 response to PHA (pg/ml) [median, IQR]	*P* value
Light infection	337	809 (695-940)	<0.001	150	474 (242-775)	0.364
Heavy infection	540	1544 (1376-1731)		226	490 (283-801)	
Children (≤19 yr)	504	1766 (1561-1999)	<0.001	289	534 (319-841)	0.040
Adult (>19yr)	990	1185 (1086-1294)		393	472 (258-728)	
Male	590	1307 (1189-1437)	0.219	286	588 (347-884)	<0.001
Female	904	1434 (1283-1603)		396	460 (259-698)	

Parasite specific DNA loads of *A. duodenale, N.americanus and A.lumbricoides* were categorized as low load (Ct≥30) and high load (Ct<30), irrespective of infection with *T. trichiura* of which only microscopy data were available. A subject was defined to have a heavy infection when a high DNA load was measured for either one of the helminth species. A light infection refers to subjects with low DNA loads (Ct≥30) for both of these helminth species, including subjects that are helminth negative. Data were tested by Student's t-test.

8

EFFECT OF DEWORMING ON TYPE 2 AND REGULATORY RESPONSES REVEALED BY MASS CYTOMETRY

Karin de Ruiter, Dicky L. Tahapary*, Koen A. Stam*, Vincent van Unen, Thomas Höllt, Boudewijn P.F. Lelieveldt, Frits Koning, Erliyani Sartono, Johannes W.A. Smit, Taniawati Supali and Maria Yazdanbakhsh

*Both authors contributed equally

Manuscript Submitted

ABSTRACT

Numerous studies have shown that helminths can have a profound role in shaping immune responses to vaccines, allergens or autoantigens, by inducing strong type 2 and regulatory responses, however, the degree of heterogeneity of such cells has not been studied before. Mass cytometry, which provides a method that allows in depth profiling of immune responses, was used to profile type 2 and regulatory immune cells in Europeans not exposed to helminth infections, and in Indonesians who were infected with soil-transmitted helminths (STH), before and 1 year after deworming. The use of Hierarchical Stochastic Neighbor Embedding (HSNE) in Cytosplore allowed the identification of very distinct immune signatures in Europeans and Indonesians, showing expanded frequencies of Th2 cells, in particular CD161$^+$ cells, and regulatory T cells, but only those expressing CTLA4 and co-expressing CD38, HLA-DR, ICOS or CD161, in STH-infected Indonesians. It was also possible to analyse ILC2s, which are difficult to study in peripheral blood, and to show that these cells are expanded in STH-infected Indonesians. The expansion of type 2 cells was confirmed functionally through analysis of type 2-cytokine producing cells, whereas IL-10 production alone could not capture the difference seen in regulatory T cells observed through phenotypic characterization. However, CD11c$^+$ B cells were the main IL-10 producers among B cells in Indonesians, a subset which was almost absent in Europeans. In addition to ILC2s and CD4$^+$ T cells, CD8$^+$ T cells as well as γδ T cells were found to be producers of type 2 cytokines in STH-infected Indonesians. A number of these expanded responses were shown to be driven by current helminth infection as they decreased following treatment and clearance of infection. These results provide us with a detailed insight into the types of cells that participate in strong type 2 and regulatory networks, and show that treatment of helminths affects specific groups of cells in these immune networks.

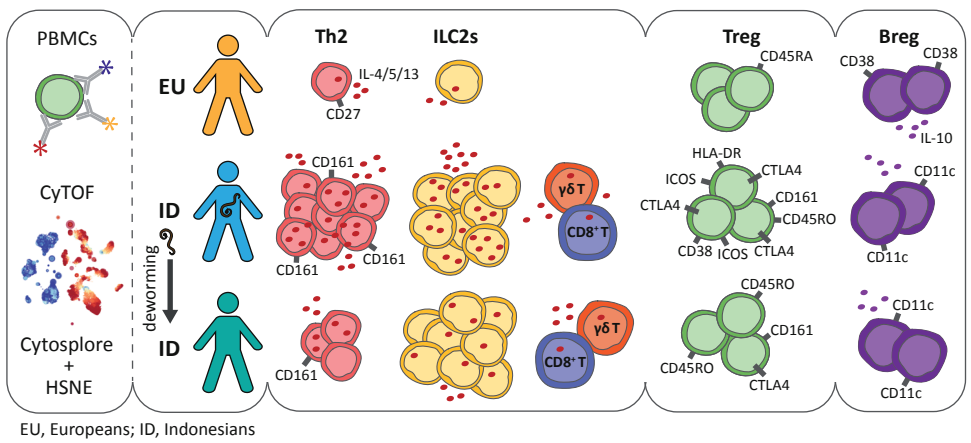

Graphical abstract

INTRODUCTION

Parasitic helminths represent one of the most prevalent infections affecting nearly one-third of the population worldwide (1), and are known as the strongest natural inducers of type 2 immune responses (2). These are characterized by CD4$^+$ T helper 2 (Th2) cells secreting the hallmark cytokines interleukin (IL)-4, IL-5 and IL-13, systemic and localized eosinophilia, expansion of basophils and mast cells, goblet cell hyperplasia and the production of IgE (3). There is evidence for a role of type 2 immune responses in controlling the number of parasites through direct killing or expulsion, and in inducing tissue repair, necessary to protect against damage caused by tissue-migrating helminths (4). In addition, an innate source of type 2 cytokines, termed group 2 innate lymphoid cells (ILC2s) described in both mice (5-7) and humans (8) are also part of the "type 2 immune system". Whereas murine ILC2s have been shown to contribute to anti-helminth immunity (5-7), information about their role in human helminth infections is lacking, and it has been challenging to study these cells considering their low frequency in peripheral blood (9).

Studies have shown that helminths can have a profound role in shaping immune responses to vaccines, allergens or autoantigens, and besides polarizing the immune system towards a strong type 2 immune response, their modulatory effects can be attributed to the induction of a strong regulatory network (2). Regulatory T cells (Tregs), expressing FOXP3, are an important component of such a network, and mediate their effects through cytokine-mediated suppression (e.g. IL-10 and TGF-β) and the expression of suppressory molecules such as cytotoxic T lymphocyte antigen 4 (CTLA4) (10). Several studies in animal models and humans show that helminth infections are associated with increased Treg frequencies and/or functional capacity (11-14). Although longitudinal studies assessing the effect of deworming on Tregs are rare, we recently found that not Treg frequencies, but the expression of CTLA4 on CD4$^+$ T cells significantly declined in anthelmintic-treated individuals (15).

To fully understand the diverse immune modulatory processes mediated by helminths and identify specific cells that might be important, we performed unbiased immune profiling of Indonesians residing in a rural area of Indonesia, who were infected with soil-transmitted helminths (STH), and 1 year after 3-monthly anthelmintic treatment, were free of these infections. Mass cytometry (Cytometry by time-of-flight; CyTOF) was applied, which allows high-resolution dissection of the cellular composition of the immune system by the simultaneous measurement of 37 cellular markers at the single-cell level.

A well-established technique for mass cytometry data analysis is t-distributed Stochastic Neighbour Embedding (t-SNE) (16), an algorithm that allows visualization of all concurrent marker expression profiles of cells on a two-dimensional plot in an unbiased fashion. However, t-SNE does not scale well to large amounts of data. Recently introduced techniques, such as Uniform Manifold Approximation and Projection (UMAP) (17) and Hierarchical Stochastic Neighbor Embedding (HSNE) (18) promise to overcome this scaling problem. Here, we applied HSNE, as implemented in Cytosplore (19), to visualize

and cluster the data. This allowed efficient visualization of our dataset containing 20 million cells without the need for downsampling of the data, while preserving single-cell resolution. These methods were applied to study the effect of helminths on the immune cell phenotype *ex vivo*, in addition to determination of functional effects in terms of cytokine production. Moreover, immune profiles were compared to those of healthy Europeans who had not been exposed to helminths.

MATERIALS AND METHODS

Study population

Samples in this study were part of the SugarSPIN trial, a household-based cluster-randomized double-blind trial that was conducted in three villages in Nangapanda, Ende district of Flores island (East Nusa Tenggara), Indonesia (20). The trial was approved by the ethics committee of Faculty of Medicine, Universitas Indonesia (FKUI) (ref: 549/H2·F1/ETIK/2013), and filed by the ethics committee of Leiden University Medical Center (LUMC). The trial is registered as a clinical trial (Ref: ISRCTN75636394). Written informed consent was obtained from participants prior to the study.

All subjects selected for the current study were infected with soil-transmitted helminths at baseline (Table 1), and cleared their infection after 1 year of albendazole treatment. The treatment consisted of a single tablet of albendazole (400 mg; PT Indopharma Pharmaceutical, Bandung, Indonesia) for three consecutive days, and this regimen was given every three months for a total of four rounds (maximum of 12 tablets in total), between May 2014 and February 2015. Before the start of drug administration and 6 weeks after the last round of drug administration, blood and stool samples were collected as previously described (20).

With regards to the European samples, we collected venous blood of 10 healthy volunteers who had not been exposed to helminths for PBMC isolation. Except for sex and age (Table 1), no additional data were collected.

Parasitology

Aliquots of fresh stool samples were frozen at -20°C in the field study centre and subsequently at -80°C at the Department of Parasitology of FKUI and LUMC for DNA extraction. Stool DNA isolation and real-time PCR were performed pairwise (baseline and follow-up). DNA isolation from stool was performed as described elsewhere (21). Multiplex real-time polymerase chain reaction (PCR) was performed to simultaneously detect the presence of hookworm (*Ancylostoma duodenale*, *Necator americanus*), *Ascaris lumbricoides*, *Trichuris trichiura*, and *Strongyloides stercoralis,* using a method described previously (21). Stool samples were considered positive by PCR when cycle threshold (Ct) values were <50.

Table 1. Characteristics of the study population.

Characteristic	Europeans (n=10)	Indonesians (n=10)
Age, years (median, min, max)	32.0 (26-55)	35.9 (18-56)
Sex, female, *n*	5	5
Eosinophil count, %, (GM, min, max)	na	13.7 (9-28)
Total IgE, IU/mL, (GM, min, max)	na	823 (124-7753)
Helminth infection by PCR, No.		
Single	na	5
Multiple		5

GM, geometric mean; na, not applicable

Eosinophil count and total IgE

A Giemsa-stained peripheral thin blood smear was read to assess the differential white blood cell count, resulting in a relative percentage of basophils, eosinophils, neutrophils, lymphocytes and monocytes. Total IgE was measured in serum as described previously (22).

PBMC cryopreservation

After diluting heparinised venous blood 2x with HBSS, PBMCs were isolated using Ficoll density gradient centrifugation within 12 hours after blood collection. The HBSS contained 100 U/mL penicillin G sodium and 100 µg/mL streptomycin. After washing twice with HBSS, the PBMCs were cryopreserved in RPMI 1640 containing 20% of heat-inactivated foetal calf serum (FCS; Bodinco, Alkmaar, the Netherlands) and 10% dimethyl sulfoxyde (DMSO). The RPMI medium contained 1 mM pyruvate, 2 mM L-glutamine, penicillin G and streptomycin. Cryovials containing the cell suspension were transferred to a Nalgene Mr Frosty Freezing Container (Thermo Scientific, Waltham, MA, USA) which was placed at a -80°C freezer for a minimum of 4 hours. Subsequently, vials were stored in liquid nitrogen until analysis. The cryopreserved PBMCs collected in the field were shipped in a liquid nitrogen dry vapour shipper from Jakarta, Indonesia, to Leiden, the Netherlands, for analysis.

Mass cytometry antibody staining

Two antibody panels were designed to 1) phenotype immune cells *ex vivo* and 2) assess cytokine production after 6 hours of stimulation with phorbol 12-myristate 13-acetate (PMA) and ionomycin. Details on antibodies used are listed in Supplementary table S1 and S2. Antibody-metal conjugates were either purchased or conjugated using a total of 100 µg of purified antibody combined with the MaxPar X8 Antibody Labelling Kit (Fluidigm, South San Francisco, CA, USA) according to manufacturer's protocol V7. The conjugated antibody was stored in 200 µL Antibody Stabilizer PBS (Candor Bioscience, GmbH, Wangen, Germany) at 4°C. All antibodies were titrated on study samples.

On the day of the staining, cryopreserved PBMCs were thawed with 50% FCS/RPMI medium at 37°C and washed twice with 10% FCS/RPMI medium. Next, $3x10^6$ cells per sample, used for phenotyping (Panel 1), were temporarily stored on ice while another $3x10^6$ cells per sample were transferred to 5 ml round-bottom Falcon tubes (BD Biosciences, Bedford, MA, USA) for 6 hours of incubation in 10% FCS/RPMI with 100 ng/mL PMA (Sigma; cat.P8139) and 1 µg/mL ionomycin (Sigma; cat. I0634). After 2 hours of incubation at 37°C, 10 µg/mL brefeldin A (Sigma; cat. B7651) was added after which the cells were incubated for 4 more hours. Subsequently, the cells were washed with PBS and resuspended in MaxPar staining buffer (Fluidigm) before continuing with the antibody staining (Panel 2).

For phenotyping (Panel 1), the staining was based on MaxPar Nuclear Antigen Staining Protocol V2 (Fluidigm). First, cells were washed with MaxPar staining buffer and centrifuged for 5 minutes at 300g in 5 mL eppendorf tubes. Then, the cells were incubated with 1 mL 500x diluted 500 µM Cell-ID Intercalator-103Rh (Fluidigm) in staining buffer at room temperature for 15 minutes to identify dead cells. After washing with staining buffer, cells were incubated with 5 µL Human TruStain FcX Fc-receptor blocking solution (BioLegend, San Diego, CA, USA) and 40 µL staining buffer at room temperature for 10 minutes. Then, 50 µL of freshly prepared surface antibody cocktail was added and incubated at room temperature for another 45 minutes. Subsequently, cells were washed 2x with staining buffer and fixed and permeabilized using the eBioscience FOXP3/Transcription factor staining buffer set (eBioscience, cat. 00-5523-00). After cells were incubated with 1 mL of the freshly prepared Fix/Perm working solution (prepared according to the manufacturer's instructions) for 45 minutes, cells were washed 2x with 1x Permeabilization buffer at 800g for 5 minutes. Next, 50 µL of the intranuclear antibody cocktail was added to 50 µL of cells resuspended in 1x Permeabilization buffer and incubated for 30 minutes at room temperature. Following the incubation, cells were washed once with 1x Permeabilization buffer and twice with staining buffer, before being stained with 1 mL 1000x diluted 125 µM Cell-ID Intercalator-Ir (Fluidigm) in MaxPar Fix and Perm buffer (Fluidigm) at 4°C overnight to stain all cells. After 3 washes with staining buffer and centrifugation at 800 g, cells were stored as a pellet at 4°C and measured within 2 days.

To assess the cytokine production of PBMCs (Panel 2), the staining was based on MaxPar Cytoplasmic/Secreted Antigen Staining Protocol V3. While the surface staining was performed exactly as described above, cells were afterwards fixed by incubating them with 1 mL of freshly prepared 1x MaxPar Fix I buffer (Fluidigm) for 20 minutes at room temperature. Next, cells were washed 3x with MaxPar Perm-S buffer (Fluidigm) and 50 µL of cytokine antibody cocktail was added to 50 µL of cell suspension and incubated for 40 minutes at room temperature. Then, cells were washed 3x with staining buffer and stained with Cell-ID Intercalator-Ir as described above.

Mass cytometry data acquisition

Measurement of samples was randomised per subject to avoid bias, but samples belonging to the same subject were stained and measured together. Samples were measured with a Helios™ mass cytometer (Fluidigm), which was automatically tuned according to Fluidigm's recommendations. Before measuring, cells were counted, washed with Milli-Q water, passed over a cell strainer, and brought to a concentration of $1.0x10^6$ cells/mL with 10% EQ Four Element Calibration Beads (Fluidigm) in Milli-Q water. Mass cytometry data were acquired and analysed on-the-fly, using dual-count mode and noise-reduction on. Next to channels to detect antibodies, channels for intercalators (103Rh, 191Ir, 193Ir), calibration beads (140Ce, 151Eu, 153Eu, 165Ho, and 175Lu) and background/contamination (133Cs, 138Ba, 206Pb) were acquired. After data acquisition, the mass bead signal was used to normalize the short-term signal fluctuations with the reference EQ passport P13H2302 during the course of each experiment. When applicable, normalized FCS files were concatenated using Helios software, without removing beads.

Mass cytometry data analysis

FlowJo V10 for Mac (FlowJo LLC, Ashland, OR, USA) was used to gate out beads and we discriminated live, single $CD45^+$ immune cells with DNA stain and event length. The selected cells were exported as FCS files and analysed using novel HSNE (18), as implemented in Cytosplore (19, 23). HSNE constructs a hierarchy of non-linear similarities that can be interactively explored with a stepwise increase in detail up to the single-cell level (19). Briefly, the data exploration starts with the visualization of the embedding at the highest level, the overview level, where the layout of the landmarks (representative cells) indicates similarity in the high-dimensional space. The landmark size reflects its area of influence (AoI), containing cells that are well-represented by the landmark, and the similarity of two landmarks is defined as the overlap of their respective AoIs. Colouring of the landmarks is used to represent marker expressions. At the overview level, a group of landmarks (also referred to as cluster) can be selected, by manual gating based on visual cues such as marker expression, or by performing unsupervised Gaussian mean shift (GMS) clustering (23, 24) of the landmarks based on the density representation of the embedding. Next, we can zoom into this selection by means of a more detailed embedding and visualize all selected landmarks in a next level. While this process can be repeated until the data level is reached where each dot represents a single cell, this is not imperative and we often clustered at an intermediate level without reaching the data level. The number of hierarchical levels depended on the input-data size.

Before HSNE was applied, data were transformed using a hyperbolic arcsin with a cofactor of 5. Furthermore, within Cytosplore, an extra channel called 'SampleTag' was added to the FCS files to be able to identify from which sample an event originated after HSNE.

Clusters produced in Cytosplore were analysed using R software (R x64 version 3.5.1; R Foundation for Statistical Computing, Vienna, Austria, http://www.r-project.org/) and RStudio (Rstudio, Inc., Boston, MA, USA, www.rstudio.com). The package 'cytofast' was used to produce heatmaps, scatterplots showing subset abundance and histograms showing the median signal intensity distribution of markers (25).

Statistical Analysis

Statistical analyses were performed using R software. To compare subpopulation and cluster abundance between Europeans and Indonesians pre-treatment unpaired *t* tests were used. Paired *t* tests were applied to compare pre- and post-treatment samples of Indonesians. Total IgE levels and eosinophil counts were log-transformed for analysis and paired *t* tests were used in GraphPad Prism (GraphPad Software, San Diego, CA, USA). Spearman's correlation was used to assess the relationship between the frequency of Tc2 cells and type 2 cytokine-producing CD8$^+$ T cells. *P* values <.05 were considered statistically significant.

RESULTS

Distinct immune signatures between Europeans and Indonesians

Study population characteristics are shown in Table 1. To analyse the cellular composition of the immune system at high-resolution, we developed a 37-metal isotope-tagged monoclonal antibody panel (Table S1) which allowed the identification of the six major immune lineages (CD4$^+$, CD8$^+$, γδ T cells, B cells, myeloid cells and innate lymphoid cells (ILCs; CD3$^-$CD7$^+$)), and major subpopulations and detailed cell clusters within. Importantly, by using the t-SNE-based HSNE (19), we could explore the full mass cytometry dataset containing 20.3 million live CD45$^+$ cells at the single-cell level without the need for downsampling. At the overview level, landmarks (representative cells) depict the global composition of the entire immune system and distinguished the major immune lineages, which were annotated based on lineage marker expression overlays (Fig. 1A-B). Quantification of cell frequencies revealed a significantly higher frequency of B cells in Indonesians (*P* = .03), but no other differences were found between Europeans and Indonesians at the lineage level (Fig. 1C, Fig. S1). Next, CD4$^+$ T cell landmarks, representing 6.3 million cells, were selected at the overview level (Fig. 1B) and a new higher resolution embedding was generated at the second level of the hierarchy (Fig. 1D), revealing subpopulations within the CD4$^+$ T cell lineage (Fig. 1D). Stratification by origin of the samples revealed a strikingly different distribution of the CD4$^+$ T cells between European and Indonesian individuals, visualized by cell density plots (Fig. 1E). Different cellular distributions were also observed within other lineages (CD8$^+$, γδ T cells, B cells, myeloid cells and ILCs) (Fig. 1E), suggesting distinct immune signatures between Europeans and Indonesians in both the innate and adaptive immune compartment.

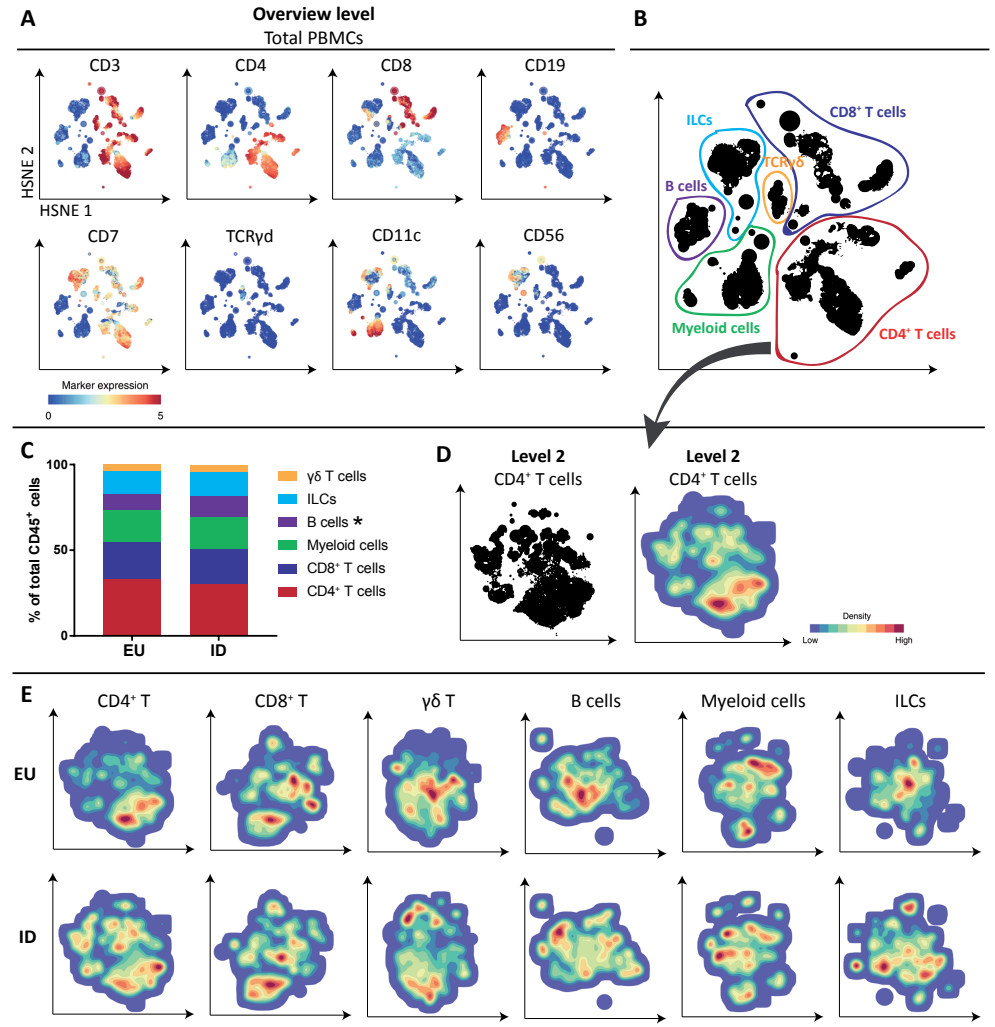

Figure 1. Distinct immune signatures between Europeans and Indonesians. A. First HSNE level embedding of 20.3 million cells. Colour represents arsin5-transformed marker expression as indicated. Size of the landmarks represents AoI. **B.** The major immune lineages, annotated on the basis of lineage marker expression. **C.** Comparison of lineage proportions relative to total cells between Europeans (EU) and Indonesians (ID). Differences between EU and ID were tested with Student's *t* test. **P* <.05. **D.** Second HSNE level embedding of the CD4$^+$ landmarks selected from the overview level of total PBMCs, as indicated by the red encirclement. Both landmarks (left panel) and the density features of the CD4$^+$ T cells (right panel) are shown. Density is indicated by colour. **E.** Density plots per lineage, stratified by sample origin, and therefore illustrating the differences between EU and ID.

A CD161⁺ subpopulation of Th2 cells is expanded in Indonesians and decreases after anthelmintic treatment

Within the CD4⁺ T cells, a distinct population of Th2 cells was found that expressed GATA3, CD25, CD127, CD45RO and chemoattractant receptor-homologous molecule expressed on Th2 (CRTH2), the latter being the most reliable marker to identify human Th2 cells (26) (Fig. 2A). The frequency of total Th2 cells was significantly higher in Indonesians compared to Europeans (*P* = .003) and importantly, deworming resulted in a significant decrease (*P* = .008) (Fig. 2B). This is in line with the observation that the proportion of circulating eosinophils as well as serum levels of total IgE, both markers of the type 2 response, significantly decreased in the STH-infected Indonesian individuals after treatment (Fig. S2).

Further analysis of Th2 cells revealed 22 phenotypically distinct clusters using the GMS clustering (Fig. 2C) and generated a heatmap showing the distinct marker expression profiles for each cluster (Fig. 2G). Th2 cells were found to be heterogeneous and based on the expression of the lectin-like receptor CD161 and CD27, the latter which is lost on highly differentiated memory CD4⁺ T cells (27, 28), three subpopulations could be identified (CD161⁺CD27⁻, CD161⁻CD27⁻ and CD161⁻CD27⁺ Th2 cells; Fig. 2C-D). Visualization of Th2 cells by density plots (Fig. 2E) showed that the proportion of CD161⁺ Th2 cells was expanded in Indonesians compared to Europeans, although the difference fell short of statistical significance, but a significant decrease was observed after anthelmintic treatment (*P* = .01) (Fig. 2F). Deeper analysis at the cluster level revealed three clusters within the CD161⁺ Th2 population that significantly declined upon deworming, characterized as CD161⁺CD7⁻ KLRG1⁻, CD161⁺CD7⁻KLRG1⁺ and CD161⁺CD7⁺KLRG1⁻ (Fig. 2G). In contrast, after one year of treatment we observed a significant increase of three CD7⁺ Th2 clusters that only weakly expressed GATA3 and CRTH2 (Fig. 2G).

Although Indonesian blood samples contained more Th2 cells, the proportion of poorly differentiated CD27⁺ Th2 cells was significantly higher in Europeans (*P* = .019) (Fig. 2F) and this difference was in particular seen in the CCR7⁻ cluster within the CD27⁺ Th2 cell subpopulation (Fig. 2G). This finding indicates the relatively low presence of highly differentiated memory effector Th2 cells in the immune system of Europeans.

Overall frequency of ILC2s is expanded in Indonesians but does not decrease after anthelmintic treatment.

When 2.8 million ILCs (CD3⁻CD7⁺), which include NK cells and helper-like ILCs, were analysed at a more detailed level, the embedding of a CD25⁺CD127⁺CD161⁺ subpopulation revealed 2 distinct clusters that were phenotyped as ILC2s and ILC3s, based on the expression of CRTH2 and c-Kit, respectively (Fig. 3A). It was found that other markers such as GATA3, KLRG1, CD45RA and CCR6 could also be expressed by ILC2s and/or ILC3s (Fig. 3A). Consistent with previous work (29), we observed that while GATA3, the Th2 master transcription factor, was highly expressed in CRTH2⁺ ILC2s, it was also expressed in CRTH2⁻ ILCs and can therefore not exclusively be used to define ILC2 cells.

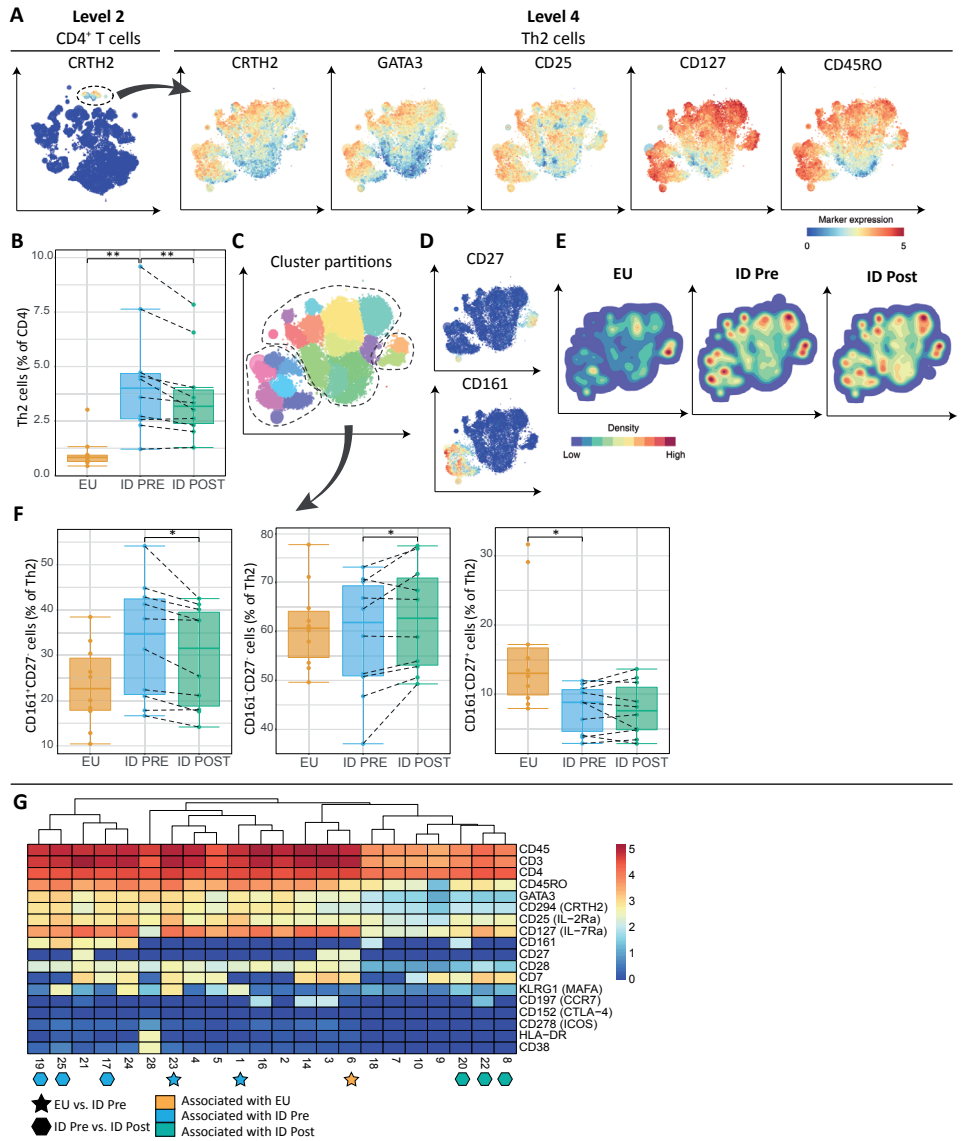

Figure 2. A CD161⁺ subpopulation of Th2 cells is expanded in Indonesians and decreases after anthelmintic treatment. A. Fourth HSNE level embedding of the CRTH2⁺ landmarks (Th2 cells) selected from the second HSNE level embedding of 6.3 million CD4⁺ T cells, as indicated by the black encirclement. Colour represents arsin5-transformed marker expression as indicated. Size of the landmarks represents AoI. **B.** Frequency of Th2 cells relative to CD4⁺ T cells. Differences between Europeans (EU) and Indonesians pre-treatment (ID Pre) were tested with Student's *t* test, while differences between ID Pre and ID Post were assessed using paired *t* tests. ***P* <.01. **C.** Cluster partitions of Th2 cells using density-based GMS clustering. The black encirclement indicates three subpopulations, whose frequencies are shown in f. **D.** Marker expression of CD27 and CD161 on Th2 cells. **E.** Density features of Th2 cells illustrating the different distribution of cells between EU, ID Pre and ID Post. **F.** Frequency of three Th2 subpopulations (CD161⁺CD27⁻, CD161⁻CD27⁻, CD161⁻CD27⁺) relative to total Th2 cells. **P* <.05. **G.** A heatmap summary of median expression values (same colour ▸

coding as for the embeddings) of cell markers expressed by CRTH2⁺ clusters identified in c. and hierarchical clustering thereof. To compare cluster abundance between EU and ID Pre Student's *t* test was used, while paired *t* test was used to compare ID Pre and ID Post. Coloured symbols below the clusters indicate statistical significance.

In contrast to ILC3s, the proportion of ILC2s was significantly higher in Indonesians compared to Europeans (P = .003), and did not change after anthelmintic treatment (Fig. 3B). Further characterization of ILC2s resulted in 8 phenotypically distinct clusters that were mainly distinguished by the expression of KLRG1, CD45RA and CCR6 (Fig. 3C). Except for a higher frequency of KLRG1⁺CCR6⁻ ILC2s (cluster 2) present in STH-infected Indonesians and a lower frequency of KLRG1⁺CCR6⁺ ILC2s (cluster 5) compared to Europeans, no significant differences at the cluster level were observed (Fig. 3D).

Not Treg frequency, but their expression of CTLA4 is induced by helminth infections

Regulatory T cells (Tregs) were characterized as FOXP3⁺CD25^{high}CD127^{low} cells and appeared as a clearly distinct subpopulation within CD4⁺ T cells (Fig. 4A). The frequency of Tregs, when assessed as a whole, did not differ between Europeans and Indonesians, nor changed after deworming (Fig. 4B). However, the immune profile of Indonesians consisted of significantly more effector Tregs expressing CD45RO (P = .036) (Fig. 4C), whereas in Europeans, a clear population of Tregs was positioned in the naïve, CD45RA⁺, compartment (Fig. 4A,D). In line with previous studies describing Tregs as phenotypically and functionally heterogeneous (10), we found several subpopulations within the effector Treg compartment expressing CTLA4, HLA-DR, CD38 and/or ICOS (Fig. 4E). A significant proportion of the effector Tregs expressed CTLA4, a marker that is associated with the suppressive function of Tregs (30). In concordance with this, the proportion of CTLA4⁺ Tregs was significantly higher in Indonesians compared to Europeans (P = .007) and decreased after treatment (P = .052) (Fig. 4F).

Next, we identified 27 phenotypically distinct clusters within Tregs (Fig. 4G-H). Analysis at the cluster level revealed that the frequencies of 6 out of 27 clusters were significantly higher in Indonesians compared to Europeans, which could be distinguished by the expression of only CTLA4⁺, or co-expressing CD38 and/or HLA-DR and/or ICOS (Fig. 4H). One of these clusters (cluster 7) expressing CTLA4, HLA-DR, CD38 and ICOS decreased significantly upon deworming, suggesting that this population of effector Tregs is particularly important in the immune response induced by STH.

Of note, among the CTLA4⁺ Tregs, we identified a cluster expressing CD161 (cluster 25; Fig. 4H), characterizing a subpopulation that was previously described as the major source of Treg-derived proinflammatory cytokines with the ability to produce IL-17 under inflammatory conditions (31, 32). The proportion of CD161⁺ Tregs was significantly higher in Indonesians compared to Europeans (P = .001) but did not change after deworming (Fig. 4I).

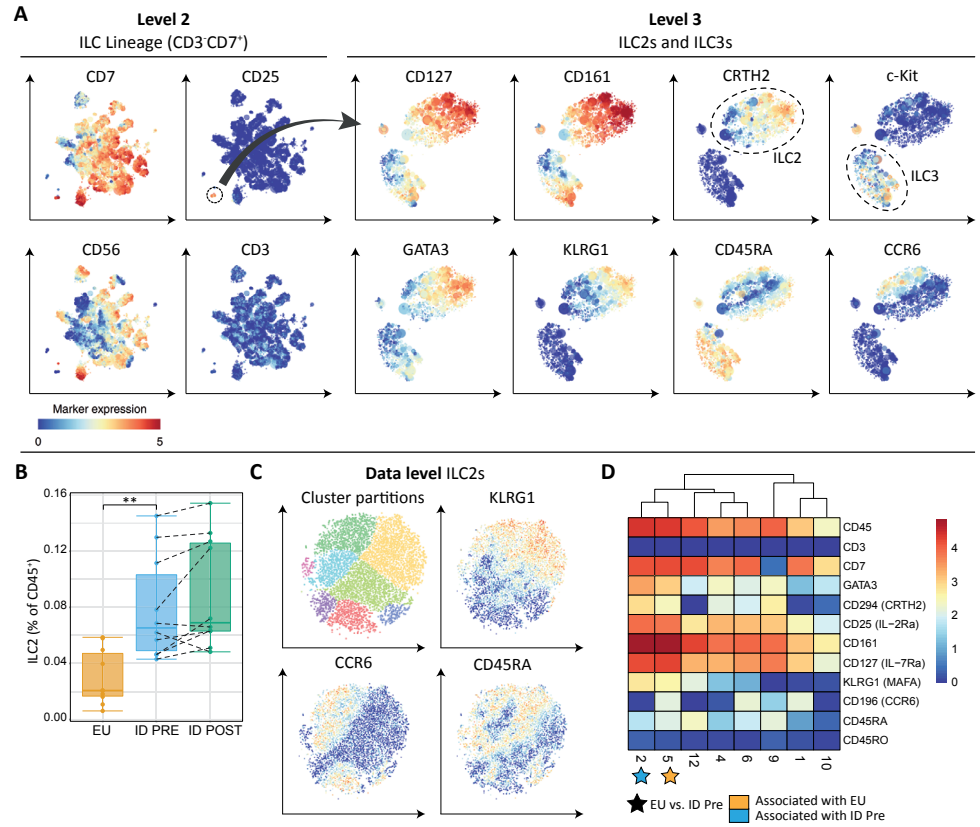

Figure 3. Overall frequency of ILC2s is expanded in Indonesians but does not decrease after anthelmintic treatment. A. The right panel shows the third HSNE level embedding of the CD25⁺CD161⁺CD127⁺ landmarks selected from the second HSNE embedding of 2.8 million ILCs (CD3⁻CD7⁻), as indicated by the black encirclement. Next to a distinct cluster of CRTH2⁺ ILC2s, a cluster of cKit⁺ ILC3s was found. Colour represents arsin5-transformed marker expression as indicated. Size of the landmarks represents AoI. **B.** Frequency of ILC2s relative to total CD45⁺ cells. Differences between Europeans (EU) and Indonesians pre-treatment (ID Pre) were tested with Student's *t* test, while differences between ID Pre and ID Post were assessed using paired *t* tests. ***P* <.01. **C.** Data level embedding of ILC2s. The upper left panel shows the cluster partitions using GMS clustering, whereas the other panels show the expression of KRLG1, CCR6 and CD45RA. **D.** A heatmap summary of median expression values (same colour coding as for the embeddings) of cell markers expressed by ILC2 cell clusters identified in c. and hierarchical clustering thereof. To compare cluster abundance between EU and ID Pre Student's *t* test was used, while paired *t* test was used to compare ID Pre and ID Post. Coloured symbols below the clusters indicate statistical significance.

Type 2 cytokine-producing cells in Indonesians (ILC2s, CD4⁺, CD8⁺ and γδ T cells) and their alteration after deworming

Following the phenotypic characterization of the cells, the cytokine-producing capacity of the cells was analysed to assess functional type 2 immune cells. PBMCs from identical donors as described above, were stimulated with PMA/ionomycin for 6h and subsequently

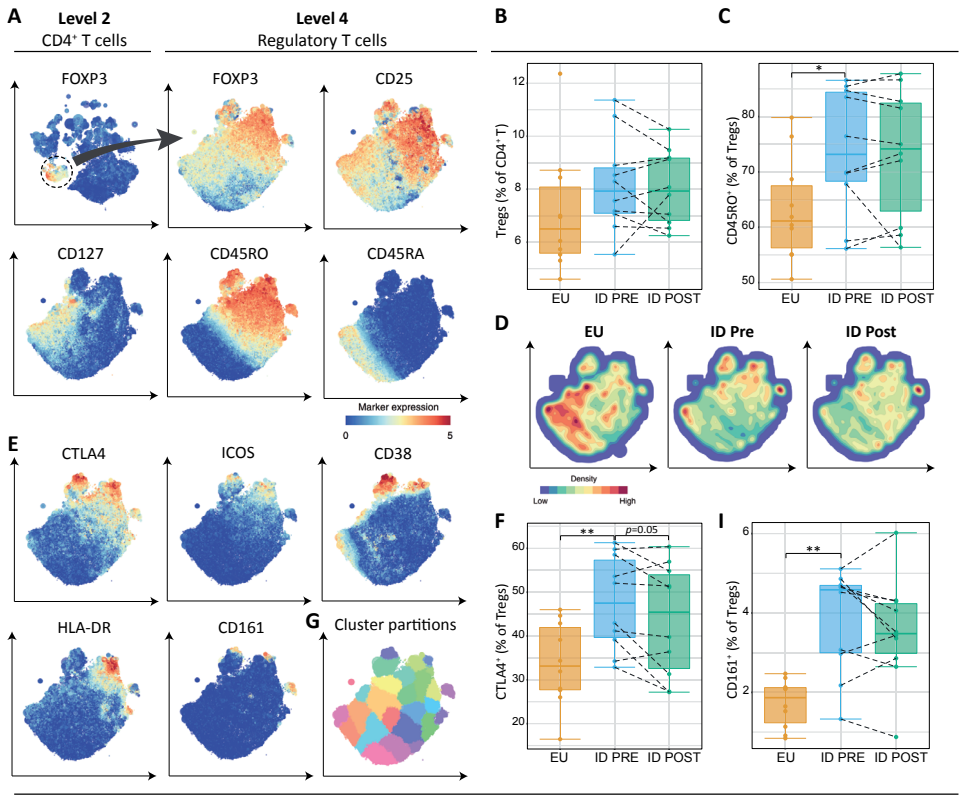

Figure 4. Not Treg frequency, but their expression of CTLA4 is induced by helminths. A. Fourth HSNE level embedding of the FOXP3⁺ landmarks (Tregs) selected from the second HSNE embedding of 6.3 million CD4⁺ T cells, as indicated by the black encirclement. Colour represents arsin5-transformed marker expression as indicated. Size of the landmarks represents AoI. **B.** Frequency of Tregs relative to CD4⁺ T cells. Differences between Europeans (EU) and Indonesians pre-treatment (ID Pre) were tested with Student's *t* test, while differences between ID Pre and ID Post were assessed using paired *t* tests. **C.** Frequency of CD45RO⁺ effector Tregs relative to total Tregs. **P* <.05. **D.** Density features of Tregs illustrating the different distribution of cells between EU, ID Pre and ID Post. **E.** Marker expression of CTLA4, ICOS, CD38, HLA-DR and CD161 by Tregs. **F.** Frequency of CTLA4⁺ Tregs relative to total Tregs. **P* <.05; ***P* <.01. **G.** Treg cluster partitions using GMS clustering. **H.** A heatmap summary of median expression values (same colour coding as for the embeddings) of cell markers expressed by FOXP3⁺ Treg clusters identified in g. and hierarchical clustering thereof. To compare cluster abundance between EU and ID Pre Student's *t* test was used, while paired *t* test was used to compare ID Pre and ID Post. Coloured symbols below the clusters indicate statistical significance. **I.** Frequency of CD161⁺ Tregs relative to total Tregs. **P* <.05.

stained with a 37-metal isotope-tagged monoclonal antibody panel which included the following cytokine antibodies: IFNγ, TNFα, IL-2, IL-17, IL-10 and IL-4/IL-5/IL-13 (simultaneously assessed and hereafter referred to as 'type 2 cytokines').

Type 2 cytokine-producing CD45⁺ cells were analysed in Cytosplore and clustering on surface markers clearly revealed four distinct type 2 cytokine-producing subpopulations (Fig. 5A-D, Fig. S3). Th2 cells and ILC2s have been described as the main producers of type 2-cytokines, and this was confirmed by the finding that the median signal intensity (MSI) of type 2 cytokines was highest in CD4⁺ T cells and ILC2s (Fig. 5E). However, we also identified a cluster of γδ T cells and multiple CD8⁺ T cell clusters producing type 2 cytokines, although the MSI of IL-4/5/13 was lower compared to CD4⁺ T and ILC2 cells (Fig. 5E). Interestingly, whereas ILC2s did not produce IFNγ, a CD25⁻ proportion of CD4⁺ and CD8⁺ T cells, and all γδ T cells co-expressed IFNγ (Fig. 5E-F).

Density plots of type 2 cytokine-producing cells revealed striking differences between Europeans and STH-infected Indonesians (Fig. 5C). While Indonesians not only exhibited a significantly higher frequency of type 2 cytokine-producing cells (Fig. 5G), the number of cellular sources for these cytokines also appeared to be expanded (Fig. 5C-D,H). In both populations it were mainly CD4⁺ T cells that produced type 2 cytokines, however, the ILC2 and γδ T cell subpopulations that were found in Indonesians, were much less pronounced in Europeans. Importantly, the proportion of type 2 cytokine-producing cells significantly declined after deworming ($P < .001$) (Fig. 5G) and this can be attributed to a significant decrease in type 2 cytokine-producing CD4⁺ T ($P < .001$) and ILC2s ($P = .004$) (Fig. 5H).

When cells were phenotyped *ex vivo*, we identified a GATA3⁺ cluster (2.1% of CD8⁺ T cells) within a subpopulation of CD45RO⁺CCR7⁻CD161⁻CD56⁻ CD8⁺ T cells (Fig. 6A-B), a subset previously defined as type 2 cytotoxic T cells (Tc2) cells (33, 34). In addition, Tc2 cells expressed CRTH2, CD25, CD127 and CD7 (Fig. 6B). Although Tc2 frequencies did not change after deworming, its proportion correlated strongly with the type 2 cytokine-producing CD8⁺ T cells (r=0.87, $P < .001$; Fig. 6C), suggesting that Tc2 cells are the source of Th2 cytokines within the CD8 lineage. However, it should be noted that the frequency of Tc2 cells ranged widely from 0.09-16.8% of CD8⁺ T cells among individuals, and 56% of the cells within the Tc2 subpopulation were from one individual (including both before and after treatment samples).

IL10-producing B and CD4⁺ T cells revealed by mass cytometry

Similar to what was described above, we sought cells that produced the suppressory cytokine IL-10. The IL-10-producing CD45⁺ cells were analysed in Cytosplore

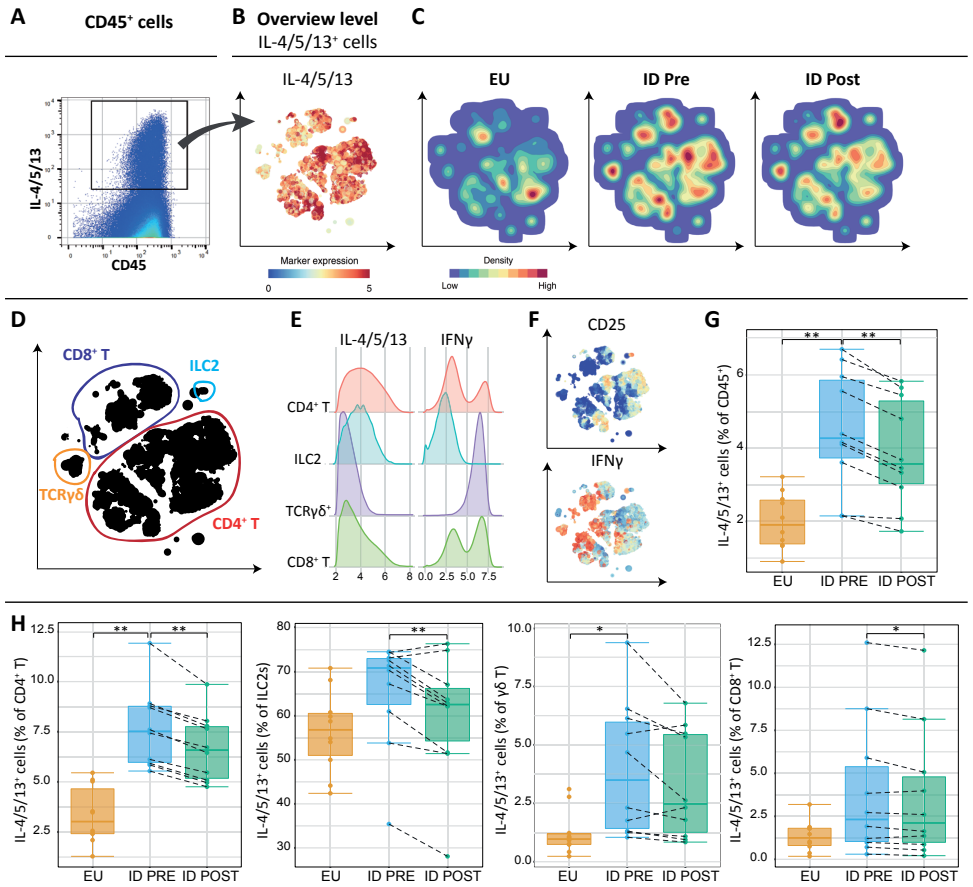

Figure 5. Type 2 cytokine-producing cells in Indonesians (ILC2s, CD4⁺, CD8⁺ and γδ T cells) and their alteration after deworming. A. IL-4/5/13⁺ cells were manually gated using Flowjo. Data from one representative individual is shown. **B.** First HSNE level embedding of total IL-4/5/13⁺ cells, clustered on surface markers. Colour represents arsin5-transformed marker expression as indicated. Size of the landmarks represents AoI. **C.** Density features of IL-4/5/13⁺ cells illustrating the different distribution of cells between Europeans (EU), Indonesians pre- (ID Pre) and post-treatment (ID Post). **D.** The major immune cell subpopulations producing type 2 cytokines, annotated on the basis of lineage marker expression (*See Fig. S3*). **E.** Histogram showing the median signal intensity (MSI) distribution of IL-4/5/13 and IFNγ for the subpopulations identified in d. **F.** Marker expression of CD25 and IFNγ by IL-4/5/13⁺ cells. **G.** Frequency of total IL-4/5/13-producing cells relative to total CD45⁺ cells. Differences between EU and ID Pre were tested with Student's *t* test, while differences between ID Pre and ID Post were assessed using paired *t* tests. ***P* <.01. **H.** Frequency of IL-4/5/13-producing clusters identified in d. relative to total CD4⁺ T, ILC2, γδ T or CD8⁺ T cells. **P* <.05; ***P* <.01.

(Fig. 7A-B) and clustering on surface markers revealed a major cluster of CD4⁺ T cells, and minor clusters of CD8⁺ T cells, CD4⁻CD8⁻ T cells and B cells (Fig. 7C-D, Fig. S4). Similar frequencies of total IL-10-producing cells (relative to CD45⁺ cells) were observed among Europeans and Indonesians, and these did not change after anthelmintic treatment (data

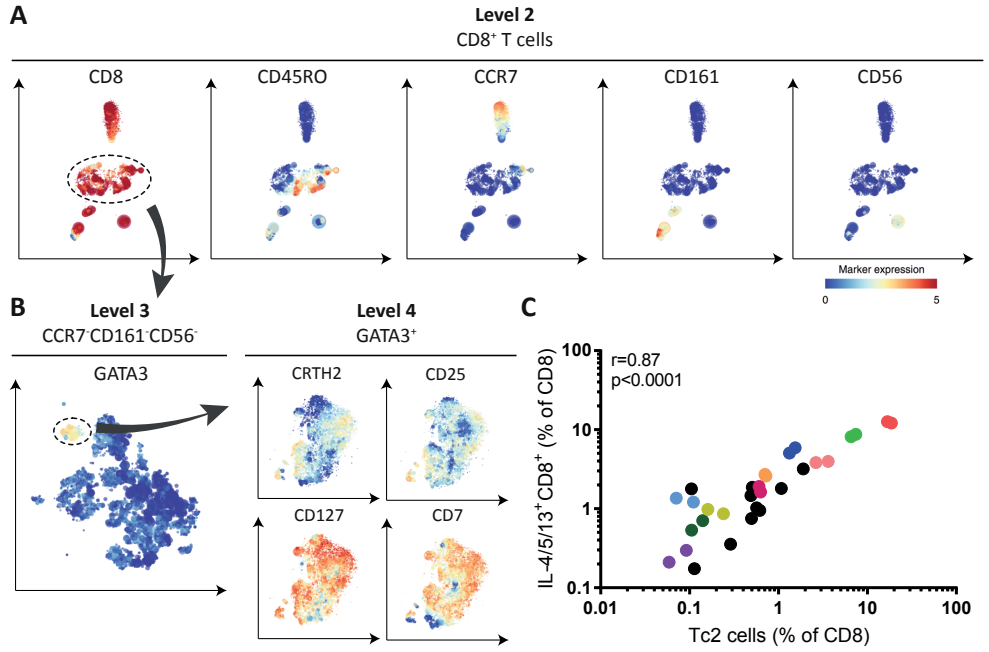

Figure 6. Tc2 cells are the source of type 2 cytokines produced by CD8⁺ T cells. A. CCR7⁻CD161⁻CD56⁻ landmarks were selected from the second level HSNE embedding of CD8⁺ T cells, as indicated by the black encirclement. **B.** From the next level embedding, GATA3⁺ landmarks were selected and their marker expression is shown at the fourth level embedding. Colour represents arsin5-transformed marker expression as indicated. Size of the landmarks represents AoI. **C.** Correlation of GATA3⁺CD8⁺ T (Tc2) cells identified in b. and IL-4/5/13-producing CD8⁺ T cells identified in Fig. 5D. Colours indicate paired samples (pre and post treatment) from Indonesian individuals. Spearman's rank correlation was used for statistical analysis.

not shown). Also regarding the IL-10⁺ subpopulations (CD4⁺, CD8⁺, CD4⁻CD8⁻ T and B cells), no significant differences were found (data not shown).

Interestingly, a distinct population of IL-10⁺ B cells (0.5% of total B cells) was identified and further analysis showed that it consisted of three clusters, namely CD11c⁺CD38⁻, CD11c⁻CD38⁺ and CD11c⁻CD38⁻ cells (Fig. 7E). Whereas the composition of IL-10⁺ B cells did not change after deworming, IL-10⁺ B cells from Indonesians clearly contained more CD11c⁺CD38⁻ cells compared to Europeans, who had relatively more CD11c⁻CD38⁺ IL-10⁺ B cells (Fig. 7F). These results indicate a different phenotype of IL-10⁺ B cells in the two populations, which is in line with the finding that the immune system of Indonesians contained significantly more CD11c⁺ B cells as assessed by phenotypic markers compared to Europeans (data not shown).

When IL-10-producing CD4⁺ T cells were clustered on cytokines, four clusters were identified which all expressed type 2 cytokines but varied in terms of co-expression of other cytokines (IFNγ, TNFα, and/or IL-2) (Fig. 7G-H). When considering all CD4⁺ T cells producing IL-10 and type 2 cytokines, irrespective of other cytokines, their frequency was

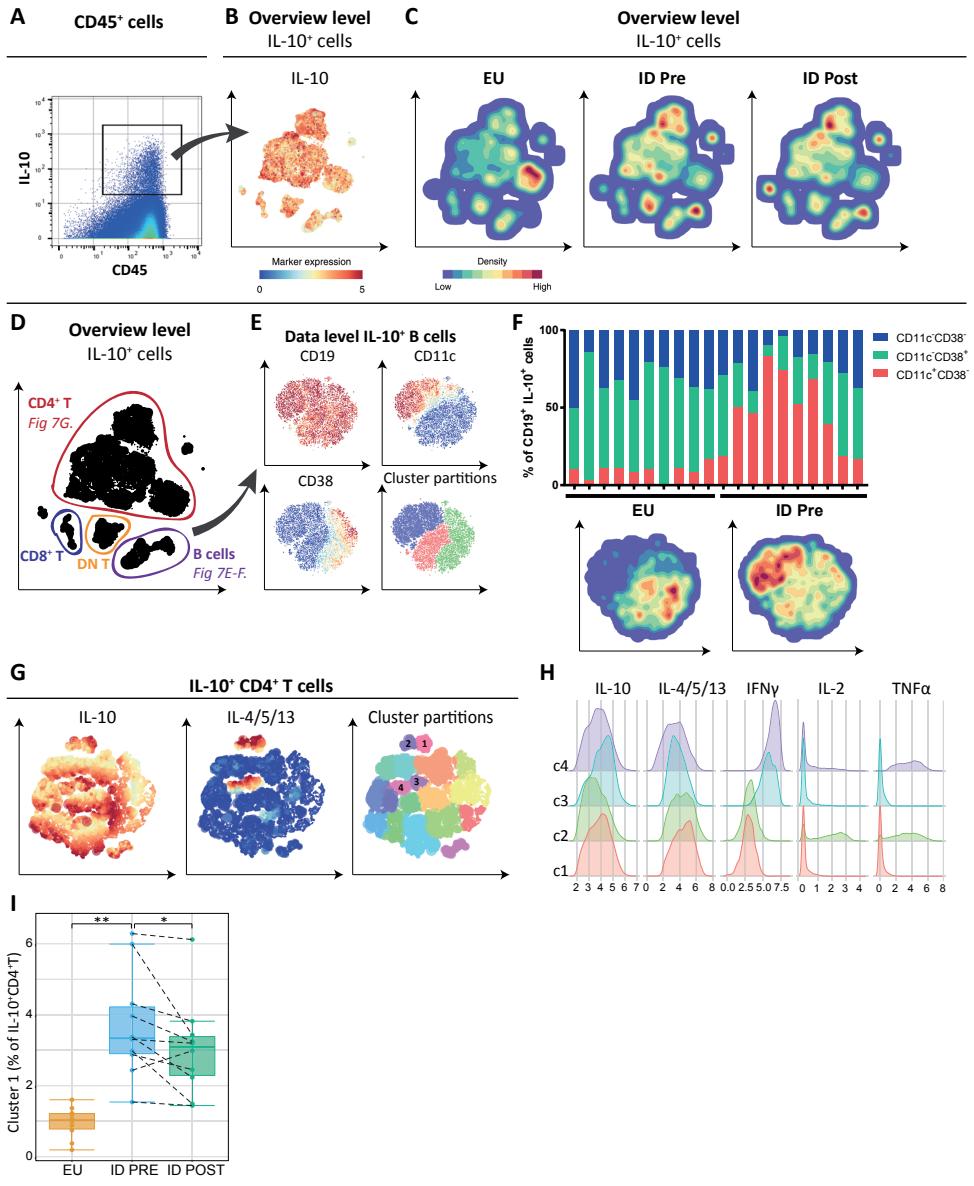

Figure 7. IL-10-producing B and CD4⁺ T cells revealed by mass cytometry. A. IL-10⁺ cells were manually gated using Flowjo. Data from one representative individual is shown. **B.** First HSNE level embedding of total IL-10⁺ cells, clustered on surface markers. Colour represents arsin5-transformed marker expression as indicated. Size of the landmarks represents AoI. **C.** Density features of IL-10⁺ cells illustrating the different distribution of cells between Europeans (EU), Indonesians pre- (ID Pre) and post-treatment (ID Post). **D.** The major immune cell subsets producing IL-10, annotated on the basis of lineage marker expression (*See Fig. S4*). **E.** Data level embedding of IL-10⁺ B cells and the cluster partitions using GMS clustering (lower right panel). **F.** Relative composition of IL-10⁺ B cells, comparing EU and ID Pre. Below, density features of IL-10⁺ B cells are shown illustrating the different distribution of cells between EU and ID Pre. **G.** First level HSNE embedding of IL-10⁺CD4⁺ landmarks selected in d. and clustered on cytokines. Four IL-4/5/13⁺ clusters were identified as indicated in the right panel showing the cluster partitions. **H.** Histograms showing the median signal intensity (MSI) distribution of cytokines for the four clusters identified in g. **I.** Frequency of cluster 1, co-expressing IL-4/5/13 and IL-10 (identified in g), relative to total IL-10-producing CD4⁺ T cells. Differences between EU and ID Pre were tested with Student's *t* test, while differences between ID Pre and ID Post were assessed using paired *t* tests. **P* <.05; ***P* <.01.

significantly higher in Indonesians compared to Europeans (*P* < .001; data not shown). However, only the cluster that was negative for IFNγ, TNFα, and IL-2 (cluster 1) decreased significantly after deworming (*P* = .041; Fig. 7I).

DISCUSSION

There are large population differences in immune responses that, although in part can be explained by genetic factors, seem to be largely driven by environmental exposures (35). One such exposure is to helminths, that are ubiquitous in many parts of the world. These parasites induce strong type 2 and regulatory responses and can shape vaccine efficacy or influence the development of inflammatory diseases. By understanding these responses in depth it will be possible to devise interventions that could help vaccine responses or curtail inflammation that damages tissues and organs. To this end, mass cytometry was applied to analyse type 2 and regulatory immune cells of healthy Europeans, as well as of STH-infected Indonesians before and one year after deworming, thereby starting to understand the differences in the immune response of populations living in different geographical areas.

Here, we have identified and shown the enhanced presence of Th2 and ILC2 cells, both sources of the type 2 cytokines IL-4, IL-5 and IL-13, in STH-infected Indonesians compared to Europeans. When considering the cells by their phenotype, Th2 cell frequencies significantly decreased after deworming, but the frequencies of ILC2s remained unchanged. However, the frequency of ILC2s producing type 2 cytokines declined after anthelmintic treatment, indicating decreased functional ILC2 activity. There is very little known about the role of ILC2s in human helminth infections. Although the identification of CRTH2 as a marker of human ILC2s (8) has been a great advantage, only two studies have analysed ILC2s in the context of human helminth infections (36, 37). In a cross-sectional study, Boyd et al. found a higher frequency of c-Kit⁺ ILCs (reported as Lin⁻CD45⁺CD127⁺) in filarial-infected adults (36), however, c-Kit⁺ ILCs have been described to contain both ILC2s and ILC3s (38), and here we did not detect c-Kit⁺ ILC2s. Another study showed that the proportions of ILC2s (reported as Lin⁻CD45⁺CD127⁺CRTH2⁺CD161⁺), when expressed as percentage of Lin⁻CD45⁺CD127⁺ cells, were significantly lower in *Schistosoma haematobium*-infected African children (6-9 years) when compared to age and sex matched uninfected individuals and increased 6 weeks after clearing the infection (37). In our study, when based on phenotypic characterization, there was a tendency for ILC2 frequencies to be higher (although not statistically significant) after deworming. However, decreased functional ILC2 activity in terms of cytokine production was observed and as this study did

not analyse the cytokine production by the cells, it is difficult to compare it with our data. As suggested by the authors (37), the reduction observed in infected individuals might be a consequence of ILC2s migrating and accumulating at the site of infection, or a decline in the generation or maintenance of the cells.

Unlike ILC3s, only one (functional) subset of ILC2s has been characterized in healthy humans (38). We identified 8 ILC2 clusters based on the heterogeneous expression of KLRG1, CD45RA and CCR6, but the significance of these is currently unknown and requires further investigation. Interestingly, we identified CD45RA$^+$c-Kit$^+$ ILC3s that did not express CCR6, a marker previously described to be expressed by ILC3s (29, 38), and hypothesize that this subpopulation might consist of the recently described ILC precursors (ILCPs), as these cells lack CCR6 expression and are CD45RA$^+$ (39).

There is increasing evidence that Th2 cells can be heterogeneous. For example, a minority subpopulation of Th2 cells termed pathogenic effector Th2 (peTh2) cells, found in patients with allergic eosinophilic inflammatory diseases, have been described that have enhanced effector function (27, 40). PeTh2 cells are characterized as CD161$^+$hPGDS$^+$CD27$^-$ Th2 cells, expressing IL-5 in addition to IL-4 and IL-13 and respond to innate stimuli including IL-25, IL-33 and TSLP indicating that they have innate-like properties (27). Although chronic antigen exposure is thought to drive peTh2 differentiation from conventional Th2 cells, it is unknown whether peTh2 cells are induced by or play a role in human helminth infections (27). Anarudha et al. previously identified IL-5$^-$IL-4$^+$IL-13$^+$ and IL-5$^+$IL-4$^+$IL-13$^+$ human CD4$^+$ T cell subpopulations in the context of filariasis, but the expression of CD161 was not assessed (41). Here, we describe the enhanced presence of a peTh2-like CD27$^-$ CD161$^+$ subset of Th2 cells in STH-infected individuals which significantly decreased after deworming. However, whether these cells are identical to peTh2 cells needs to be investigated in future studies.

Unlike Th2 cells, Tregs have been described as a heterogeneous population and previous work showed that HLA-DR (42), ICOS (43) and CD38 (44) are differentially expressed within the FOXP3$^+$ Treg population, marking cells with distinct capacities and modes of suppression. While Tregs expressing HLA-DR or CD38 were shown to be highly suppressive compared to their negative counterparts (42, 44), the expression of ICOS seems to define a Treg subset that has the capacity to produce large amounts of IL-10, in contrast to ICOS$^-$ Tregs producing mainly TGF-β (43). By using mass cytometry, we could not only confirm the presence of these distinct Treg phenotypes in our study population, but also visualize the marker distribution which revealed that all HLA-DR$^+$, ICOS$^+$ and CD38$^+$ cells were found within the CTLA4$^+$ Treg subset. Similar to CD25 and GITR, CTLA4 is a T cell activation marker (10) and has been shown to correlate with FOXP3 expression in human CD4$^+$ T cells (45). Experimental models showed that CTLA4 is crucial for the suppressive function of Tregs through the modulation of APCs (30) and its interaction with CD80 and CD86 on conventional T cells (46).

Although Treg frequencies were not expanded in helminth infected individuals and no treatment-related change was seen, consistent with previous work in children from

the same study area (14, 15), the proportion of CTLA4$^+$ Tregs was significantly higher in helminth infected individuals and declined after treatment which is in line with previous reports (15, 47). Analysis at the cluster level revealed that the CTLA4$^+$ clusters in particular, often co-expressing ICOS and/or HLA-DR and/or CD38, were expanded in Indonesians compared to Europeans, indicating that helminths induce a particular Treg phenotype which could be represented by cells with increased regulatory capacity.

Besides Th2 cells and ILC2s being a source of type 2 cytokines, we identified Tc2 cells (type 2 cytokine-secreting CD8$^+$ T cells (33)) and a cluster of γδ T cells, which were capable of producing type 2 cytokines. Although Tc2 cells have recently been found to be enriched in patients with eosinophilic asthma (34), this subset has rarely been investigated, and therefore the current study is one of the first to characterize these cells in the context of human helminth infections.

Like Tc2 cells, not much is known about type 2 cytokine-producing γδ T cells, although their existence has been described before (48-52). Inagaki et al. showed a protective role of γδ T cells against infection with *N. brasiliensis* in mice, which was associated with the production of type 2 cytokines, in particular IL-13 (49). However, to our knowledge, the presence of type 2 cytokine-producing γδ T cells in human helminth infection has not been reported before. Here, we identified type 2 cytokine-producing γδ T cells, and showed that these cells were present in helminth-infected individuals, indicating their possible participation in the development of Th2 responses. However, further studies are required to investigate the function of Tc2 and type 2 cytokine-producing γδ T cells.

IL-10 producing B cells, known as regulatory B cells (Bregs), represent a relatively rare cell type within the human immune system that can suppress inflammatory responses (53). Although the frequency of IL-10 producing B cells was similar in Europeans and Indonesians and deworming did not affect their frequency, the phenotype of these cells was strikingly different with relatively more CD11c$^+$CD38$^-$, and less CD11c$^-$CD38$^+$ IL-10$^+$ B cells present in Indonesians. CD11c$^+$ B cells are increasingly recognized as a distinct population of memory B cells, and have been shown to expand in settings of chronic infections such as HIV, malaria and TB as well as in several autoimmune diseases (54, 55). In line with this, we found a significantly expanded population of CD11c$^+$Tbet$^+$ B cells in helminth-infected Indonesians compared to Europeans, of which a small fraction appeared capable of producing IL-10. Whereas CD38 has previously been reported as a marker for human Bregs (53), the expression of CD11c has not yet been associated with Bregs and further studies investigating the suppressive properties of CD11c$^+$IL-10$^+$ B cells will be needed.

Our study has a number of limitations. The small number of study subjects, the lack of placebo-treated individuals and the possibility that other infections are affected by deworming.

The work described here provided a detailed insight into the types of cells that participate in the strong type 2 and regulatory response induced by helminths. We demonstrate the advantage of using mass cytometry combined with HSNE, which allowed the identification of rare cell populations, such as ILC2s, Tc2 cells and Bregs, and provided

an opportunity to analyse the heterogeneity within Th2 cells and Tregs. Therefore this study forms the basis for the analysis of the identified cell subpopulations by flow cytometry in larger studies, not only in helminth infections, but also in other disease settings, as well as for their further functional characterization.

ACKNOWLEDGEMENTS

We would like to thank the volunteers who participated in this study. We would also like to thank all field workers from Universitas Indonesia and Nangapanda; Yvonne Kruize, Sanne de Jong and Astrid Voskamp for their help with the study. This work was supported by the Royal Netherlands Academy of Arts and Science (KNAW), Ref 57-SPIN3-JRP and Universitas Indonesia (Research Grant BOPTN 2742/H2.R12/HKP.05.00/2013.).

REFERENCES

1. Hotez PJ, Brindley PJ, Bethony JM, King CH, Pearce EJ, Jacobson J. Helminth infections: the great neglected tropical diseases. The Journal of clinical investigation **2008**; 118(4): 1311-21.
2. Maizels RM, Yazdanbakhsh M. Immune regulation by helminth parasites: cellular and molecular mechanisms. Nature reviews Immunology **2003**; 3(9): 733-44.
3. Allen JE, Wynn TA. Evolution of Th2 immunity: a rapid repair response to tissue destructive pathogens. PLoS pathogens **2011**; 7(5): e1002003.
4. de Ruiter K, Tahapary DL, Sartono E, et al. Helminths, hygiene hypothesis and type 2 diabetes. Parasite immunology **2017**; 39(5).
5. Moro K, Yamada T, Tanabe M, et al. Innate production of T(H)2 cytokines by adipose tissue-associated c-Kit(+)Sca-1(+) lymphoid cells. Nature **2010**; 463(7280): 540-4.
6. Neill DR, Wong SH, Bellosi A, et al. Nuocytes represent a new innate effector leukocyte that mediates type-2 immunity. Nature **2010**; 464(7293): 1367-70.
7. Price AE, Liang HE, Sullivan BM, et al. Systemically dispersed innate IL-13-expressing cells in type 2 immunity. Proceedings of the National Academy of Sciences of the United States of America **2010**; 107(25): 11489-94.
8. Mjosberg JM, Trifari S, Crellin NK, et al. Human IL-25- and IL-33-responsive type 2 innate lymphoid cells are defined by expression of CRTH2 and CD161. Nat Immunol **2011**; 12(11): 1055-62.
9. Simoni Y, Newell EW. Dissecting human ILC heterogeneity: more than just three subsets. Immunology **2018**; 153(3): 297-303.
10. Sakaguchi S, Miyara M, Costantino CM, Hafler DA. FOXP3+ regulatory T cells in the human immune system. Nature reviews Immunology **2010**; 10(7): 490-500.
11. Maizels RM, Smith KA. Regulatory T cells in infection. Adv Immunol **2011**; 112: 73-136.
12. Metenou S, Nutman TB. Regulatory T cell subsets in filarial infection and their function. Frontiers in immunology **2013**; 4: 305.
13. Watanabe K, Mwinzi PN, Black CL, et al. T regulatory cell levels decrease in people infected with Schistosoma mansoni on effective treatment. The American journal of tropical medicine and hygiene **2007**; 77(4): 676-82.
14. Wammes LJ, Hamid F, Wiria AE, et al. Regulatory T cells in human geohelminth infection suppress immune responses to BCG and Plasmodium falciparum. European journal of immunology **2010**; 40(2): 437-42.
15. Wammes LJ, Hamid F, Wiria AE, et al. Community deworming alleviates geohelminth-induced immune hyporesponsiveness. Proceedings of the National Academy of Sciences of the United States of America **2016**; 113(44): 12526-31.
16. van der Maaten L, Hinton G. Visualizing Data using t-SNE. J Mach Learn Res **2008**; 9: 2579-605.
17. McInnes L HJ. UMAP: Uniform Manifold Approximation and Projection for Dimension Reduction. https://arxivorg/pdf/180203426pdf **2018**.
18. Pezzotti N, Hollt T, Lelieveldt B, Eisemann E, Vilanova A. Hierarchical Stochastic Neighbor Embedding. Comput Graph Forum **2016**; 35(3): 21-30.
19. van Unen V, Hollt T, Pezzotti N, et al. Visual analysis of mass cytometry data by hierarchical stochastic neighbour embedding reveals rare cell types. Nature communications **2017**; 8(1): 1740.
20. Tahapary DL, de Ruiter K, Martin I, et al. Helminth infections and type 2 diabetes: a cluster-randomized placebo controlled SUGARSPIN trial in Nangapanda, Flores, Indonesia. BMC infectious diseases **2015**; 15: 133.
21. Tahapary DL, de Ruiter K, Martin I, et al. Effect of Anthelmintic Treatment on Insulin Resistance: A Cluster-Randomized, Placebo-Controlled Trial in Indonesia. Clin Infect Dis **2017**; 65(5): 764-71.
22. Wiria AE, Prasetyani MA, Hamid F, et al. Does treatment of intestinal helminth infections influence malaria? Background and methodology of a longitudinal study of clinical, parasitological and immunological parameters in Nangapanda, Flores, Indonesia (ImmunoSPIN Study). BMC infectious diseases **2010**; 10: 77.
23. Hollt T, Pezzotti N, van Unen V, et al. Cytosplore: Interactive Immune Cell

Phenotyping for Large Single-Cell Datasets. Comput Graph Forum **2016**; 35(3): 171-80.
24. Comaniciu D, Meer P. Mean shift: A robust approach toward feature space analysis. Ieee T Pattern Anal **2002**; 24(5): 603-19.
25. Beyrend G, Stam K, Hollt T, Ossendorp F, Arens R. *Cytofast*: A workflow for visual and quantitative analysis of flow and mass cytometry data to discover immune signatures and correlations. Computational and Structural Biotechnology Journal **2018**.
26. Cosmi L, Annunziato F, Galli MIG, Maggi RME, Nagata K, Romagnani S. CRTH2 is the most reliable marker for the detection of circulating human type 2 Th and type 2 T cytotoxic cells in health and disease. European journal of immunology **2000**; 30(10): 2972-9.
27. Mitson-Salazar A, Prussin C. Pathogenic Effector Th2 Cells in Allergic Eosinophilic Inflammatory Disease. Front Med (Lausanne) **2017**; 4: 165.
28. Mahnke YD, Brodie TM, Sallusto F, Roederer M, Lugli E. The who's who of T-cell differentiation: human memory T-cell subsets. European journal of immunology **2013**; 43(11): 2797-809.
29. Simoni Y, Fehlings M, Kloverpris HN, et al. Human Innate Lymphoid Cell Subsets Possess Tissue-Type Based Heterogeneity in Phenotype and Frequency. Immunity **2017**; 46(1): 148-61.
30. Wing K, Onishi Y, Prieto-Martin P, et al. CTLA-4 control over Foxp3+ regulatory T cell function. Science (New York, NY) **2008**; 322(5899): 271-5.
31. Pesenacker AM, Bending D, Ursu S, Wu Q, Nistala K, Wedderburn LR. CD161 defines the subset of FoxP3+ T cells capable of producing proinflammatory cytokines. Blood **2013**; 121(14): 2647-58.
32. Afzali B, Mitchell PJ, Edozie FC, et al. CD161 expression characterizes a subpopulation of human regulatory T cells that produces IL-17 in a STAT3-dependent manner. European journal of immunology **2013**; 43(8): 2043-54.
33. Seder RA, Le Gros GG. The functional role of CD8+ T helper type 2 cells. J Exp Med **1995**; 181(1): 5-7.
34. Hilvering B, Hinks TSC, Stoger L, et al. Synergistic activation of pro-inflammatory type-2 CD8(+) T lymphocytes by lipid mediators in severe eosinophilic asthma. Mucosal Immunol **2018**.
35. Brodin P, Jojic V, Gao T, et al. Variation in the human immune system is largely driven by non-heritable influences. Cell **2015**; 160(1-2): 37-47.
36. Boyd A, Ribeiro JM, Nutman TB. Human CD117 (cKit)+ innate lymphoid cells have a discrete transcriptional profile at homeostasis and are expanded during filarial infection. PloS one **2014**; 9(9): e108649.
37. Nausch N, Appleby LJ, Sparks AM, Midzi N, Mduluza T, Mutapi F. Group 2 innate lymphoid cell proportions are diminished in young helminth infected children and restored by curative anti-helminthic treatment. PLoS neglected tropical diseases **2015**; 9(3): e0003627.
38. Spits H, Artis D, Colonna M, et al. Innate lymphoid cells--a proposal for uniform nomenclature. Nature reviews Immunology **2013**; 13(2): 145-9.
39. Lim AI, Li Y, Lopez-Lastra S, et al. Systemic Human ILC Precursors Provide a Substrate for Tissue ILC Differentiation. Cell **2017**; 168(6): 1086-100 e10.
40. Mitson-Salazar A, Yin Y, Wansley DL, et al. Hematopoietic prostaglandin D synthase defines a proeosinophilic pathogenic effector human T(H)2 cell subpopulation with enhanced function. The Journal of allergy and clinical immunology **2016**; 137(3): 907-18 e9.
41. Anuradha R, George PJ, Hanna LE, et al. Parasite-antigen driven expansion of IL-5(-) and IL-5(+) Th2 human subpopulations in lymphatic filariasis and their differential dependence on IL-10 and TGFbeta. PLoS neglected tropical diseases **2014**; 8(1): e2658.
42. Baecher-Allan C, Wolf E, Hafler DA. MHC class II expression identifies functionally distinct human regulatory T cells. Journal of immunology (Baltimore, Md : 1950) **2006**; 176(8): 4622-31.
43. Ito T, Hanabuchi S, Wang YH, et al. Two functional subsets of FOXP3+ regulatory T cells in human thymus and periphery. Immunity **2008**; 28(6): 870-80.
44. Patton DT, Wilson MD, Rowan WC, Soond DR, Okkenhaug K. The PI3K p110delta regulates expression of CD38 on regulatory T cells. PloS one **2011**; 6(3): e17359.
45. Yagi H, Nomura T, Nakamura K, et al. Crucial role of FOXP3 in the development and function of human CD25+CD4+ regulatory T cells. Int Immunol **2004**; 16(11): 1643-56.
46. Paust S, Lu L, McCarty N, Cantor H. Engagement of B7 on effector T cells by regulatory T cells prevents autoimmune disease. Proceedings of the National Academy of Sciences of the United States of America **2004**; 101(28): 10398-403.
47. Garcia-Hernandez MH, Alvarado-Sanchez B, Calvo-Turrubiartes MZ, et al. Regulatory T Cells in children with intestinal parasite infection. Parasite immunology **2009**; 31(10): 597-603.
48. Ferrick DA, Schrenzel MD, Mulvania T, Hsieh B, Ferlin WG, Lepper H. Differential production of interferon-gamma and interleukin-4 in response to Th1- and Th2-stimulating pathogens by gamma delta T cells in vivo. Nature **1995**; 373(6511): 255-7.
49. Inagaki-Ohara K, Sakamoto Y, Dohi T, Smith AL. gammadelta T cells play a protective role during infection with Nippostrongylus brasiliensis by promoting goblet cell function in the small intestine. Immunology **2011**; 134(4): 448-58.
50. Zuany-Amorim C, Ruffie C, Haile S, Vargaftig BB, Pereira P, Pretolani M. Requirement for gammadelta T cells in allergic airway inflammation. Science (New York, NY) **1998**; 280(5367): 1265-7.
51. Spinozzi F, Agea E, Bistoni O, et al. Increased allergen-specific, steroid-sensitive gamma delta T cells in bronchoalveolar lavage fluid from patients with asthma. Ann Intern Med **1996**; 124(2): 223-7.
52. Krug N, Erpenbeck VJ, Balke K, et al. Cytokine profile of bronchoalveolar lavage-derived CD4(+), CD8(+), and gammadelta T cells in people with asthma after segmental allergen challenge. American journal of respiratory cell and molecular biology **2001**; 25(1): 125-31.
53. Mauri C, Menon M. The expanding family of regulatory B cells. Int Immunol **2015**; 27(10): 479-86.
54. Karnell JL, Kumar V, Wang J, Wang S, Voynova E, Ettinger R. Role of CD11c(+) T-bet(+) B cells in human health and disease. Cellular immunology **2017**; 321: 40-5.
55. Winslow GM, Papillion AM, Kenderes KJ, Levack RC. CD11c+ T-bet+ memory B cells: Immune maintenance during chronic infection and inflammation? Cellular immunology **2017**; 321: 8-17.

SUPPLEMENTAL DATA

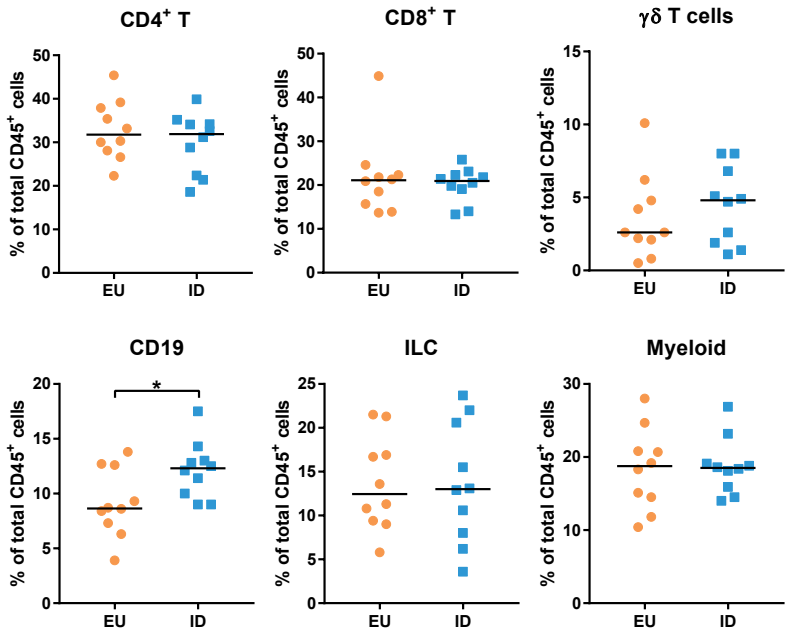

Supplementary Figure S1. Lineage frequencies. Scatterplots comparing lineage frequencies of Europeans (EU) and Indonesians (ID). Median is shown. Differences between EU and ID Pre were tested with Student's t-test. *P <.05.

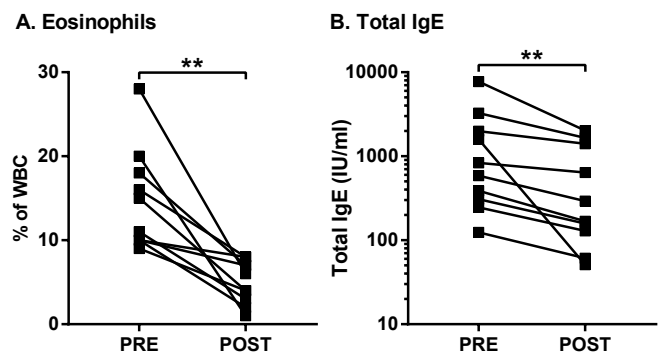

Supplementary Figure S2. Eosinophil counts and total IgE levels. A. Eosinophil counts expressed as percentage of white blood cells (WBC) and **B.** Serum levels of total IgE of Indonesians pre- and post-anthelmintic treatment. **P <.01.

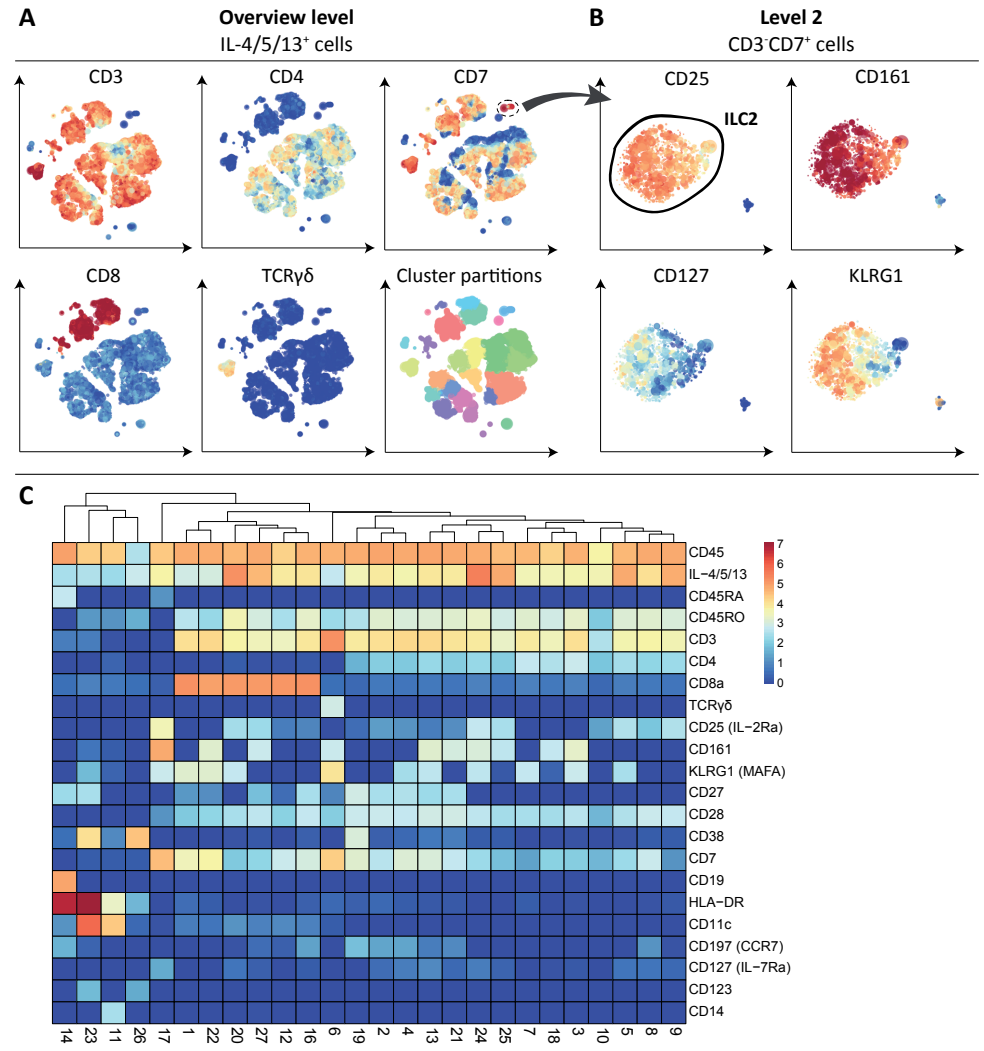

Supplementary Figure S3. Type 2-cytokine producing cells. A. First level embedding of IL-4/5/13$^+$ cells clustered on surface markers and cluster partitions of IL-4/5/13$^+$ cells using GMS clustering (lower right panel). The expression of CD4 was reduced as a consequence of the stimulation. Colour represents arsin5-transformed marker expression as indicated. Size of the landmarks represents AoI. **B.** Second level embedding of the CD3$^-$CD7$^+$ landmarks selected from the first level in a, as indicated by the black encirclement, allowed the identification of ILC2s. **C.** A heatmap summary of median expression values of cell markers expressed by IL-4/5/13$^+$ cells identified in a. and hierarchical clustering thereof.

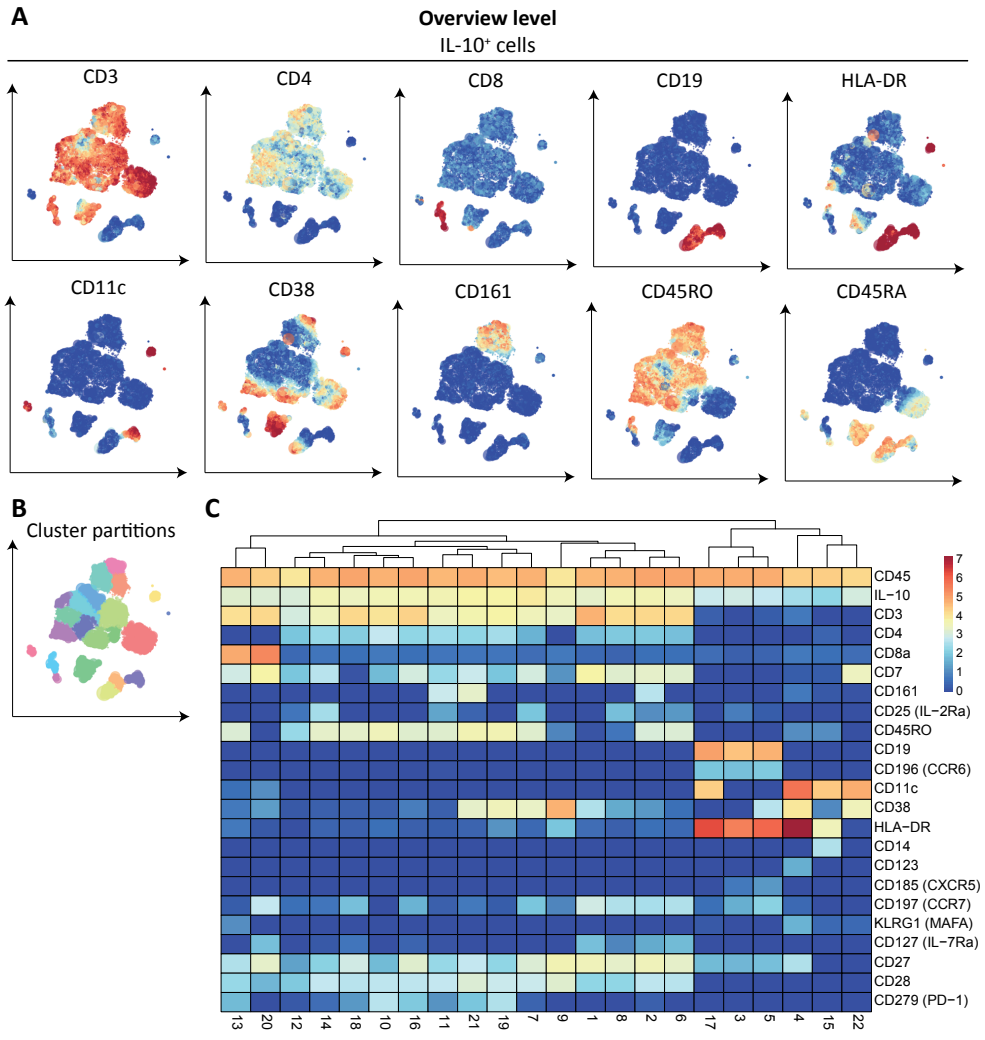

Supplementary Figure S4. IL-10 producing cells. A. First level embedding of IL-10⁺ cells clustered on surface markers. The expression of CD4 was reduced as a consequence of the stimulation. Colour represents arsin5-transformed marker expression as indicated. Size of the landmarks represents AoI. **B.** Cluster partitions of IL-10⁺ cells using GMS clustering. **C.** A heatmap summary of median expression values of cell markers expressed by IL-10⁺ cells identified in b. and hierarchical clustering thereof.

Supplementary table S1. Antibody panel 1 (Phenotyping).

Label	Specificity	Clone	Vendor	Catalogue number	Dilution
^{89}Y	CD45	HI30	Fluidigm[a]	3089003B	200x
^{113}CD	CD45RA	HI100	eBioscience[b]	83-0458-42	50x
^{141}Pr	CD196 (CCR6)	G034E3	Fluidigm	3141003A	100x
^{142}Nd	CD19	HIB19	Fluidigm	3142001B	200x
^{143}Nd	CD117 (c-Kit)	104D2	Fluidigm	3143001B	100x
^{145}Nd	CD4	RPA-T4	Fluidigm	3145001B	100x
^{146}Nd	CD8a	RPA-T8	Fluidigm	3146001B	200x
^{147}Sm	CD183 (CXCR3)	G025H7	BioLegend[c]	353733	100x
^{148}Nd	CD14	M5E2	BioLegend	301843	100x
^{149}Sm	CD25 (IL-2Ra)	2A3	Fluidigm	3149010B	100x
^{150}Nd	CD185 (CXCR5)	J252D4	BioLegend	356902	100x
^{151}Eu	CD123	6H6	Fluidigm	3151001B	100x
^{152}Sm	TCRγδ	11F2	Fluidigm	3152008B	50x
^{153}Eu	CD7	CD7-6B7	Fluidigm	3153014B	100x
^{154}Sm	CD163	GHI/61	Fluidigm	3154007B	100x
^{155}Gd	CD278 (ICOS)	C398.4A	BioLegend	313502	50x
^{156}Gd	CD294 (CRTH2)	BM16	BioLegend	350102	50x
^{158}Gd	CD122 (IL-2Rb)	TU27	BioLegend	339015	100x
^{159}Tb	CD197 (CCR7)	G043H7	Fluidigm	3159003A	100x
^{160}Gd	FOXP3	PCH101	eBioscience	14-4776-82	50x
^{161}Dy	KLRG1 (MAFA)	REA261	Miltenyi[d]	Special order	100x
^{162}Dy	CD11c	Bu15	Fluidigm	3162005B	200x
^{163}Dy	CD152 (CTLA-4)	BNI3	BioLegend	369602	100x
^{164}Dy	CD161	HP-3G10	Fluidigm	3164009B	100x
^{165}Ho	CD127 (IL-7Rα)	AO19D5	Fluidigm	3165008B	200x
^{166}Er	Tbet	4B10	BioLegend	644825	50x
^{167}Er	CD27	O323	Fluidigm	3167002B	200x
^{168}Er	HLA-DR	L243	BioLegend	307651	200x
^{169}Tm	GATA3	REA174	Miltenyi	130-108-061	50x
^{170}Er	CD3	UCHT1	Fluidigm	3170001B	100x
^{171}Yb	CD28	CD28.2	BioLegend	302937	200x
^{172}Yb	CD38	HIT2	Fluidigm	3172007B	200x
^{173}Yb	CD45RO	UCHL1	BioLegend	304239	100x
^{174}Yb	CD335 (NKp46)	92E	BioLegend	331902	100x
^{175}Lu	CD279 (PD-1)	EH 12.2H7	Fluidigm	3175008B	100x
^{176}Yb	CD56	NCAM16.2	Fluidigm	3176008B	100x
^{209}Bl	CD16	3G8	Fluidigm	3209002B	400x

[a]Fluidigm, South San Francisco, CA, USA. [b]eBioscience, San Diego, CA, USA. [c]Biolegend, San Diego, CA, USA. [d]Miltenyi Biotech, Bergisch Gladbach, Germany. CCR, C-C chemokine receptor. CD, cluster of differentiation. CRTH2, prostaglandin D2 receptor 2. CXCR, CXC chemokine receptor. FOXP3, forkhead box P3. HLA-DR, human leukocyte antigen-D-related. IL-2R, interleukin-2 receptor. IL-7Rα, interleukin-7 receptor α. KLRG1, killer cell lectin-like receptor subfamily G member 1. MAFA, mast cell function-associated antigen. PD-1, programmed cell death protein. TCR, T-cell receptor. Markers in grey were stained intranuclear, while all other markers were stained on the cell surface.

Supplementary table S2. Antibody panel 2 (Cytokine production).

Label	Specificity	Clone	Vendor	Catalogue number	Dilution
^{89}Y	CD45	HI30	Fluidigm[a]	3089003B	200x
^{113}CD	CD45RA	HI100	Ebioscience[b]	83-0458-42	50x
^{141}Pr	CD196 (CCR6)	G034E3	Fluidigm	3141003A	100x
^{142}Nd	CD19	HIB19	Fluidigm	3142001B	200x
^{143}Nd	CD117 (c-Kit)	104D2	Fluidigm	3143001B	100x
^{144}Nd	IL-2	MQ117H12	BioLegend[c]	500339	400x
^{145}Nd	CD4	RPA-T4	Fluidigm	3145001B	100x
^{146}Nd	CD8a	RPA-T8	Fluidigm	3146001B	200x
^{147}Sm	CD183 (CXCR3)	G025H7	BioLegend	353733	100x
^{148}Nd	CD14	M5E2	BioLegend	301843	100x
^{149}Sm	CD25 (IL-2Ra)	2A3	Fluidigm	3149010B	100x
^{150}Nd	CD185 (CXCR5)	J252D4	BioLegend	356902	100x
^{151}Eu	CD123	6H6	Fluidigm	3151001B	100x
^{152}Sm	TCRγδ	11F2	Fluidigm	3152008B	50x
^{153}Eu	CD7	CD7-6B7	Fluidigm	3153014B	100x
^{154}Sm	CD163	GHI/61	Fluidigm	3154007B	100x
^{155}Gd	IFNγ	B27	BioLegend	506521	400x
^{156}Gd	CD294 (CRTH2)	BM16	BioLegend	350102	50x
^{158}Gd	CD122 (IL-2Rb)	TU27	BioLegend	339015	100x
^{159}Tb	CD197 (CCR7)	G043H7	Fluidigm	3159003A	100x
^{160}Gd	TNFα	MAb11	BioLegend	502941	400x
^{161}Dy	KLRG1 (MAFA)	REA261	Miltenyi[d]	Special order	100x
^{162}Dy	CD11c	Bu15	Fluidigm	3162005B	200x
^{163}Dy	IL-17	BL168	BioLegend	512331	400x
^{164}Dy	CD161	HP-3G10	Fluidigm	3164009B	100x
^{165}Ho	CD127 (IL-7Ra)	AO19D5	Fluidigm	3165008B	200x
^{166}Er	IL-10	JES39D7	Fluidigm	3166008B	400x
^{167}Er	CD27	O323	Fluidigm	3167002B	200x
^{168}Er	HLA-DR	L243	BioLegend	307651	200x
^{169}Tm	IL-4	MP4-25D2	Fluidigm	3169016B	400x
^{169}Tm	IL-5	TRFK5	BioLegend	500829	400x
^{169}Tm	IL-13	JES105A2	BioLegend	504309	400x
^{170}Er	CD3	UCHT1	Fluidigm	3170001B	100x
^{171}Yb	CD28	CD28.2	BioLegend	302937	200x
^{172}Yb	CD38	HIT2	Fluidigm	3172007B	200x
^{173}Yb	CD45RO	UCHL1	BioLegend	304239	100x
^{175}Lu	CD279 (PD-1)	EH 12.2H7	Fluidigm	3175008B	100x
^{176}Yb	CD56	NCAM16.2	Fluidigm	3176008B	100x

[a]Fluidigm, South San Francisco, CA, USA. [b]eBioscience, San Diego, CA, USA. [c]Biolegend, San Diego, CA, USA. [d]Miltenyi Biotech, Bergisch Gladbach, Germany. CCR, C-C chemokine receptor. CD, cluster of differentiation. CRTH2, prostaglandin D2 receptor 2. CXCR, CXC chemokine receptor. HLA-DR, human leukocyte antigen-D-related. IL-2R, interleukin-2 receptor. IL-7Rα, interleukin-7 receptor α. KLRG1, killer cell lectin-like receptor subfamily G member 1. MAFA, mast cell function-associated antigen. PD-1, programmed cell death protein. TCR, T-cell receptor. Markers in grey were stained intracellular, while all other markers were stained on the cell surface.

9

SUMMARIZING DISCUSSION

Adapted from: Helminths, Hygiene Hypothesis and Type 2 Diabetes.

Karin de Ruiter*, Dicky L. Tahapary*, Erliyani Sartono, Pradana Soewondo,
Taniawati Supali, Johannes W.A. Smit and Maria Yazdanbakhsh

*Both authors contributed equally

Parasite Immunology (2017)

WHAT WAS ALREADY KNOWN ABOUT HELMINTHS, THEIR IMMUNOMODULATORY EFFECTS AND THE ASSOCIATION WITH TYPE 2 DIABETES?

Helminth parasites are the strongest natural inducers of type 2 immunity, and landmark studies have shown that conditions which induce type 2 immune responses improve metabolic disorders (1-6). Furthermore, in several epidemiological studies an inverse association between helminth infections and the prevalence of type 2 diabetes (T2D) or metabolic syndrome was found (7-11). However, the cross-sectional design of these studies have prevented conclusions on the causal relationship between helminth infections and T2D in humans.

Although the mechanisms underlying the potential association between helminth infections and T2D are still largely unknown, experimental infections with helminths or helminth-derived molecules in high fat diet-induced obese mice have indicated that changes in the immune cell composition, in particular in white adipose tissue, contribute to the insulin-sensitizing effects. While obese adipose tissue is characterized by pro-inflammatory type 1 cytokines, a type 2 cytokine environment is present in metabolic tissues under homeostatic, insulin sensitive conditions. Group 2 innate lymphoid cells (ILC2s) and $CD4^+$ T helper 2 (Th2) cells produce the type 2 cytokines interleukin (IL)-4, IL-5 and IL-13 in healthy adipose tissue and sustain a white adipose tissue (WAT) eosinophil and alternatively macrophage (AAM) axis that is largely driven by eosinophil-produced IL-4 (1, 12). Of note, whereas a recent study showed an association between soil-transmitted helminth (STH) infections and insulin sensitivity in humans, no indication for differences in systemic inflammation between subjects with and without STH infections was found (11).

The induction of a strong regulatory network involving regulatory T cells (Tregs) is another important hallmark of helminth infections which might explain the possible beneficial effects of helminth infections. Although filarial antigen-mediated improvement in glucose tolerance in obese mice was shown to occur independently of Tregs (5), the establishment of a regulatory network may contribute to the control of overt immune responses, restricting the chronic low-grade inflammation in adipose tissue that is key to the development of insulin resistance (13). Wammes et al. recently found that not Treg frequencies, but the expression of CTLA4, a molecule expressed by Tregs and involved in putting the brake on immune activation, significantly declined in anthelmintic-treated individuals, indicating that helminths have a modulatory effect on Tregs resulting in increased regulatory capacity (14).

In addition to modulation of the host immune response, helminth infections might confer protection against the development of T2D through caloric restriction, induced by changes in digestion and decreased absorption of nutrients (15, 16). It was previously shown that helminth infections were associated with a lower body mass index (BMI) and waist hip ratio (WHR). However, after adjustment for BMI, the negative association

between STH infections and HOMA-IR persisted, indicating that this association cannot be explained by effects of STH infections on BMI alone (11).

Taken together, previous work has identified the interplay between helminths, inflammation and metabolic homeostasis as an exciting new area that needs further dissection.

HOW DID OUR STUDIES ADVANCE THE FIELD?

Helminths and metabolic homeostasis

To investigate the causal relationship between helminth infections and the development of T2D, we assessed the effect of anthelmintic treatment on changes in insulin resistance (IR), in an area endemic for STH on Flores Island, Indonesia. To this end, a double-blind, household-cluster-randomized, placebo-controlled trial was conducted which is described in **chapter 2**. During one year, study participants (≥ 16 years of age) received four rounds of albendazole or matching placebo with three-month intervals, for three consecutive days. In **chapter 3** we describe the trial outcomes, showing that intensive anthelmintic treatment significantly reduced STH prevalence, as well as infection intensity. Moreover, type 2 immune responses, assessed by eosinophil counts and total IgE levels in peripheral blood, were significantly reduced in albendazole-treated subjects. Although treatment did not lead to an increase of whole-body IR, assessed by homeostatic model assessment of IR (HOMA-IR), at the community level, a significant increase in HOMA-IR was observed among helminth-infected subjects. The latter was accompanied by a significant increase in BMI, and pathway analysis showed that adjustment for BMI and eosinophil count attenuated the treatment effect on HOMA-IR among helminth-infected subjects. Altogether, this is the first cluster-randomized trial in humans demonstrating the causal relationship between helminth infections and whole-body IR in an area endemic for STH. However, it should be noted that the anthelmintic treatment-induced increase in IR might have a relatively small contribution to the multi-factorial pathogenesis of IR, and the assessment of other more established factors such as diet and physical activity will be needed to investigate this.

Experimental infections with helminths in obese mice have enabled us to investigate the potential mechanisms by which helminths can influence metabolic outcomes. Moreover, the identification of single, active helminth-derived molecules has gained increasing attention, as administration of these molecules eliminates the potential helminth-induced pathological condition, and excludes the possibility that the beneficial effects of helminth infections on metabolic homeostasis are simply a result of parasitism. **Chapter 4** builds on previous work showing that chronic treatment with a mixture of *Schistosoma mansoni* soluble egg antigens (SEA) improved whole-body metabolic homeostasis in high-fat diet (HFD)-induced obese mice (4). In this chapter, we investigated the effects of two plant-produced glycosylation variants of omega-1 (ω1), a glycoprotein present in SEA which was previously identified as the major immunomodulatory component in SEA (17, 18), on whole-body metabolic homeostasis. Both recombinant ω1 glycovariants decreased fat mass and

improved whole-body metabolic homeostasis in obese mice, an effect associated with increased adipose tissue Th2 cells, eosinophils and AAM. The use of mice deficient for STAT6, a transcription factor which is essential for IL-4/IL-13 receptor-mediated signaling, allowed us to assess whether type 2 immunity induced by either SEA or ω1 is required for its metabolic effects. Remarkably, although the metabolic effects of SEA were abolished (data not shown), those of ω1 were still observed, despite the abrogation of the Th2-mediated immune response in these Stat6-deficient mice. In addition, ω1 was found to inhibit food intake in both WT and Stat6-deficient mice, suggesting that the improvement of metabolic homeostasis in insulin-resistant obese mice by plant-produced recombinant ω1 glycovariants is independent of their Th2-inducing capacities, and may be explained by brain-mediated inhibition of food intake and/or immune-independent direct interaction of ω1 with metabolic cells. Further studies are required to investigate the anorexigenic effect of ω1, which might be a specific property of this molecule since it was not described previously when mice were chronically infected with *S. mansoni* or treated with SEA (4). Thus, although the schistosome egg antigen mixture improves metabolic homeostasis through type 2 immune responses, the single molecule ω1, which is capable of inducing strong type 2 responses, improves metabolic homeostasis, but not through its effect on type 2 immune responses.

In summary, our work on helminth infections and metabolic disorders, in both human and mice, has provided valuable insights into the effects of helminths and their molecules on metabolic homeostasis (**Figure 1**). The clinical trial revealed that in helminth-infected subjects, anthelmintic treatment significantly increases IR, highlighting the need for education and prevention strategies for noncommunicable diseases such as T2D, to go hand in hand with infectious disease control measures such as mass drug administration programs. Furthermore, repetitive injections of ω1 in a pathogen-free setting were found to have a beneficial effect on metabolic homeostasis in obese mice. However, as this effect appeared independent of the Th2-inducing capacity of ω1, it questions the role of type 2 immune cells in this particular experimental model.

Immune modulation by helminths

In the subsequent chapters, we further characterized the immunomodulatory effects of helminths as these might be associated with improved metabolic homeostasis. Eosinophilia is a well-known hallmark of helminths, and considering the presumed role of WAT eosinophils in maintaining whole-body metabolic homeostasis, we assessed the effect of STH infections on the activation status and responsiveness of eosinophils. In addition, neutrophil activation was analyzed as, despite a recent study showing enhanced neutrophil activation in subjects infected with helminths (19), little is known about the role of neutrophils during helminth infections. **Chapter 5** describes a field-applicable method that was developed to monitor changes in the expression of certain granulocyte surface molecules by flow cytometry, in order to assess granulocyte activation. As we were limited

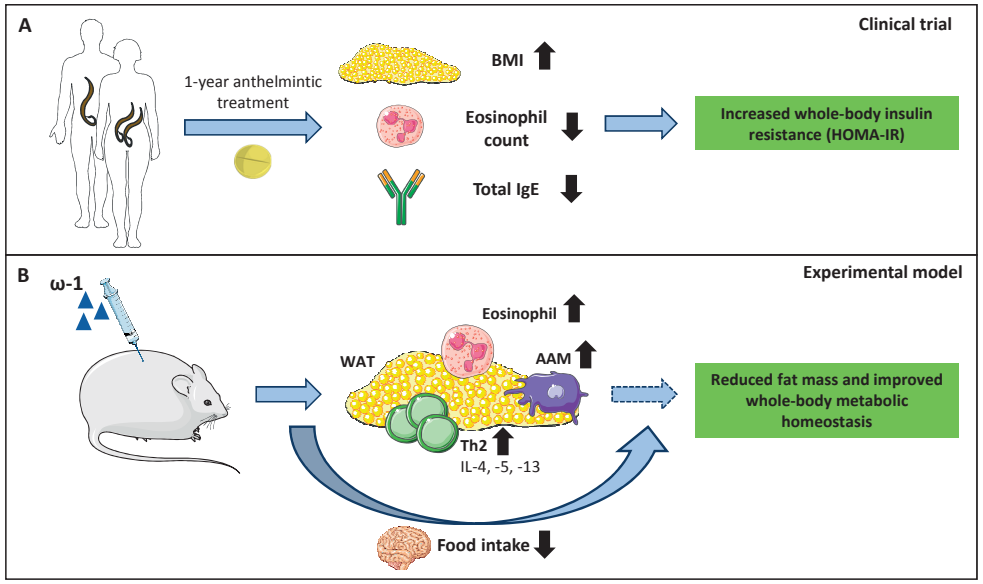

Figure 1. Summary of findings demonstrating the causal relationship between helminths or the helminth-derived molecule ω1 and whole-body metabolic homeostasis. This figure summarizes the results described in chapter 3 & 4. A) Intensive anthelmintic treatment in an STH-endemic area significantly reduced both STH infection prevalence and intensity, as well as its related type 2 immune responses (eosinophil counts and total IgE levels), while BMI increased. Deworming did not lead to an increase of whole-body IR at the community level, but it increased IR among those with a microscopy-detected STH infection. B) Treatment of obese mice with plant-produced recombinant ω1 glycovariants decreased fat mass and improved whole-body metabolic homeostasis, independent of its Th2-inducing capacity (indicated by the arrows with dashed lines), and may be explained by brain-mediated inhibition of food intake (indicated by the arrow with uninterrupted lines). BMI, body mass index; AAM, alternatively activated macrophages; WAT, white adipose tissue.

by the resources at the field study site with no direct access to a flow cytometer, we set up a method to analyze granulocyte activation markers in whole-blood samples that were lysed, fixed and cryopreserved. Although marker intensities varied when comparing fresh and fixed granulocytes, most likely due to intracellular staining and increased eosinophil autofluorescence as a consequence of fixation, it was shown that the responsiveness to stimuli could still be clearly measured after fixation.

We applied this method in our clinical trial (chapter 2) and collected samples for flow cytometric analysis from a subset of 300 subjects, before and after one year of albendazole treatment. **Chapter 6** describes that, although anthelmintic treatment effectively reduced the prevalence of helminth infections and circulating eosinophil numbers (similar to the results described in Chapter 3), helminths did not affect the activation status, nor responsiveness of eosinophils and neutrophils as assessed by the expression of activation markers (CD11b, CD35, CD69, CD66b and CD62L). Serum levels of eosinophil granule proteins represent another measure of eosinophil activation, as these cytotoxic proteins

are released upon eosinophil degranulation. Whereas the levels of major basic protein (MBP), eosinophil cationic protein (ECP) and eosinophil-derived neurotoxin (EDN) were not different between helminth-infected and uninfected subjects at baseline, treatment significantly reduced the levels of EDN in those infected at baseline. In contrast to previous studies (19-26), the findings in this chapter indicate that STH infections do not induce increased eosinophil activation, although they do increase eosinophil numbers. However, it should be noted that this applies to eosinophils circulating in the peripheral blood, and it might be different at the site of infection or in the case of tissue-residing eosinophils. This study is the first placebo-controlled trial studying the effect of helminth infections on granulocyte activation and derives strength from its large sample size. Nevertheless, future studies, preferentially analyzing fresh instead of fixed eosinophils, are needed to investigate this further.

Besides eosinophilia, the type 2 response induced by helminths is also characterized by high levels of IgE and elevated signature cytokines such as IL-5. In **chapter 7** we assessed the effect of anthelmintic treatment on these two different components - total plasma IgE levels and IL-5 responses to mitogen PHA - of the Th2-mediated response, by analyzing immunological data obtained from a previously conducted randomized placebo-controlled trial of three-monthly single-dose albendazole treatment in an area highly endemic for STH (27). Remarkably, we showed that two years of anthelmintic treatment might have differential effects on different arms of Th2-mediated responses. Whereas IgE levels significantly declined in albendazole-treated subjects, IL-5 production by peripheral blood cells in response to PHA was not significantly affected by the treatment and rather tended to increase. The latter could be described as reversed T-cell hyporesponsiveness, a phenomenon which has been associated with chronic helminth infections and is thought to be mediated by Tregs (28). However, in **Chapter 8** (see below), we observed a significant reduction in PMA+ionomycin stimulated cells producing IL-4/IL-5/IL-13 after albendazole treatment, which supports the decrease seen in total IgE, yet it contrasts with the increased IL-5 production in PHA-stimulated whole blood. A combination of higher responsiveness to PHA, a different composition of cells in whole blood producing IL-5, and the stimuli used could account for this anomaly. This raises the question whether different types of Th2 cells are involved in various arms of the type 2 response.

As the sample collection during our field study progressed, so did the technology to study immune cells, and in **chapter 8** we used a recently developed platform termed mass cytometry (cytometry by time-of-flight; CyTOF) to get a better understanding of immune modulation by helminths and to identify specific cells that might be important in this process. Mass cytometry is an advanced form of flow cytometry that allows single-cell analysis of more than 40 different cellular markers, without the need for spectral compensation (29). Together with advances in computational analysis approaches such as Hierarchical Stochastic Neighbor Embedding (HSNE) (30), implemented in Cytosplore (31, 32), mass cytometry has emerged as a powerful tool to dissect the cellular composition of the immune system at a single-cell level.

We performed unbiased immune profiling of Indonesians who were infected with STH, before and 1 year after 3-monthly anthelmintic treatment, as well as of healthy European volunteers who had not been exposed to helminths. Expanded populations of total Th2 cells and ILC2s, but not Tregs, were found in STH-infected Indonesians compared to Europeans. After deworming, the frequency of Th2 cells significantly decreased and this was marked by a decrease in $CD161^+$ Th2 cells, a subpopulation which might be identical to previously described pathogenic effector Th2 cells (33). Interestingly, whereas anthelmintic treatment did not affect the frequency of ILC2s, the proportion of ILC2s producing type 2 cytokines declined after treatment, indicating decreased functional activity. Whereas ILC2s represent the innate source of type 2 cytokines, little is known about their role in human helminth infections and this is partly due to their low frequencies in peripheral blood. Here, we demonstrated a helminth-induced expansion of ILC2s in blood and future studies are needed to investigate their relative contribution to the different effector arms of the type 2 immune response.

Although the frequency of total Tregs was similar in Europeans and Indonesians, the use of mass cytometry allowed us to investigate the heterogeneity within Tregs. A significantly expanded population of $CTLA4^+$ Tregs was identified in STH-infected Indonesians compared to Europeans, which decreased after deworming. CTLA4 is a molecule which is crucial for the suppressive function of Tregs (34) and interestingly, further analysis showed that this $CTLA4^+$ subpopulation contained clusters expressing HLA-DR, CD38 and/or ICOS, all markers which have been associated with distinct Treg capacities and modes of suppression (35-37). Taken together, this indicates that helminths induce a particular Treg phenotype which could be represented by cells with increased regulatory capacity.

The use of mass cytometry also enabled us to identify rare cell populations such as type-2 cytokine producing $CD8^+$ T cells (termed Tc2 cells) and γδ T cells, subsets which were expanded in STH-infected Indonesians but did not change after treatment. Moreover, IL-10 producing B cells (regulatory B cells; Bregs) were identified and $CD11c^+$ B cells were shown to be the main IL-10 producers among B cells in Indonesians, a subset which is almost absent in Europeans.

Collectively, these results provide us with a detailed insight into the specific cell populations that participate in the type 2 and regulatory networks, and show that treatment of helminths affects specific cell subsets in these networks. In addition, we demonstrated that the combined use of mass cytometry and HSNE allowed us to identify rare cell populations in blood, such as ILC2s, Tc2 cells and Bregs.

In summary, the data presented in chapter 6, 7 and 8 have shed light on the immunomodulatory effects of helminths involving different components of the immune response. Whereas chapter 6 focused on eosinophil activation, chapter 7 studied the effects of anthelmintic treatment on IgE levels and the production of IL-5 in response to PHA, followed by a detailed characterization of circulating Th2 cells, ILC2s and Tregs before and after deworming in chapter 8. Regarding the beneficial effects of helminth infections on metabolic homeostasis, our work showed that $CD161^+$ Th2 cells, $CTLA4^+$ Tregs and ILC2s are of particular interest and enhancement of these populations might reduce systemic inflammation, and hence should be further analyzed. Whereas the relative contribution of each cell type to the beneficial effects of helminth infections in humans remains unknown, the helminth-induced regulatory network involving Tregs is thought to play a key role. However, experimental studies describing the effects of helminth-derived molecules on Tregs residing in WAT have shown inconclusive results. Previous work showed that treatment with ω1 (6), as well as with filarial antigens (5), resulted in increased Treg abundance in WAT of obese mice, while we demonstrated no change in WAT Treg frequencies following repetitive injections with ω1 (chapter 4). Moreover, a single footpad injection of ω1 increased both the percentage of total Tregs and of $CTLA4^+$ Tregs in the draining lymph nodes of non-obese diabetic (NOD) mice, indicating the potential of helminth-derived molecules to upregulate the suppressive function of Tregs (38). Therefore, further studies are needed to elucidate the functional role of Tregs in WAT in the context of helminth infections and metabolic homeostasis.

DIRECTIONS FOR FUTURE RESEARCH

Effects of deworming on type 2 and regulatory immune responses: Part II

Recent advances in cellular immunology methodologies and computational analysis approaches have now enabled detailed profiling of the immune system. However, mass cytometry is currently still limited by its slow throughput compared to flow cytometry. When considering large scale clinical trials, the application of this technique therefore provides the point of departure for larger studies. By using flow cytometry, future studies can further explore the findings described in chapter 8 in a larger subset of the study population, including placebo-treated individuals, to assess whether the observed effects can be truly attributed to the removal of helminths and to investigate if changes in the immune profile are reflected in clinical outcomes (e.g. changes in HOMA-IR). In addition, cellular assays can be performed to further investigate the function of particular cell populations. For example, suppression assays in which Tregs and T effector cells are co-cultured in the presence of blocking antibodies, can be used to evaluate the suppressive function of Tregs expressing CTLA4 and/or HLA-DR and/or CD38 and/or ICOS that were found to be expanded in STH-infected Indonesians.

To assess the effect of deworming on the cytokine production of immune cells, cells need to be stimulated *ex vivo*. Whereas stimulation with PMA+ionomycin (used in chapter 8) is very strong, non-specific, and not even mediated via the T cell receptor complex, stimulation with helminth-antigens is more physiological and will provide insight into the function of antigen-specific T cells. For example, stimulation with schistosomal antigens (schistosome soluble egg (SEA) and adult worm antigens (AWA)) was previously used to investigate the adaptive immune responses in *Schistosoma haematobium*-infected schoolchildren (39, 40). However, up to now, it has been challenging to isolate STH-derived antigens which can induce detectable cytokine responses.

Controlled human infections

Although longitudinal field studies in areas endemic for helminths provide a unique opportunity to study the real-life biological settings of infection, the interpretation of the results is complicated due to the presence of other infections that could be affected by treatment, the chance of reinfection and the observation that protective effects of helminths might persist long after treatment. Meanwhile, controlled human infections (CHI) in which healthy volunteers are experimentally infected with helminths, have generated much interest as a complementary approach to study the host-pathogen interaction in a very specific and controlled manner (41). CHI models will allow the characterization of the dynamics of immune responses that develop to helminth infections in a highly controlled setting, and will enable the assessment of helminth-induced effects on metabolic homeostasis. Moreover, these models can be used to study the therapeutic potential of helminth-derived molecules.

Another advantage of the CHI model compared to a field setting where clinical resources are limited, is the possibility to obtain human adipose tissue biopsies from helminth-infected individuals. Although experimental infections with helminths or helminth-derived molecules have shown that the type 2 immune pathways in WAT have protective roles that support maintenance of metabolic homeostasis, little is known about the effects on the immune cell composition of human WAT. However, additional insights on tissue-resident cells might be more relevant for the control of metabolic homeostasis, compared to circulating immune cells which are most often studied in helminth-infected individuals. Previous work identified ILC2s in human adipose tissue and found that frequencies are lower in obese compared to non-obese individuals (42). The same was observed for Tregs, whose frequencies appear to decrease in obese individuals (13). It would be very interesting to study these immune cell frequencies in WAT of obese individuals in the setting of a controlled helminth infection, the hypothesis being that type 2 and regulatory immune cells will expand after infection, thereby promoting insulin sensitivity. Moreover, the use of WAT biopsies would allow the study of macrophages, cells that are absent in peripheral blood but have shown to play a key role in the association between helminths and metabolic homeostasis.

Although white adipose tissue is the most studied organ in terms of immune-metabolic interactions in the context of obesity and metabolic disorders, it will also be interesting to explore the impact of helminths and helminth-derived molecules on other metabolic tissues such as brown adipose tissue, pancreas, liver, brain, muscle and intestine. These (predominantly rodent) studies will provide a deeper understanding of how the immune and metabolic systems interact to support metabolic homeostasis. To this end, novel technologies such as imaging mass cytometry (43), which couples high-density analysis by mass cytometry to conventional histology, could be used to study cell interactions in the context of the tissue microenvironment.

Gut microbiome

Besides alteration of the immune response, changes in the composition of the gut microbiome might be another possible helminth-mediated mechanism associated with improved metabolic homeostasis. Although a recent study reported the impact of human gut microbiome on insulin sensitivity (44) and chronic *Trichuris muris* infection was shown to alter the host microbiota *in vivo* (45), there have been no studies specifically studying the interaction between helminth infections, gut microbiome and insulin resistance. Interestingly, in mice, helminth infections are associated with an increase of intestinal short-chain fatty acids (SCFA) (46), the end products of dietary carbohydrates fermentation, which have been shown to play an important role in the control of body weight and insulin sensitivity (47).

Despite the growing interest in the analysis of the composition of the human gut microbiome, sample collection, storage techniques and bacterial DNA extraction methods are key steps required for the accuracy of these studies (48). While immediate freezing of fecal samples at -20˚C or below is considered the gold standard for microbiome preservation, this approach is not feasible for many field studies in remote areas (49). Studies showed that long-term sample storage at room temperature or multiple freeze-thaw cycles alters microbial community stability, while preservation methods improve stability but could alter community structure (50). Therefore, the microbiome field urgently needs a sampling method which can be readily applied outside of a clinical or well-equipped environment and which produces an accurate representation of the microbiota composition (48). Recently developed commercial kits such as OMNIgene GUT (DNA Genotek), allowing storage of fecal samples at room temperature, are now available and these might be suitable for large-scale field studies since there is no need for cold-chain transportation.

CONCLUDING REMARKS

This thesis has contributed to further understanding of immune modulation exerted by soil-transmitted helminths and how this can affect the development of type 2 diabetes. Every experimental study design has its pros and cons, and whereas this work has been based on a large-scale field study conducted in a rural area of Indonesia and an animal model of HFD-induced obese mice, the implementation of the controlled human infection model is expected to provide complementary insights into the mechanisms underlying the beneficial effects of helminths on metabolic homeostasis. Moreover, by investigating the effects of helminth-derived molecules on the immune response, future studies may offer new insights towards the development of novel therapeutics for the treatment of metabolic disorders.

REFERENCES

1. Wu D, Molofsky AB, Liang HE, et al. Eosinophils sustain adipose alternatively activated macrophages associated with glucose homeostasis. Science (New York, NY) 2011; 332(6026): 243-7.
2. Bhargava P, Li C, Stanya KJ, et al. Immunomodulatory glycan LNFPIII alleviates hepatosteatosis and insulin resistance through direct and indirect control of metabolic pathways. Nat Med 2012; 18(11): 1665-72.
3. Yang Z, Grinchuk V, Smith A, et al. Parasitic nematode-induced modulation of body weight and associated metabolic dysfunction in mouse models of obesity. Infection and immunity 2013; 81(6): 1905-14.
4. Hussaarts L, Garcia-Tardon N, van Beek L, et al. Chronic helminth infection and helminth-derived egg antigens promote adipose tissue M2 macrophages and improve insulin sensitivity in obese mice. FASEB journal: official publication of the Federation of American Societies for Experimental Biology 2015; 29(7): 3027-39.
5. Berbudi A, Surendar J, Ajendra J, et al. Filarial Infection or Antigen Administration Improves Glucose Tolerance in Diet-Induced Obese Mice. J Innate Immun 2016; 8(6): 601-16.
6. Hams E, Bermingham R, Wurlod FA, et al. The helminth T2 RNase omega1 promotes metabolic homeostasis in an IL-33- and group 2 innate lymphoid cell-dependent mechanism. FASEB journal : official publication of the Federation of American Societies for Experimental Biology 2016; 30(2): 824-35.
7. Aravindhan V, Mohan V, Surendar J, et al. Decreased prevalence of lymphatic filariasis among diabetic subjects associated with a diminished pro-inflammatory cytokine response (CURES 83). PLoS neglected tropical diseases 2010; 4(6): e707.
8. Chen Y, Lu J, Huang Y, et al. Association of previous schistosome infection with diabetes and metabolic syndrome: a cross-sectional study in rural China. The Journal of clinical endocrinology and metabolism 2013; 98(2): E283-7.
9. Shen SW, Lu Y, Li F, et al. The potential long-term effect of previous schistosome infection reduces the risk of metabolic syndrome among Chinese men. Parasite immunology 2015; 37(7): 333-9.
10. Hays R, Esterman A, Giacomin P, Loukas A, McDermott R. Does Strongyloides stercoralis infection protect against type 2 diabetes in humans? Evidence from Australian Aboriginal adults. Diabetes research and clinical practice 2015; 107(3): 355-61.
11. Wiria AE, Hamid F, Wammes LJ, et al. Infection with Soil-Transmitted Helminths Is Associated with Increased Insulin Sensitivity. PloS one 2015; 10(6): e0127746.
12. Molofsky AB, Nussbaum JC, Liang HE, et al. Innate lymphoid type 2 cells sustain visceral adipose tissue eosinophils and alternatively activated macrophages. J Exp Med 2013; 210(3): 535-49.
13. Cipolletta D. Adipose tissue-resident regulatory T cells: phenotypic specialization, functions and therapeutic potential. Immunology 2014; 142(4): 517-25.
14. Wammes LJ, Hamid F, Wiria AE, et al. Community deworming alleviates geohelminth-induced immune hyporesponsiveness. Proceedings of the National Academy of Sciences of the United States of America 2016; 113(44): 12526-31.
15. Stephenson LS, Latham MC, Ottesen EA. Malnutrition and parasitic helminth infections. Parasitology 2000; 121 Suppl: S23-38.
16. Bethony J, Brooker S, Albonico M, et al. Soil-transmitted helminth infections: ascariasis, trichuriasis, and hookworm. Lancet 2006; 367(9521): 1521-32.
17. Everts B, Perona-Wright G, Smits HH, et al. Omega-1, a glycoprotein secreted by Schistosoma mansoni eggs, drives Th2 responses. J Exp Med 2009; 206(8): 1673-80.
18. Everts B, Hussaarts L, Driessen NN, et al. Schistosome-derived omega-1 drives Th2 polarization by suppressing protein synthesis following internalization by the mannose receptor. J Exp Med 2012; 209(10): 1753-67, S1.
19. Rajamanickam A, Munisankar S, Bhootra Y, Dolla CK, Nutman TB, Babu S. Elevated Systemic Levels of Eosinophil, Neutrophil, and Mast Cell Granular Proteins in Strongyloides Stercoralis Infection that Diminish following Treatment. Frontiers in immunology 2018; 9: 207.
20. Mawhorter SD, Stephany DA, Ottesen EA, Nutman TB. Identification of surface molecules associated with physiologic activation of eosinophils. Application of whole-blood flow cytometry to eosinophils. Journal of immunology (Baltimore, Md : 1950) 1996; 156(12): 4851-8.
21. Fujiwara RT, Cancado GG, Freitas PA, et al. Necator americanus infection: a possible cause of altered dendritic cell differentiation and eosinophil profile in chronically infected individuals. PLoS neglected tropical diseases 2009; 3(3): e399.
22. Silveira-Lemos D, Teixeira-Carvalho A, Martins-Filho OA, Oliveira LF, Correa-Oliveira R. High expression of co-stimulatory and adhesion molecules are observed on eosinophils during human Schistosoma mansoni infection. Memorias do Instituto Oswaldo Cruz 2006; 101 Suppl 1: 345-51.
23. Gazzinelli-Guimaraes PH, Bonne-Annee S, Fujiwara RT, Santiago HC, Nutman TB. Allergic Sensitization Underlies Hyperreactive Antigen-Specific CD4+ T Cell Responses in Coincident Filarial Infection. Journal of immunology (Baltimore, Md : 1950) 2016; 197(7): 2772-9.
24. Tischendorf FW, Brattig NW, Buttner DW, Pieper A, Lintzel M. Serum levels of eosinophil cationic protein, eosinophil-derived neurotoxin and myeloperoxidase in infections with filariae and schistosomes. Acta tropica 1996; 62(3): 171-82.
25. Tischendorf FW, Brattig NW, Lintzel M, et al. Eosinophil granule proteins in serum and urine of patients with helminth infections and atopic dermatitis. Tropical medicine & international health : TM & IH 2000; 5(12): 898-905.
26. Reimert CM, Tukahebwa EM, Kabatereine NB, Dunne DW, Vennervald BJ. Assessment of Schistosoma mansoni induced intestinal inflammation by means of eosinophil cationic protein, eosinophil protein X and myeloperoxidase before and after treatment with praziquantel. Acta tropica 2008; 105(3): 253-9.
27. Hamid F, Wiria AE, Wammes LJ, et al. A longitudinal study of allergy and intestinal helminth infections in semi urban and rural areas of Flores, Indonesia (ImmunoSPIN Study). BMC infectious diseases 2011; 11: 83.
28. Maizels RM, Yazdanbakhsh M. Immune regulation by helminth parasites: cellular and molecular mechanisms. Nature reviews Immunology 2003; 3(9): 733-44.
29. Simoni Y, Chng MHY, Li S, Fehlings M, Newell EW. Mass cytometry: a powerful tool for dissecting the immune landscape. Curr Opin Immunol 2018; 51: 187-96.
30. Pezzotti N, Hollt T, Lelieveldt B, Eisemann E, Vilanova A. Hierarchical Stochastic Neighbor Embedding. Comput Graph Forum 2016; 35(3): 21-30.
31. Hollt T, Pezzotti N, van Unen V, et al. Cytosplore: Interactive Immune Cell Phenotyping for Large Single-Cell Datasets. Comput Graph Forum 2016; 35(3): 171-80.
32. van Unen V, Hollt T, Pezzotti N, et al. Visual analysis of mass cytometry data by hierarchical stochastic neighbour embedding reveals rare cell types. Nature communications 2017; 8(1): 1740.
33. Mitson-Salazar A, Prussin C. Pathogenic Effector Th2 Cells in Allergic Eosinophilic Inflammatory Disease. Front Med (Lausanne) 2017; 4: 165.
34. Wing K, Onishi Y, Prieto-Martin P, et al. CTLA-4 control over Foxp3+ regulatory T cell function. Science (New York, NY) 2008; 322(5899): 271-5.
35. Baecher-Allan C, Wolf E, Hafler DA. MHC class II expression identifies functionally distinct human regulatory T cells. Journal of immunology (Baltimore, Md: 1950) 2006; 176(8): 4622-31.
36. Ito T, Hanabuchi S, Wang YH, et al. Two functional subsets of FOXP3+ regulatory T cells in human thymus and periphery. Immunity 2008; 28(6): 870-80.
37. Patton DT, Wilson MD, Rowan WC, Soond DR, Okkenhaug K. The PI3K p110delta regulates expression of CD38 on regulatory T cells. PloS one 2011; 6(3): e17359.
38. Zaccone P, Cooke A. Helminth mediated modulation of Type 1 diabetes (T1D). International journal for parasitology 2013; 43(3-4): 311-8.
39. Meurs L, Labuda L, Amoah AS, et al. Enhanced pro-inflammatory cytokine responses following Toll-like-receptor ligation in Schistosoma haematobium-

infected schoolchildren from rural Gabon. PloS one 2011; 6(9): e24393.
40. Schmiedel Y, Mombo-Ngoma G, Labuda LA, et al. CD4+CD25hiFOXP3+ Regulatory T Cells and Cytokine Responses in Human Schistosomiasis before and after Treatment with Praziquantel. PLoS neglected tropical diseases 2015; 9(8): e0003995.
41. Roestenberg M, Hoogerwerf MA, Ferreira DM, Mordmuller B, Yazdanbakhsh M. Experimental infection of human volunteers. The Lancet Infectious diseases 2018.
42. Brestoff JR, Kim BS, Saenz SA, et al. Group 2 innate lymphoid cells promote beiging of white adipose tissue and limit obesity. Nature 2015; 519(7542): 242-6.
43. Giesen C, Wang HA, Schapiro D, et al. Highly multiplexed imaging of tumor tissues with subcellular resolution by mass cytometry. Nat Methods 2014; 11(4): 417-22.
44. Pedersen HK, Gudmundsdottir V, Nielsen HB, et al. Human gut microbes impact host serum metabolome and insulin sensitivity. Nature 2016; 535(7612): 376-81.
45. Houlden A, Hayes KS, Bancroft AJ, et al. Chronic Trichuris muris Infection in C57BL/6 Mice Causes Significant Changes in Host Microbiota and Metabolome: Effects Reversed by Pathogen Clearance. PloS one 2015; 10(5): e0125945.
46. Zaiss MM, Rapin A, Lebon L, et al. The Intestinal Microbiota Contributes to the Ability of Helminths to Modulate Allergic Inflammation. Immunity 2015; 43(5): 998-1010.
47. Canfora EE, Jocken JW, Blaak EE. Short-chain fatty acids in control of body weight and insulin sensitivity. Nat Rev Endocrinol 2015; 11(10): 577-91.
48. Hill CJ, Brown JR, Lynch DB, et al. Effect of room temperature transport vials on DNA quality and phylogenetic composition of faecal microbiota of elderly adults and infants. Microbiome 2016; 4(1): 19.
49. Song SJ, Amir A, Metcalf JL, et al. Preservation Methods Differ in Fecal Microbiome Stability, Affecting Suitability for Field Studies. mSystems 2016; 1(3).
50. Debelius J, Song SJ, Vazquez-Baeza Y, Xu ZZ, Gonzalez A, Knight R. Tiny microbes, enormous impacts: what matters in gut microbiome studies? Genome Biol 2016; 17(1): 217.

&

NEDERLANDSE SAMENVATTING

Parasitaire worminfecties en het immuunsysteem

Naar schatting is een kwart van de wereldbevolking geïnfecteerd met parasitaire wormen. Deze infecties worden voornamelijk aangetroffen in tropische landen, in gebieden met slechte hygiënische omstandigheden. De meest voorkomende parasitaire wormen leven in het maag-darm kanaal, zoals mijnwormen (*Necator*, *Ancylostoma*), spoelwormen (*Ascaris*) en zweepwormen (*Trichuris*). Een geïnfecteerd persoon kan via zijn/haar ontlasting de bodem besmetten met wormeieren. Nieuwe personen worden vervolgens geïnfecteerd wanneer ze de wormeieren inslikken via besmet voedsel of vieze handen. Sommige wormlarven, zoals die van mijnworm, kunnen de intacte huid binnendringen. Zowel kinderen als volwassenen kunnen op deze wijze geïnfecteerd raken als zij bijvoorbeeld geen schoenen dragen. De levenscyclus van de wormen wordt in stand gehouden doordat de eieren en larven zich in de darmen van een geïnfecteerd persoon ontwikkelen tot volwassen wormen die weer nieuwe eieren produceren. Hoewel de wormen soms tot tien jaar in de darmen aanwezig blijven, verlopen de infecties vaak zonder klachten.

Het afweersysteem, ook wel immuunsysteem genoemd, beschermt ons tegen ziekteverwekkers zoals virussen, bacteriën en parasitaire wormen. De ziekteverwekkers die het lichaam weten binnen te dringen worden opgewacht door een gemengde verzameling van witte bloedcellen (immuuncellen) met verschillende functies (bijv. T-helpercellen, B cellen, dendritische cellen, monocyten, macrofagen, 'killercellen', eosinofielen en neutrofielen). Het type ziekteverwekker bepaalt welke witte bloedcellen in actie komen. Virale of bacteriële infecties activeren veelal T-helper-1 (Th1) cellen, terwijl parasitaire wormen Th2 cellen activeren en een type 2-afweerreactie opwekken. Het is van groot belang dat de verschillende componenten van het afweersysteem in balans zijn en dit wordt aangestuurd door onder andere regulatoire T (Treg) cellen. Bij een worminfectie is deze immuunregulatie in het voordeel van zowel de geïnfecteerde persoon (de gastheer) als van de worm. In de gastheer zorgt immuunregulatie er namelijk voor dat de schade aan de omliggende weefsels die gepaard gaat met afweerreacties beperkt blijft, terwijl de worm niet wordt aangevallen door een sterke afweerreactie en dus langer kan overleven.

Wormen en diabetes type 2

Studies hebben aangetoond dat de door een worminfectie geactiveerde type 2 en regulatoire afweercellen, mogelijk een beschermend effect hebben op de ontwikkeling van andere ziektes waarbij het immuunsysteem ontregeld is. Dit betreft bijvoorbeeld allergieën en auto-immuunziekten. Ook bij mensen met overtollig vetweefsel (obesitas) zijn de verschillende componenten van het afweersysteem uit balans en dit vergroot de kans op diabetes type 2. Patiënten met diabetes type 2 zijn minder gevoelig voor insuline, het hormoon dat ervoor zorgt dat glucose uit het bloed kan worden opgenomen

door lichaamscellen, zodat het gebruikt kan worden om energie van te maken. Als cellen echter niet meer reageren op insuline, oftewel insuline resistent zijn geworden, blijven bloedsuikerspiegels hoog en dit kan op lange termijn zenuwen en bloedvaten beschadigen. In muizen is aangetoond dat gezond vetweefsel wordt gekenmerkt door de aanwezigheid van type 2-afweercellen die de werking van insuline bevorderen. In het vetweefsel van muizen met overgewicht daarentegen, ontstaat een chronische ontsteking die gepaard gaat met een type 1-afweerreactie. Deze type 1-afweercellen belemmeren de werking van insuline. Zie figuur 2 in hoofdstuk 1 voor een illustratie waarin bovenstaande wordt samengevat.

Aangezien worminfecties een type 2-afweerreactie opwekken en geassocieerd worden met een versterkte immuunregulatie, hebben wij onderzocht of worminfecties, of moleculen afkomstig van wormen, een beschermend effect hebben op de ontwikkeling van diabetes type 2. Tevens is onderzocht hoe worminfecties de activatie van verschillende soorten witte bloedcellen beïnvloeden. Dit onderzoek is uitgevoerd in de vorm van een klinische studie en daarnaast is er gebruik gemaakt van een muismodel.

Het effect van ontwormen op de ontwikkeling van diabetes type 2

Het effect van worminfecties op de ontwikkeling van diabetes type 2 kan worden onderzocht door de ene helft van een onderzoeksgroep te behandelen tegen worminfecties en de andere helft met een placebo. Dit hebben wij gedaan in een gebied waar veel mensen met wormen zijn besmet, in het 'SugarSPIN' project op Flores, Indonesië. **Hoofdstuk 2** beschrijft het studieprotocol dat is gebruikt om te onderzoeken of worminfecties een gunstig effect hebben op insuline resistentie, een veelgebruikte indicator en voorspeller voor de ontwikkeling van diabetes type 2. Gedurende 1 jaar is de onderzoeksgroep behandeld en deelnemers ontvingen hiervoor elke 3 maanden, 3 dagen achter elkaar medicatie tegen worminfecties (albendazole) of een placebo. Naast het uitvoeren van antropometrische metingen (lengte, gewicht, heup- en tailleomvang), zijn er voor en na de behandeling bloed, urine en feces monsters verzameld om veranderingen in insuline resistentie (en andere metabole parameters) en afweersysteem te kunnen meten. **Hoofdstuk 3** beschrijft de onderzoeksresultaten van deze studie. De behandeling tegen wormen heeft ertoe heeft geleid dat het aantal worminfecties na 1 jaar sterk verlaagd was. Toen we het effect van de behandeling op insuline resistentie onderzochten, bleek dat er een kleine, maar significante toename in insuline resistentie was opgetreden in de groep mensen die voor aanvang van de behandeling geïnfecteerd waren. Dit resultaat is het eerste directe bewijs in mensen dat worminfecties een beschermend effect kunnen hebben op insuline resistentie, en dus op de ontwikkeling van diabetes type 2. Daarnaast bleek dat de toename in insuline resistentie voornamelijk was toe te wijzen aan een toename in Body Mass Index (BMI) en een afname in het aantal eosinofielen, een bepaald type witte bloedcellen dat betrokken is bij type 2-afweerreacties.

Het mogelijk beschermende effect van parasitaire wormen op insuline resistentie is ook onderzocht in muizen met overgewicht. Ten opzichte van het SugarSPIN project,

bieden deze experimenten meer mogelijkheden om het onderliggende mechanisme te onderzoeken. Het is bijvoorbeeld mogelijk om de compositie van immuuncellen in het vetweefsel te bekijken, iets wat in mensen een stuk lastiger is. Daarnaast is het muismodel erg geschikt om onderzoek te doen naar moleculen afkomstig van wormen, die in staat zijn om het gunstige effect van een worminfectie te reproduceren om de ontwikkeling van diabetes type 2 in obesitas tegen te gaan. Om die reden is in **hoofdstuk 4** onderzocht of omega-1, een eiwit van *Schistosoma*-eitjes dat sterke Th2-sturende capaciteiten heeft, de insulinegevoeligheid in muizen met overgewicht kan bevorderen. Muizen op een hoog-vet-dieet die herhaaldelijk werden geïnjecteerd met omega-1 werden minder dik, de cellen in het lichaam namen glucose sneller op en de muizen waren gevoeliger voor insuline, in vergelijking met soortgenoten die niet met omega-1 werden behandeld. Dit ging gepaard met een type 2-afweerreactie in het vetweefsel. Om te onderzoeken of het positieve effect van omega-1 op insulinegevoeligheid echt veroorzaakt wordt door de type 2-afweerreactie, hebben we dit experiment ook uitgevoerd in zogenaamde STAT6-*knockout* muizen op een hoog-vet-dieet. Deze muizen zijn genetisch gemanipuleerd waardoor er geen type 2-afweerreactie kan worden opgewekt. Tegen de verwachting in, bevorderde omega-1 de insulinegevoeligheid ook in deze muizen wat aantoont dat het effect onafhankelijk is van de type 2-afweerreactie. Zowel de normale als de STAT6-*knockout* muizen, beide behandeld met omega-1, aten minder dan hun soortgenoten die niet met omega-1 werden behandeld. Dit resultaat suggereert dat dit eiwit mogelijk een effect heeft op de signalering in de hersenen die de voedselinname reguleert. Om deze hypothese te toetsen is echter verder onderzoek nodig.

Zie figuur 1 in hoofdstuk 9 voor een illustratie die de resultaten van hoofdstuk 3 en 4 samenvat.

Het effect van ontwormen op de verschillende componenten van het afweersysteem

In de volgende hoofdstukken hebben we het effect van worminfecties op de verschillende type witte bloedcellen in mensen verder onderzocht, omdat dit het positieve effect van wormen op insuline resistentie mogelijk zou kunnen verklaren. Tijdens een veldstudie zoals het SugarSPIN project zijn de onderzoeks-voorzieningen beperkt. Hierdoor zijn er methodes nodig waarmee we cellen kunnen invriezen zodat ze naar Nederland kunnen worden getransporteerd voor verder onderzoek. **Hoofdstuk 5** beschrijft de ontwikkeling van de methode om bepaalde soorten witte bloedcellen, namelijk eosinofielen en neutrofielen, in te vriezen tijdens een veldstudie zodat de activatie status van deze cellen later gemeten kan worden. Het is bekend dat eosinofielen onderdeel uitmaken van de type 2-afweerreactie, terwijl neutrofielen over het algemeen meer betrokken zijn bij type 1-afweerreacties. Deze methode is toegepast tijdens het SugarSPIN project in Indonesië en **hoofdstuk 6** beschrijft de studie waarin we in een deel van de totale onderzoeksgroep hebben onderzocht of worminfecties resulteren in een verhoogde activatiestatus van eosinofielen en neutrofielen. Hoewel het aantal eosinofielen in het

bloed sterk afnam in de groep mensen die behandeld was tegen wormen, was er tegen de verwachting in geen verschil in de activatiestatus van de eosinofielen en neutrofielen. Dit kan worden verklaard door het feit dat dit type witte bloedcellen zich voornamelijk in de weefsels bevindt. Het is daarom mogelijk dat de activatiestatus van de cellen in het bloed geen goed beeld geeft van wat zich afspeelt in de weefsels. Daarnaast kan het zijn dat de activatiestatus toch nauwkeuriger kan worden bepaald in cellen die niet ingevroren zijn geweest.

Naast Th2 cellen en eosinofielen, wordt de type 2-afweerreactie ook gekenmerkt door een toename van IgE, een antilichaam geproduceerd door B cellen, en bepaalde cytokines (eiwitten die belangrijk zijn voor de communicatie tussen cellen) zoals IL-4, IL-5 en IL-13. **Hoofdstuk 7** beschrijft dat de behandeling tegen wormen verschillende effecten kan hebben op de verschillende componenten van de type 2-afweerreactie. In vergelijking met de groep mensen die een placebo-behandeling kregen, resulteerde de behandeling tegen wormen namelijk in een afname in de concentratie van IgE, terwijl de productie van IL-5 niet significant veranderde en eerder leek toe te nemen. Het is de eerste keer dat deze verschillende effecten zijn aangetoond in één onderzoeksgroep. Het resultaat is een aanwijzing dat men rekening moet houden met de verschillende effecten op de type 2-afweerreactie in studies naar de invloed van parasitaire wormen op de ontwikkeling van ontstekingsziekten.

Tot slot is er in **hoofdstuk 8** gebruik gemaakt van een recentelijk ontwikkelde techniek genaamd 'Massa cytometrie' (CyTOF), waarmee het mogelijk is om de expressie van 37 specifieke eiwitten (markers), cel voor cel, te bestuderen en zo de complexiteit van het afweersysteem in detail te onderzoeken. Door de cellen van Indonesische mensen met een worminfectie voor en na behandeling met elkaar te vergelijken, hebben we onderzocht welke specifieke cellen binnen de type 2-afweerreactie en de Treg cellen een rol spelen tijdens worminfecties. Daarnaast hebben we het afweersysteem van deze Indonesische mensen vergeleken met een groep gezonde Europeanen. De geconstateerde verschillen in het afweersysteem tussen Europeanen en Indonesiërs kunnen van belang zijn voor het begrip van de toenemende hoeveelheid mensen met diabetes type 2, en mogelijk bijdragen aan de ontwikkeling van oplossingen voor dit probleem. Daarnaast is deze kennis van belang voor de ontwikkeling van vaccins. Er zijn namelijk wereldwijd verschillen in de werkzaamheid van vaccins en dit wordt deels toegewezen aan veranderde levensomstandigheden (verbeterde hygiëne, minder blootstelling aan bacteriën en parasieten) in Westerse landen, waardoor er vermoedelijk plaatsgebonden verschillen in het afweersysteem zijn opgetreden.

Conclusie

Het onderzoek beschreven in dit proefschrift biedt nieuwe inzichten in de interactie tussen parasitaire wormen, het afweersysteem en de ontwikkeling van diabetes type 2. De studies laten zien dat zowel worminfecties in mensen, als de toediening van wormmoleculen in muizen met obesitas, een positief effect hebben op de insulinegevoeligheid en hierdoor het

risico op diabetes type 2 verkleinen. Hoewel dit werk aantoont dat de type 2-afweerreactie en Treg cellen belangrijke en complexe onderdelen van ons afweersysteem vormen, zal toekomstig onderzoek moeten uitwijzen hoe cruciaal de rol van deze afweerreacties is in de ontwikkeling van ontstekingsziektes waarbij een type 2-afweerreactie wenselijk is, zoals diabetes type 2. De verwachting is dat studies waarbij gezonde proefpersonen onder gecontroleerde omstandigheden worden geïnfecteerd met parasitaire wormen ("Controlled Human Infections") hier aan bij zullen dragen.

ACKNOWLEDGEMENTS / DANKWOORD

I would like to thank all the people who, in one way or the other, have contributed to the work described in this thesis.

First I would like to thank my promotores and co-promotor. Maria, thank you so much for the opportunity to start this project, the trust you gave me, your energy and enthusiasm, and your continuous support – no matter the distance in between. I have learned a lot from you. Tania, without your fieldwork experience this project would not have succeeded. Thanks for your guidance and support, for composing a great team of fieldworkers and for taking care of the (always challenging) transport of samples, dry ice and liquid nitrogen. Bruno, thank you for the opportunity to be involved in the in vivo studies and your welcome advice whenever needed.

I would also like to thank Erliyani for sharing your fieldwork experience with Dicky and me, teaching us how to prepare and conduct a field study and always being there to answer our questions. I am also very grateful to Yvonne, you taught me how to work in the "Nangapanda lab" and to always think of creative solutions. Thank you Jan, for your advice and support throughout the project.

I would also like to thank my paranymphs. Dicky, my partner in crime, I have very much enjoyed working together with you for 4 years. Your social skills and commitment have been crucial for the successful completion of the field study. Thank you for being my guide into the Indonesian culture. Astrid, with the joint use of mass cytometry we started to team up and you have been a great support to me. In addition, I have enjoyed our non-CyTOF related conversations and laughter.

I would also like to thank many other people at the department of Parasitology for your help in- and outside the lab and doing fun things together such as the movie nights, paragliding, a mud masters obstacle run, lab outings and the diving weekends in Zeeland. In particular Koen and Yoanne (*Thanks for the 'gezelligheid' in the office, the discussions and laughs*), Sanne (*Thanks for your FACS and CyTOF support and for always being helpful*), Jacqueline (*Thanks for your help sorting thousands of samples*), Mikhael and Eddy (*Thanks for your help in Nangapanda*), Katja (*Thanks for sharing the last-months-of-your-PhD-issues*), Leonard, Beatrice and Marijke (*Lab outing committee 2016!*), Abena, Alice, Alwin, Angela, Arifa, Bart, Corrie, Dian, Eric, Eunice, Firdaus, Frank, Hermelijn, Jantien, Laudine, Leonie, Linda, Lisette, Łucja, Maria K., Marie-Astrid, Marije, Mathilde, Meta, Michelle, Noemí, Patrick, Ron, Simone and Suzanne. Furthermore, I would like to thank the CyTOF team including Vincent, Rene and Marjolijn for their advice and help. Jeanine and Ivonne, thank you for your statistical help. Leo, Edward, Bart and Selma, thank you for the nice collaboration regarding the granulocyte work.

My appreciation also goes to my Indonesian Parasitology colleagues. Terima kasih banyak Yenny, Pak Dirman, Yossi, Eka, Difa, Pita, Femmy, Elisa, Audi, Devy, Sovie, Budi, Pak Warto and Elton. You have all contributed greatly to the field study. I would also like to thank Dr. Helda Sihotang, Bapak Camat Berdadus Idu, all health workers from Nangapanda Primary Healthy Centre, as well as the local health cadres, in particular Yuyun and Mufida. Thanks to all the study participants.

Lieve Linde, Nicoline, Sophie, Kim, Willemien, Anouk, Marian, Marga, Frederik, Anne en Marloes, bedankt voor jullie vriendschap, support en interesse in mijn onderzoek!

Tot slot wil ik mijn lieve ouders en zus bedanken. Jullie hebben me van advies, steun en afleiding voorzien wanneer nodig. Dank dat jullie altijd voor me klaar staan!

CURRICULUM VITAE

Karin de Ruiter was born on 20 September 1988 in Renkum, the Netherlands. After completing grammar school in Wageningen (scholengemeenschap Pantarijn) in 2006, she started to study Life Science and Technology, Major Biomedical Sciences, at the University of Groningen. She obtained her Bachelor's degree in 2009, and this was followed by a *cum laude* Master's degree in Medical Pharmaceutical Sciences in 2011. During her Master's, Karin first worked on an internship within the Endothelial Biomedicine & Vascular Drug Targeting Group at the University Medical Center Groningen, and did her final internship at the Department of Pharmacokinetics, Toxicology and Targeting at the University of Groningen. Thereafter, at the same department, she conducted research on the targeted delivery of IFNγ to activated hepatic stellate cells in liver fibrosis. In 2013 she moved to Leiden to start a PhD project at the Department of Parasitology under the supervision of Prof. Dr. Maria Yazdanbakhsh. For this collaborative research project between the Faculty of Medicine, Universitas Indonesia (FKUI), Jakarta, Indonesia and Leiden University Medical Center (LUMC), she often travelled to Indonesia to work with a team and conduct a large immunoepidemiological field study on Flores island, East Indonesia, which culminated in the work presented in this thesis.

LIST OF PUBLICATIONS

de Ruiter K, Tahapary DL*, Stam KA*, van Unen V, Höllt T, Lelieveldt BPF, Koning F, Sartono E, Smit JWA, Supali T, Yazdanbakhsh M. *Mass cytometry reveals heterogeneity of type 2 and regulatory cells driven by helminth infections.* Submitted.

Jochems SP*, **de Ruiter K***, Solorzano C*, Voskamp A*, Mitsi E, Nikolaou E, Carniel BF, Pojar S, German EL, Reine J, Schanoski A, Hill H, Robinson R, Weight C, Durrenberger PF, Heyderman RS, Gordon S, Smits HH, Urban B, Rylance J, Collins A, Wilkie M, Lazarova L, Leong S, Yazdanbakhsh M, Ferreira DM. *Defining mucosal immunity using mass cytometry following experimental human pneumococcal challenge.* Submitted.

van der Zande HJP*, Hussaarts L*, Pelgrom LR, Garcia-Tardon N, Hoving L, **de Ruiter K**, Otto F, van der Zon G, Embgenbroich M, Katiraei S, Willems van Dijk K, Everts B, Yazdanbakhsh M, van Harmelen V , Burgdorf S, Guigas B. *Mannose receptor deficiency protects against high-fat diet-induced insulin resistance by reducing pro-inflammatory activation of macrophages.* Submitted.

de Ruiter K, Tahapary DL, Sartono E, Nutman TB, Smit JWA, Koenderman L, Yazdanbakhsh M. *The effect of helminths on granulocyte activation: a cluster-randomized placebo-controlled trial in Indonesia*. J Infect Dis. 2018 Nov 17 [Epub ahead of print].

van Staveren S, Ten Haag T, Klöpping M, Hilvering B, Tinnevelt GH, **de Ruiter K**, Piacentini MF, Roelands B, Meeusen R, de Koning JJ, Jansen JJ, Vrisekoop N, Koenderman L. *Multi-dimensional flow cytometry analysis reveals increasing changes in the systemic neutrophil compartment during seven consecutive days of endurance exercise.* Plos One. 2018 Oct 30;13(10):e0206175.

Tahapary DL*, **de Ruiter K***, Kurniawan F*, Djuardi Y, Wang Y, Nurdin SME, Iskandar E, Minggu D, Yunir E, Guigas B, Supali T, Rensen PCN, Sartono E, Soewondo P, Harbuwono DS, Smit JWA, Yazdanbakhsh M. *Impact of rural-urban environment on metabolic profile and response to a 5-day high-fat diet.* Sci Rep. 2018 May 25;8(1):8149.

de Ruiter K, van Staveren S, Hilvering B, Knol E, Vrisekoop N, Koenderman L, Yazdanbakhsh M. A field-applicable method for flow cytometric analysis of granulocyte activation: Cryopreservation of fixed granulocytes. Cytometry A. 2018 May;93(5)540-547.

Tahapary DL, **de Ruiter K**, Martin I, Brienen EAT, van Lieshout L, Djuardi Y, Djimandjaja CC, Houwing-Duistermaat JJ, Soewondo P, Sartono E, Supali T, Smit JW, Yazdanbakhsh M. *Effect of anthelmintic treatment on leptin, adiponectin, and leptin to adiponectin ratio: a randomized controlled trial.* Nutr Diabetes. 2017 Oct 16;7(10):e289.

Tahapary DL*, **de Ruiter K***, Martin I, Brienen EAT, van Lieshout L, Cobbaert CM, Soewondo P, Djuardi Y, Wiria AE, Houwing-Duistermaat JJ, Sartono E, Smit JW, Yazdanbakhsh M, Supali T. *Effect of Anthelmintic Treatment on Insulin Resistance: A Cluster-Randomized Placebo-Controlled Trial in Indonesia.* Clin Infect Dis. 2017 Sep 1;65(5):764-771.

de Ruiter K*, Tahapary DL*, Wammes LJ, Wiria AE, Hamid F, van Lieshout L, Smit JWA, Houwing-Duistermaat JJ, Sartono E, Supali T, Yazdanbakhsh M. *The effect of three-monthly albendazole treatment on Th2 responses: Differential effects on IgE and IL-5.* Parasite Immunol. 2017 Jun;39(6).

de Ruiter K*, Tahapary DL*, Sartono E, Soewondo P, Supali T, Smit JWA, Yazdanbakhsh M. *Helminths, hygiene hypothesis and type 2 diabetes.* Parasite Immunol. 2017 May;39(5).

Tahapary DL*, **de Ruiter K***, Martin I, van Lieshout L, Guigas B, Soewondo P, Djuardi Y, Wiria AE, Mayboroda OA, Houwing-Duistermaat JJ, Tasman H, Sartono E, Yazdanbakhsh M, Smit JW, Supali T. *Helminth infections and type 2 diabetes: a cluster-randomized placebo controlled SUGARSPIN trial in Nangapanda, Flores, Indonesia.* BMC Infect Dis. 2015 Mar 18;15:133.

*Equal contribution